論文 / 著書情報
Article / Book Information

題目(和文)	小型IoT向けのLED方式小型光無線給電
Title(English)	LED-based Portable Optical Wireless Power Transmission for Compact IoT
著者(和文)	周 宇環
Author(English)	Zhou Yuhuan
出典(和文)	学位:博士（工学）, 学位授与機関:東京工業大学, 報告番号:甲第11935号, 授与年月日:2021年3月26日, 学位の種別:課程博士, 審査員:宮本 智之,小山 二三夫,植之原 裕行,德田 崇,宮島 晋介,丸山 武男
Citation(English)	Degree:Doctor (Engineering), Conferring organization: Tokyo Institute of Technology, Report number:甲第11935号, Conferred date:2021/3/26, Degree Type:Course doctor, Examiner:,,,,,
学位種別(和文)	博士論文
Type(English)	Doctoral Thesis

LED-based Portable Optical Wireless Power Transmission for Compact IoT

by

Yuhuan Zhou

Department of Electrical and Electronic Engineering
Electrical and Electronic Engineering
Tokyo Institute of Technology

DOCTORAL DISSERTATION
1 March 2021

Adviser
Associate Professor Tomoyuki MIYAMOTO, Dr. Eng

Tokyo Institute of Technology
4259 Nagatsuta, Midori-ku, Yokohama 226-8503, JAPAN

Abstract: For Internet-of-things (IoT) terminals, wiring and battery exchange are less effective power supplying methods due to excessive installation and maintenance works cost. Optical wireless power transmission (OWPT) is promising candidate, and its advantages of long transmission distance, good directionality, and portable size are attractive. In this research, light emitting diode (LED) based OWPT system that realized portable size, large electricity power supply amount and high functionality was designed and demonstrated by simulation and experiment. Around 400 mW output power was achieved from GaAs solar cell from 1 m transmission distance by portable near infrared LED-based OWPT system. Based on the analysis of the system, the characterization between system parameters and possible performance was investigated, implicit challenges and future prospect of LED-based OWPT system was discussed and clarified.

Table of Contents

Chapter 1. Introduction

1.1 Background

1.1.1 Internet of things investigation

Internet of things (IoT) plays an indispensable role in today's informatization and digitization society and is rapidly gaining ground in the scenario of modern wireless telecommunications. It includes various kinds of devices such as smart phone, computers, and daily necessities which embedded sensors, software and other technologies for the purpose of connecting and exchanging data with other devices and systems over internet and forming a cyber-physical system (CPS).[1] In fact, IoT technologies are nowadays assumed to be one of the key pillars of the fourth industrial revolution due to significant potential in innovations and useful benefits for the population.[2] Especially, with the fifth generation (5G) mobile network is about to become popular on a large scale, which can significantly enlarge the scope and scale of coverage of IoT by increased the capacity and speed to provide reliable and speedy connectivity to the numerous IoT terminals at same time, the more and more rapidly growing of IoT is predictable.[3]

The major significant trend of IoT in recent years is the explosive growth of devices connected and controlled by internet. A prediction of future connected devices over internet is shown in Fig. 1.1. The graph shows a growth of devices such as phones, tablets, laptops, etc. The real substantial growth is predicted from all other types of connected small devices in areas like home automation, smart energy, health care, transportation, asset tracking and many others which will be a real candidate to be IoT devices. The rise of IoT technologies is currently undergoing intense development, and according to projections for the next 10 years, it is estimated that over 125 billion IoT devices are expected to be connected.[4]

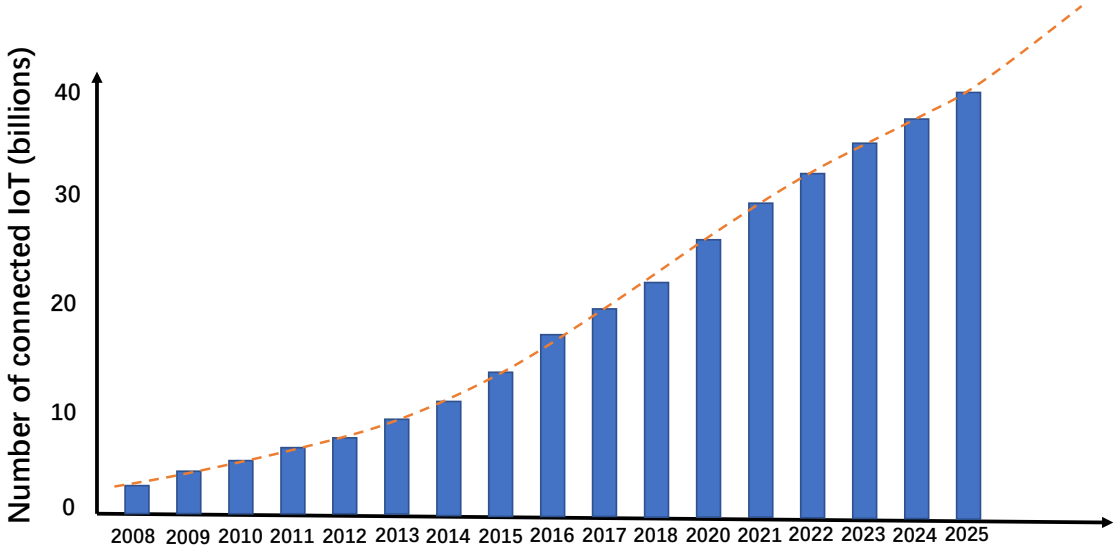

Fig. 1.1 Growth of devices[5]

The applications of IoT covers almost fields in society. The application areas of IoT can be mainly divided in 8 categories, which is shown in Table 1.1.[6]

Table 1.1 Categories of IoT application areas

Categories	Examples
Smart home	Google Home
Healthcare	Fitbit electronic wristbands
Transportation	ETC
Industry	Smart manufacturing
Agriculture	Humidity sensor
Power management	Smart grid
Smart city	Smart parking
Wearable gadgets and smart appliances	Key tracker

In smart home, the IoT devices are a part of the concept of home automation. With the popularization of broadband services, smart home products involve all aspects. Residents can control home appliances such as lighting, air-conditions

media or checking home security system and camera system remotely at anytime and anywhere. Smart home is one of the most rapidly growing area of IoT applications. Now the most popular ones include Google Home, Amazon Echo, Apple's HomePod, Samsung's SmartThings Hub and Xiaomi's Mi Smart Home.[7][8][9][10][11]

The IoT for medical and health related purposes references as "Internet of Medical Things (IoMT)" or "Smart Healthcare". It is an application of collecting data of body condition and creating a digitized healthcare system, connecting available medical resources and healthcare services. It can also be used to enable remote health monitoring and emergency notification. These health monitoring devices can range from blood pressure and heart rate monitors to advanced devices capable of monitoring specialized implants, such as pacemakers, Fitbit electronic wristbands, or advanced hearing aids.[12][13][14][15][16][17][18][19][20][21]

The application of IoT technology in transportation area is relatively mature and application of the IoT extends to all aspects of transportation system. With the increasing population of vehicles, traffic congestion has become a major problem of city transportation system. Real-time monitoring of traffic conditions and timely transferring information to drivers by IoT devices allow drivers timely adjust their route, which effectively alleviating traffic pressure. Electronic Toll Collection (ETC) which set up at highway intersections can eliminate the need for payment card picking and returning time. The bus tracking system allows passengers to check route and arrival time of the bus and determine their freely. The roadside parking management system, which based on cloud computing platform combined with IoT and mobile payment technology, can share parking space resources and improve parling space utilization.[22][23][24]

The IoT in industry area, which is also known as Industrial Internet of Things (IIoT), is a platform for diversified integration and mutual exploration of different elements, which can connect various sensors, controllers, computer numerical control (CNC) machine tools and other production equipment. By applying perception technology, communication technology, transmission technology,

data processing technology and control technology to all stages of production, batching, warehousing to achieve digital and intelligent producing and controlling, it can improve product quality and reducing product costs and resource consumption.[25][26][27]

The agricultural IoT refers to the IoT that participates in automatic control through various instruments and meters in real time or as parameters of automatic control. It can provide a scientific basis for the precise adjustment to achieve the purpose of increasing production, improving quality, regulating the growth cycle, and improving economic benefits. In agriculture field, various sensors are used to detect the physical quantities such as temperature, relative humidity, PH value, light intensity, soil nutrients, CO_2 concentration and others to ensure that crops have a good and suitable growth environment. The realization of remote control enables technicians to monitor and control the environment of multiple greenhouses or cultivated fields.[28][29]

The energy-consuming IoT devices can connect with internet and communicate with utilities for the purpose of optimizing the energy consumption. These devices allow for remote control by users, or central management via a cloud-based interface, and enable functions like scheduling. Smart grid is a good example of IoT application in power management area. The systems collect and process the information related to energy to improve the efficiency of electricity producing and distributing. The electric utilities can collect data from users and manage distribution automation devices by using advanced metering infrastructure (AMI) internet-connected devices.[30][31]

The smart city is metropolitan scale deployment and integration of different categories of IoT devices such as transportation IoT or power management IoT to enable better management of cities. There are several planned or undergoing programs of smart city. For instance, Cisco has started a smart city project of deploying technologies for Smart Wi-Fi, Smart Safety & Security, Smart Lighting, Smart Parking, Smart Transports, Smart Bus Stops, Smart Kiosks, Remote Expert for Government Services (REGS) and Smart Education in the five km area in the city of Vijaywada.[32][33][34][35][36][37][38][39][40][41][42][43][44][45]

The last category of IoT application area is some small IoT terminals and tags that be wearable or easy installing on other objects. The main function of such IoT devices is tracking position or recording certain information, such as smart sports bracelet, smart camera, pet positioning collar or key tracker.[46][47]

It should be noted that, the boundaries of the categories shown in Table 1.1 is blurred. The category of a certain IoT devices is based on various factors such as function, application scenario, size, etc. Generally, a IoT device that belongs multiple categories is possible and normal. For example, a smart watch can belong to both healthcare area and wearable gadgets IoT area, and a temperature sensor IoT terminal can belong to smart home area, industry area, agriculture area and smart city.

The application scenarios of IoT devices area extensive. However, bulk of issues and challenges exist, such as Heterogeneity, quality of service (QoS), security and privacy, power consumption and so on.[48] Among these issues, power consumption is always the most basic but core problem. Basically, the current power supply methods of IoT devices are wiring and using battery. The application scenarios of IoT can be simply divided as fixed installed and movable. As for a certain part of IoT devices such as most IIoT, the working location and environment is unchanged, thus wiring is the simplest method of stable power supplying. However, wiring requests laying work, laying space and wires maintenance, which causes excessive labour and money. Moreover, the required excess space of wiring limits usage environment. Such as smart doorbell camera that installed outdoor or ETC installed on car ceiling, it is difficult to ensure required space of wiring.

Generally, IoT device has several typical work states of an advertisement and connection events, which is shown in Fig. 1.2.

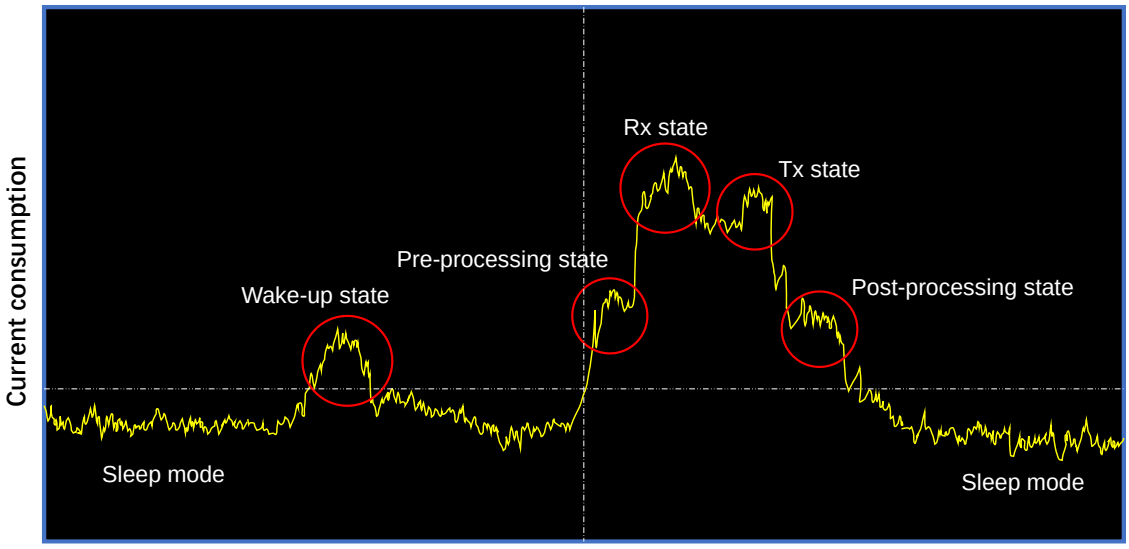

Fig. 1.2 Connection event states of typical IoT

The sleep mode, or power saving mode, which is the connection intervals between two work cycles of the IoT terminal. The power consumption of the sleep mode is usually constrained at the minimum level. The wake-up state, which is the stage that IoT actives by fixed intervals (timer) or a certain trigger, and performs the tasks related to the system initialization. The pre-processing state, which is the stage that IoT terminal processes preparation of the radio to transmit (Tx) and receive (Rx) data packets. The Rx state and Tx state are the stages that IoT terminal process the information receiving and transmitting tasks. Finally, the post-processing state processes the received data packets, and also sets the timer for the next connection event in some applications.[49] The power consumption will vary depending on each state.

The average current Ion during IoT awake period can be calculated by:

$$I_{on} = \frac{\sum_{i=1}^{N_S}(T_{Si}I_{Si})}{T_{on}} \tag{1.1}$$

Here the T_{on} is the period of connection event, and T_{Si} is the time of each state and I_{Si} is the corresponding current consumption. N_s represents the number of states and i is the state index.[50] The total average current I_{avg} that includes both awake period and sleep period can be obtained by:

$$I_{avg} = \frac{I_{on}T_{on}+I_{sleep}(T_{ci}-T_{on})}{T_{ci}} \tag{1.2}$$

The I_{sleep} is the current consumption of sleep state, and T_{ci} represent the period of an individual operation which includes both connection state and sleep state. Thereby, the battery lifetime is given by:

$$T_{bat} = \frac{C_{bat}}{I_{avg}} \tag{1.3}$$

The T_{bat} is the battery lifetime in hours, and C_{bat} is the battery capacity in mAh. According to the equations, apart from objective factors such as C_{bat}, the battery lifetime of IoT is closely related with the IoT performance. Extending the period of connection state, shortening connection interval and speeding up work cycle, increasing data packets capacity, all of these high functions and performance will shorten battery lifetime. Conclusively, the action of high function of IoT is supported by high power consumption, which is inversely proportional to the battery lifetime. The Fig. 1.3 shows the connection interval and data packets capacity versus battery lifetime of IoT device.

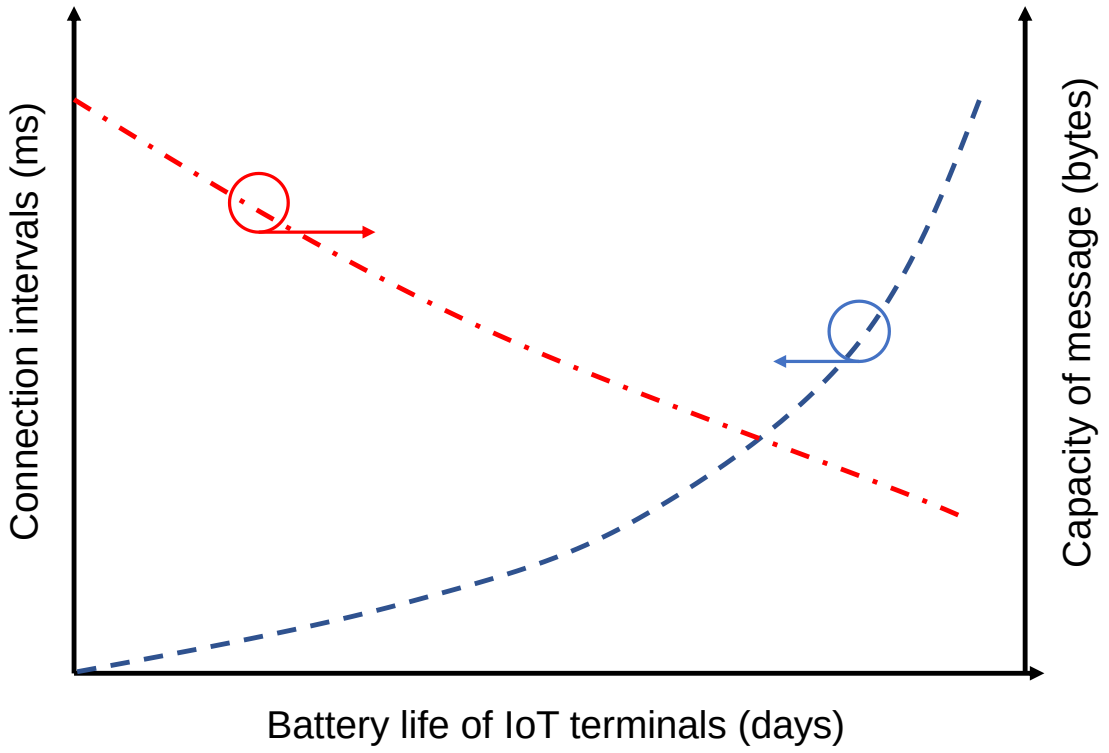

Fig. 1.3 Characteristics of battery life of IoT based on connection interval and capacity of message[49]

In the recent years, increasing the lifetime of IoT devices has been a hot research topic. The power consumption of IoT terminals can be constrained by compressing the capacity of data packets of every mote.[53] At the aspect of communication protocol, the lifetime of IoT terminals can be improved through data aggregation by intermediate hops[51] and using fare routing protocols,[52] or applying more efficient MAC protocol.[54] However, the researches stated above didn't solve the essential issue of the easy supplementing electrical power of IoT battery. Essentially, the burden of replacing or recharging battery of IoT device is unavoidable.

Furthermore, if the battery replacement must be arranged periodically, then the difference of the remained power amount between each IoT terminal battery across the certain region will be a severe factor. On such regard, it must be considered that extra labour, money and time will be costed by each intervention, and also, it might cause trouble to the citizens in some cases. On the other hand, if the battery usage of different IoT devices is much different, the battery replacement schedule becomes more complicated. IoT terminals are usually small devices with limited processers, memory and batteries. They are usually capture data from the environment and send messages wirelessly to a central mote, which is often called a gateway. According to the way of messages are generated, the IoT applications can be divided into two categories: the first category is that the nodes report data at fixed intervals, which means the IoT terminal is active by the built-in timer, and the second category is that the nodes report data asynchronously, which means the IoT terminals is active by certain triggers. Most of IoT applications for monitoring purpose are the example of the former, while the IoT terminals for sensing purpose will be an example of the latter, where the IoT terminals only send messages when certain status of the environment changed. As for the IoT terminal acts periodically, the power consumption of all the terminals in the same network is very similar due to the operation conditions of all devices is almost the same. Therefore, due to the power consumption of all IoT terminals is similarly decreased as time passes, the battery replacement schedule for such category IoT devices is relatively easy.

Whereas, the power consumption of the IoT terminal that acts by certain trigger is much different depends on the installed position, functions and status of the environment, therefore the battery replacement schedule is very difficult to make due to much difference on the remained power of the individual battery. In addition, if take into account that different categories IoT devices installed at a certain region, some of them are operated with different fixed intervals, and some of them are active by different triggers, the remained power of each IoT terminals will be much different. Besides, since the battery replacement intervention is unavoidable and relatively frequent, if only the IoT batteries that out of power are replaced every time, the rest of IoT terminals will soon deplete their battery and accelerate the next intervention of battery replacement. While if replace the batteries of all IoT terminals periodically, it becomes a large waste of money and labour, and also cause large trouble to the daily life of the citizens. Such process is worsened in the practical condition that diverse IoT terminals installed and various scenarios existed.[55]

Moreover, the trend of IoT technology is developing towards the direction of more intelligent, smaller and more complex functions, which means higher performance and smaller battery capacity. The contradiction between the request of higher performance of IoT device and its smaller battery capacity has become more and more prominent, and the power consumption issue of IoT devices is becoming acute. Considering the extensive increasing of connected IoT devices in the coming decade, every home or workplace may have dozens of high performance IoT devices averagely, wiring and installing a large number of sockets is not realistic, and periodically replacing or rechanging the battery must become a burden not only for specific technicians but also individuals. Thus, even the power saving technology of the IoT devices is advancing, its performance and function expansion are restricted by power consumption issues. Therefore, it is very critical to study a new type of power supply method which provides the power to IoT devices easily without wiring or even installing batteries. It is envisaged that such novel wireless power supply technology can conveniently provide long-distance power for IoT terminals anytime and anywhere, eliminating the burden of wiring or replacing batteries. The wireless power supply device has simple

configuration and small size, and the receiving end is easy-installing, and can be adapted to most IoT terminals. The IoT terminal can guarantee several times the previous lifetime without sacrificing functionality.

1.1.2 Investigation of wireless power transmission technologies

In order to propose a new power supply method and solve the power supplying issue of IoT terminals, representative power supplying methods are investigated, and the merits and drawbacks of each approach is analysed and listed in the Table 1.2.

Table 1.2 Representative power supplying methods

Power supply methods	Advantages	Disadvantages
Wiring	No battery need, stable and high-power supplying	Location fixed, laying space and laying work needed, maintenance needed
Battery only	High degree of freedom, stable power supplying	Power amount limited, replacement and recharging needed
Energy harvesting	Recharging constantly and unlimited	Low power supplying, largely depends on environment and unstable
WPT	High power supplying remotely and stably, high degree of freedom, no environment dependence	Need to design device separately

Wiring, which is the most common power supplying method, can provide very high power stably. However, as discussed in section 1.1.1, laying work and maintenance is required, which cost excessive labor and money.[56] Besides, the requirement of laying space limits the possible working scenarios. With the development of IoT technology and its increasing diverse and flexible application scenarios, the request of non-wiring will become much more common.

Using battery is a traditional solution to the demand of high degree of freedom and flexible working scenario of electrical devices. Whereas, the periodical battery recharging or replacement is becoming a burden. Not to mention that in the diverse working scenarios of IoT devices, some of IoT terminals are difficult to contact and charge. One example is the dynamic fleet flow monitoring IoT sensor which is usually installed at high places such as top of the bracket of a street lamp or ceiling of an overpass. Every time replacing or recharging the battery via cable, it takes a lot of time and effort to build and get access to the IoT sensors. Specifically, in some scenarios, the traffic section needs to be deactivated in order to complete the battery replacement or recharging work, which greatly increases the labour and financial costs.[57]

Energy harvesting, also known as energy scavenging, is the process of harvesting driven power from ambient environment and external sources, such as solar power, thermal power, wind power and salinity power.[58] As for energy harvesting, only very small amount power can be obtained from the ambient environment but constantly, which makes it become an effective and green power supplying method for low-energy electronics. Typical example is the solar-powered calculator that shown in Fig. 1.4.[59] It is equipped with a small solar panel and rechargeable button battery. Because of the weak power consumption of calculator, the button batter can provide most of its power demand during work, and in the rest of non-working time, the solar panel can continuously harvest solar energy and recharge the built-in battery, then greatly extending its lifetime. However, critical issues also exist of energy harvesting. Firstly, energy harvesting method can only provide very low power to the device, and usually the charging rate of power harvesting is much lower than the power consumption rate of electronics. This means that energy harvesting approach is only suitable for the electronics that are used less frequently. For such kind of electronics, it stays unworked state most of the time, thus the drawback of lower power recharging can be compensated by long charging time. Secondly, energy harvesting is harvesting energy from ambient environment passively, which makes it largely depend on the environmental conditions. For instance, for solar energy harvesting device, the possible conditions such as cloudy, rainy, foggy or night

time will all deteriorate charging efficiency greatly. Consequently, energy harvesting is a kind of power supplying method that largely depends on ambient environment condition and cannot provide power stably, and its environment dependent characteristic also largely limits the working environment of devices.

Fig. 1.4 Solar-powered calculator (Casio, HS-8VA)

The wireless power transmission technology might be a promising solution of IoT's power consumption issue. Wireless power transmission (WPT), which also known as wireless energy transmission (WET), is a kind of non-contact power transmission technology. The transmitter transfers the electrical energy into other forms of relay energy (such as electromagnetic field energy, optical energy, microwaves and mechanical waves, etc.), and after a certain distance of transmission, then the receiver converts the relay energy into electrical energy to realize the mode of wireless power transmission.[60] Comparing with other power supply methods, WPT technology can supply high and unlimited power stably and remotely, and moreover, its efficiency is not related with environment conditions. WPT technology is useful to power electrical devices where interconnecting wires are inconvenient, hazardous, or are not possible, and also suitable for the electronics that need to change places frequently.[61] Considering

the various working environment of IoT terminals that discussed in section 1.1.1, WPT technology is a perfect choice of power supply method to recharge the IoT battery easily and remotely. If power supply become wireless and include the communication that is already wireless, the required wires for the IoT devices is not simply reduced by one, but becomes 0. For this reason, it is expectable that a wireless IoT terminal in which power supply and communication are both wireless will lead to the revolutionary changing of the concept of IoT technology, or even reshape the social market economy and values, and bring huge economic benefits and social promotion.

WPT is a generic term for a number of different technologies for transmitting energy by means of electromagnetic field.[62][63][64] The WPT technologies which listed in the Table 1.3 is differ in the distance over which they can transfer power efficiently, whether the transmitter must be directed at the receiver, the frequency of the electromagnetic field, and in the type of electromagnetic energy they use.[65]

Table 1.3 The typical WPT technologies

Technology	Range	Directivity	Frequency
Inductive coupling	Short	Low	Hz - MHz
Resonant inductive coupling	Middle	Low	kHz - GHz
Capacitive coupling	Short	Low	kHz - MHz
Magnetodynamic coupling	Short	N. A	Hz
Microwaves	Long	High	GHz
Light waves	Long	High	THz

In electrical engineering,[66][67] when two conductors are configured such that change in current passing through one wire induced a voltage at both ends of the other wire through electromagnetic induction, the two conductors are called inductively coupled or magnetically coupled.[68] According to the Ampere's circuit law, a changing in the current trough the first wire creates a changing magnetic

field around it, and by the Faraday's law of induction, the changing magnetic field induces an electromotive force (EMF or voltage) in the second wire.[63][67] As shown in Fig. 1.5, the power supply end and the power receiving end are connected by high-frequency electromagnetic waves to form a circuit. The coupling between the two wires can be enhanced by winding the two wires into coils, and the magnetic field of the transmitting side can pass through the receiving coil if the two coils are placed tightly with alignment. The inductive coupling is the leading and relatively mature technology in WPT application area. It is the most common technology of WPT, which an efficiency of up to 95% or more can be achieved (as in case of transformers), and the applications that already been commercialized include electric tooth brush[66], mobile battery charging, industrial heaters and so on. However, its transmission distance is limited in extremely short distance, which is usually in the range of several mm to several tens cm. Besides, the misalignment of coils is a big issue, and unintentional inductive coupling can cause signals from one circuit to be induced into nearby circuits, which called cross-talk, and is a form of electromagnetic interference.[69] Moreover, the large size and weight of wire coils of both transmitter and receiver is also a limitation of application scenarios.

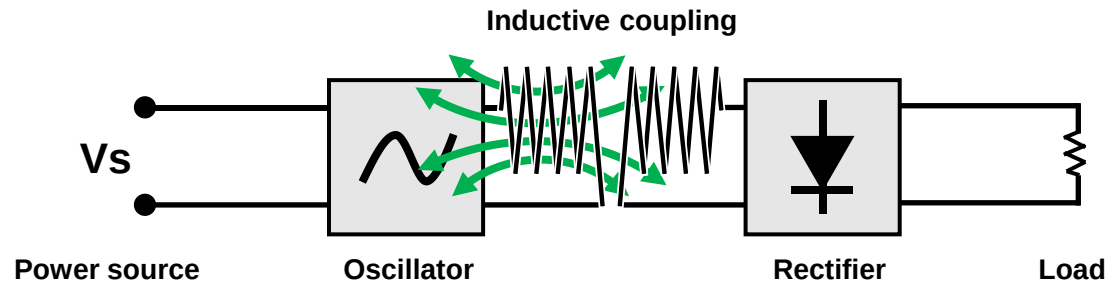

Fig. 1.5 Schematic illustration of inductive coupling

As for inductive coupling, the power transmission distance can be extended by configuring resonance circuits on one or both transmitting and receiving sides, which is the concept of resonant inductive coupling.[70] When the coupled coli of one or both sides resonate, the coupling will become stronger. [71][72] In inductive coupling, in order to receive the magnetic field as much as possible, the receiving

side coil is placed as close as possible to feeding side coil and accurately aligned, which causes very short transmission distance. Once the transmission distance extends, majority of the energy is wasted as resistive losses on the feeding side coil, and makes the inductive coupling power transmission becomes highly inefficient. Whereas, if the resonance circuits are applied at the feeding or receiving side and driving the transmitting side coil at the receiving side resonant frequency, the coupling becomes stronger and transmission distance extended as well, so that significant power can be transmitted between the coils over a range of several tens of cm to 1 m at reasonable efficiency. In addition, another merit of resonant inductive coupling is that it will not be affected by coils misalignment anymore.[73] The efficiency of up to 70% can be achieved by resonant inductive coupling.

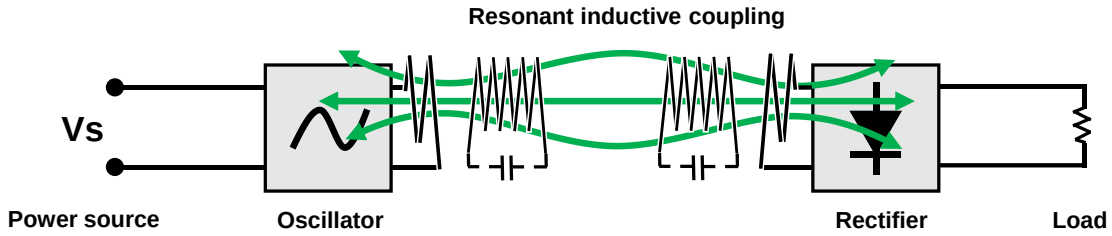

Fig. 1.6 Schematic illustration of resonant inductive coupling

Capacitive coupling is also known as electric field coupling or electrostatic coupling. A coupling capacitor connects two circuits in series, and the energy is transferred from transmitting side to receiving side by electric field.[74] Since the energy propagates as electric field, it can penetrate though metal materials that obstruct the transmission path. Moreover, compared with the inductive coupling, the requirements of accurate alignment between the transmitting and receiving side are less stringent. The main issue of capacitive coupling method in WPT power supply applications is that the capacitor offers a high resistance or impedance to the DC voltage, while only the desired AC voltage can pass through the coupling capacitor with a low resistance. Thus, rectifier circuit is necessary for the IoT devices with built-in battery. Besides, capacitive coupling has only been able to used practically in lower power applications, because the very high

voltages on electrodes required to transmit significant power can be hazardous, and can cause unpleasant side effects such as noxious ozone production.[66][68]

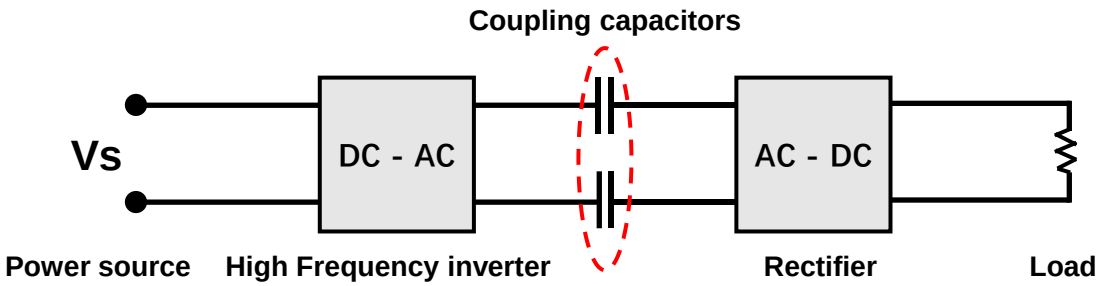

Fig. 1.7 Schematic illustration of capacitive coupling

The Magnetodynamic coupling is a kind of low-frequency wireless electrical power transmission technology that operates around hundreds Hz. In order to harvest enough power at low operating frequency, method of rotating rare-earth permanent magnets by motor is used to generate a strong enough time-varying magnetic field.[75] There are two approaches of receiving and transferring the power at secondary side. First method is configuration of another magnet with a generator. When the magnet at feeding side is rotated by the motor, the magnetic field causes the receiving side magnet to turn, then drives a generator to create electrical power. The energy goes from electrical to mechanical and back to mechanical, and then to electrical. The second approach is configuring an inductive coil as the receiver. The electrical power is induced in the receiving coil by the time-varying magnetic field, which is like an electrical generator.[76] The magnetodynamic coupling has the merit of low frequency operation, thus the RF radiation hazard is almost avoided, and a slow-varying magnetic field from rotating permanent magnets is able to penetrate various non-magnetic materials, including conductive bio-tissues and implant-grade stainless steel housing without significant loss. Magnetodynamic coupling can achieve over 90% efficiency over distance of 10 cm to 15 cm.[77] However, the two energy conversions make its efficiency less than electrical system like inductive coupling. The WPT technologies that discussed above are belongs to short-range or mid-range WPT technologies. In the very short region of the transmitter, the oscillating

electric and magnetic fields are separate and power can be transmitted via electric fields by capacitive coupling between metal electrodes, or via magnetic fields by inductive coupling between coils of wire. These fields are not radiative, meaning the energy stays within a short distance of the transmitter.[78] If there is not receiving device within their limited range to “couple” to, no power leaves the transmitter.[79] The range of these fields is short, and depends on the size and shape of the “antenna” devices, which are usually coils of wire. Thus, the size of transmitter or receiver antenna increases rapidly if transmission distance is expected to be extended. On the other hand, fields that power transmitted decrease exponentially with distance, so if the distance between the two antennas is much larger than the diameter of the antennas, very little power will be received.[80] Resonant inductive coupling can increase the coupling between the antennas greatly, allowing efficient transmission at somewhat greater distance, while its fields are still non-radiative and decrease exponentially with transmission distance increasing. There is also another method of WPT based on piezoelectric,[81] in which Piezoelectric crystal[82] like Quartz, Rochelle salt, Berlinite (A1P04), Topaz, Tourmaline, Cane sugar, Bone, Tendon, Silk, Enamel, Dentin, Barium Titanate (BaTi03) can convert mechanical energy into electrical energy and vice-versa. Piezoelectric provides an option for energy transmission where power cannot be delivered by electromagnetic means, but it can still transmit power through a very short distance. Therefore, these WPT technologies cannot be applied for long range power transmission.

In order to transmit power beyond the short transmission range of the transmitter, the electric and magnetic fields need to be perpendicular to each other and propagate as an electromagnetic wave, such as radio waves, microwaves or light waves. This part of the energy is radiative, meaning it leaves the antenna whether or not there is a receiver to absorb it.[71] As a method using high frequency, there is a long-distance power feeding method using the microwave beam shown in Fig. 1.9. Since the radiation beam of microwaves is used, it is possible to supply power to a remote location. Microwaves are generated from electric power on the power feeding side, and microwaves are converted to DC electric power by a receiver that combines rectenna and a rectifying device on the receiving side.

Since the beam spreads due to the diffraction of electromagnetic waves in space, it is difficult to receive the entire beam. The application of a phased array method that uses a large number of antennas to control the input high-frequency phase is being studied for generating a large microwave beam for a wavelength with little diffraction and controlling beam direction.[83] By controlling and synchronizing the phases and amplitudes of the microwaves sent from each antenna element of the array, a desired beam shape can be produced and a precisely focused beam can be directed in any direction. In addition to the studies of several W class, there are also research cases such as 10 kW, and it has been proved that relatively high-power transmission is possible. With this method, the feeding efficiency can be as high as 50% or more by making the receiving antenna size sufficiently large. However, since the realistic receiving antenna size is limited, the feeding efficiency of transmission distance about 10-100 m is expected to be 5-10% due to the spread beam size with increasing distance. Merits of Microwaves WPT technology is its property of high atmosphere penetrating, while the issues are the large size of phased antenna array, the cost of beam control system, and the difficulty in increasing the practical efficiency.

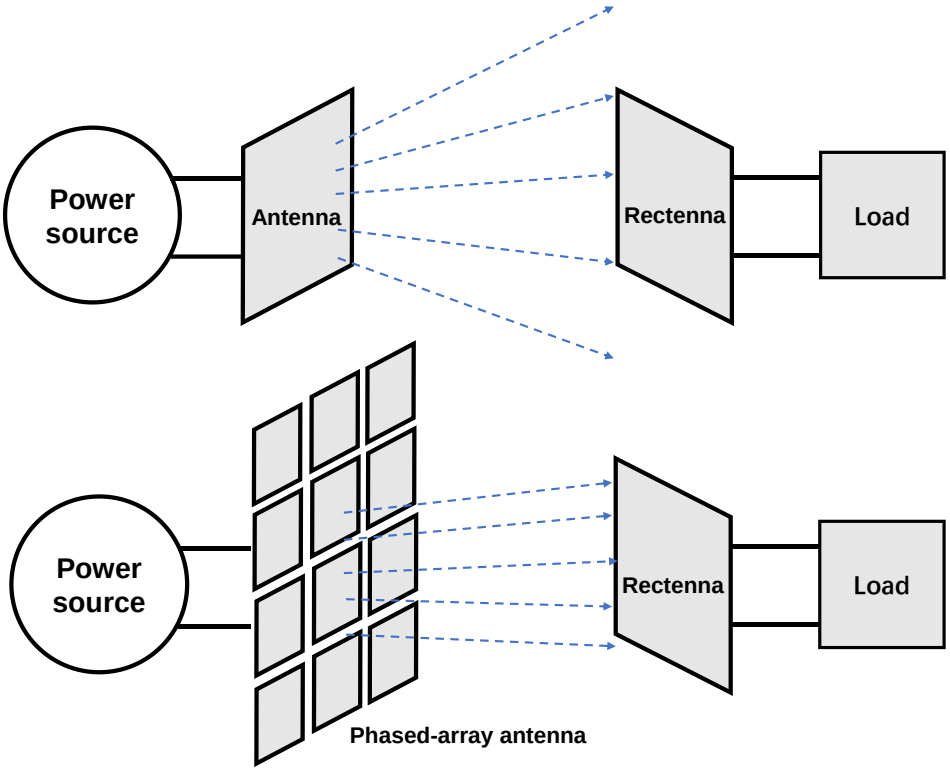

Fig. 1.8 Schematic illustration of microwave power transmission

Basically, the amount of power emitted as electromagnetic waves by an antenna depends on the ratio of the antenna's size D_{ant} to the wavelength of the waves λ. At low frequencies *f* where the antenna is much smaller than the size of the waves ($D_{ant} << \lambda$), very little power is radiated. Thus, the near-field devices above, which use lower frequencies, radiate almost none of their energy as electromagnetic radiation. Therefore, large antennas size combines with high frequency waves can increase the part of power that radiate as electromagnetic waves. However, even antennas about the same size as the wavelength ($D_{ant} \approx \lambda$) such as monopole or dipole antennas which can radiate power efficiently, the electromagnetic waves are radiated in all directions (omnidirectionally), so if the receiving antenna is far away, only a small amount of the radiation will be received.[84] Consequently, these can be used for short range, inefficient power transmission but not for long range transmission.[85] Microwaves WPT technology can be used for long distance transmission because of ultra-high frequency, but antenna arrays composed of numerous

antenna elements are necessary to produce a high directionality beam. Since the pitch of antenna array is wavelength scale, a large size of transmitter is unavoidable.

Besides, the method of using high frequency and high-power waves to achieve electromagnetic radiation still has a critical issue, which is the electromagnetic noise interference to the target and surrounding devices.[86] And also, the effect of electromagnetic waves on human body is an issue too. Moreover, since the frequency bands in radio wave region is a limited source, the allocation and regulation on available radio frequency (RF) bands specially for WPT purposes is expectable.

Conclusively, among the WPT technologies that discussed above, each of them has more or less unavoidable issues if use as power supply method for IoT devices, such as power supply distance limitation, size and weight increase, peripheral leakage of high frequency noise and corresponding RF bands regulation, etc, and although commercialized application and development of these technologies are progressing in various ways, the range of feasible and compatible devices is still largely limited.

Fortunately, there is another kind of energy that is radiative and propagates as electromagnetic wave, which is light waves. Same as microwaves that its electromagnetic radiation can be concentrated into a narrow beam with high directionality by a high gain antenna, the radiation of light waves can be focused by using optical system and aimed at the receiver, which can be used for long range power transmission. The wireless power transmission based on optical energy is referred as optical wireless power transmission (OWPT).[87] OWPT system has high compact level and light weight because of using semiconductor light source and solar cell, and unlike microwaves, the size of antenna (optical system) is not exactly related with its directionality and transmission distance.[88] Thus, long-range transmission can be easily achieved by small dimension device. Besides, a simple circuit of OWPT system can handle the work of remote power supplying due to components of OWPT are all DC operating. Since no high frequency is generated in OWPT, the feature of no electromagnetic noise interference is expected. In another word, the features of OWPT are promising

because it perfectly solves the issues of existing WPT technologies, such as short transmission range, poor directionality, large size and weight of devices, noise interference and so on. Therefore, OWPT is promising as a potential candidate method of supplying power remotely to IoT devices. The Fig. 1.9 shows the characteristics of system efficiency of the typical WPT technologies based on transmission distance.[89]

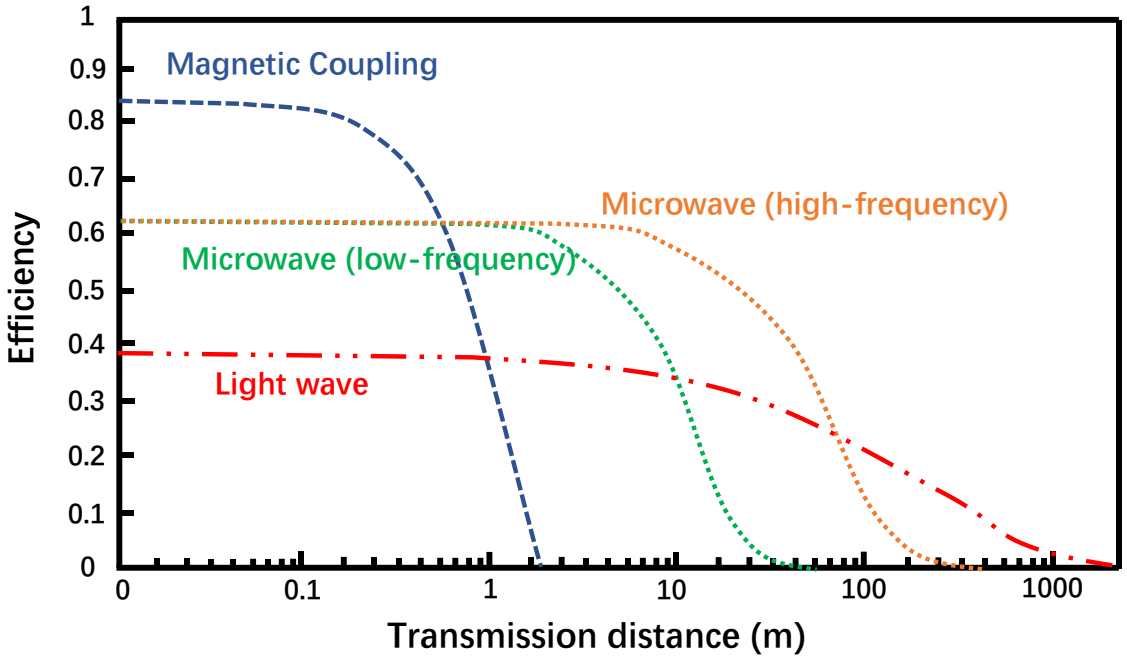

Fig. 1.9 Theoretical calculation of system efficiency of WPT technologies

1.2 Optical wireless power transmission

In this section, the concept of OWPT system will be introduced firstly. Then, the history of OWPT technology and its current research conditions is discussed respectively. Next, the merits and features of OWPT is described, and the potential applications scenarios of OWPT is investigated. In final part of this section, the open issues of current OWPT technology are represented.

1.2.1 Concept of optical wireless power transmission

Optical wireless power transmission is a simple and basic principle in which the energy is propagating as the electromagnetic radiation that close to the visible

region of the spectrum, and light beam can be received and conversed into electrical power on photovoltaic cells at remote position. A practical OWPT system[90] is shown in the Fig. 1.10, in addition to the basic light source and receiver, various sub-system or technologies might be required, such as specifically designed optical system to control the beam shape and target the receiver correctly, beam scanning system which can provide power to mobile targets constantly, target detection technology is able to detect the motion state of objects in a specific area and realize the functions such as the selection of the optimal transmission line or pause the power transmission urgently to prevent the possible hazard from being exposed under high intensity light beam, and communication technology that allows real-time information exchanging between feeding side and receiving side, etc, and advanced systemization that links these functions and systems is indispensable.

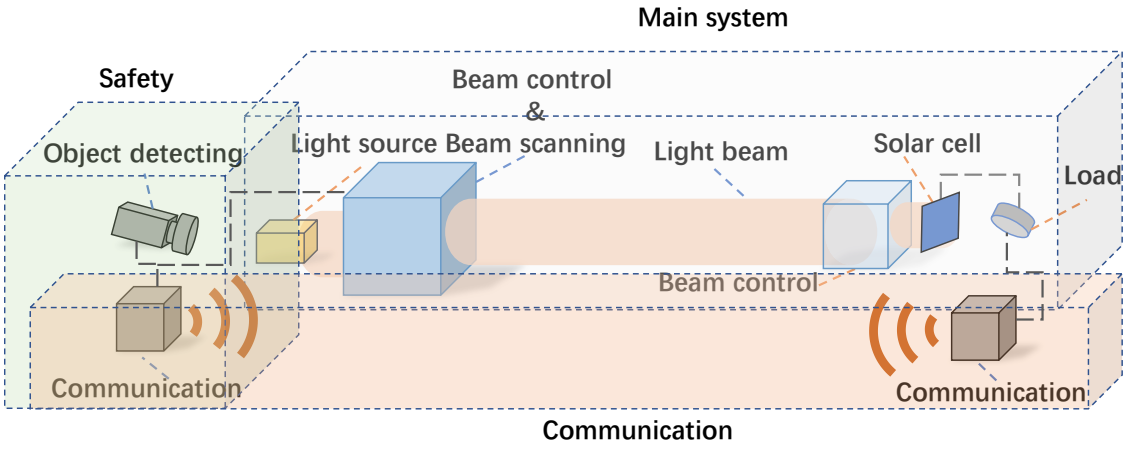

Fig. 1.10 Schematic diagram of the functional composition of the OWPT system

1.2.2 History of optical wireless power transmission

The OWPT system consists of two main components, which are the light source and the receiver, and the history of the research on optical wireless power transmission technology is highly related with the research of both light source and receiver. Therefore, it is difficult to determine the specific beginning of the research history of OWPT technology itself. From the perspective of the light source, Theodore Maiman of the Hughes Research Laboratories confirmed the

first operation of the laser through experiments on May 16, 1960.[91] The laser has high efficiency and high power, and can be used as the typical light source of the OWPT system. Therefore, it can be said that the research on the light source of the OWPT system has begun since the laser was first operated in 1960. In the research and development of solar cells as receivers of the OWPT system, the report of the Bell Laboratories in 1954 on the first modern solar cells can be regarded as the starting point for subsequent research and development of the solar cell.[92] Since the OWPT system can be implemented by using high-efficiency light sources and solar cells, so it can be said that the 1970s is regarded as the beginning of the research of optical wireless power transmission technology. From such time, optical wireless power transmission technology became not only a concept but also a possibility

However, since it was reported, the research and development of laser light sources and solar cells has been in a hot field, but the development and progress of OWPT technology has been relatively slow. In recent years, because the communication channel has been completely wireless, the demand for wireless power transmission has also increased. At the same time, as the efficiency of light sources and light energy receivers increases and costs decrease, high-efficiency optical wireless power transmission becomes possible. In addition, because advanced sensing technology and control technology are available at current stage, the safety hazards of high-power light sources have also been resolved. Therefore, research on optical wireless power transmission technology and related field has gradually been paid attention in recently years.

1.2.3 Current condition of optical wireless power transmission

In recently years, the research on optical wireless power transmission technology has been valued. The Fig. 1.11 shows the search results of the publications on Google Scholar based on the key works related with optical wireless power transmission technologies. It can be seen that the research interest in the field of OWPT is generally rising rapidly in recent years. In this section, some significant research reports and literatures is listed.

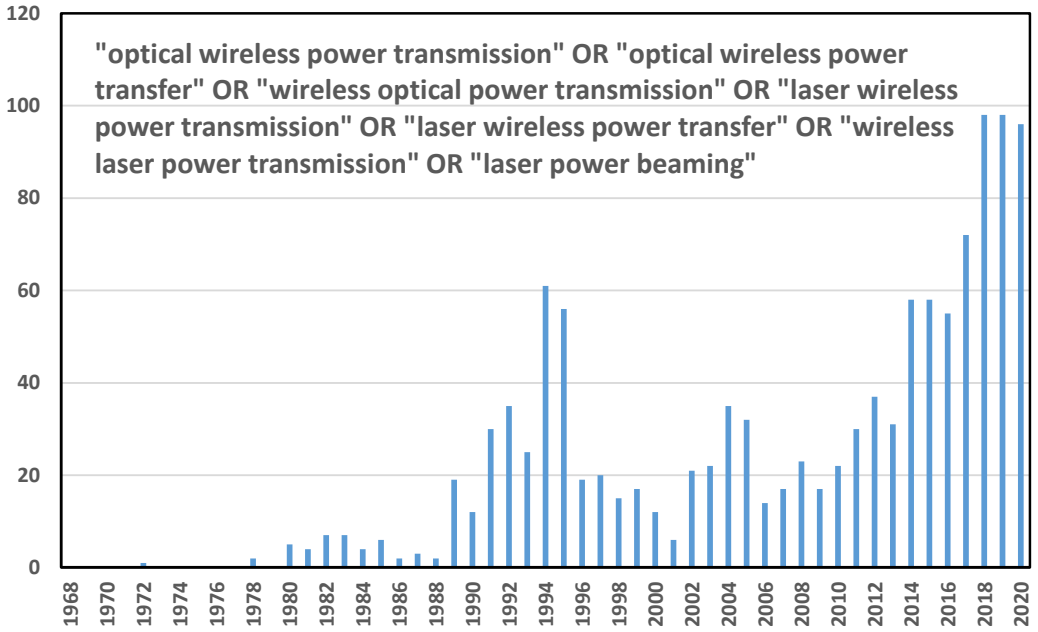

Fig. 1.11 The trends in the number of publications about OWPT technology

In 2003, Steinsiek and Schafer used a frequency doubled solid state laser at 532nm to supply the power to a moving rover under the transmission distance from 30 m to 200 m.[93] The experiment proved that a complete wireless power transmission link between a transmitter and a distant receiver system is feasible.

In 2015, Miyamoto et al. reported an OWPT experiment with 975 nm near-infrared (NIR) vertical cavity surface emitting laser (VCSEL) array and silicon solar cells.[94] As high as 33% power generation efficiency of Si-solar cell was confirmed.

Also, in 2015, laser-based wireless power transmission experiment on 50 m to 100 m apart airships was carried out by Shi Dele.[95] 13.43W peak received power was measured under 88W input power, which corresponded to the transfer efficiency of 15.26%.

In 2016, John Fakidis et al. reported the experiments of indoor laser-based WPT system with small cells at nighttime, which systematically analyzed the performance of OWPT system in the absence of ambient light.[96]

In 2018, Katsuta and Miyamoto reported 15% efficiency of an OWPT system using GaAs solar cell and VCSELs.[97]

In 2018, Takashi Tokuda et al. reported the ultra-small implantable optogenetic stimulator which is power by optical energy wirelessly. A CMOS control circuit for an integrated photovoltaic (PV) power transfer/harvesting platform is proposed.[98] The device has around 1 mm^3 dimension and 2.3 mg weight, and can be driven by 860 nm wavelength light.

In 2019, Wei Wang et al. of Chinese Academy of Sciences reported a novel OWPT technology, which is transmitting power with high safety through the RBC (resonant beam charging) energy transmission channel for the IoT devices.[99] The repot verified that the RBC transmitter can provide up to 2 W electrical power and the maximum transmission distance is 2.6 m.

From the literature review of the OWPT technology, although there have been some studies and repots existed, the scope of the study are still narrow, and sufficient knowledge and information have not been accumulated yet. At this point, the systematic and deep research on OWPT technology is critical not only for the general public but also for researcher and developers in application areas who may use this technology, as well as specialists in various functional elements and devices that will make up this technology. On the other hand, it is considered that various devices, functional elements, and peripheral technologies used to configure the OWPT system have made great progress in recent years. By accumulating sufficient knowledge and information about these latest technologies, the research of the OWPT technology can be progressed steadily, and the characteristics and applicability of OWPT systems that can be realized in near future can be anticipated.

1.2.4 Advantages of optical wireless power transmission

Compared with other wireless power transmission approaches, optical wireless power transmission has various unique advantages especially in the applications of miniaturized devices, mobile targets, diverse scenarios and long-range power feeding needs. Specifically, about the advantages of optical wireless power transmission:

- Long transmission range: Optical wireless power transmission technology has the longest transmission range among all existed wireless

power transmission methods. Collimated monochromatic wavefront propagation allows narrow beam cross-section area for transmission over large distance. As a result, very little or no reduction in power when increasing the distance from feeding side to receiving side.

- Compact size: In the case of similar power transmission range, optical wireless power transmission system has the correspond smallest size of both transmitter and receiver among all wireless power transmission systems. On transmitter side, semiconductor light source such as semiconductor laser or light emitting diode (LED) fits into small products, portable transmitter can thus be possible. As for receiver, high directional beam of OWPT and its highly concentrated spot at the target distance makes the miniaturization of the receiver to be possible. Besides, due to the flexibility and light weight of the optical energy receiver such as photovoltaic cell, it adapts to various application scenarios of miniaturized devices or terminals.
- No radio-frequency regulation: Unlike other wireless power transmission technologies whose frequencies range are more or less overlapping with existing radio communication frequency bands, the frequency range of OWPT is above THz due to its electromagnetic radiation is based on light waves. Such frequency range is much higher than existing radio communication frequency bands, so OWPT can completely avoid electromagnetic noise interference with peripheral electronics.
- Access control: due to the light beam has high directionality, the transmitted power is propagated radiatively, and only the target receivers will be focused and accessed power transmission. Thus, the access of power transmission can be highly controlled.

According to the above discussion, it can be found that the advantages of OWPT just make up for the shortcomings of other existing wireless power transmission technologies. Therefore, OWPT is expected to complement the empty board part of the existing wireless power transmission technology in application scenarios.

1.2.5 Target application scenarios of optical wireless power transmission

According to the advantages of OWPT discussed above, the potential application

scenarios of OWPT are very diverse, covering almost all power fields.

- Aerospace: Optical wireless power transmission technology can provide power in the long transmission range as long as a direct line of sight with the target is available. Thus, aerospace is a very idea application region of OWPT. There is almost no obstruction in the space environment, and the light beam as an energy medium can transmit power to almost any location. In addition, unlike the earth environment that atmosphere existed, the energy of the light beam is hardly dissipated due to reflection or absorption in vacuum environment, so OWPT can maintain extremely high transmission efficiency even during very long-distance transmission. Laser propulsion is a potential OWPT application in aerospace area.[100] Laser propulsion is a new concept propulsion technology that uses high-energy lasers to heat the working substance, so that gas of the working substance thermally expands or generates electric current to indirectly generate thrust, and push the aircraft forward.[101] The driven aircraft are rockets, unmanned aircraft, etc. It has the advantages of high specific impulse, large effective load ratio, and low launch cost. Space-based solar power (SBSP) is another example of OWPT application in aerospace area.[102] The solar power that collected in outer space can distribute to earth or outer space station and satellites by light beam.

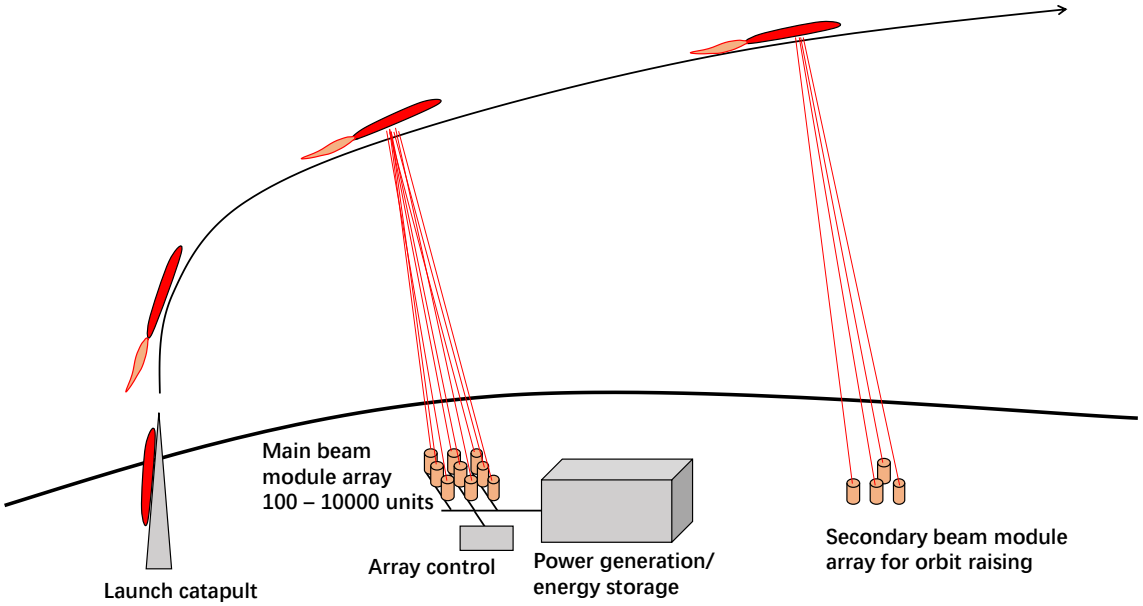

Fig. 1.12 Laser launch architecture with modular ground-based laser array

- Mobile objects: Optical wireless power transmission technology can accurately locate targets from long range distance, it can thus be applied as power supply method of mobile objects such as vehicles and drones.[103] In order to feed power to mobile objects, sub-systems of targets detection function and beam tracking function need to be embedded into OWPT system. By using OWPT for power supply, the built-in battery of mobile objects can be downsized or discarded, thereby reducing the weight and cost without sacrificing the work duration.

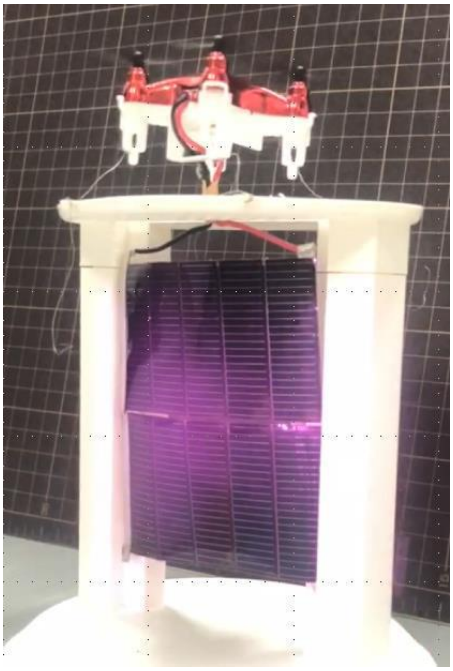

Fig. 1.13 Laser-powered drone

- Consumer electronics: Optical wireless power transmission technology can provide flexible power supply for consumer electronics, freeing them from the shackles of wires and cables. Because there is no wire restriction, electronics can be moved freely and placed anywhere in the private home or workplace as long as line of sight is available, which greatly provide convenience to the users. Besides, the beam spot can be invisible by applying infrared wavelength light sources, thereby not causing additional visual disturbance to the users in daily use.

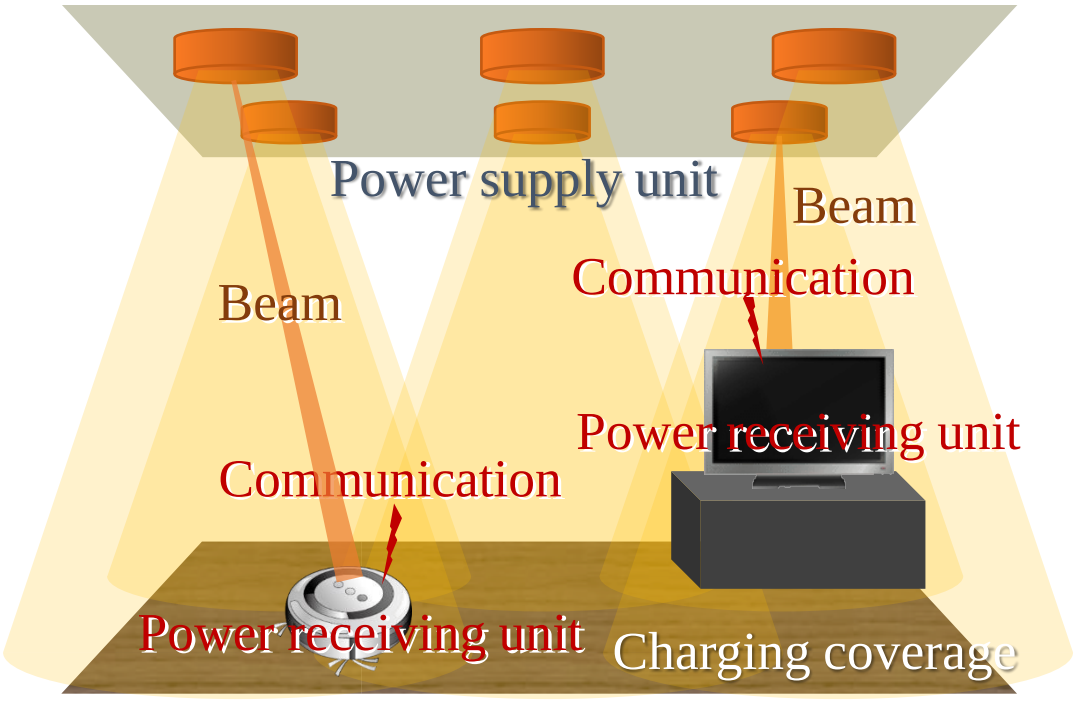

Fig. 1.14 Schematic diagram of consumer electronics charged by OWPT system indoor

- IoT devices: Due to the merit of compact size, optical wireless power transmission device can be miniaturized and portable, which makes it to be a perfect candidate power supplying method for IoT devices. Most IoT devices have the characteristics of miniaturization, and their application scenarios and working environments have high diversity. Some IoT devices are allow to be easily supplied power through wires with high efficiency. However, there are also a large number of IoT devices whose use environment cannot allow the laying of wires and can only be powered by built-in batteries, such as wearable IoT devices and outdoor sensor. There are also some IoT devices although can be powered by wires, they will change places frequently. Thus, the use of wires for power supply greatly reduces the convenience and limits the degree of freedom. These IoT devices include small speakers, WI-FI cameras, tablets, handheld game console and so on. By using OWPT to provide stable and flexible power supplying at anywhere, IoT devices can be completely wireless. Because the

OWPT can easily and remotely charge IoT devices, the power consumption issue of IoT devices can be solved, thus high-power functions and performances can be supported and realized, and also working duration can be greatly extended. In addition, because of easy recharging for the built-in battery of IoT, a large battery with high capacity is no longer a necessity. A small battery or even no battery can be sufficient to support the daily work of the IoT, so the development of IoT devices can move in the direction of miniaturization and light weight. It can be said that the application of OWPT in the field of IoT devices can completely change the design concept of IoT devices and accelerate the realization of its miniaturization and high performance.

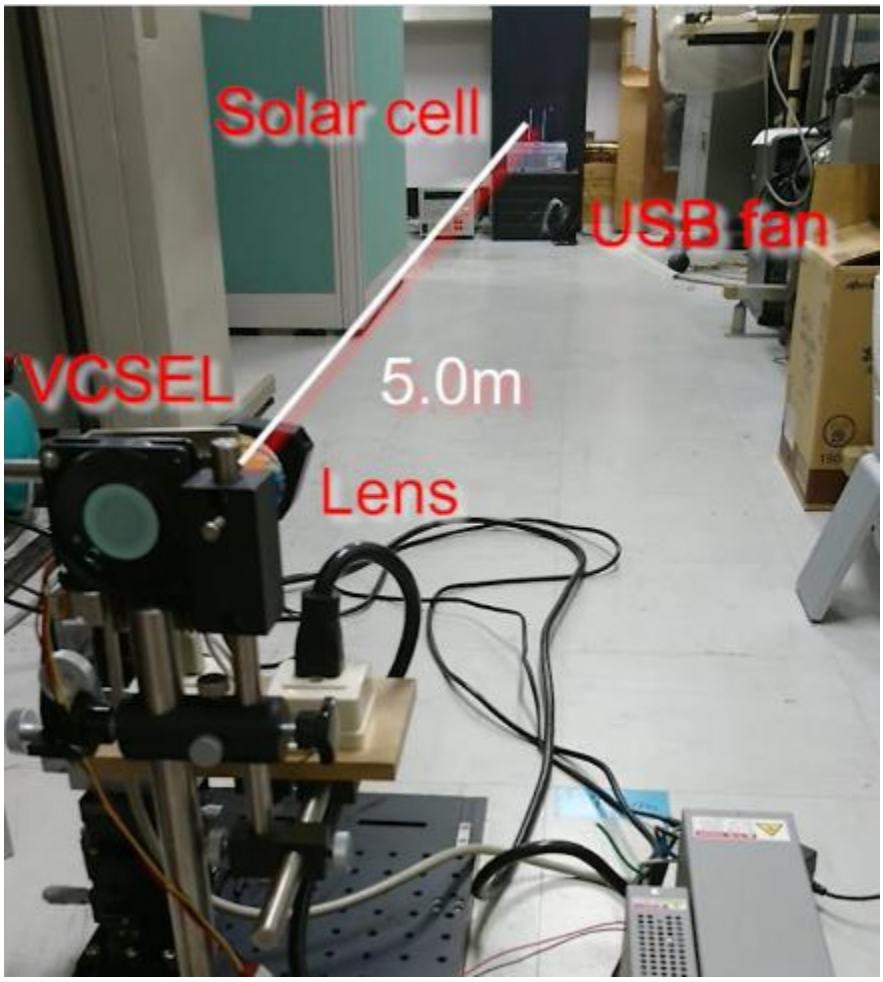

Fig. 1.15 Experiment of long-distance powering USB fan by VCSEL

1.2.6 Current issues of optical wireless power transmission

Although the potential characterizations of OWPT technology brings a number of possibilities, there are some issues to be solved before the capacities of OWPT can be fully unleashed. In this section, the current challenges of OWPT technology are discussed. Also, the promising solutions of each issues will be represented as well.

- Atmospheric scattering and absorption: As for OWPT, light beam as the energy medium will be affected by the particles and gases in the atmosphere, and such effects are caused by the mechanisms of atmospheric scattering and absorption. Although such absorption and scattering effects are not obvious in most applications of OWPT, such loss will be much more apparent in specific scenarios like space-earth power transmission or power transmission in water mist environment. Scattering occurs when the particles or large gas molecules present in the atmosphere interact with and cause the light rays to be redirected from the original path. How much scattering occurs depends on various factors such as wavelength, the abundance of the particles, and the distance travelled through the atmosphere. According to the relation between wavelength of the light beam and size of the particles, there are three types of scattering happens. When the particles are very small compared to the wavelength of light rays, such as small specks of dust or nitrogen and oxygen molecules, Rayleigh scattering occurs. It will cause shorter wavelengths such as blue light to be scattered much more than longer wavelengths.[104] Mie scattering occurs when the particles are just about the same size as the wavelength of the light rays.[105] Smoke, pollen, dust and water vapour are common causes of Mie scattering, and Mie scattering tends to affect the light rays with longer wavelengths than shorter ones. The nonselective scattering usually occurs when the particles are much larger than the wavelength of the light rays, such as water droplets and large dust particles.[106] In the condition of nonselective scattering, all wavelengths are uniformly scattered. Absorption is another main factor at work when light rays propagate and interact with the atmosphere. In contrast to scattering, this phenomenon causes molecules in the atmosphere to absorb energy at

various wavelengths. Ozone, carbon dioxide, and water vapour are the three main atmosphere constituents which absorb radiation. As for scattering issue, the wavelength of the OWPT light source should be selected according to the application scenario. For instance, the marine climate area is affected by the monsoon and foggy days throughout the year. Therefore, the use of short-wavelength light sources for optical wireless power transmission should be avoided in order to reduce the negative impact from Rayleigh scattering. The absorption of atmosphere can be restrained by choosing light wavelength based on atmospheric windows. The areas of the spectrum which are not severely influenced by atmospheric absorption are referred as atmospheric windows.[107] By doing so, the effects of atmospheric absorption can be restricted to a minimum level. Fortunately, the visible or near-infrared wavelengths that commonly used as OWPT light sources are in the range of atmospheric windows.

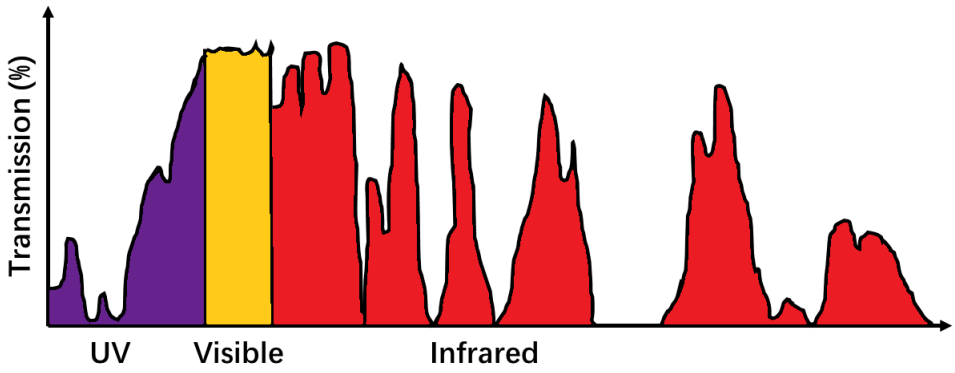

Fig. 1.16 Atmospheric windows

- Requirement of a direct line of sight: The electromagnetic radiation of OWPT is relatively short wavelengths, which makes its ability of penetrating obstacles to be low. Thus, the transmission of optical wireless power requires a direct line of sight, any objects include creatures on the

optical path will block the power transmission. This feature imposes certain restrictions on the application scenario of OWPT. For example, as for ultra-long distance optical wireless power transmission, it is very difficult to ensure that no obstructed objects are always kept within such a long-distance range under normal circumstances. Therefore, ultra-long distance OWPT will be usually applied in sparsely populated areas, rather than in urban regions. Another situation is to change the transmission to vertical direction. Generally, there are far fewer obstacles in the vertical direction than in the horizontal direction, such as the earth-space optical wireless power transmission can effectively avoid the issue of line of sight lack. In daily application scenarios, the vertical direction transmission is also useful. Such as installing the OWPT module on the ceiling of the house can effectively cover most room locations. In addition, by systematically integrating multiple power transmitters that installed in different locations of a certain space and embedding object detection function and tracking function in the control system, the OWPT system can detect the location of the transmission targets and then select and unobstructed transmission path to realize effective optical power transmission, which is also a solution of transmission path obstruction. Moreover, under certain circumstances, optical fibre can also be used as a guide of the optical energy of laser light in order to bypass obstacles, which is referred as power-over-fibre (PoF).

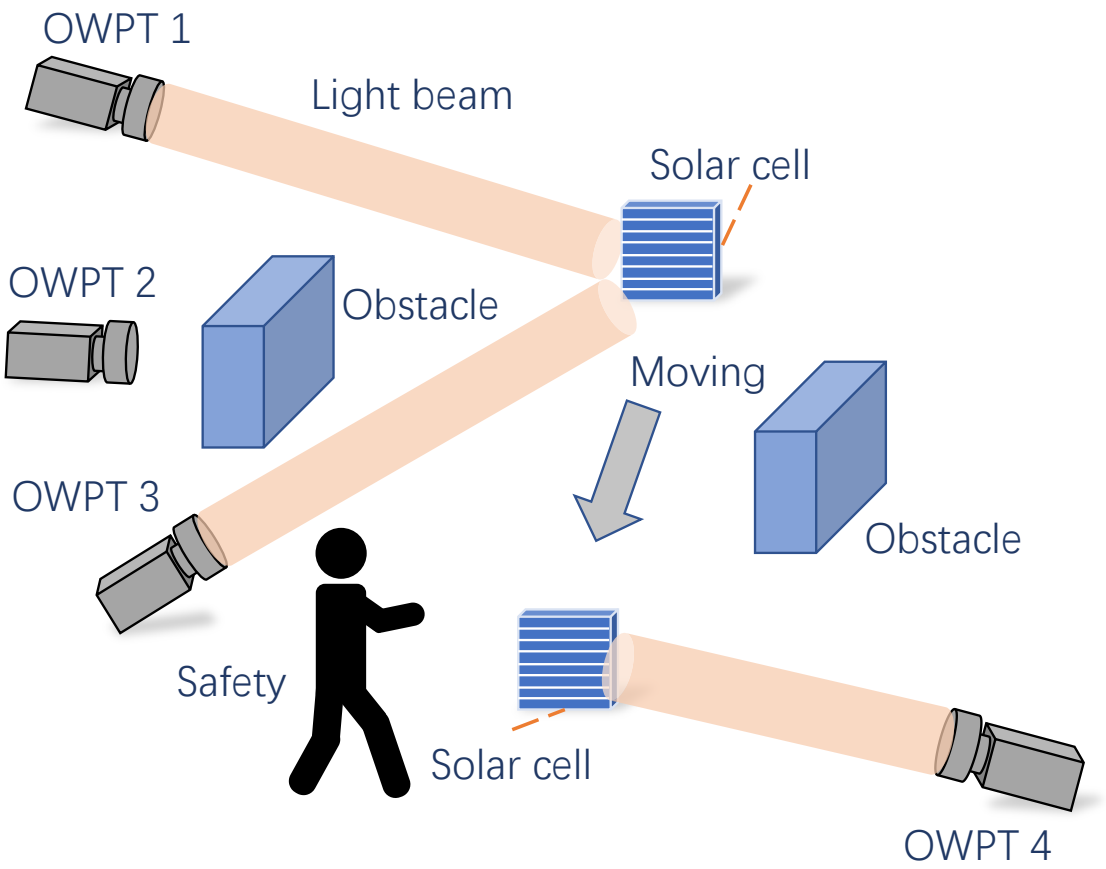

Fig. 1.17 Schematic diagram of tracking function of OWPT system for ensuring line of sight

- Relatively low efficiency: The conversion between electricity and light is limited by current technologies of semiconductor devices. The efficiency of the OWPT power transmission can be calculated by the equation (1.4):

$$\eta_{OWPT} = \eta_s \times \eta_l \times \eta_d \times \eta_p \quad (1.4)$$

The η_{OWPT} is the total efficiency of OWPT system, and η_s refers the electricity-intensity efficiency of semiconductor light source, then η_l and η_d are the efficiency of optical system and dissipation during transmission path, separately. Last, η_p represents the photovoltaic (PV) conversion efficiency of the photovoltaic cells. As for photovoltaic cells, the maximum of only 40% - 50% photovoltaic conversion efficiency can be achieved even under monochromatic light condition. Although the PV conversion efficiency of

photovoltaic cells can be increased by condensing the light beams to enhance the radiant intensity, heat will be generated by such condensing. The higher temperature of the photovoltaic cells, the more likely that nonradiative recombination (NRR) will occur and efficiency will decrease.[108] Furthermore, this nonradiative recombination also causes heat generation, and a negative chain that further reduces efficiency occurs. On the other hand, the efficiency of light source is also limited. Based on the region of the spectrum, the efficiency of the commercialized semiconductor laser currently is over 70% in infrared wavelength region and over 40% in the region of long-wavelength region, and over 40% efficiency of infrared LED and over 80% efficiency of long-wavelength LED can be achieved. This is to say, even the optical system can achieve 100% efficiency and then ignore the dissipation of the light beam during transmitting, the maximum efficiency of total OWPT system is still lower than 40%. Conclusively, there is not effective method to improve the overall efficiency of OWPT at current stage.

- Safety: Due to the high-intensity light beams that used in OWPT system, ensuring safety of surrounding objects and organisms during power transmission is a very serious point. The high-intensity beams are very harmful to the eyes of living beings, and especially the condition using laser as light source, moderate and high-power laser can burn the retina or even the skin. Infrared light beams are particularly hazardous, since body's protective glare aversion response is only triggered by visible light, while the infrared light is invisible to human. Thus, once body's eyes are under exposure of high-intensity infrared light, people won't aware of the dander but be damaged immediately. Although, the wavelength longer than about 1400 nm is absorbed by the transparent parts of the eye before it reaches the retina and relatively safe, it will cause burn damage if the intensity is high enough.[109] Thus, laser products are severely regulated by various specifications all over the world, such as IEC 60825 internationally.[110] These regulations impose upon manufacturers required safety measures, such as labelling lasers with specific warning, or mandatorily requiring technician to wear laser safety goggles when operating. In addition, safety functions such

as body detection modules and emergency braking modules are usually indispensable and used in high-power laser OWPT systems in order to ensure safety. Although the LED-based OWPT system does not have such strict regulation, the necessary safety precautions are still essential during operation to prevent possible hazard.

1.3 Feasibility of LED-based optical wireless power transmission

Currently, almost researches of OWPT are laser-based, because it has advantages such as high power, high directionality, low divergence, and narrow spectrum, and so on. The laser-based OWPT has already been proved to be a realistic remote power supply method. However, the disadvantages of lasers are also critical, such as the safety issue that stated in section 1.2.6. Therefore, research on the feasibility of light sources other than lasers is necessary. By considering the benefits such as low cost, low temperature sensitivity, recent improved efficiency and output power, small size, and sufficiently narrow spectrum for using in OWPT, a recent high-performance light-emitting diode (LED) is believed as an important candidate in the OWPT system. In this section, a brief comparison on the characterization of laser and LED in OWPT application is represented firstly to prove the feasibility of using LED as light source in OWPT system, then a brief summary of the discussion is shown. A more systematic and detailed investigation and analysis on the principles of different light sources and their characterization in the OWPT system will be discussed in section 2.2 of this thesis later.

1.3.1 Brief comparison of LED and laser performance based on OWPT system

Semiconductor laser, also known as laser diode (LD), is the most practical and important type of laser. It is small in size, long in life, and can be pumped by simple current injection. Its working voltage and current are compatible with integrated circuits, so it can be monolithically integrated with it. In terms of adaptability, semiconductor laser is a very suitable light source choice for OWPT. The main reasons of such adaptability are divided into four aspects:

monochromaticity, high intensity, high directionality and small size. Therefore, LEDs will be compared with semiconductor lasers in the above four aspects in this section to confirm the feasibility of LEDs as light source in OWPT applications.

- Monochromaticity: In most lasers, lasing begins with spontaneous emission into the lasing mode. This initial light is then amplified by stimulated emission in the gain medium. Stimulated emission produces light that matches the input signal in wavelength and polarizations, whereas the phase of emitted light is 90 degrees in lead of the stimulating light. This, combined with the filtering effect of the optical resonator gives laser light its characteristic coherence, and may give it uniform polarization and monochromaticity. The full width at half maxima (FWHM) value of array laser is usually less than 1 nm, such as 0.8 nm FWHM value of high power VCSEL array, and single laser even has narrower spectrum width, which makes laser highly monochromatic light source. Monochromatic light can greatly improve the photovoltaic conversion efficiency of solar cells, so becomes the key of OWPT system that able to achieve far higher transmission efficiency than sunlight. Unlike lasers, the light emitted from an LED is caused by the recombing of electrons in the semiconductor with electron holes and not spectrally coherent, thus its monochromaticity is worse than lasers. As for white LED, there are two primary ways of producing white colour. One is to use individual LEDs that emit three primary colours of red, green and blue, and then mix them to form white light. The other is to use a phosphor material to convert monochromatic light from a blue or UV LED to broad-spectrum white light. The spectrum of first type white LED shows the combined of three wavelengths, and the second type white LED has a peak wavelength of blue or UV light and another broadband wavelength that emitted by the phosphor, thus none of white LED has monochromaticity. On the other hand, the typical FWHM value of a monochromatic LED such as infrared LED is usually in the range of 20 nm – 30 nm. Although this value is dozens of times than laser, compared with the 500 nm FWHM value of sunlight spectrum, the spectrum of monochromatic LED is sufficiently narrow enough for improving the photovoltaic conversion efficiency of solar cells, thereby the monochromatic

LEDs can be regarded as functionally monochromatic light source in OWPT system.

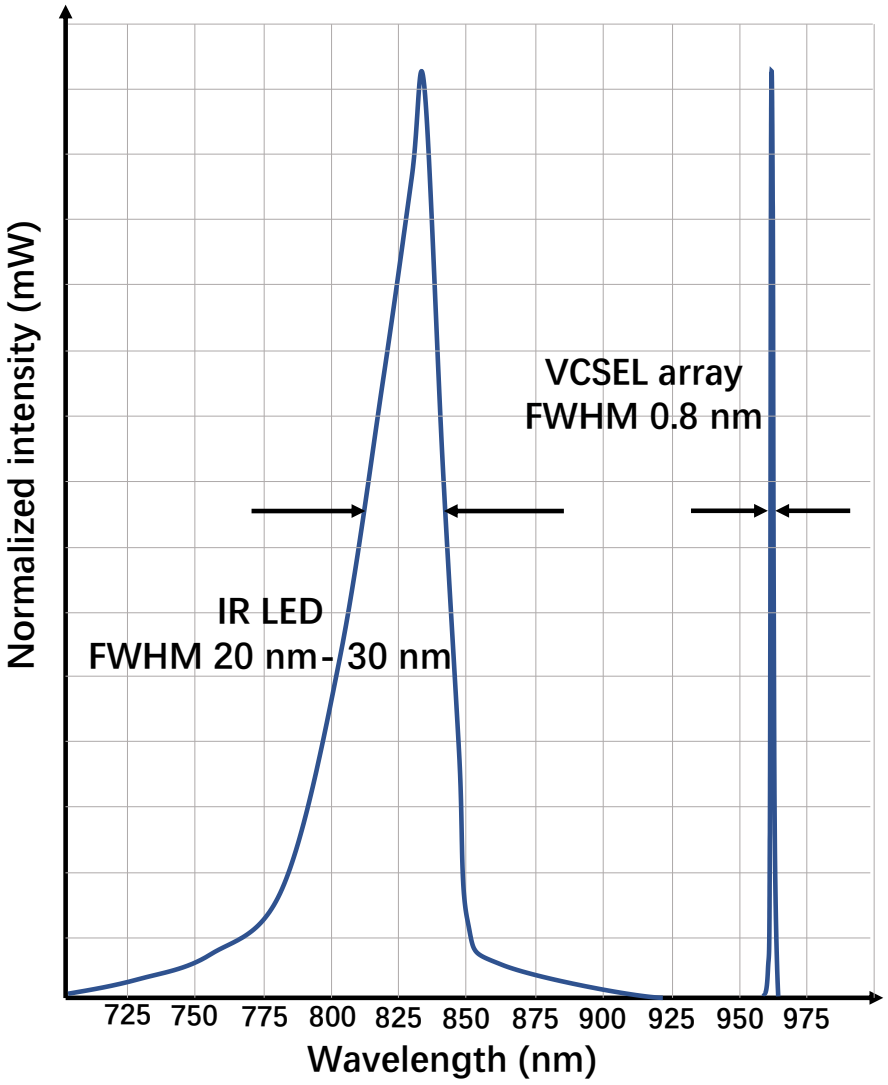

Fig. 1.18 Comparison of the spectrum between VCSEL and LED

- Intensity: According to various optical wireless power application scenarios, the required power covers the range from milliwatts to megawatts, and the difference is nearly 10 orders of magnitude. Therefore, according to the application scenarios and target devices of optical wireless power transmission, various requirements are put forward on the characteristics and power level of the light sources. Generally, the actual intensity of a several

mm^2 high-power LED emitting chip is around several watts, while for the semiconductor laser chip, such value is in the range of several watts to dozens of watts. However, such high output intensity of LD is based on a high-performance heat dissipation system. On the contrary, LEDs are generally used in relatively low-cost systems, and low cost is a major advantage of LEDs. Therefore, generally only a relatively simple heat dissipation system is configured in such systems. This is an important reason why the light output of the LED is generally lower than that of the LD when the size of the light-emitting chip is the same. Besides, due to the different emitting principles and structures, the LED is emitting from entire chip, while laser is emitting only from a small part, and as the areal chip cost necessary for economical lighting scales as input power density, areal chip cost can be much higher for LDs than for LEDs. Thus, if the size of light sources themselves is the same, the LD's emitting area is normally smaller than LED, and the practical light output difference of LED and laser will be much smaller than their radiant intensity. In fact, under the conditions of same thermal heatsinking and the same power conversion efficiency, the maximum output power of LED and LD that with same chip size may be almost the same. Sometimes the LED even show larger output due to better capability of heat resistance comparing with LD. More importantly, such high power of LD is also one of the main reasons of its possible hazard to creatures and surrounding objects. Therefore, from the aspect of safety, LED is promising as a better choice of OWPT light source than LD. In general, LD is a good light source for OWPT system to provide enough power for high power consumption electronics, but such high power of LD brings other problems at same time, such as heat dissipation issue and safety issue. Although single LED cannot provide the same high power as LD in most practical scenarios of applications, it can be used as an ideal light source in OWPT for low power consumption devices, such as small wearable devices and IoT terminals. On the other hand, by integrating multiple LEDs as light source, sufficiently large output can be realized. Moreover, LED also has the advantages of a more secure using environment and looser specifications and regulations. To sum

up, the performance of LED and LD in terms of output light intensity is comparable.

- Directionality: The temporal coherence of the laser endows the laser with the characteristics of high monochromaticity, while the spatial coherence makes the laser beam have a very small divergence angle, thereby achieving high directionality. After installing the collimation lens, a laser is able to be focused to a tight spot from long-range distance. Unlike lasers, LEDs emit light spontaneously. Without encapsulating a first-order lens, the LED chip emits light similar to a Lambertian object, which means the light intensity is approximately equals in all directions. After encapsulating the first-order lens, the beam of the LED can be restricted into a certain angle, but it still cannot achieve the same degree of directivity as the laser. The Fig. 1.19 shows the comparison of the divergence angle of a typical white LED with large divergence angle, which is usually used for illumination, and a narrow emission LED with relatively high directionality, and a VCSEL array.[111][112][113] The illumination LED usually has a large divergence angle in order to cover as large as possible area. High directional LED can normally be achieved by packaged pointed epoxy resin or metal reflective cavity, and the half-value angle is basically in the range of 5 degrees to 20 degrees. However, even comparing with VCSEL array of multi-transverse mode, the directionality of narrow emission LED is far more less. Besides, such design of high directional LED will cause unideal irradiation spot and negative influence on final output from solar cell, and this point will be discussed in section 2.2 later. Therefore, LED is unable to achieve same level directionality as laser, and cannot be collimated over long distance more importantly. This difference will lead out totally different idea on the designing direction of beam control system in OWPT.

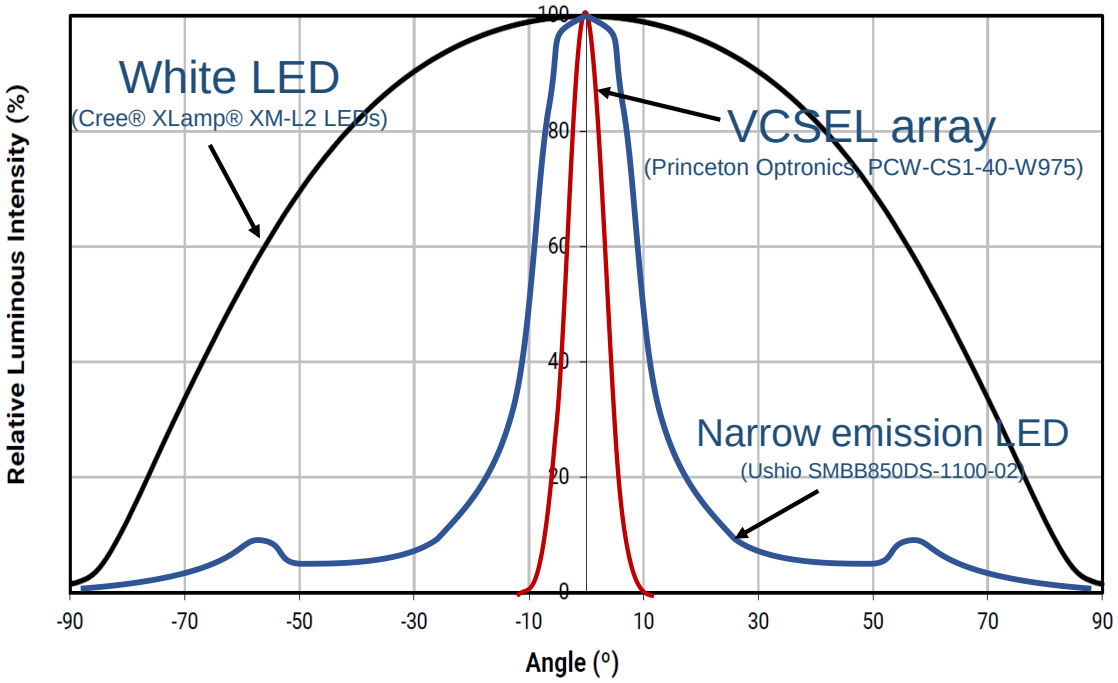

Fig. 1.19 Comparison of the divergence angle between laser, wide-emission LED and narrow-emission LED

- Compact and lightweight: Both LD and LED have the advantages of small size and light weight. Usually, the chips of both semiconductor light sources are in the size range of several square millimetres, and the weight is tens of milligrams. Therefore, in most of application scenarios, only discussing the size and weight of LD and LED chips is less meaning. Because the LED chips emits light from entire area, while the LD emits light only from a small part, the LED products thus have the advantage of being slightly smaller and lighter than LD when the area of light emitting areas of both chips are the same. On the other hand, in order to form a highly directional beam, an optical control system is necessary for both LD and LED. Because of the high directionality of the LD, its beam control system is usually simpler than LED's. Moreover, the narrower diameter of laser beam also leads out smaller aperture size of the optical element in LD beam control system than LED beam control system. Therefore, if only consider the transmitter dimension, the laser-based OWPT transmitter will be smaller than LED-based OWPT transmitter. However, this difference is only in a small range, such as 5 cm

difference in width and height. From another perspective, the LD usually has more serious heat dissipation problem than LED due to its high power, and its sensitivity to temperature is also higher than LED. Thereby, under the same conditions and compare with LED-based OWPT transmitter, it is essential to configure a better heat dissipation system, such as a larger heat sink or a fan, for a laser-based OWPT transmitter. Considering heat sink is much heavier than optical elements, the weight of laser-based OWPT transmitter will be much larger than LED-based OWPT transmitter. So, from the view of portability and combing all the above discussion, LED has unique pros as the light source of OWPT system.

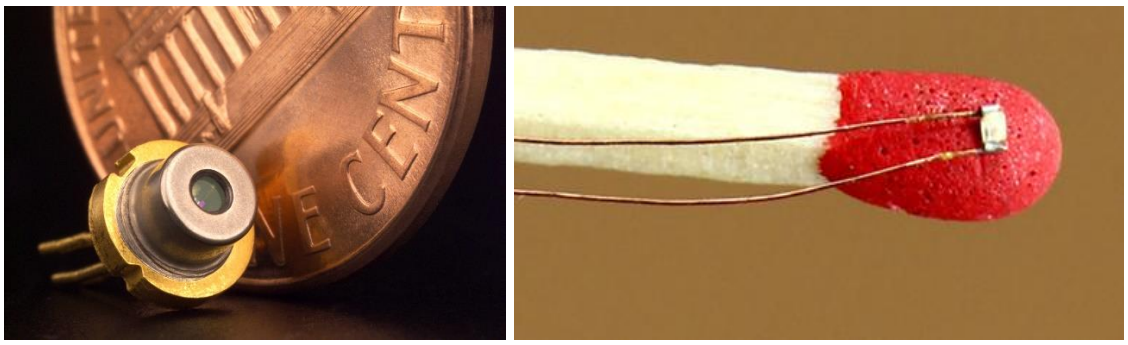

Fig. 1.20 Size of semiconductor light source (left: LD; right: LED)[114]

1.3.2 Summary of the feasibility of LED-based optical wireless power transmission

Based on the discussion shown in the section 1.3.1, the Table 1.3 lists the summary of main comparison between LED and LD as the light source of OWPT system.

Table 1.3 The main comparison between LED and LD as the light source of OWPT system

Light source	LED	LD
Monochromaticity	High	Extremely high
Intensity	High	High
Operating temperature	High	Intermediate

Heat dissipation system	Simple system is enough	High-performance system required
Directionality	Intermediate	Extremely high
Product dimension	Extremely small	Extremely small
Product regulation	Loose	Severe

Conclusively, compared to semiconductor lasers, LEDs have a sufficiently high monochromaticity to achieve efficient PV conversion of photovoltaic cells. On the other hand, on the basis of being a portable device, LED has the advantage of being lighter than semiconductor laser. In terms of intensity, although the semiconductor laser has a very considerable output, safety and strict regulation make it impossible to easily appear in the commercial market as a daily application in a short time. Because the power consumption requirements of electronic devices cover the range from a few milliwatts to several megawatts, single LED can be used as an ideal light source of optical wireless power transmission for low-power devices, and LED array is capable to supply high-level power. and its relatively loose regulation also makes it a potential candidate that be put into practical use and quickly promoted in a short time of the future. The most important point is that the different performance of LEDs and lasers directionality feature leads to different design ideas between the LED-based OWPT system and the laser-based OWPT system. Compared with lasers, non-temporal coherence ultimately causes LEDs unable to obtain ultra-high directionality, and difficult to maintain collimation over long distances as well. Therefore, LED-based OWPT systems usually have more complex optical control systems in order to accurately target the receiver at a long distance. Besides, because the LED-based OWPT system can only obtain a small enough irradiation spot and realize high-efficiency power supply at the target distance, while the power supply efficiency at un-target distances deteriorates rapidly. Therefore, in the conditions of non-zoom optical system, a system configuration for specific transmission distance and specific target irradiation size is indispensable when

designing LED-based OWPT system. On the other hand, with zoom optical system applying in the LED-based OWPT system, the transmission distance can be variable, and effective power transmission can be achieved in large-range distance.

Based on the discussion and analysis that stated above, it is proved that the LED-based OWPT system is a feasible and ideal option of wireless power supplying. Whereas, even the LED has numerous advantages and prominent features, the investigation of LED-based OWPT system has almost not been reported yet. Most of the existing literature on OWPT technology is based on LD light sources. Therefore, the research of LED-based OWPT system is far more important and urgent.

1.4 Objectives of the research

Based on discussion of the background shown above, LED-based OWPT system for compact IoT should be realized. The main objective of this research is designing a portable optical wireless power transmission system based on LED light source, which can be used to transmit significant power remotely to the IoT terminals, and evaluate its performance in various application scenarios and predict its possible potential in the future. The objectives of this research are summarized as follow:

1. Investigating the components of LED-based OWPT system, and proposing the proper selections of the components based on their characteristics in LED-based OWPT system.
2. The basic configuration design of the portable LED-based OWPT system for compact IoT.
3. Characteristics analysis of the single-LED OWPT system with different configurations and application scenarios.
4. Design and characteristics analysis of the LED-array OWPT system for achieving high output power.
5. Future prospect of the portable LED-based OWPT system for compact IoT.

In general, this research will study and compare the characteristics and performance of most existing light source, optical energy receiving devices and optical elements under the application of OWPT technology, and point out proper selection of the essential and optimal components of the LED-based OWPT system. In addition, the ideal system parameters of LED-based OWPT are provided to meet different requests in diverse application scenarios. Through this study, a guideline and research direction will be provided for the future scholars who will conduct the research of LED-based OWPT technology and those institutions that engaged in the research and development of relate or supporting technologies for OWPT.

1.5 Structure of thesis

In the chapter 1 of this thesis, the introduction of the optical wireless power transmission technology is discussed. Specifically, it discussed why the power consumption issue of IoT devices is an urgent problem to be solved, and why the existing various power supply technologies cannot satisfy the needs of various application scenarios of IoT devices, and the unique advantages of using OWPT technology to provide required power for the IoT devices. Also, the basic introduction of OWPT technology and its research status is shown. Moreover, the feasibility and merits of applying LED as the light source of OWPT system is demonstrated by comparing it with the laser-based OWPT technology that has been proven to be feasible.

In the chapter 2, the basic configuration of LED-based OWPT system is shown and compared with laser-based OWPT system. The investigation on the possible components of LED-based OWPT is provided, which are light sources, light energy receiver and optical elements. Then, based on their characteristic under OWPT application, the optimal choice of each component is analysed and represented.

The more detailed configuration and parameters discussion of LED-based OWPT system is shown in chapter 3. The main discussion in this chapter is about the optical system. Specifically, the different optical system configurations will be

compared and analysed, and the optimal configuration of LED-based OWPT is provided. Besides, the effects of each parameter, the relation between parameters and the corresponding performance is analysed by establishing mathematical model of optical system of LED-based OWPT system. Then, according to different scenarios, the appropriate value of each parameter will be given. At last, the simulation model and analysis of different kinds of LED-based OWPT system which are suitable to different application requirements is provided.

In the chapter 4, the performance confirmations of LED-based OWPT system by experiment is shown, including the experiment of LED-based OWPT system under ideal operation conditions and also unideal conditions such as oblique irradiation and irradiation with tremor. The detailed analysis of system performance (system efficiency, output power, transmitter and receiver dimension) will be provided by comparing experiment data with simulation data. Also, the experimental data of some important characteristics of LED-based OWPT system will be proposed in this section, such as the tolerance transmission range nearby the target distance, and the thermal analysis on the transmitter and receiver side, and the corresponding impacts on the final system performance.

In order to break out the power limitation of single LED chips and enhance the entire output power of LED-based OWPT system, the designing of LED-array OWPT system is discussed in chapter 5. A novel LEDs array method is proposed in this research, which can achieve much higher compact level and smaller dimension of the system than traditional array approach. Two kinds of configurations of the LED-array OWPT system are shown in this section, with different degree of emphasis on system efficiency and size of irradiation at target distance. Then, experiment data of such two LED-array OWPT systems is provided and analysed by comparing with simulation results. Besides, the discussion of the very important alignment deviation issue in the process of designing LED-array OWPT system, including the concept of alignment deviation between different optical elements array sets, the required alignment accuracy, the degradation of system performance caused by misalignment, and the possible solutions will be presented at the end of this chapter.

In the final section of this thesis, the future prospect of LED-based OWPT system

for compact IoT terminals will be discussed. The possible available performance and functions of portable LED-based OWPT system in the near decades will be estimated by investigating and analysing the progress in the research field of the components and technologies that closely related with LED-based OWPT technology. And last, the conclusion of the entire thesis will be shown. The outline of the thesis is shown in Fig. 1.21.

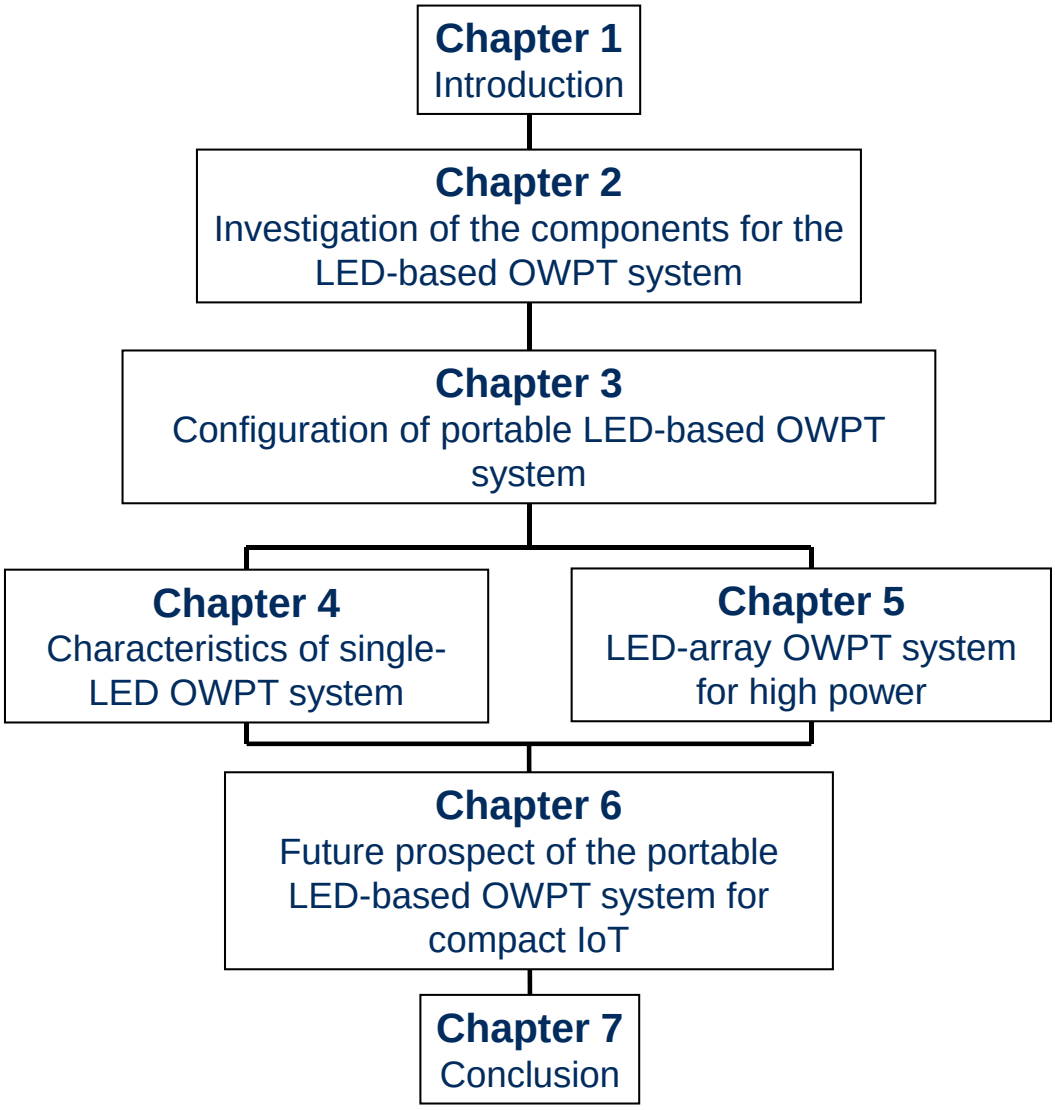

Fig. 1.21 The structure of the thesis

References

[1] H. Dai, Z. Zheng and Y. Zhang, "*Blockchain for Internet of Things: A Survey,*" IEEE Internet of Things Journal, 6 (**5**), pp. 8076-8094, 2019.

[2] Morrar, Rabeh, Husam Arman, and Saeed Mousa, "*The fourth industrial revolution (Industry 4.0): A social innovation perspective,*" Technology Innovation Management Review, 7 (**11**), pp: 12-20, 2017.

[3] Li, Shancang, Li Da Xu, and Shanshan Zhao, "*5G Internet of Things: A survey,*" Journal of Industrial Information Integration, 10, pp: 1-9, 2018.

[4] Nižetić, Sandro, et al., "*Internet of Things (IoT): Opportunities, issues and challenges towards a smart and sustainable future,*" Journal of Cleaner Production 274, 122877, 2020.

[5] Mahmoud, Mahmoud S., and Auday AH Mohamad, "*A study of efficient power consumption wireless communication techniques/modules for internet of things (IoT) applications,*" 2016.

[6] Vongsingthong, S., and S. Smanchat, "*Internet of Things: A Review of Applications & Technologies,*" Suranaree Journal of Science and Technology, 21 (**4**), pp: 359-374, 2014.

[7] Lovejoy. Ben, "*HomeKit devices getting more affordable as Lenovo announces Smart Home Essentials line,*" 2018.

[8] Prospero. Mike, "*Best Smart Home Hubs of 2018*," Tom's Guide, 2018.

[9] Chinchilla. Chris, "*What Smart Home IoT Platform Should You Use?,*" Hacker Noon, 2019.

[10] Baker. Jason, *"6 open source home automation tools,*" opensource.com, 2019.

[11] Demiris. G, Hensel. K, "*Technologies for an Aging Society: A Systematic Review of 'Smart Home' Applications,*" IMIA Yearbook of Medical Informatics, 17 (**01**), pp: 33-40, 2008.

[12] da Costa. CA, Pasluosta. CF, Eskofier. B, da Silva. DB, da Rosa Righi. R, "*Internet of Health Things: Toward intelligent vital signs monitoring in hospital wards,*" Artificial Intelligence in Medicine, 89, pp: 61–69, 2018.

[13] Engineer. A, Sternberg. EM, Najafi. B, "*Designing Interiors to Mitigate Physical and Cognitive Deficits Related to Aging and to Promote Longevity in Older Adults: A Review,*" Gerontology, 64 (**6**), pp: 612–622, 2018.

[14] Kricka. LJ, "*History of disruptions in laboratory medicine: what have we learned from predictions?,*" Clinical Chemistry and Laboratory Medicine, 57 (**3**): 308–311, 2019.

[15] Gatouillat. Arthur, Badr. Youakim, Massot. Bertrand, Sejdic. Ervin, *"Internet of Medical Things: A Review of Recent Contributions Dealing with Cyber-Physical Systems in Medicine,*" IEEE Internet of Things Journal, 5 (**5**), pp: 3810–3822, 2018.

[16] Topol, Eric, "*The Patient Will See You Now: The Future of Medicine Is in Your Hands,*" 2016.

[17] Dey. Nilanjan, Hassanien. Aboul Ella, Bhatt. Chintan, Ashour. Amira S, Satapathy. Suresh Chandra, "*Internet of things and big data analytics toward next-generation intelligence,*" Springer International Publishing, 2018.

[18] Deloitte, U. K, "*Centre for Health Solutions,*" Primary Care: Today and Tomorrow—Improving general practice by working differently, London: Deloitte, 2012.

[19] Ersue. M, Romascanu. D, Schoenwaelder. J, Sehgal. A, "*Management of Networks with Constrained Devices: Use Cases,*" IETF Internet Draft, 2014.

[20] "*Goldman Sachs Report: How the Internet of Things Can Save the American Healthcare System $305 Billion Annually,*" Engage Mobile Blog, Engage Mobile Solutions, LLC., 2018.

[21] World Health Organization, *"mHealth. New horizons for health through mobile technologies,*" World Health Organization, 2011.

[22] Mahmud. Khizir, Town. Graham E, Morsalin. Sayidul, Hossain. M.J, "*Integration of electric vehicles and management in the internet of energy,*" Renewable and Sustainable Energy Reviews, 82, pp: 4179–4203, 2018.

[23] Xie. Xiao-Feng, Wang. Zun-Jing, *"Integrated in-vehicle decision support system for driving at signalized intersections: A prototype of smart IoT in transportation,"* Transportation Research Board (TRB) Annual Meeting, Washington, DC, USA, 2017.

[24] Xie. Xiao-Feng, "*Key Applications of the Smart IoT to Transform Transportation,*" 2016.

[25] Yang. Chen, Shen. Weiming, Wang. Xianbin, "*The Internet of Things in Manufacturing: Key Issues and Potential Applications,*" IEEE Systems, Man, and Cybernetics Magazine, 4 (**1**): 6–15, 2018.

[26] Severi. S, Abreu. G, Sottile. F, Pastrone. C, Spirito. M, Berens. F, *"M2M Technologies: Enablers for a Pervasive Internet of Things,"* The European Conference on Networks and Communications (EUCNC2014), 2014.

[27] Gubbi. Jayavardhana, Buyya. Rajkumar, Marusic. Slaven, Palaniswami. Marimuthu, "*Internet of Things (IoT): A vision, architectural elements, and future directions,*" Future Generation Computer Systems, 29 (**7**), pp: 1645–1660, 2013.

[28] Meola. A, *"Why IoT, big data & smart farming are the future of agriculture,"* Business Insider. Insider, Inc., 2018.

[29] Zhang. Q, "*Precision Agriculture Technology for Crop Farming,*" Taylor & Francis, CRC Press, pp: 374, 2016.

[30] Parello. J, Claise. B, Schoening. B, Quittek. J, *"Energy Management Framework*," IETF Internet, 2014.

[31] Ersue. M, Romascanu. D, Schoenwaelder. J, Sehgal. A, "*Management of Networks with Constrained Devices: Use Cases,*" IETF Internet, 2014.

[32] Poon. L, "*Sleepy in Songdo, Korea's Smartest City,*" CityLab, Atlantic Monthly Group, 2018.

[33] Zanella. Andrea, et al., "*Internet of things for smart cities,*" IEEE Internet of Things journal, 1 (**1**), pp: 22-32, 2014.

[34] Rico. Juan, "*Going beyond monitoring and actuating in large scale smart cities,*" NFC & Proximity Solutions–WIMA Monaco, 2014.

[35] "*A vision for a city today, a city of vision tomorrow,*" Sino-Singapore Guangzhou Knowledge City, 2014.

[36] "*San Jose Implements Intel Technology for a Smarter City,*" Intel Newsroom, 2014.

[37] "*Western Singapore becomes test-bed for smart city solutions,*" Coconuts Singapore, 2014.

[38] Higginbotham. Stacey, "*A group of wireless execs aim to build a nationwide network for the Internet of things,*" Fortune.com, 2019.

[39] Freeman. Mike, *"On-Ramp Wireless becomes Ingenu, launches nationwide IoT network,*" SanDiegoUnionTribune.com, 2015.

[40] Lipsky. Jessica, "*IoT Clash Over 900 MHz Options,*" EETimes, 2015.

[41] Alleven. Monica, "*Sigfox launches IoT network in 10 UK cities,*" Fierce Wireless Tech, 2015.

[42] Merritt. Rick, "*13 Views of IoT World,*" EETimes, 2015.

[43] Fitchard. Kevin, "*Sigfox brings its internet of things network to San Francisco,*" Gigaom, 2014.

[44] Ujaley. Mohd, "*Cisco to Invest in Fiber Grid, IoT, Smart Cities in Andhra Pradesh,*" Expresscomputer, 2018.

[45] "*STE Security Innovation Awards Honorable Mention: The End of the Disconnect,*" securityinfowatch.com, 2015.

[46] Pivac. N, et al., "*Application of wearable sensory devices in predicting occupant's thermal comfort in office buildings during the cooling season,*" IOP

Conference Series: Earth and Environmental Science, 410 (**1**), IOP Publishing, 2020.

[47] Muthu. BalaAnand, et al., "*IOT based wearable sensor for diseases prediction and symptom analysis in healthcare sector,*" Peer-to-peer networking and applications, pp: 1-12, 2020.

[48] Ali. Zainab H, Hesham A. Ali, and Mahmoud M. Badawy, "*Internet of Things (IoT): definitions, challenges and recent research directions,*" International Journal of Computer Applications, 128 (**1**), pp: 37-47, 2015.

[49] Garcia-Espinosa. Eduardo, et al., "*Power Consumption Analysis of Bluetooth Low Energy Commercial Products and Their Implications for IoT Applications,*" Electronics, 7 (**12**), pp: 386, 2018.

[50] Afonso. José Augusto, António José F. Maio, and Ricardo Simoes, "*Performance evaluation of bluetooth low energy for high data rate body area networks,*" Wireless Personal Communications, 90 (**1**), pp: 121-141, 2016.

[51] N. Kimura and S. Latifi, "*A survey on data compression in wireless sensor networks,*" Information Technology: Coding and Computing, 2005 (ITCC 2005) International Conference, vol. 2, pp: 8–13, 2005.

[52] C. Schurgers and M. Srivastava, "*Energy efficient routing in wireless sensor networks,*" Military Communications Conference, 2001 (MILCOM 2001) Communications for Network-Centric Operations: Creating the Information Force, IEEE, vol. 1, pp: 357–361, 2001.

[53] J. Kolo, L.-M. Ang, S. Shanmugam, D. Lim, and K. Seng, "*A simple data compression algorithm for wireless sensor networks,*" Soft Computing Models in Industrial and Environmental Applications, Springer Berlin Heidelberg, vol. 188, pp: 327–336, 2013.

[54] T. van Dam and K. Langendoen, "*An adaptive energy-efficient mac protocol for wireless sensor networks,*" Proceedings of the 1st International Conference on Embedded Networked Sensor Systems, New York, USA, pp: 171–180, 2003.

[55] Prieto. M. Domingo, et al., "*Balancing power consumption in IoT devices by using variable packet size,*" 2014 Eighth International Conference on Complex, Intelligent and Software Intensive Systems, IEEE, 2014.

[56] Grell. Max, et al., "*Autocatalytic metallization of fabrics using Si ink, for biosensors, batteries and energy harvesting,*" Advanced Functional Materials, 29 (**1**), 2019.

[57] Backman. Jere, et al., "*IoT-based interoperability framework for asset and fleet management,*" 2016 IEEE 21st International Conference on Emerging Technologies and Factory Automation (ETFA), IEEE, 2016.

[58] Sudevalayam. Sujesha, and Purushottam. Kulkarni, "*Energy harvesting sensor nodes: Survey and implications,*" IEEE Communications Surveys & Tutorials, 13 (**3**), pp: 443-461, 2010.

[59] CASIO HS-8VA, datasheet.

[60] Pudur. Rajen, et al., "*Wireless power transmission: A survey,*" International Conference on Recent Advances and Innovations in Engineering (ICRAIE-2014), IEEE, 2014.

[61] Ibrahim. Fatin Noratika, N. A. M. Jamail, and N. A. Othman, "*Development of wireless electricity transmission through resonant coupling,*" 4th IET Clean Energy and Technology Conference (CEAT 2016), 2016.

[62] Shinohar., Naoki, “Wireless power transfer via radiowaves,” ISTE-Wiley, 2014.

[63] Gopinath. Ashwin, "*All About Transferring Power Wirelessly,*" Electronics for You, pp: 52–56, 2013.

[64] Lu. X, Wang. P, Niyato. D, Kim. D. I, Han. Z, "*Wireless Charging Technologies: Fundamentals, Standards, and Network Applications,*" IEEE Communications Surveys and Tutorials, 18 (**2**), pp: 1413–1452, 2016.

[65] Sun. Tianjia, Xie. Xiang, Zhihua. Wang, “*Wireless Power Transfer for Medical Microsystems. Springer Science & Business Media,*” pp: 5–6, 2013.

[66] Valtchev. Stanimir S, Elena N. Baikova, and Luis R. Jorge, "*Electromagnetic field as the wireless transporter of energy,*" Facta universitatis-series: Electronics and Energetics, 25 (**3**), pp: 171-181, 2012.

[67] Davis. Sam, "*Wireless power minimizes interconnection problems,*" Power Electronics Technology, 37 (**7**), pp: 10-14, 2011.

[68] Sazonov. Edward, Neuman. Michael R, "*Wearable Sensors: Fundamentals, Implementation and Applications,*" Elsevier, pp: 253–255, 2014.

[69] Zhang. Zhen, et al., "*Wireless power transfer—An overview,*" IEEE Transactions on Industrial Electronics, 66 (**2**), pp: 1044-1058, 2018.

[70] Karalis. Aristeidis, Joannopoulos. J. D, Soljačić. Marin, "*Efficient wireless non-radiative mid-range energy transfer,*" Annals of Physics, 323 (**1**), pp: 34–48, 2008.

[71] Agbinya. Johnson I, "*Wireless Power Transfer,*" River Publishers, pp: 1–2, 2012.

[72] Wilson. Tracy V, "*How Wireless Power Works,*" How Stuff Works, InfoSpace LLC, 2014.

[73] Steinmetz. Charles Proteus, "*Elementary Lectures on Electric Discharges, Waves, and Impulses, and Other Transients (2nd ed.),*" McGraw-Hill, 1914.

[74] "*Resonant Capacitive Coupling,*" www.wipo-wirelesspower.com, 2018.

[75] Ashley. Steven, "*Wireless recharging: Pulling the plug on electric cars,*" BBC website, British Broadcasting Corp, 2012.

[76] Jiang. Hao, Zhang. Junmin, Lan. Di, Chao. Kevin K, Liou. Shyshenq, Shahnasser. Hamid, Fechter. Richard, Hirose. Shinjiro, Harrison. Michael, Roy. Shuvo, "*A Low-Frequency Versatile Wireless Power Transfer Technology for Biomedical Implants,*" IEEE Transactions on Biomedical Circuits and Systems, 7 (**4**), pp: 526–535, 2012.

[77] Shahan. Zach, "*ELIX Wireless Rolls Out A 10kW Wireless EV Charger With 92% Efficiency,*" EVObsession.com, 2015.

[78] Agbinya. Johnson I, "*Wireless Power Transfer. River Publishers,*" pp. 1–2, 2012.

[79] Umenei. A. E, *"Understanding Low Frequency Non-radiative Power Transfer,*" Fulton Innovation, Inc., 2011.

[80] Schantz. Hans G, "*A real-time location system using near-field electromagnetic ranging,*" 2007 IEEE Antennas and Propagation Society International Symposium, pp: 3792–3795, 2007.

[81] Manbachi. A, and Cobbold. R.S.C, "*Development and Application of Piezoelectric Materials for Ultrasound Generation and Detection,*" Ultrasound, 19 (**4**), pp: 96–187, 2011.

[82] "*Piezoelectric Crystal Classes,*" Newcastle University, UK, 2015.

[83] Massa. A. Massa, G. Oliveri, F. Viani, P. Rocca, Oliveri. Giacomo, Viani. Federico, Rocca. Paolo, "*Array designs for long-distance wireless power transmission – State-of-the-art and innovative solutions,*" IEEE, 101 (**6**), pp: 1464–1481, 2013.

[84] Karalis. Aristeidis, Joannopoulos. J. D, Soljačić. Marin, "*Efficient wireless non-radiative mid-range energy transfer,*" Annals of Physics, 323(**1**), pp: 34-48, 2008.

[85] Tan. Yen Kheng, "*Energy Harvesting Autonomous Sensor Systems: Design, Analysis, and Practical Implementation,*" CRC Press, pp. 181–182, 2013.

[86] Puers. R, "*Omnidirectional Inductive Powering for Biomedical Implants,*" Springer Science & Business Media, pp: 4–5, 2008.

[87] Sahai. Aakash, Graham. David, "*Optical wireless power transmission at long wavelengths,*" 2011 International Conference on Space Optical Systems and Applications (ICSOS), pp: 164–170, 2011.

[88] T. Miyamoto, "*Optical wireless power transmission using VCSELs,*" Proc. SPIE 10682, 2018.

[89] Putra, Alexander William Setiawan, Hirotaka Kato, and Takeo MARUYAMA, "*Infrared LED marker for target recognition in indoor and outdoor applications of optical wireless power transmission system,*" Japanese Journal of Applied Physics, 2020.

[90] W. J. Robinson, Jr., "*The feasibility of wireless power transmission for an orbiting astronomical station,*" NASA Technical Memorandum X-53701, 1968.

[91] T. H. Mainman, "*Stimulated Optical Radiation in Ruby,*" Nature, vol. 187, pp: 493-494, 1960.

[92] A. Goetzberger, and C. Hebling, "*Photovoltaic materials, past, present, future,*" Solar Energy Materials and Solar Cells, 62, (**1-2**), pp: 1-19, 2000.

[93] Frank Steinsiek, W. P. Foth, K. H. Weber, Christian Schafer, H. J. Foth, "*Wireless power transmission experiment as an early contribution to planetary exploration missions,*" 54th IAF, Bremen, 2003.

[94] Masaki Hirota, Shiich Iio, Yoshimi Ohta, Yuusuke Niwa, Tomoyuki Miyamoto, "*Wireless power transmission between a NIR VCSEL array and silicon solar cells,*" 20th Microoptics Conference (MOC'15), Fukuoka, Japan, 2015.

[95] Shi Dele, Ma Zongfeng, Wu Shichen, Zang, Jiande, Huang Xiujun, "*Laser Wireless Power Transmission System Designing and Experiment between Airships,*" CITCS, 2015.

[96] John Fakidis, Stefan Videv, Stepan Kucera, Holger Claussen, Harald Haas, "*Indoor Optical Wireless Power Transfer to Small Cells at Nighttime,*" Journal of Lightwave Technology, 34 (**3236**), 2016.

[97] Yuki Katsuta, Tomoyuki Miyamoto, "*Design and experimental characterization of optical wireless power transmission using GaAs solar cell and series-connected high-power vertical cavity surface emitting laser array,*" Jpn. J. Appl. Phys, 57 (**08PD01**), 2018.

[98] Tokuda, Takashi, et al., "*1 mm^3-sized optical neural stimulator based on CMOS integrated photovoltaic power receiver,*" AIP Advances, 8 (**4**), 2018.

[99] Wang. Wei, et al., "*Wireless energy transmission channel modelling in resonant beam charging for IoT devices,*" IEEE Internet of Things Journal, 6 (**2**), pp: 3976-3986, 2019.

[100] Landis. Geoffrey A, "*Applications for space power by laser transmission,*" Laser Power Beaming, Vol. 2121, International Society for Optics and Photonics, 1994.

[101] Yu. Haichao, et al., "*Brief review on pulse laser propulsion,*" Optics & Laser Technology, 100, pp: 57-74, 2018.

[102] Glaser. Peter E, "*An overview of the solar power satellite option,*" IEEE Transactions on Microwave Theory and Techniques, 40 (**6**), pp: 1230-1238, 1992.

[103] Du. Yao, et al., "*Trajectory Design of Laser-Powered Multi-Drone Enabled Data Collection System for Smart Cities,*" 2019 IEEE Global Communications Conference (GLOBECOM), IEEE, 2019.

[104] Young. Andrew T, "*Rayleigh scattering,*" Applied Optics, 20 (**4**), pp: 533, 1981.

[105] Wiscombe. Warren J, "*Improved Mie scattering algorithms,*" Applied optics, 19 (**9**), pp: 1505-1509, 1980.

[106] Suriza. A. Z., et al., "*Preliminary analysis on the effect of rain attenuation on Free Space Optics (FSO) propagation measured in tropical weather condition,*" the 2011 IEEE International Conference on Space Science and Communication (IconSpace), IEEE, 2011.

[107] Liou. K.N, "*An Introduction to Atmospheric Radiation (2nd ed.),*" Academic, pp: 119, 2002.

[108] Shockley. W, Read. W. T, "*Statistics of the Recombinations of Holes and Electrons,*" Physical Review, 87 (**5**), pp: 835–842, 1952.

[109] Bader. Osama, and Harvey Lui, "*Laser safety and the eye: hidden hazards and practical pearls,*" American Academy of Dermatology Annual Meeting Poster Session, Washington, DC, USA, 1996.

[110] "*Safety of laser products - Part 1: Equipment classification and requirements (2nd ed.),*" International Electrotechnical Commission, 2007.

[111] Cree XLamp XM-L2, datasheet.

[112] USHIO smbb850ds-1100-02, datasheet.

[113] Princeton Optronics PCW-CS1-40-W975, datasheet.

[114] "*Laser diode,*" In Wikipedia, Retrieved 14 January 2021, Available at: https://en.wikipedia.org/wiki/Laser_diode.

Chapter 2. Investigation on the components of the LED-based OWPT system

2.1 OWPT system configuration

In this section, the basic configuration and designing of OWPT system is shown. The general designing of the LED-based OWPT system and the laser-based OWPT system is introduced, and emphasized the differences of designing between the two systems. Moreover, the necessary performance and characteristics of the LED-based OWPT system that specially used for powering compact IoT terminals is analysed.

2.1.1 Basic configuration of general OWPT system

Simply, the basic configuration of a general OWPT system consists of light source, optical receiving device and beam control system. The light source converts electrical energy into light energy and realizes long-distance power transmission. In order to achieve high efficiency of electrol-optical conversion and high intensity output, semiconductor lasers and monochromatic LEDs are the most ideal choices at current stage. The receiver needs to effectively convert the light energy that transmitted over a long distance back into electrical energy, and the usual choice is photovoltaic cells (solar cells). The functions of the beam control system are mainly divided into two. The first one is to control the divergence angle of the beam to form a highly directional beam, so as to achieve precise pointing to the target at long distance. The second function is to concentrate light and enhancing the radiant intensity, thereby increasing the photovoltaic conversion efficiency of the receiver. It should be mentioned that, the beam control system is not a critical module in some special application scenarios of OWPT. In the case that the transmission distance is short enough and the power required is very low, it is not required to used optical system to form a sharp beam or concentrate the intensity, such as powering subcutaneous ultra-small implantable devices. Therefore, the optical system can be removed for simplifying configuration and miniaturization of the devices. On the other hand, under the premise that this research is based on the application of remote power supply for IoT devices, the beam control

system is indispensable. In addition to the above basic configuration, some secondary modules are needed according to the application scenarios. For instance, although there is no need to configure rectifier circuit at the receiving side since the output of the photovoltaic cells is DC current, in order to achieve load matching, usually a Maximum Power Point Tracking (MPPT) module is necessary on the load side.[1] For another example, the application scenarios of OWPT can be divided into charging the built-in battery of the target electronics, or directly driving the devices which without battery. The devices usually have different power consumption in different operation stages, such as power consumption of drones in level flighting, hovering and ascending actions varies greatly. In the case of directly driving the no-battery devices, if the transmitter always supply power at a constant amount, the power exceeding the demand cannot be absorbed by the target devices and converted into thermal energy on the surface of photovoltaic cells. The heat can easily cause devices deterioration and damage. Therefore, it is necessary to configure the adaptive power adjust function based on the transmitter-receiver real time communication module. The Fig. 2.1 shows the basic configuration of the general OWPT system.

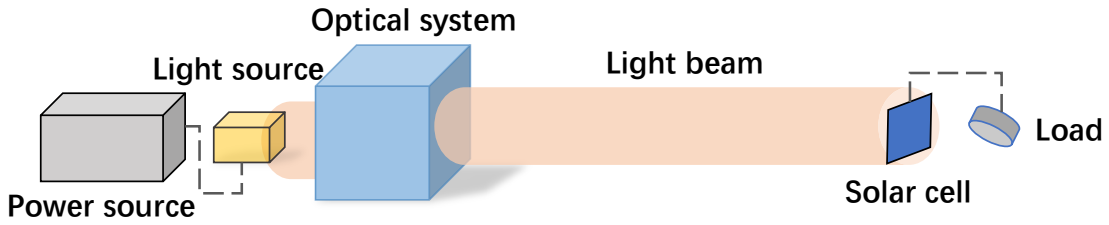

Fig. 2.1 The basic configuration of general OWPT system

2.1.2 Basic difference between LED-based and laser-based OWPT system

As the main two light sources of optical wireless power transmission technology, the design of the OWPT system that uses LED and laser as the light source is very different because of their distinct emitting principles and properties. This difference is mainly reflected in the beam control system designing. The temporal coherence of laser gives it very high directionality. Laser light from gas or crystal

lasers is highly collimated. Usually, the divergence of high-quality laser beam is commonly less than 1 milliradian, which is below 0.06 degree, and can be much less for large-diameter beams. Such as the divergence of a 1064 nm beam produced by the Nd:YAG laser, which has ideal beam quality (M^2=1), is only 0.34 mrad (0.019 degree).[2] Even in the condition of semiconductor laser, which emits less-collimated light due to the short cavity, applying a collimation lens can easily achieve high collimation. The collimated beam has parallel rays, and therefore will be spread minimally as it propagates in very long range. Thus, as for laser-based OWPT system, the beam shape will be relatively straight, and corresponding irradiation size will be unchanged on different positions of the transmission path. In other word, the beam control system of laser-based OWPT system usually contains only on collimation lens, and more importantly, laser-based OWPT system has the ability to achieve effective power transmission at different transmission distances without changing any configuration. Besides, the aperture of collimation lens can be small because of the small divergence of laser. The Fig. 2.2 shows the basic configuration of a laser-based OWPT system.

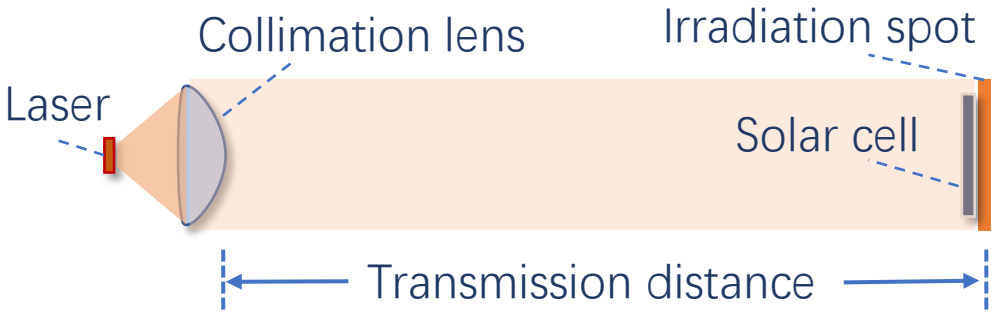

Fig. 2.2 The basic configuration of laser-based OWPT system

The designing of LED-based OWPT system is different. The high directional LEDs such as pointed epoxy resin package or metal reflective cavity package still have usually above 5-degree divergence angle. Even if a collimation lens is applied, the divergence is difficult to be controlled in a very small angle, and the

beam will show a very obvious divergence trend during propagation, so it is hard to achieve precis pointing. Due to this issue, the designing direction of LED-based OWPT system is more like trying to “aim at” rather than “align” the target. Generally, a more complicated and large optical system is necessary to constrain the divergence of light beam and decrease the size of irradiation spot at target distance, and multiple optical elements might be necessary according to the requirement. On the other side, the theoretical limit minimum size of irradiation of laser-based and LED-based OWPT system is not a major difference. According to the principle of etendue of the optical system, the size of the irradiation spot is related with the exit pupil of the optical system, and a lager exit pupil can realize smaller size of irradiation spot. In the condition of laser, such fact can also be explained by the Rayleigh criterion, which describes the that under collimated light, the minimum spot size is inversely proportional to the beam size. Therefore, in theory, the laser-based and LED-based OWPT system can both obtain a sufficiently small irradiation spot at any distance. The difference is that, in order to achieve a small spot, the laser-based OWPT system only needs to increase the beam diameter as well as aperture size of collimation lens, while the LED-based OWPT system needs to increase the beam divergence, lens aperture size, length between each two optical elements and also might sacrifice part of intensity. Thus, the sacrifice on the dimension of optical system of laser-based OWPT system is much smaller than that of the LED-based OWPT system, and with the irradiation spot size deceasing or transmission distance extending, such difference will become more and more obvious. Besides, as the discussion shown in section 1.3, with similar size of products, the emitting chip size of laser is commonly smaller than LED, thus also lead out smaller irradiation size. All the reasons above explain why LED-based OWPT system usually has larger irradiation spot than laser-based OWPT system. Another important difference is, LED-based OWPT system can only achieve accurate focus on near the target distance, and effective power transmission at the position beyond this range is difficult. Therefore, an optical system configuration for specific transmission distance and specific target irradiation size is indispensable when designing LED-

based OWPT system. The Fig. 2.3 shows the basic configuration of a LED-based OWPT system.

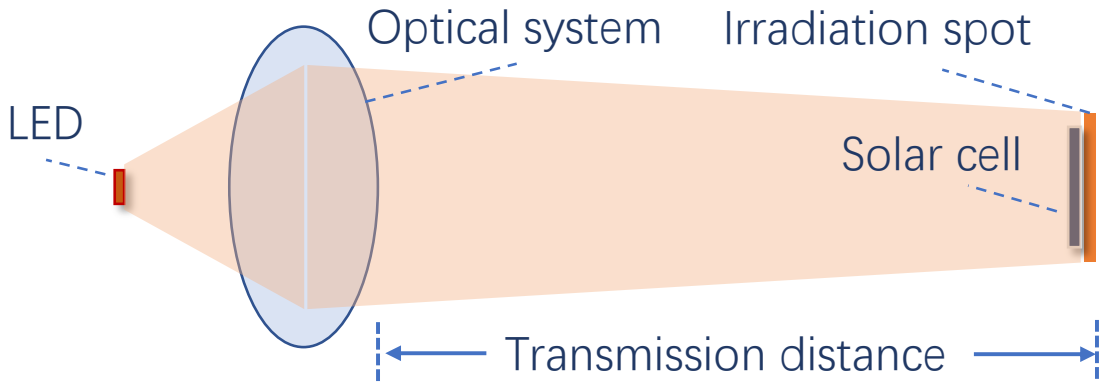

Fig. 2.3 The basic configuration of LED-based OWPT system

2.1.3 OWPT system for powering compact IoT devices

Unlike the general OWPT systems, some characteristics of the system need to be met in the envisaged application that using OWPT system to supply power remotely for compact IoT devices, which is decided by the specific scenario of powering IoT terminals.

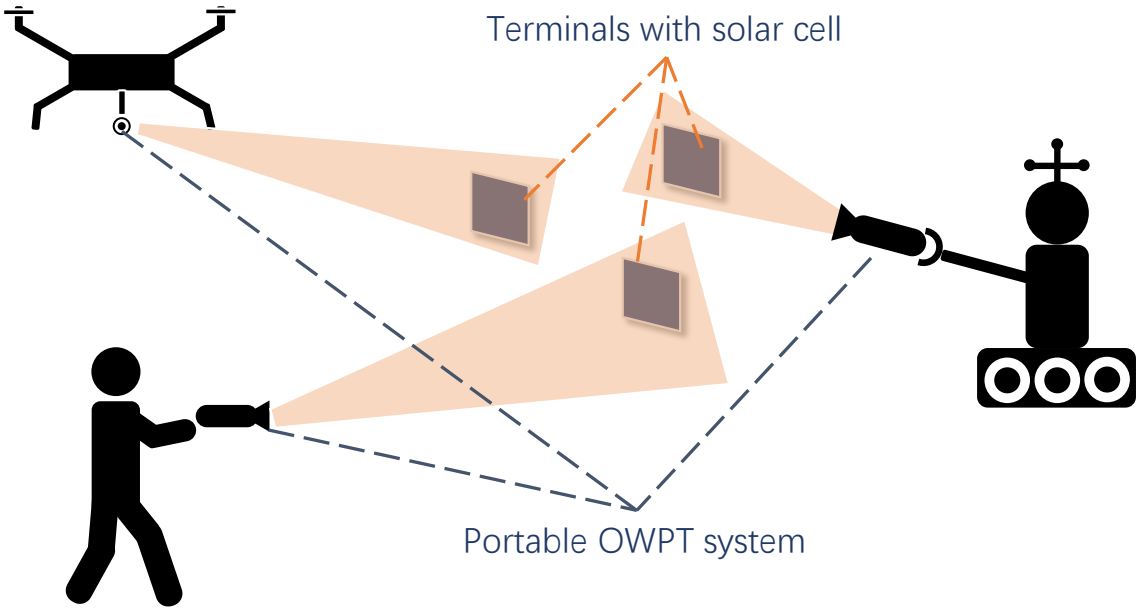

Fig. 2.4 Application scenarios of portable OWPT system

The first feature is portable size and weight. The IoT-OWPT system is assumed to have a small dimension and light enough weight to meet the requirement of portability. The Fig. 2.4 shows the envisioned application scenarios of the IoT-OWPT system. The portability is specifically manifested as it can be held by human easily or able to installed on robot or drone. Portability allows IoT-OWPT device to be easily moved or installed no matter it is used by hand-hold or fixed position. There is no clear definition of the size and weight of portable devices, the devices that in the range from smart phones to laptop computers all belongs to the category of portable devices. The envisaged IoT-OWPT system of this research is to be held by a user with one hand and perform power supply operations easily, thus the maximum size of the OWPT transmitter is limited in 15 cm × 15 cm × 15 cm, and the target shape of the transmitter is flashlight-like. Weight is another important factor of a portable device. Although the OWPT transmitter can be installed at a certain position during power transmission, operating by human hand-hold or installing on robot and drone are also critical application scenarios. In the case of human hand-hold, although a normal adult can easily hold several kilograms of objects with one hand, in the application of

optical wireless power transmission, the operator needs to keep one hand motionless during power supply process to achieve precise focusing, and tremor is unavoidable in such case. The tremor will be exacerbated as the weight of device or charging time increases. On the other hand, in the case of installing OWPT system on robot or drone, heavy weight of the device also causes power consumption of carrier increasing. Thus, the weight of the IoT-OWPT transmitter needs to be light enough. Currently, almost the weight of all handheld devices on the commercial market is less than 1 kg, and most of them are in the range of 300 g to 700 g. Although the transmitter of OWPT system consists of light source, heat sink and optical system, considering that the weight of optical elements is generally small, and the weight can be further reduced by selecting some special lenses such as Fresnel lenses. Besides, the material of the heat sink is usually copper or aluminium, so it is light as well.[3] Therefore, it is considered feasible to control the transmitter of the IoT-OWPT system within 700 g and can be held by one hand of human for relatively long time easily. The Fig. 2.5 shows the schematic diagram of the portable transmitter of OWPT system.

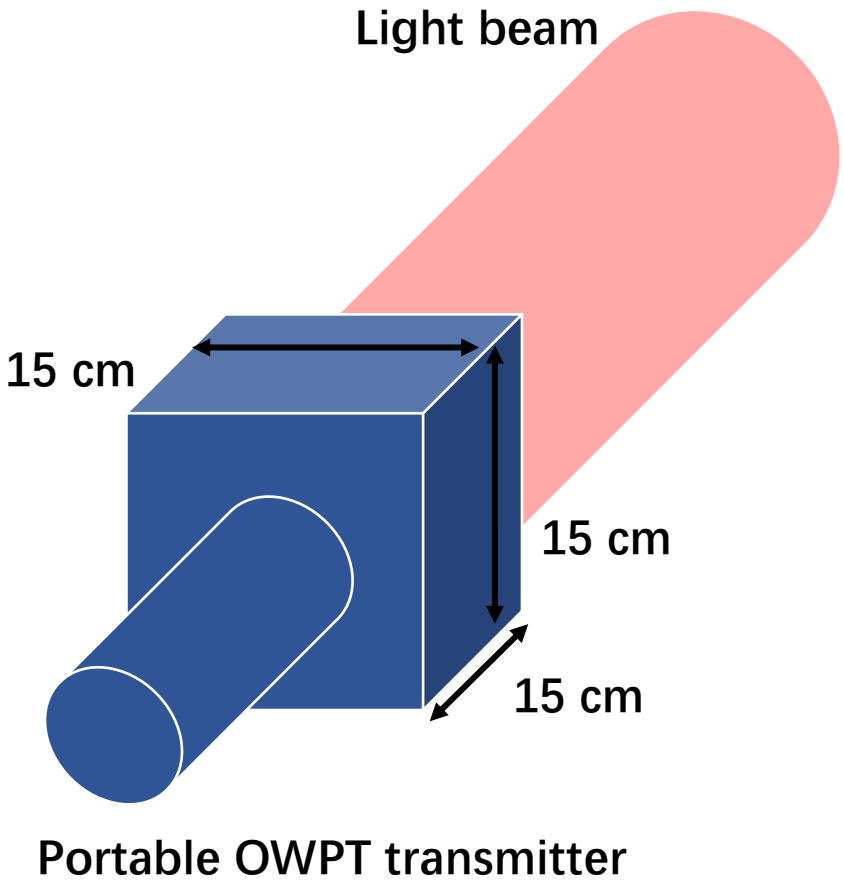

Fig. 2.5 Schematic diagram of the portable transmitter of OWPT system

The second point is the receiver size. Since the IoT terminals are expected to have carious forms and size, the receiver should be small enough to compatible with different type and size IoT terminals. The size of receiver is decided by the irradiation size of the system at the target transmission distance. Taking into account the limitation of portable size of the transmitter, the irradiation size of the LED-based OWPT system cannot be controlled extremely small, especially when the target transmission distance is very long. Therefore, the size of receiver should be decided based on the target transmission distance. In addition, whether it is operated by human-hold or installed on drone, tremor may occur during power transmission, so the size of receiver can be appropriately larger than the irradiation spot to reduce the efficiency deterioration caused by irradiation displacement. In this research, the target size of the receiver should be in the

range of 1 cm^2 – 50 cm^2 for different application scenarios by estimation. In addition, the efficiency of solar cells differs depending on the type, and the output voltage changes depending on the series connection form. Moreover, even with the same light intensity irradiation, the efficiency of the receiver (photovoltaic cell) varies depending on the light intensity distribution. The type of photovoltaic cell to be applied and the series connection structure should be optimized in consideration of the required characteristics on the terminal side and the characteristics of the voltage conversion circuit. In this research, the photovoltaic cell itself is assumed to be a commercially available product, the optimization of the solar cell itself and the pursuit of maximum efficiency are not performed. However, the characteristics directly affected by the photovoltaic cell characteristics, such as the effect of the light intensity distribution on the efficiency of the photovoltaic cell and the amount of power supplied, are considered in the research. The Fig. 2.6 shows the schematic diagram of the terminal with the receiver of the OWPT system attached.

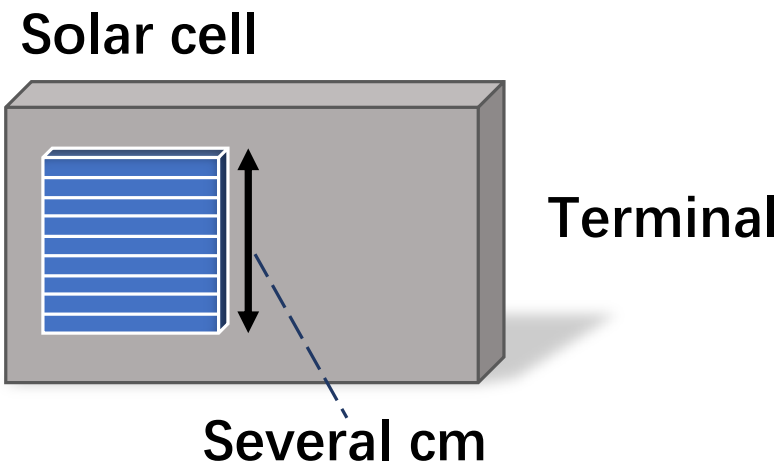

Fig. 2.6 Schematic diagram of the receiver of OWPT system

The third feature of IoT-OWPT system is the output power. Considering the target application is IoT terminal which usually has relatively low power consumption

compared with other electronics, the supplied power of OWPT that specifically designed for compact IoT will lower as well, usually under 1 W. The exchange of sacrificing the supplied power of IoT-OWPT is the advantages of simplified configuration, miniaturization and low cost. For a power supply system, the higher supplied power can allow the target devices to achieve the features of more advanced functions (longer communication range, larger data pack, shorter connection interval, etc), extending operation duration, reducing built-in battery capacity and size, shorten the recharging time and so on. Even for relatively low power device such as IoT-OWPT system, the output power pursued should be as high as possible if other conditions permit. Therefore, it does not very meaningful to discuss the upper limit of the supplied power of the IoT-OWPT system, but the minimum output power should be focused. In this research, this minimum output power of the IoT-OWPT system is also defined as the threshold value for judging whether the effectively power supply can be achieved or not. The power consumption of IoT terminals varies according to different applications and working stage. In awake stage, the power consumption is usually from several milliwatts to dozens of milliwatts, and this value declines to below 0.01 mW in sleep stage, or power saving mode. Depending on the duty cycle, the power consumption of the IoT terminals is normally between a few tenths of 1 milliwatt to a few milliwatts in a working cycle.[4] The Fig. 2.7 shows an example of characteristics of charging power and working cycles of three peripheral IoT devices under Bluetooth low energy (BLE) protocol. The average power consumption is under the condition of 1000 ms connection interval and a voltage of 3 V. The Fig. 2.7 shows the available working cycles of the IoT terminals after charging by different power for 1 s. Because comparing the connection interval, the duration of awake time is very short, and the connection intervals is just set as 1 s, thus the working cycles value shows in the Fig. 2.7 can also be regarded as the working duration in seconds. Since the power consumption of different IoT terminals varies a lot, the characteristics shown in the Fig. 2.7 are also very different. For instance, the available working cycles of Intel A-101 is more than three times of TI CC2540 after 1 s charging by OWPT system. However, if take the standard that a single-time charging can support an IoT terminal working for

a whole day, and choose Cypress CY8CKIT-042-BLE-A, which is at the average power consumption level of three different IoT devices, as a reference, then 100 mW should be a reasonable value as minimum requirement of IoT-OWPT system output power. Every 1 s charged by 100 mW power OWPT system, the IoT terminals can work 2000 cycles, which is roughly equals to 2000 s, or 33 mins. Thereby, if the IoT terminals can be recharged under same conditions 1 mins every day, around 33 h working duration is available. This is just a very rough calculation. The power consumption of different IoT devices is very various, and the awake stage of some IoT terminals is not triggered by timer either, thus the connection interval is irregular. However, this calculation also not includes the possible optical energy harvesting from ambient light, and the practical output power of IoT-OWPT system will be several times than this value. From the perspective of comparing with the irradiance of sunlight, the rationality of choosing 100 mW as the value of judging whether the OWPT system can effectively supply power can also be confirmed. According to rough estimation based on the photovoltaic conversion efficiency of the solar cell, about 300 mW total intensity is required to provide an output of 100 mW. Considering that the light irradiation spot of the OWPT system at the target distance is usually very small, which has the side length about 2 cm – 3 cm, then the average radiant intensity of the irradiation spot can be roughly calculated to be about 35 mW/cm^2-75 mW/cm^2. Such value is approximately equivalent to half the irradiance of the sunlight (AM1.5G: 100 mW/cm^2).[5] However, the irradiance of sunlight can only be available during the day, while the irradiance becomes 0 at night. Therefore, the average solar irradiance in a day and night is about 50 mW/cm^2. Therefore, the OWPT system with minimum 100 mW output can still achieve roughly same irradiance with the sunlight. Thus, it is considered reasonable to regard 100 mW as a threshold value for judging whether the IoT-OWPT system can effectively supply power to the IoT terminals.

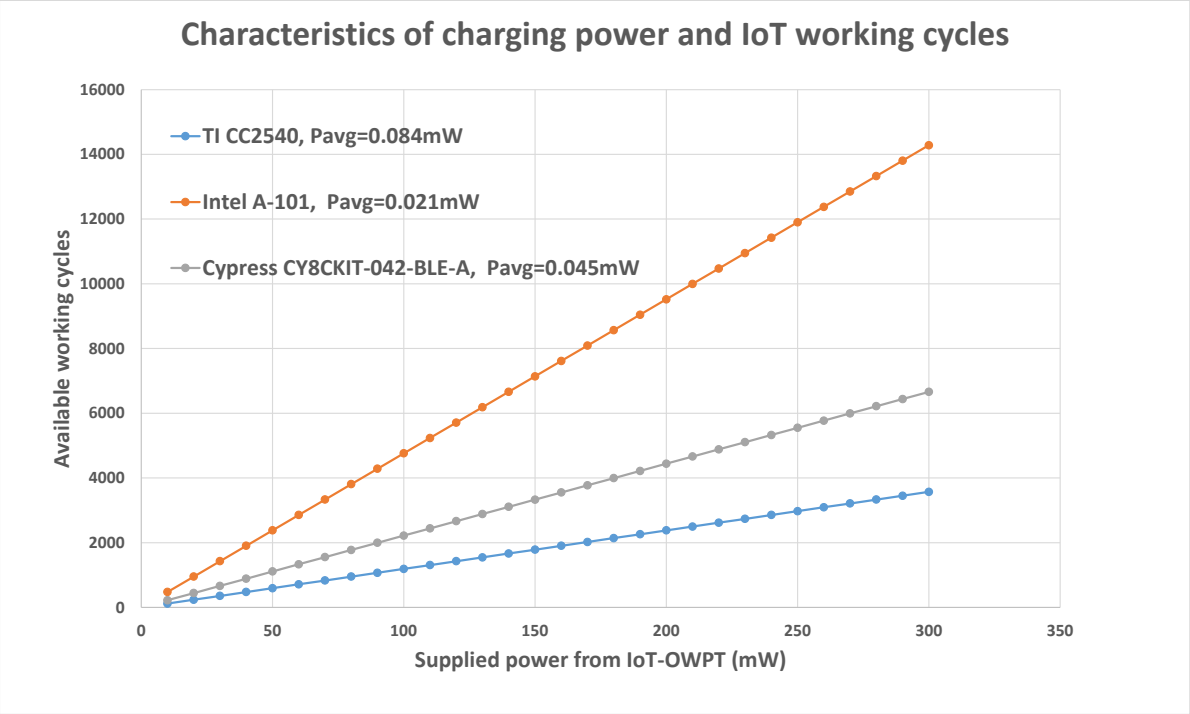

Fig. 2.7 Characteristics of charging power and IoT working cycles

The next consideration of IoT-OWPT system is the transmission distance. The sufficiently long transmission distance allows users to reduce extra movement, and increases the available space of power transmission. Generally, as a long-distance wireless power transmission device, the transmission distance should be as far as possible. However, for the LED-based OWPT system that specially designed for IoT terminals, the designed transmission distance should not be too far, and the reasons are mainly divided into two. The first reason is the LED-based OWPT system which designed for too long transmission distance will lose portability. As discussed in section 2.1.2, an optical system configuration for specific transmission distance and specific target irradiation size is indispensable when designing LED-based OWPT system. In the cause of ensuring the irradiation size is small enough, the dimension of LED-based OWPT system will increase rapidly with the extension of the designed transmission distance, and thus become no longer portable. Therefore, the pursued portability of the LED-based OWPT system inherently limits the possibility of a particularly long

transmission distance. Secondly, in the case of human-hold or installed on drone, tremor may occur during power transmission, which will cause the irradiation displacement at target distance. The tremors are usually divided into panning direction and angular direction. The effects from panning direction on irradiation displacement is relatively low, which is usually in the range of several millimetres, and the degree of the displacement will not exacerbate with the increase of transmission distance. However, in the cause of angular direction tremor, the displacement of the irradiation will increase proportionally with the increasement of the transmission distance. In short-distance (up to 3 m) power transmission scenarios, the negative effects caused by tremor can be solved by simple methods such as slightly increasing the size of receiver, while under very long transmission distance conditions, such negative effects can only be solved by installing extra modules such as beam scanning function or anti-tremor function. Thereby, the transmission distance of portable LED-based OWPT system specially powering compact IoT should be designed in a proper range. By various simulation and experiment data, 100 mm – 3 m is believed as the appropriate transmission range of portable LED-based OWPT system.

In addition, there are some unique situations and issues in the application scenario of powering IoT by IoT-OWPT system, such as the tremor problem that has been already mentioned in previous part of this section, the reflection loss at the receiving side under the condition of oblique irradiation, and the method of achieving accurate focusing when the light source is invisible light. These are all points that need to be solved in practical applications. The detailed discussion and analysis on them will be shown in the later chapters of the paper.

2.2 Investigation of OWPT light sources

Although in this study, it has been determined that using LED as the light source of the portable OWPT system, and the reasons and feasibility are briefly explained in section 1.3, based on the particularity of the OWPT application, it is also necessary to systematically investigate and compare the typical light sources from the aspects of light output, electro-optical conversion efficiency,

centre wavelength, width of spectrum (monochromaticity), beam characteristics, and dimension of light source. The term of “light source” consists of various categories based on different light emitting principles. Emitting based on combustion such as sunlight, candles and gas lamp, and lighting devices including incandescent lamp, fluorescent lamp and discharge lamp are traditional light sources. Currently, the semiconductor light sources are also commonly used everywhere.

Table 2.1 The typical categories of light sources

Categories	Light source	Efficiency (%)
Combustion	Candle	0.04
	incandescent gas mantle	0.2
Incandescent light bulb	Incandescent lamp	1-2
	Halogen lamp	2-3
Fluorescent tube	Hot cathode fluorescent lamp	10-15
Discharge lamp	High-pressure mercury lamps	5-10
	Metal halide lamp	15-20
Amplified spontaneous emission	Superluminescent diode	20-50
LED	White LED	30-40
	Monochromatic LED	10-50
Laser	Semiconductor laser	30-70
	Photoexcitation laser	20-50

The Table 2.1 lists main types of light sources and their corresponding efficiency.[6] In the application of optical wireless power transmission, the light source needs satisfy the features of:

- Easy beam forming
- High intensity output
- High conversion efficiency
- Monochromaticity

Many of the above features are interrelated in OWPT applications. For instance, a certain kind of light source has very high intensity output, however the beam cannot be formed as sharp beam, or its spectrum width is too large, then the receiver is unable to convert sufficient power for the load. Therefore, in theory, the light source of OWPT system is required to meet all the above characteristics at the same time. The applications of most light sources listed in Table 2.1 are designed only for illumination, so their original design is to maximize the brightness, expand the divergence angle and make the distribution uniform.[7] Those light sources include various traditional types of incandescent bulb, fluorescent tube and so on. The beam of such kind of light sources is not easy to control, and the spectrum is too width to ensure monochromaticity, hence low photovoltaic conversion efficiency on receiver side is predictable. Besides, their optical conversion efficiency is very low, generally. Light sources with a conversion efficiency of about 10% or less are considered to have problems in applicability when considering the purpose for the power supply function. Thereby, such illumination light sources are believed not suitable to be applied as an effective light source of OWPT technology.

Superluminescent diode (SLD) is an edge-emitting semiconductor light source based on superluminescence, and developed rapidly in recent years.[8][9][10][11] It combines the high power and brightness of laser diodes with the low coherence of coherence of conventional light-emitting diodes. As a new type light source, when an electrical forward voltage is applied an injection current across the active region of the SLD is generated. Like most semiconductor devices, a SLD consists

of a p-doped section and a n-doped section. Electric current will flow from the p-doped section to the n-doped section and across the active region that is sandwiched in between the two sections. During this process, light is generated through spontaneous and random recombination of negative electrons and positive holes and then amplified after passing through the waveguide. Unlike laser diodes, SLDs are designed to have only one-time single pass amplification for the spontaneous emission generated along the waveguide, thus insufficient feedback to achieve lasing action.[12] Therefore, comparing with the laser diodes, the output power of the SLDs is generally lower when the drive current is the same, which means lower electro-optical conversion efficiency. Besides, the p-n junction of the SLD is designed in the way that electrons and holes have multiple possible states with different energies. Therefore, the recombination of electron and holes generates light waves with a broad range of frequencies, which means the light emitted from a SLD has a broadband spectrum. In summary, SLD is a light source with the characteristics between LD and LED. It is based on amplified spontaneous emission (ASE), and has high spatial coherence and low temporal coherence, which means that it has similar monochromaticity with LED, while its directionality property is close to LD.[13] In terms of characteristics, SLD has the possibility of becoming a light source of OWPT system. However, the output power of the SLDs that existed in commercial market is insufficient, usually in the range of tens to dozens milliwatts, and the efficiency is not outstanding as well.[14][15][16] The essential reason is the current research on SLD technology is far from insufficient. The research progress and number of publishes of SLD is much lower than that of LED and LD, which can be attributed to the insufficient attraction of SLD to scholars and the market. If take this factor into consideration, the progress of performance improvement for the OWPT system based on SLD may be slow in the next few years or decades. Therefore, SLD has the potential and possibility as the light source of OWPT system, but it is not the proper choice under the existing technology.

Combining all typical light sources, laser and LED are the proper light source for OWPT system. Both laser and LED meet the requirements of easy beam forming,

high output, high conversion efficiency and monochromaticity. It should be note that the term “easy beam forming” dose not exactly equal with “high directionality” here. The typical LEDs for illumination purpose usually have half-angle over 40 degrees, and the semiconductor laser with several micrometre square aperture commonly has divergence angle in the range of 20 – 40 degrees. However, a first-order lens, or packaged lens is usually installed on the LED chips and easily control the divergence angle in proper range, and the high spatial coherence of laser makes accurately beam arrangement to be possible. Thus, even large divergence angle is common of LED and laser, them all satisfy the requirement of “easy beam forming”.

According to the gain medium, lasers can be divided into gas lasers, solid-state lasers, semiconductor lasers and dye lasers, and besides, free-electron lasers have been developed recent years. However, due to the merits such as mature technology, rapid development, low cost, small products, and most importantly, relatively high overall-efficiency compared with other lasers, semiconductor laser, or laser diode (LD) is believed as best choice among laser categories.[17] Although there are other types of laser has unique features and is valuable and potential to be applied in OWPT system, such as the fibre laser that is able to obtain excellent light beam quality with high output in a relatively small size,[18][19] the principle and designing of them as light source in OWPT application is similar with semiconductor laser. Considering this research is using LED as the target light source of the portable OWPT system and studies its feasible performance and potential application scenarios under current technology and in the future prospects, this paper only uses semiconductor laser as the representative of all lasers, and then compare with LED. In the following sections of this thesis, the term “laser” only represents the semiconductor laser. Other types of lasers will be expressed in full names, such as “solid-state laser”.

In addition to the advantages that stated above, both LEDs and LDs has the merits of micro devices and direct driven by electricity, which makes simple configuration and small modules is possible. Currently, as high-power light source, LEDs are mainly used for illumination and displays, and semiconductor

lasers are used for processing, heat treatment, photoexcitation, lighting, displays, optical plate radar, and various sensing. Since research and development are becoming more active in response to these market expansions, characteristic improvement of them is still progressing rapidly. In the next few years, several times or even dozens of times of output improvement for both LEDs and LDs can be expected. Therefore, they considered to be effective light source for portable OWPT.

From the above viewpoints, in the follow part of this section, the detailed investigation and study of the basic principles, structure, materials, designing of laser and LED will be shown, as well as the characteristics related with the OWPT system performance, such as intensity output, directionality, efficiency, and temperature sensitivity. Finally, it is necessary to focus on the detail information of various severe regulations of laser products, and discuss the possible hazard of lasers in order to explain reason and necessity of this research that focusing on the OWPT system with LEDs as the light source.

2.2.1 Semiconductor laser

The laser diode is a light source semiconductor laser invented in the 1960s, also known as laser diode. LASER is an abbreviation of "Light Amplification by Stimulated Emission of Radiation", usually abbreviated as LD. Since it can produce light with exactly the same properties such as wavelength and phase, high coherence is its biggest feature.

The Fig. 2.8 can be used to explain the basic light-emitting principle of semiconductor. The p-n junction in the laser diode is formed by two doped semiconductor layers, and a depletion region is formed between the n-type semiconductor and p-type semiconductor as a result of the difference in electrical potential between two semiconductor layers where they are in physical contact. In the depletion region, there is no charge carrier existed. When the p-n junction is forward electrical biased by an external power source, the holes and electrons are injected from opposite sides of the p-n junction into the depletion region. Holes are injected from the p-doped, and electrons from the n-doped,

semiconductor. When an electron and a hole are existing in the same region, they will randomly recombine and emit a photon with energy equal to the difference between the electron's original state and the hole's original state. This is the process of spontaneous emission.[20] On the other hand, when the current density is increased and the accumulated carrier concentration becomes sufficiently high, the light emitting layer has a light amplification characteristic based on the stimulated emission.[21][22] Stimulated emission is a phenomenon that before electrons and holes recombine, a nearby photon with energy equal to the recombination energy can cause recombination by stimulated emission. This generates another photon with the same frequency, polarization, phase and propagation direction as the original photon. Thereby, the stimulated emission will cause amplification of the light beam in the injection region, and such gain enhances with the increasing number of electrons and holes inject into the junction. Then, some photons randomly drifting in the depletion region and hit the highly reflective mirror of optical cavity vertically and reflect back along their original path. The reflected photons are reflected again on a reflector at the other side of the optical cavity and such process will repeat innumerable time. This process is called laser oscillation. During the movement of photons, more and more photons are generated due to the avalanche effect. Finally, a certain portion of the intracavity beam is allowed to transmit through at the partially reflective mirror as the laser beam.

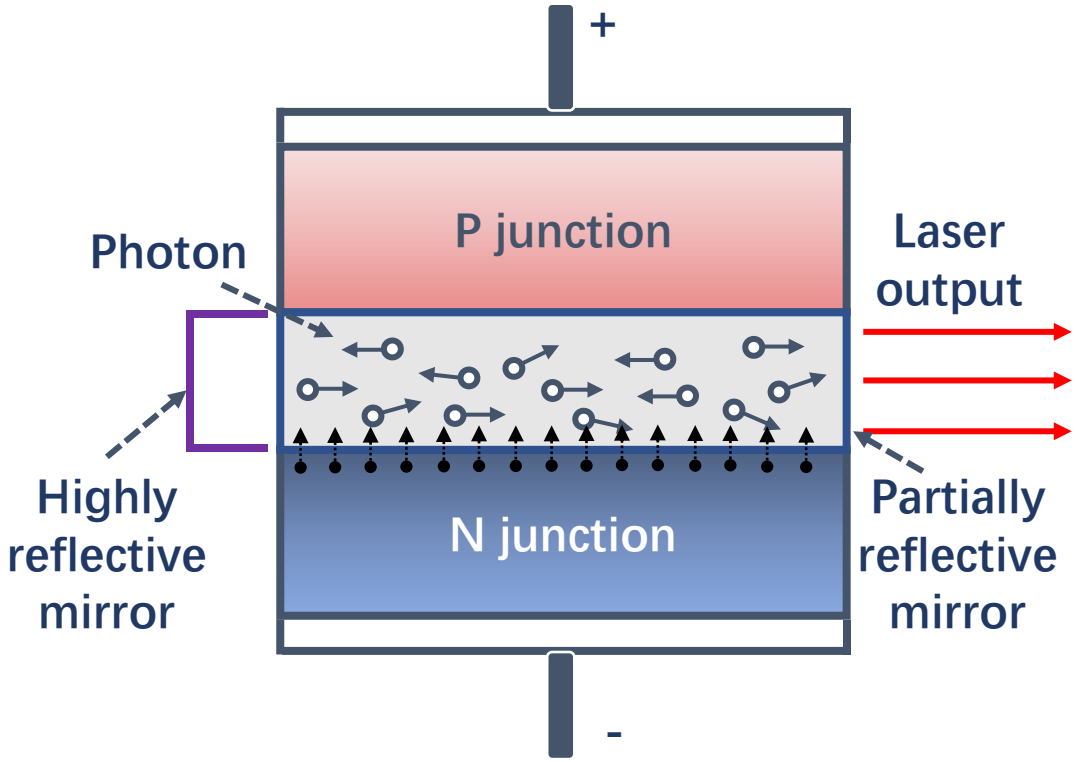

Fig. 2.8 Schematic diagram of laser construction

On the principle of light emission, the LD emits light based on stimulated emission, and all photons have the same frequency, polarization and phase, thus high coherence is available. In terms of architecture, the LD has an optical cavity, so the avalanche effect can excite more photons during the process of photon reflection in the optical cavity. In order to form a stable oscillation, the laser medium must provide enough gain to compensate for the optical loss caused by the cavity and the laser output, and continuously increase the optical field in the optical cavity. This requires a sufficiently strong current injection, which is enough population inversion. The higher the population inversion degree, the greater the gain obtained, that requires a certain current threshold condition. When the laser reaches the threshold, light with a specific wavelength can resonate in the optical cavity and be amplified, and finally form a laser and output continuously. Because of the resonation and amplify, LD can produce very high intensity output.

Similarly, the output of the LD can be enhanced by increasing the injection current. The Fig. 2.9 shows the current-optical output characteristics (I-L characteristics) of a semiconductor laser. Generally, the conversion efficiency of the injected energy amount to the optical output (dP/dI) is important. On the other hand, the temperature rise due to the heat generated by the diode is a major factor that constrains its optical output. Therefore, it is important to reduce the threshold value that essential to laser oscillation in order to reduce energy that is ineffective for laser emission to suppress heat generation.

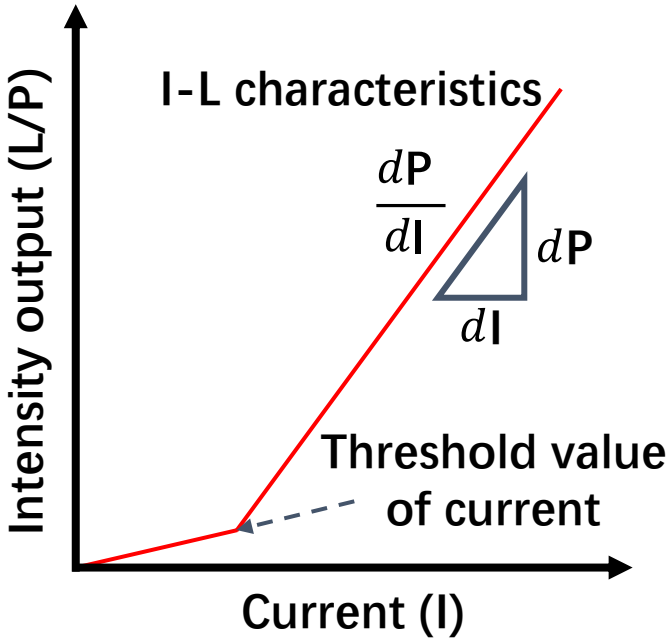

Fig. 2.9 The current-optical output characteristics (I-L characteristics) of LD

There is a great variety of different semiconductor lasers, spanning wide parameter regions and many different application areas:

- Edge emitting laser diodes: the laser output is emitted from the edge surface of the laser diode, and the laser beam is generally high quality and a few milliwatts output power. The edge-emitting laser diodes are

commonly used in laser pointers, in CD players, and for optical fibre communications.

- External cavity diode lasers: such laser contain a laser diode as the gain medium of a longer optical cavity, which often have the merits as tuneable wavelength, relatively ease-of-use and low price. External cavity diode lasers are commonly used in laboratories.

- Broad area laser diodes: they are edge-emitting laser diodes with an emitting region has the shape of a broad stripe. The output power is usually high (a few watts), while the beam quality is relatively poor. They are often used for pumping solid-state lasers.

- High-power diode bars: a one-dimensional array of broad-area emitters is contained in this laser, and tens of watts laser output with poor beam quality is available with such lasers. They are often used for welding, surface treatments and medical lasers.

- High-power stacked diode bars: they contain a number of diode bars which are arranged in the form of a stack. They can generate extremely high output power (hundreds or thousands of watts), however the beam quality is also poor, which is much lower than single diode bar. They are often used for welding, hardening, alloying and cladding of metallic surfaces.

- Surface emitting lasers (VCSELs): the direction of laser output is perpendicular to the wafer, with a lower output power (a few milliwatts) and high beam quality. They are often used for sensing, detecting, scanning and LiDAR.

- Optically pumped surface-emitting external-cavity semiconductor lasers (VECSELs): they are the semiconductor lasers based on surface-emitting semiconductor gain chip and laser resonator. The laser output are usually a few watts power with excellent beam quality. They are often used for projection displays.

- Quantum cascade lasers: they are a special kind of semiconductor lasers and usually emit mid-infrared light, sometimes in the terahertz region. They are commonly used for trace gas analysis.

In this thesis, according to factors such as suitability of OWPT application and cost, the main discussion is focused on edge emitting laser and surface emitting laser. The Fig. 2.10 shows the schematic diagram of two configurations. They have the individual advantages and disadvantages, the brief discussion on the two configuration LD will be shown below.

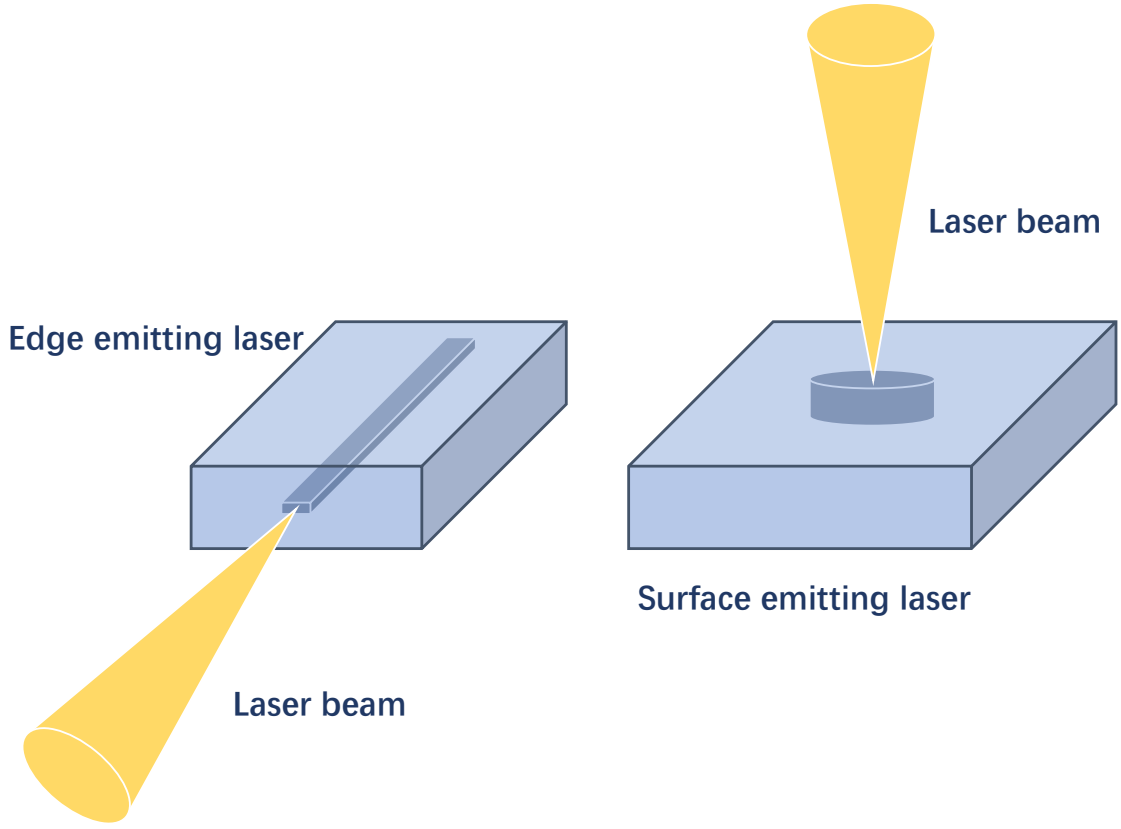

Fig. 2.10 Constructions of edge emitting laser and surface emitting laser

In an edge emitting laser, the light is reflected in the optical cavity horizontally, and emitted from the edge surface. The optical cavity of the edge emitting laser is a Fabry-Perot cavity, and its end surfaces act as reflectors.[23][24] The reflection of the light is caused by the index of refraction difference between the air and

gain medium. The edge emitting laser can host multiple modes during the operating, and due to its optical cavity is relatively long, high output power is available under the condition of single diode. Under single mode, a single edge emitting laser can achieve the output power from 1 W to several watts.

On the other hand, edge emitting laser has several drawbacks. First, because of the geometry of the design, the vertical thickness of the active region is small. Therefore, the emitted laser beam is not a perfect circular Gaussian beam, but deformed in one direction. This means the beam quality of edge emitting laser is relatively low. Second, in edge emitting laser, it is usually cleaving the semiconductor wafer to form the specularly reflector. Since the end facets are created by cleaving, a high degree of smoothness is hard to obtain. Moreover, edge emitting lasers also suffer from catastrophic optical damage (COD) at the facets, which will deteriorate the reliability of the laser.

In addition to the edge emitting laser that emits light from the edge of the semiconductor laser, the surface emitting laser such as the Vertical-Cavity Surface-Emitting Laser (VCSEL) is a kind of semiconductor laser that emits light from the surface of the substrate. Due to various merits, a large market of surface emitting laser has been formed in recent years.[25][26][27] The main gain medium of surface emitting laser is a series of quantum wells, and Bragg reflectors are configured as the reflection mirror for achieving compact setup.[28] Unlike the edge emitting laser that the light is reflected horizontally, the light in the surface emitting laser bounces up and down. The surface emitting laser has many merits such as high productivity, high stability, low cost comparing with edge emitting laser. Besides, the surface emitting laser do not suffer from COD like edge emitting laser due to the end facets are designed differently with edge emitting laser.[29] The low output power is the main drawback of surface emitting laser. Since the main VCSEL is realized as a minute device with a light emitting area diameter of about 3-15 μm, it is used as a low power consumption laser whose light output is 1-2 orders of magnitude smaller than that of milliwatt. Due to such low power consumption characteristic, it is practically used for short-distance communication as well as sensor applications such as laser mouse or LiDAR.

However, although output power of a single VCSEL is relatively low, separately from independent drive, a two-dimensional array can be formed on one semiconductor chip.[29] By integrating and manufacturing a large number of single VCSELs as shown in Fig. 2.11, it is possible to effectively increase the area and achieve high output. According to the number of integrated chips, a light output of several watts to thousands of watts can be obtained. On the other hand, such approach of array will destroy its coherence characteristic.

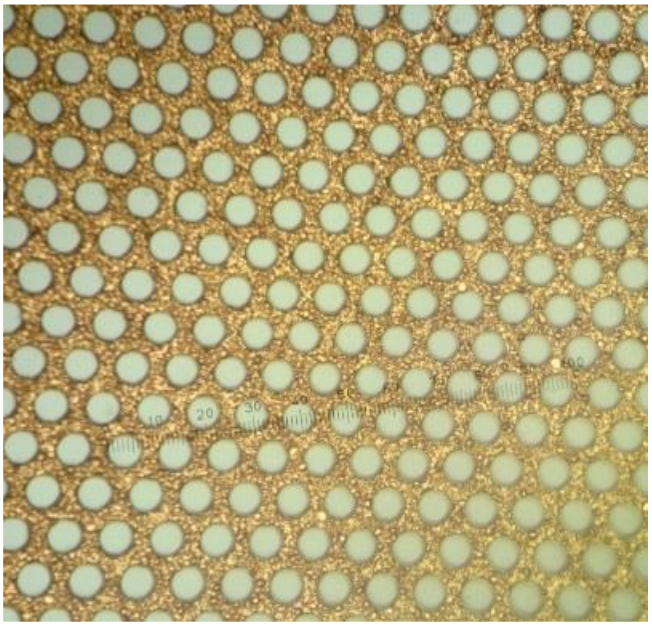

Fig. 2.11 Micrograph of two-dimensional VCSEL array

In addition to the VCSEL array that integrates a large number of minute VCSELs, there are cases where a large VCSEL with a diameter of several 100 μm class is designed as a single device.[30] However, non-uniformity of current injection is likely to occur if the diameter is increased, and heat dissipation in the central part is also likely to be an issue. In addition, for such kind of large VCSEL, the optical beam is also difficult to control.

The Fig. 2.12 shows the relationship between the VCSEL chip area and optical output. It can be confirmed that the optical output of VCSEL is roughly

proportional to the chip area. In VCSELs, heat dissipation is as important as the edge emitting laser. Optical output is closely related to efficiency and heat dissipation. There is room for improvement in efficiency of VCSELs, and an increase in optical output can be expected while maintaining the area.

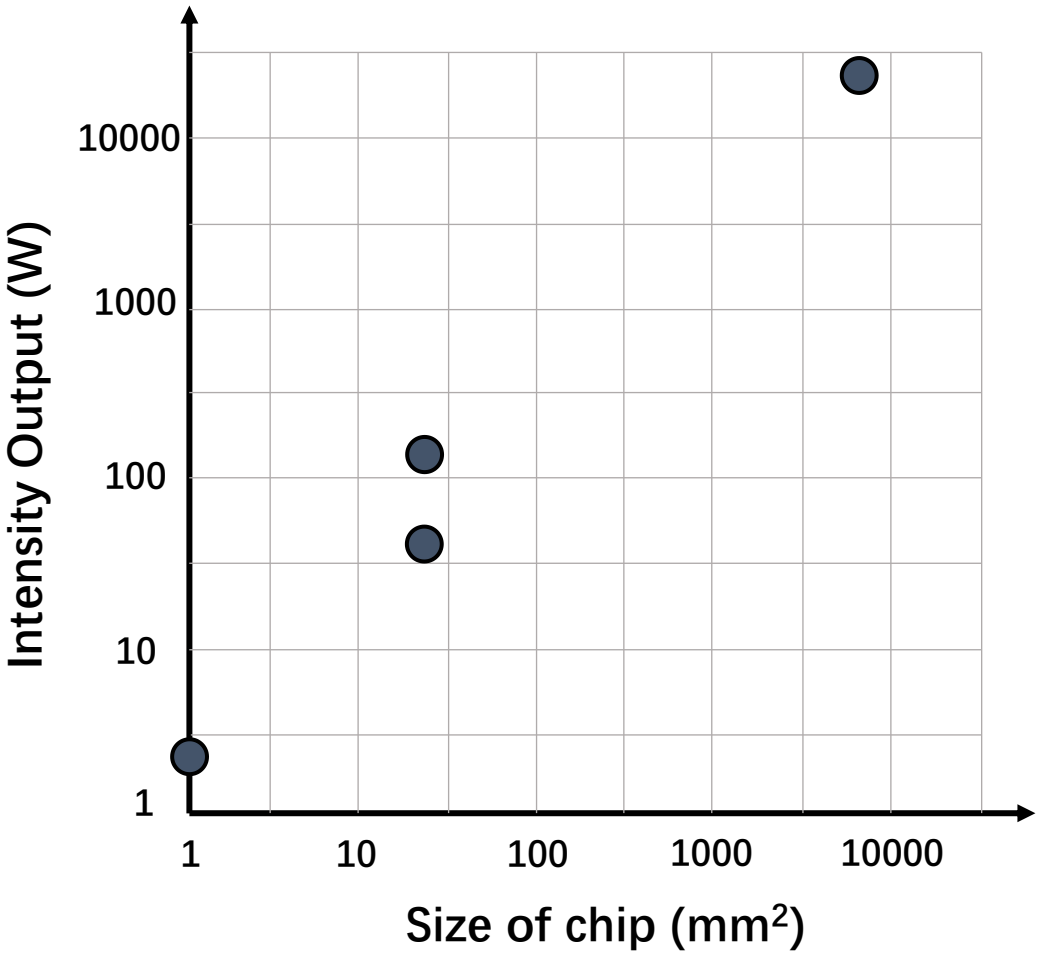

Fig. 2.12 Characteristics of the intensity output and chip size of the commercial VCSEL array

Common materials for semiconductor lasers (and for other optoelectronic devices) are GaAs (gallium arsenide), AlGaAs (aluminum gallium arsenide), GaP (gallium phosphide), InGaP (indium gallium phosphide), GaN (gallium nitride), InGaAs (indium gallium arsenide), GaInNAs (indium gallium arsenide nitride), InP (indium

phosphide), GaInP (gallium indium phosphide). These are all direct bandgap semiconductors. Indirect bandgap semiconductors such as silicon do not exhibit strong and efficient light emission. As the photon energy of a laser diode is close to the bandgap energy, compositions with different bandgap energies allow for different emission wavelengths. As for semiconductor laser, a wide range of wavelengths is accessible with different devices, covering much of the visible, near-infrared, and midinfrared spectral region. Some devices also allow for wavelength tuning. The Table 2.2 shows the major LD materials and corresponding wavelength.[31]

Table 2.2 Major LD materials and corresponding wavelength

Material	Wavelength range
AlGaN	350-400 nm
GaInN	375-440 nm
ZnSSe	447-480 nm
ZnCdSe	490-525 nm
AlGaInP/GaAs	620-680 nm
$Ga_{0.5}In_{0.5}P$/GaAs	670-680 nm
GaAlAs/GaAs	750-900 nm
GaAs/GaAs	904 nm
InGaAs/GaAs	915-1050 nm
InGaAsP/InP	1100-1650 nm
InGaAsSb	2000-5000 nm
PbCdS	2700-4200 nm
Quantum cascade	3000-50000 nm
PbSSe	4200-8000 nm
PbSnTe	6500-30000 nm

PbSnSe	8000-30000 nm

Apart from the above-mentioned inorganic semiconductors, organic semiconductor compounds might also be used for semiconductor lasers.[32] However, the corresponding technology of organic semiconductor is still immature, but it has been developed due to it has found an attractive prospect for mass production with low prices. So far, only optically pumped organic semiconductor lasers have been demonstrated, whereas for the electrical pumping organic semiconductor lasers, it is difficult to realize high efficiency.

2.2.2 Light-emitting diode

The light-emitting diode (referred to as LED) is a semiconductor electronic component that can convert electrical energy into optical energy. The electronic component of light-emitting diode appeared as early as 1962, and it could only emit infrared light with low intensity.[33] Then, the LED was later developed in other monochromatic colours. Today, the available spectrum of LED has spread to visible light, infrared and ultraviolet light, and the intensity has also increased to a considerable level. At present, LED have been widely used in indoor and outdoor lighting, displays, traffic lights, automotive lights, TFT-LCD display backlights, optical fibre communications, and so on.

The emitting principle of LED is spontaneous emission, which is exactly the same as the first-stage light emitting of the LD. Like ordinary diodes, LEDs are composed of a P-N junction and also have unidirectional conductivity, but the difference point is LEDs can emit light. The schematic illustration of the LED light emitting is shown in Fig. 2.13. The p-n junction is a combination of an n-type semiconductor with majority electrons (negatively charged) and a p-type semiconductor with majority holes (positively charged). When a forward voltage is applied to the semiconductor, electrons and holes will move and recombine at the junction. It is in the process of recombining that a large amount of energy is generated, and this energy is released in the form of light. Compared with

traditional light sources (such as incandescent lamps) that first convert electric energy into heat and then into light energy, LEDs can achieve high efficiency, because electric energy can be directly converted into light energy, skipping the additional conversion into heat which will cause extra energy wasted.

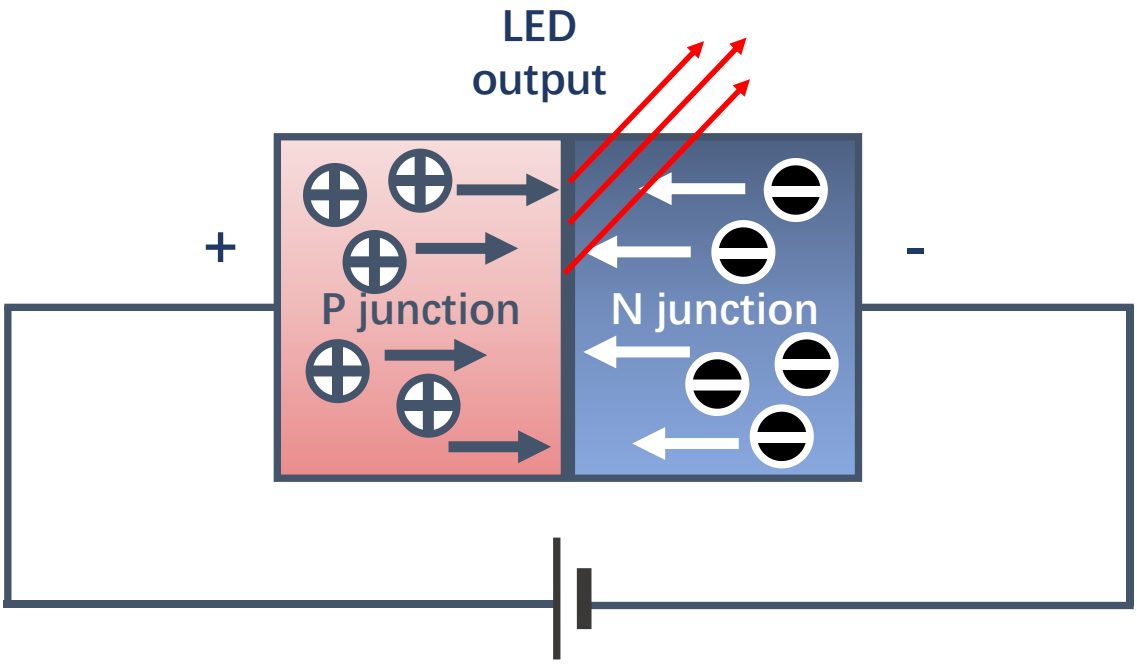

Fig. 2.13 Schematic diagram of LED construction

Throughout the history of LED development, there are several important turning points. Although LED appeared as early as 1962, it could only emit low-intensity infrared light in the early days, so it was only used in remote control circuits or as indicator lights, and could not be used for lighting application.

In the 1970s, breakthroughs were made in the research and development of LEDs. The efficiency of the LED based on GaAsP material reached 1 lm/W by using the nitrogen doping process, and they were able to emit red, orange and yellow light. Subsequently, the GaP green chip LED was developed. By the end of the 1970s, LEDs had appeared in red, orange, yellow, green, emerald and other colors. In the mid-1980s, the use of gallium arsenide and aluminum

phosphide led to the birth of the first generation of high-brightness red, yellow, and green LEDs, with a luminous efficiency of 10 lumens/watt. However, there are still no blue and white LEDs at this time. Because only the invention of blue LED can realize full-color LED display, which has huge market value.

In 1993, during his inauguration at Nichia Corporation in Japan, Shuji Nakamura successfully invented the blue LED based on semiconductor materials of gallium nitride (GaN) and indium gallium nitride (InGaN) by infiltrating nitrogen into semiconductor materials. Before it appeared, because the white light could not be synthesized through the RGB system, the light effect and brightness of the LED were not high, thus the LEDs could not be used in the field of lighting. Therefore, in 1995, Shuji Nakamura used indium nitride to invent the high-intensity green LED. Then in 1998, white LEDs were made by integrating the red, green, and blue LEDs. Since then, the successful development of green and white LEDs marks the official entry of LEDs into field of lighting, which is the most critical milestone in the development of LED lighting.[34][35]

The wavelength of LED is determined by the energy required for electrons to cross the band gap of the semiconductor. Generally, a small semiconductor crystal with size ranging from 0.3×0.3 mm^2 to 2×2 mm^2 is configured in a LED light source, and the wavelength of the emitted light of the LED is determined by the band gap of such semiconductor. Specifically, the wavelength is decided by the required energy for electrons to cross the band gap. The most common crystals used in the LEDs are the mixtures of periodic table Group III and Group V elements, and by controlling the relative proportions of different semiconductor elements and adding different dopants to change the electronic properties of the crystalline lattice, the emission light output with different wavelength can be realized. Unlike the monochromatic LED, white LED is realized by using multiple semiconductors or adding light-emitting phosphor in the blue LED. The Table 2.3 shows the inorganic semiconductor materials used in traditional LEDs and the corresponding colours.[36]

Table 2.3 Colour, wavelength and corresponding materials of typical LEDs

Colour	Wavelength	Materials
Ultraviolet	395 nm	InGaN/SiC
Blue Violet	430 nm	GaN/SiC
Super Blue	470 nm	GaN/SiC
Green	520 nm	InGaN/Sapphire
Pure Green	555 nm	GaP/GaP
Green-Yellow	567 nm	GaP/GaP
Yellow	585 nm	GaAsP/GaP
Orange	605 nm	GaAsP/GaP
Super Orange	612 nm	AlGaInP
Super Red	633 nm	AlGaInP
Ultra Red	660 nm	GaAlAs/GaAs
Near-Infrared	700 nm	GaP/GaP
Infrared	880 nm	GaAlAs/GaAs

Unlike a laser, the light emitted from an LED is neither spectrally coherent nor even highly monochromatic. However, its spectrum is sufficiently narrow that it appears to the human eye as a pure colour. The typical spectrum characteristic of LEDs is shown in the Fig. 2.14. The FWHM (full width at half maximum) of a typical monochromatic LED is usually in the range of 20 – 70 nm, and in the range or 535 nm to 585 nm spectrum range, the FWHM of LED is slightly wide, this is because that these LEDs configured a secondary phosphor that is excited by a violet or ultraviolet primary LED, thus the corresponding spectral profile is broadened and the output power is declined.

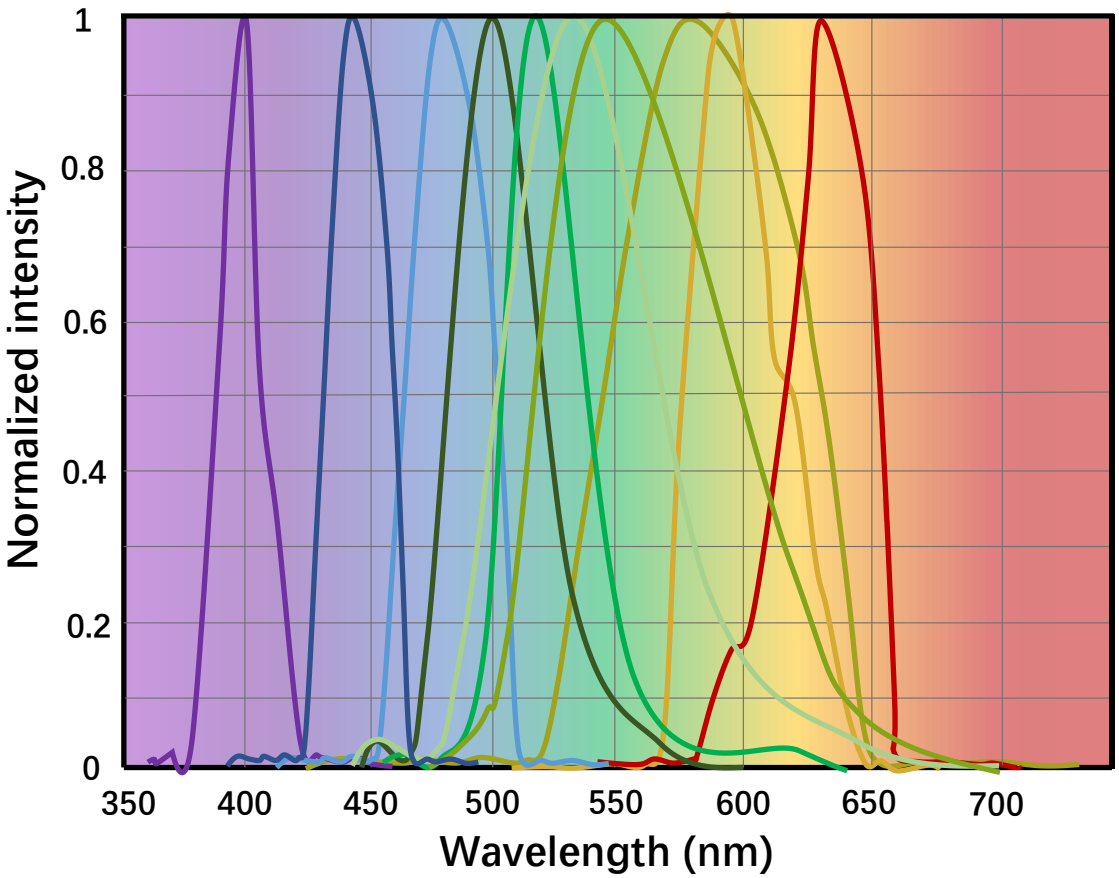

Fig. 2.14 Spectrum characteristics of LEDs

Unlike the monochromatic LED, the white LED usually has broad spectrum due to its special principle of illumination. Generally, the white light is generated based on different semiconductor materials that are monochromatic. There are two approaches of generating white lite. The firs method is combining three different diodes in a single envelope, or different monochromatic semiconductor materials in a single chip. The second approach utilizes a violet or ultraviolet LED to excite a secondary phosphor, then the mixed light tends to appear white colour. The Fig. 2.15 shows the spectrum characteristics of the white LED based on two approaches.

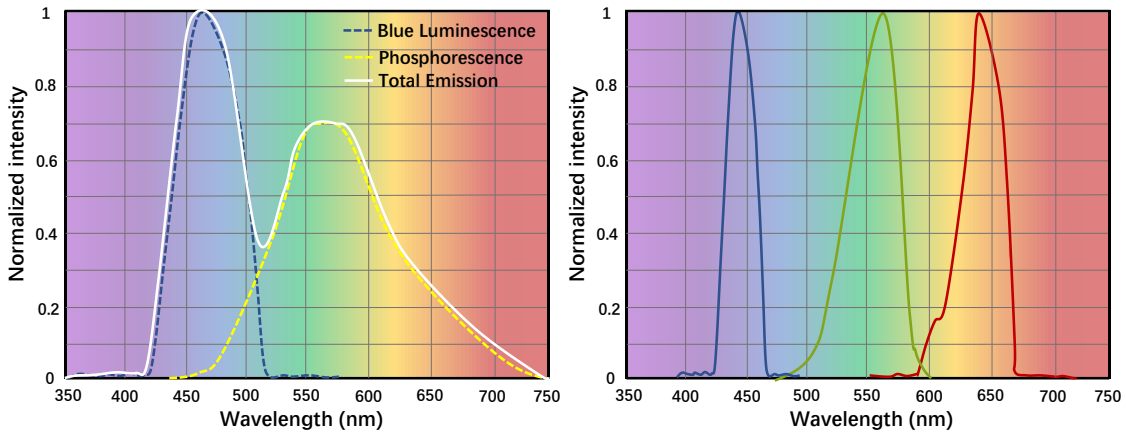

Fig. 2.15 Spectrum characteristics of white LEDs

There are several critical factors of the LED designing that will largely decide the characteristics of the LED, which are the elements used for the n-type and p-type semiconductors, the physical geometry, the designing of the package lens, and configuration of the light escape route. The basic constructure of a typical LED consists of a small size semiconductor crystal, which is the light-emitting chip, a substrate for the semiconductor crystal to mount on, and in most cases, a package lens is applied on the substrate to rearrange the distribution of the emitting light rays.[37] The light-emitting chip of the LED has a size up to several mm^2, and the package lens varies between 2 mm to 10 mm. Generally, the cathode is attached on the bottom face of the substrate, while the anode is connected at the top face of the chip by a gold bonding wire. The grid electrode pattern and the position that the gold bonding wire connected will also influence the intensity distribution of the irradiation spot. Due to these different designs, the LEDs have various wavelengths, radiation pattern, shape and size. Most LEDs features a hemispherical geometry, while based on the requirement of the radiation pattern, rectangular, square, triangular, or polygonal geometry LEDs are also existed.

As shown in the Fig. 2.16, there are two kinds of popular LED package designs, which are the edge emitting LED (Fig. 2.16 (a)) and the surface emitting LED (Fig. 2.16 (b)). The edge emitting LED that shown in the Fig. 2.16 (a) is usually used

as the indicator lamp for the electronic appliances, while surface emitting LED that shown in the Fig. 2.16 (b) is usually used for lighting and displays applications. The Epoxy resins are usually for the package lens of both types LEDs. In the edge emitting LED, a reflector cup is usually configured inside of the package lens, and the light emitting chip is secured at the centre position of the conical reflector cup. The cathode lead is soldered on the reflector cup, while the anode is connected to the chip with a bonding wire.[38] The light emitted from the sides of the LED is reflected by the reflector cup and then propagates forward with a relatively small divergence. The schematic diagram of a flip chip surface emitting LED is shown in the Fig. 2.16 (b). Compared wit the traditional surface mount technology (SMT) LEDs, the flip chips diode is directly mounted on a heat sink slug that can be soldered onto a printed circuit board, therefore the heat dissipation is enhanced, and the light output can be improved around 15% as well. A silicon encapsulant is applied on the LED chip to restrain the total internal reflection of emitted wavefronts and improve the light extraction efficiency. The cathode is connected with the bottom surface of the chip directly, while the anode is connected with the top surface of the chip by a gold bonding wire.[39]

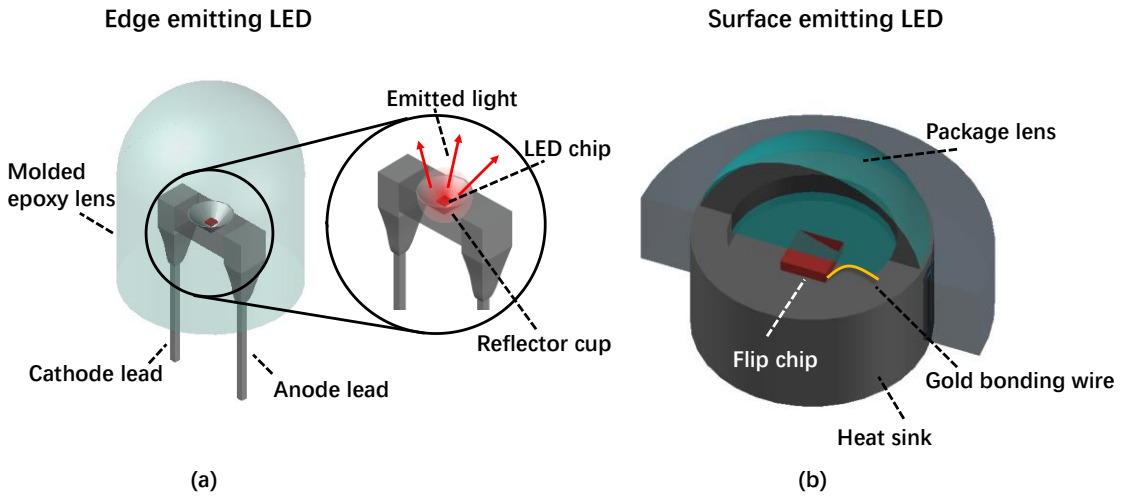

Fig. 2.16 Architecture of LED package designs

As for the characteristic of the radiation, the LED chip shows an emission profile of Lambertian emission pattern, of which the intensity propagates omnidirectionally with roughly same amount. Once the package lens applied on the LED chip, the intensity profile is inversely proportional to the divergence angle of the light rays, tends to show Gaussian distribution. Based on the structure of the package lens, most of surface emitting LEDs show wider divergence, while majority of the edge emitting LEDs has a very narrow or approximately collimated light beam due to a reflector cup is applied in order to collect the light from four sides of the chip, however the size of the irradiation spot will be enlarged accordingly. The edge emitting LEDs emit light from a small region on the sides of the chip in a complex pattern that axis-dependent. Therefore, the radiation pattern of the edge emitting LEDs is asymmetric, which has a fast axis and slow axis.

The radiation pattern of the LEDs is determined by the geometry of the package lens and the design criteria of the semiconductor crystal. The Fig. 2.17 shows the different designs of the package lens and the corresponding emission profile of LEDs. The planar, hemispherical and parabolic package lenses are shown in the Fig. 2.17 (a), Fig. 2.17 (b), and Fig. 2.17 (c), respectively. The corresponding emission profile of LEDs with different package lens is shown in the Fig. 2.17 (d). It is easy to find that the LED with parabolic package lens shows the best feature of high directionality. In addition to the geometry of the package lens, clear lenses without colour and any diffusion additives are another important factor to realize high intensity output, which is critical for the OWPT application. Besides, for adapting different application scenarios or design requirements, custom-shaped package lens or lensless LEDs will be another important factor. At current stage, there is no LED that specially designed for the OWPT application, however, it is expectable in the near future.

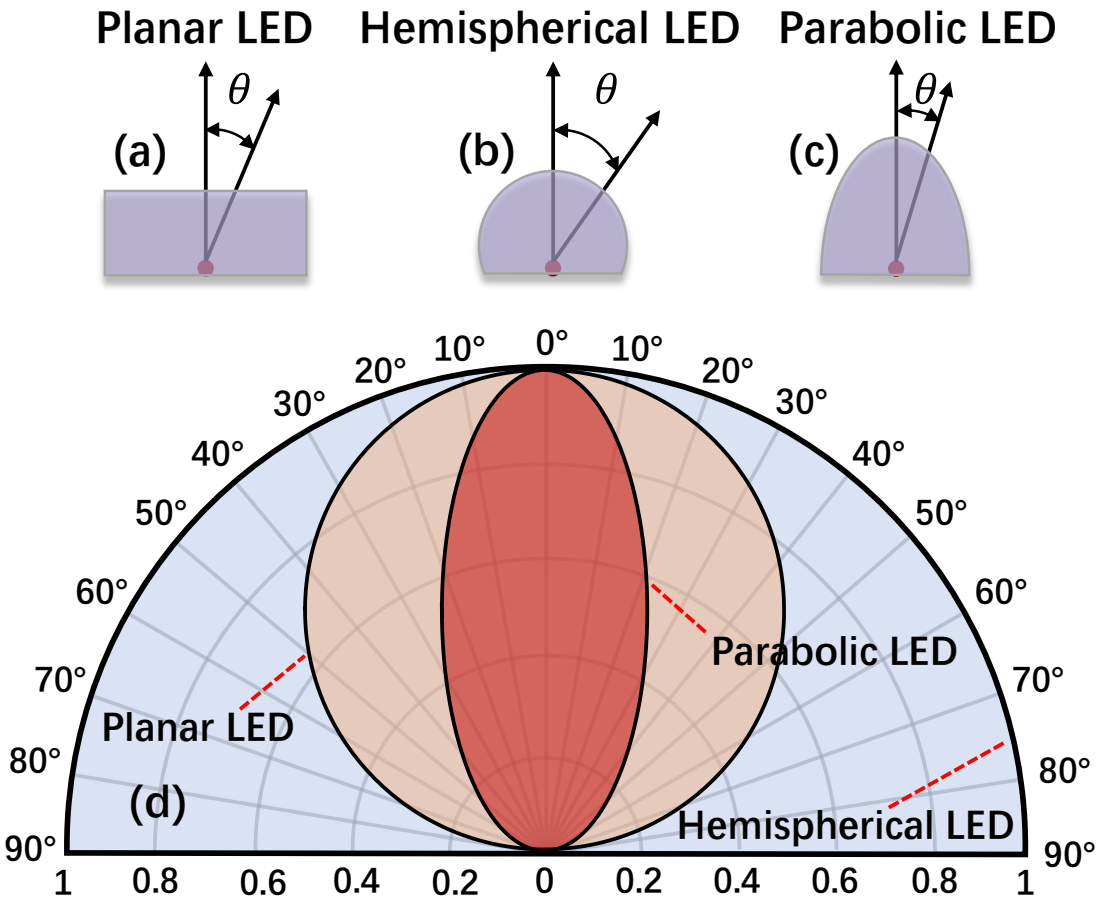

Fig. 2.17 Far-field emission patterns of LEDs with different package lens

In LED construction and design, the non-radiative recombination is one of the important factors that suppresses the maximization and extraction of the light output. Thus, one of the primary goals when designing the LED is to enhance the radiative recombination of charge carriers, which can be realized by choosing semiconductor materials and doping to improve quantum efficiency. On the other hand, maximizing the escape light is another important factor to enlarge the intensity output of the LED. Due to the chip of LED plays like a Lambertian object, the light emitted from the chip is isotropic in all directions.[40] Whereas, due to the total internal reflection (TIR) inside of the package lens, only a part of light component can be successfully escaped from the package lens and enter into the outside environment. Generally, around 50% of the intensity will be lost before

entering the outside environment due to the total internal reflection and other phenomena, and such value will decline if the light rays have larger divergence angle. According to Snell's law, only when the outgoing wavefronts intersects the interface between the two media at an angle less than the critical angle, can the light rays cross the interface from a medium with a higher refractive index to a medium with a lower refractive index.[41] The remained light will be lost in the primary medium. As a result, the light rays emitted from a LED chip will go through the total internal reflection loss twice before entering the external environment, the first loss occurs when the light emitted from the semiconductor crystal and enters into the package lens, and the second loss happens when the light escapes from the LED package lens to the external environment. The Fig. 2.18 shows the schematic diagram of the TIR loss during the light emitted from the LED chip and finally escaped into the external environment. As shown in the Fig. 2.18, the semiconductor layer has a refractive index n_s, while the package lens has a low refractive index of n_e. The light rays emitted from the LED chip at angles within the escape cone can cross the interface between the semiconductor layer and package lens with minimal TIR loss, while the rays with angles larger than the escape cone will suffer from the TIR at the interface and cannot enter into the package lens. When the light rays reach the boundary of the package lens, part of rays lost by the TIR again.[42] However, during this process, due to the curvature of the epoxy dome, most light rays reach the boundary of package lens at nearly right angle. Therefore, the TIR loss on the interface of package lens and external environment is relatively small, and majority of light rays can escape into the outside.

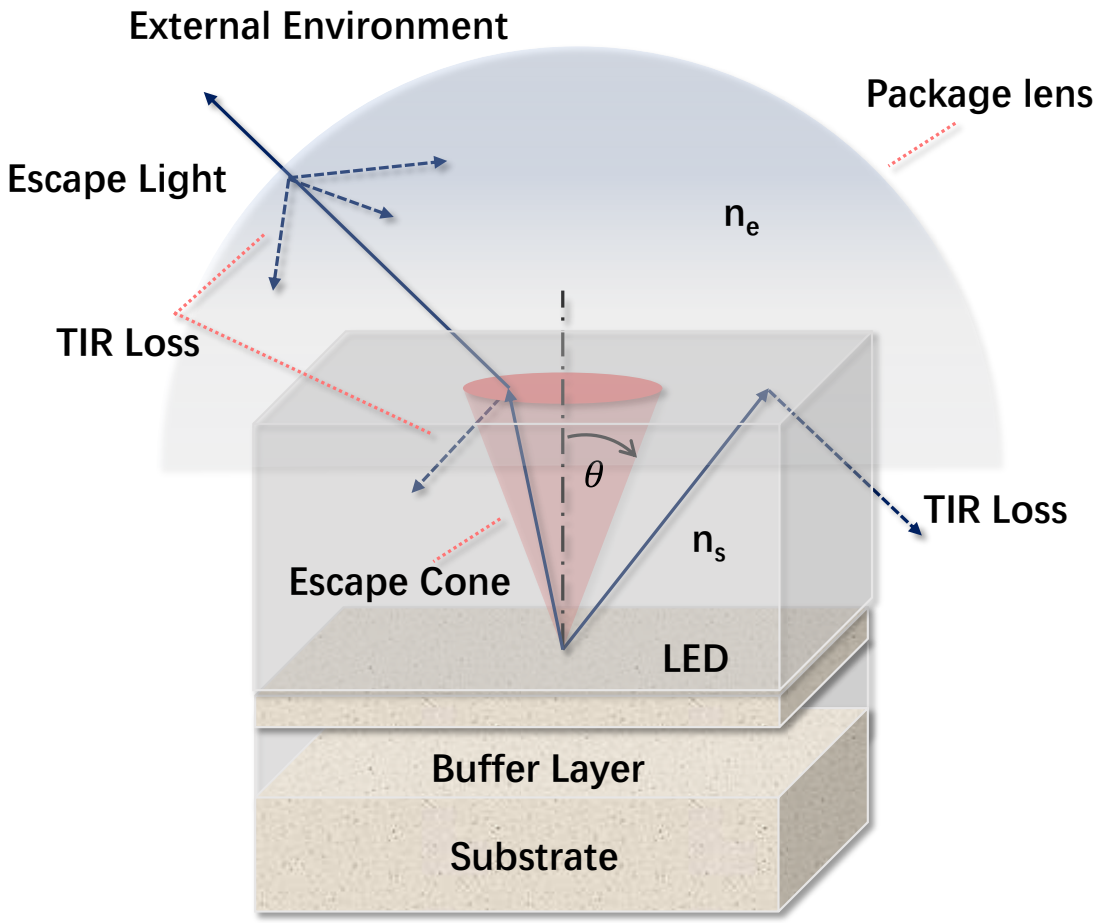

Fig. 2.18 LED light escape cone

As the energy source of the power supply system, the output power of the LED is one of the most critical factors. The output power of the LED is roughly proportional to the size of the active chip, and the output power of the currently commercially available high-power LEDs is around 1 W/mm^2. The Fig. 2.19 shows the output power of typical high-power LEDs with small active chip size.

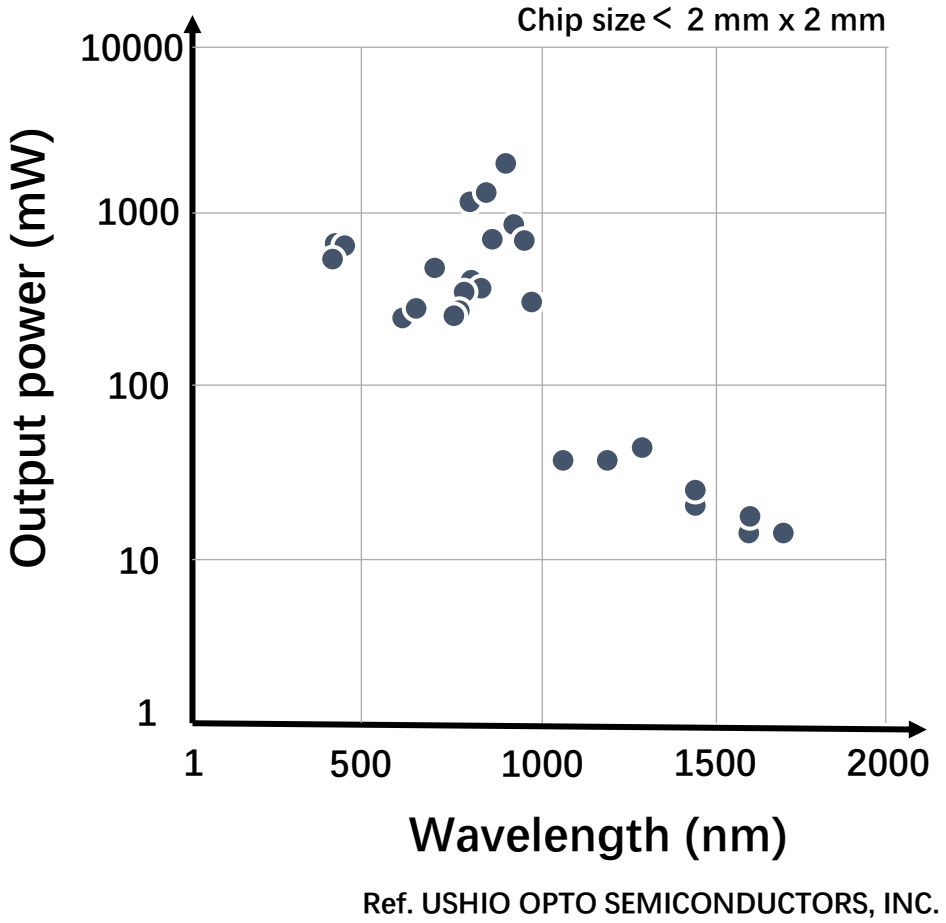

Fig. 2.19 Characteristics of output power of high-power LEDs in market

According to the Fig. 2.19, in the 800 nm – 900 nm region, the LED can achieve more than 1 W output intensity, and averagely 0.4 W is available in the region of visible light and infrared light. In order to enable existing LEDs to provide an output of more than several watts, the usual method is to increase the size of the LED chip or integrate multiple LED chips into one module. However, such high-output LEDs usually require high power consumption. As the electric current increases, the efficiency of the LED will decrease accordingly. Heating also increases with higher currents, which compromises LED lifetime. Most importantly, in the application of OWPT, the increasing size of emitting chip will rapidly enlarge the final irradiation size at the target transmission distance. Therefore, although the total intensity that can be obtained with a large-chip LED

is increased, under the IoT-OWPT application condition that the receiver size is assumed to be small and the intensity cannot be collected completely, the final output of the OWPT system may not be improved. On the contrary, the decrease in LED efficiency caused by the increase in current will reduce the overall efficiency of the OWPT system. Therefore, LEDs with such large-size chips are not the target light source of the OWPT system. The principle of selecting the LED as the light source of the OWPT system is that the size of the LED chip should be as small as possible while maintaining certain high output, high efficiency and high directivity.

2.2.3 Comparison between LED and LD in the application of OWPT

Based on the discussion stated above, the detailed comparison between LED and LD under the condition of OWPT application will be shown in this section.

First is the discussion of intensity output. Generally, under the premise of small size chip semiconductor devices, semiconductor lasers inject a high current density (10 kA/cm^2 class) into the light emitting region (active region). As a result, heat generation in a narrow area increases, so it is usually difficult to make the entire semiconductor chip emit light. On the other hand, since LEDs emit light with high efficiency at a low current density (10-100 A/cm^2 class), the heat generation density is also small, so it is common to emit light from the entire chip. Since the current density corresponds to the light output density, the difference in the light output density is about 2-3 orders of magnitude.

For both semiconductor lasers and LEDs, the temperature rise due to heat generation greatly affects the limitation of characteristics. Generally, LEDs emit light in the entire chip, and semiconductor lasers emit light in a region of several tens of percent from the chips. If assume that the efficiency of the entire semiconductor devices is equivalent, the difference of intensity output from LED and LD should be much smaller than the difference of current density. In other words, it is unlikely that there will be a large difference in the intensity output per chip size of LEDs and LDs. In fact, the LDs and LEDs that on the commercial market have a chip size of about 1 mm square and an intensity output of about 1

to several watts, and the difference in light output is at the level of several times. In summary, although the output of LED and LD is slightly different under the same size products, it can be said that the intensity output of two devices is on the same order of magnitude. The intensity output of LED and LD is proportional with the emitting area. In the case of integrating multiple chips to form an array, both LEDs and LDs can provide sufficiently high intensity.

The second discussion is the efficiency of light sources. The semiconductor light sources, including LED and LD, are current driven devices. The electro-optical conversion efficiency (PCE: power conversion efficiency, or WPE: wall plug efficiency) is the ratio between output intensity and input electricity power. The Fig. 2.20 shows the simple relation between the output intensity and input current. Generally, the diode in turned on and starts to realize light output when the input current is higher than the threshold current. The efficiency of the light source reaches the peak at a position relatively close to the threshold current. As the input current continuously increasing, the intensity output decreases as the junction temperature enhancing, thus the electro-optical conversion efficiency begins to decline.

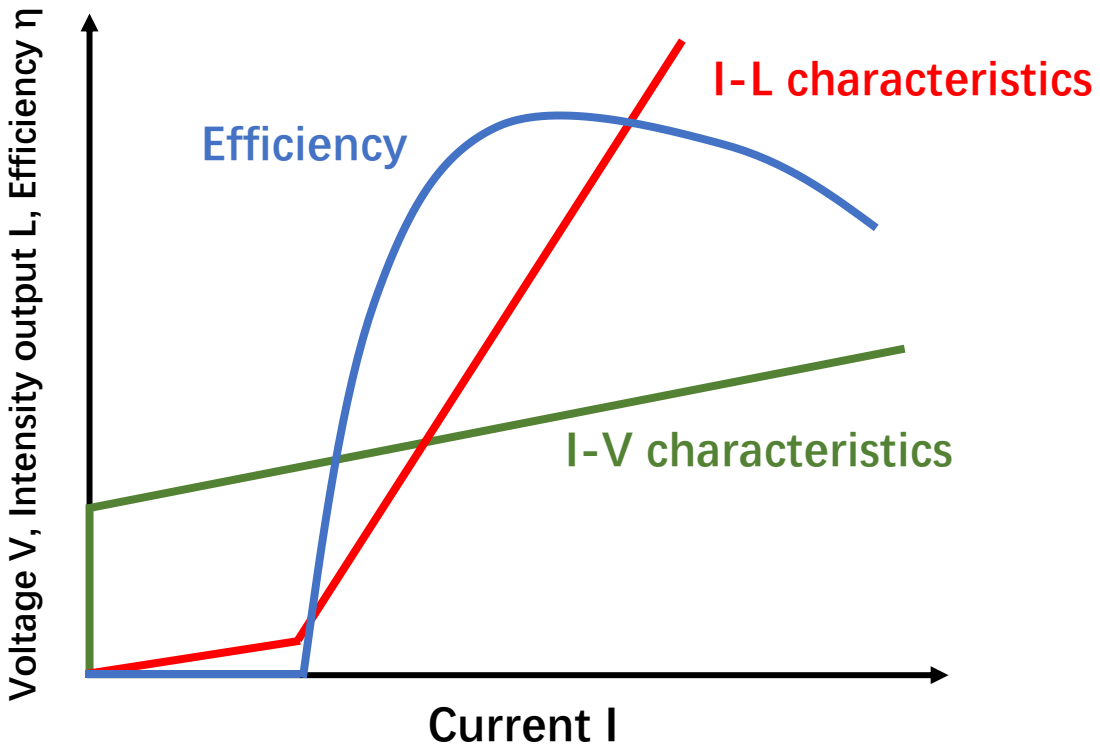

Fig. 2.20 The relation between current, voltage, intensity output, efficiency of LD

The Fig. 2.21 shows the examples of the electro-optical conversion efficiency of edge-emitting lasers, surface-emitting lasers and LEDs. The efficiency values of LDs that shown in Fig. 2.21 are mainly reported value of papers, while the values of LEDs are based on commercial devices.

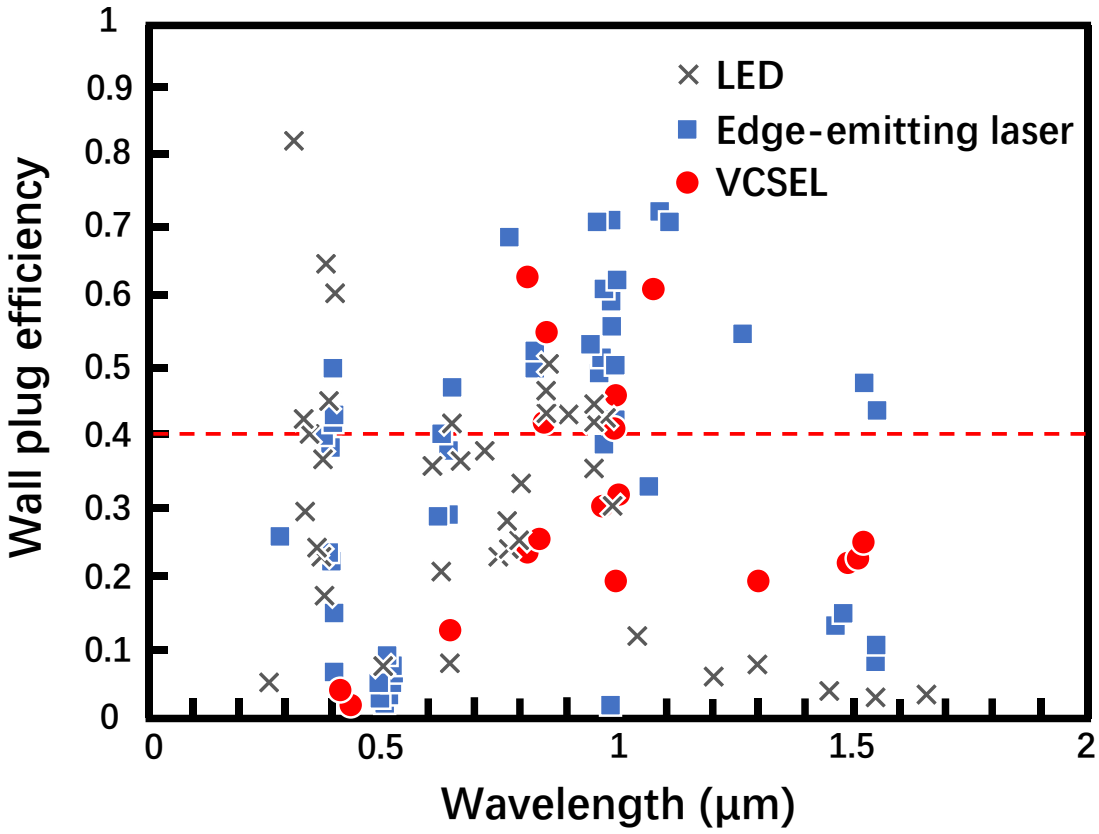

Fig. 2.21 The wall plug efficiency of different light sources in commercial market

From the values shown in Fig. 2.21, the efficiency of edge-emitting laser is over 40% in a wide range from ultraviolet (400 nm wavelength) to infrared (1600 nm wavelength). In the near-infrared region, there are many reports of above 70% efficiency. However, in the green-yellow region (500 nm – 600 nm), the efficiency of edge-emitting laser is relatively low.

Regarding the efficiency of VCSEL, similar to the edge-emitting laser, the maximum efficiency is achieved in the near-infrared region because of many technical and physical advantages. Comparing with edge-emitting laser, the efficiency of VCSEL is about 10% - 20% lower. However, it is believed that VCSEL is more advantageous in the OWPT application. As the discussion shown in 2.2.1, VCSEL is more reliable than edge-emitting laser. Besides, the irradiance of edge-emitting laser is an elliptical shape with high intensity at centre region,

while the VCSEL emits light from the entire surface of the chip, thus regular shape irradiation with even intensity distribution is able to obtained. Such uniform irradiance is advantageous if consider its effect to the photovoltaic conversion efficiency at the receiving side. In other words, the applicability of the OWPT system should not be judged only by the efficiency of the device itself. Considering the characteristics of the device itself and the possible chain reaction of these characteristics in OWPT application scenarios, VCSELs have an efficiency comparable to or even surpassing that of edge-emitting lasers.

Until the early 1990s, the efficiency of LEDs was generally around only a few percent, and it was thought that the efficiency was far below that of semiconductor lasers. Currently, the high efficiency of LEDs is already achieved by numerous commercial products, and LEDs are also becoming an indispensable device in the field of lighting. The actual efficiency of commercialized LEDs is around 30% - 40%. In addition, LEDs are highly efficient at low currents, it has been reported about 84% efficient at low current densities of 5 A/cm^2.[43] Although this a special case of very low current density, the efficiency that exceeding the reported highest efficiency value of semiconductor lasers is a fact. Thus, the efficiency of LEDs is comparable to that of semiconductor lasers, including practical characteristics.

The third comparison between LEDs and LDs is the spectrum, or monochromaticity. The spectrum characteristic of LEDs is also different from the LDs due to the differences in light emission principles that already mentioned. The FWHM of the spectrum is normally only about several nanometre even in the case of lasers array. On the other hand, the spectrum FWHM value of the LED is strongly influenced by the energy distribution of the carriers which injected into the emitting layer, and it varies depending on the wavelength. The typical FWHM value of LED spectrum is around several tens of nanometre, which means several tens of times of the LD spectrum. In the application of OWPT, the influence of the FWHM value of spectrum is mainly reflected in the photovoltaic conversion efficiency of the solar cell at the receiving end. The conversion efficiency of solar cells is greatly affected by the photon energy of light, which is closely related to

the wavelength. In the case of LEDs, the FWHM value of the spectrum is in the range of tens nanometres, and the corresponding difference on photon is usually below 0.1 eV. Compared with the photon energy of visible and near-infrared light which is greater than 1 eV, the influence of the spectrum width on the photon energy is less than 10%. Taking into account process such as photovoltaic conversion of solar cells, the effect of the relatively wide spectrum of LEDs on the overall efficiency of OWPT can be considered to be small enough. Therefore, in OWPT applications, both LED and LD can be regarded as sufficiently excellent monochromatic light sources, and the difference of monochromatic characteristics is negligible.

According to the discussion shown above, the from the aspects of intensity output, electro-optical efficiency, and monochromaticity, LEDs and LDs are almost no different in the application of OWPT. However, there is a big difference in the light beam characteristics. A laser emits a light beam in a specific direction due to its light emission principle. Depending on the diffraction principle of light and the laser structure, there is some degree of divergence of the laser beam, but basically the laser beam propagates in the direction perpendicular to the reflector that constitutes the laser cavity. While the LED is more like a Lambertian object that emits light in all directions. Although it is possible to limit the direction to some extent by changing the internal structure or package lens, the light emission direction is basically wide. Such light beam characteristics have a great influence on the designing and applications of OWPT system. Even the irradiation direction of LEDs is in a wide range, it is possible to generate a light beam that propagating in a specific direction by designing a specific beam control system. Light utilization efficiency can be improved by configuring the beam control system, but it affects the irradiation distance, irradiation size, efficiency, and size of the light source module. For this reason, issues existed if apply LEDs as light source of OWPT, especially in the case of very long transmission distance. In other words, considering only the performance of the light source, the LED-based OWPT system has more restrictions in application scenarios than laser-based OWPT because of the difference in beam characteristics. However, if there are no major

restrictions on the size of the light source module and receiver, or in the scenario of relatively short transmission distance as about 1 m, LEDs can still be applied as a high-efficiency light source to OWPT system.

From the aspect of performance, the intensity output, electro-optical efficiency, monochromaticity, and directionality of LEDs and LDs are compared. In terms of light source of OWPT system, LED is the same excellent candidate as LD, but slightly limited in application scenarios. However, the comparison between the two should not only be discussed through the performance of the device itself, but also in the application of OWPT. Compared with LD, LED has two obvious advantages in the application of OWPT, namely higher tolerance of temperature and loose products regulation. These two aspects will be discussed next.

Generally, due to the structure and light emission principle, LD is easier to generated heat on the junction and also more sensitive to the operating temperature. The Fig. 2.22 shows the characteristics of operating temperature of several typical LEDs and LDs. According to the different intensity output level, three groups of LEDs and LDs with different wavelengths and different outputs were selected, and their operating temperatures were compared. Specifically, LED (KT DDLM31.13, Osram, 87.5 mW intensity output, 528 nm wavelength)[44] and semiconductor laser (PLT5 520B, Osram, 80 mW, 520 nm wavelength)[45] is first group; LED (LE B Q8WP, Osram, 1950 mW intensity output, 459 nm wavelength)[46] and semiconductor laser (PLPT5 450KA, Osram, 2200 mW, 447 nm wavelength)[47] is the second group; and; LED (LE B Q7WP, Osram, 3500 mW, 459 nm wavelength)[48] and semiconductor laser (PLPT9 450LA_E, Osram, 3000 mW, 447 nm wavelength)[49] is the third group.

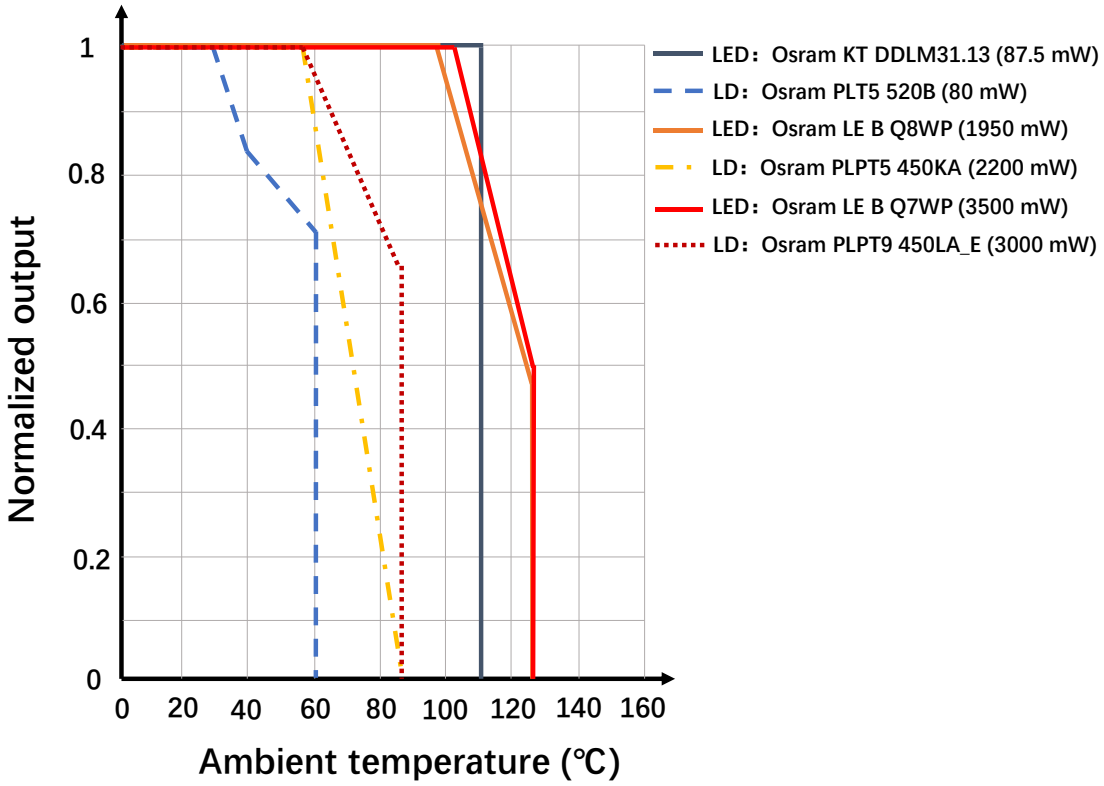

Fig. 2.22 Operating temperature of LEDs and LDs with different output classes

From the Fig. 2.22 ,although the parameters of intensity output and centre wavelength are different of three groups, it can be see that the difference in operating temperature of LED and LD consistent. When the temperature of the devices crosses a threshold value, the forward current starts to decline. Once the temperature keeps increasing and exceeds the range of operating temperature, the forward current will drop to zero and the device stop working. In the comparison of these LEDs and LDs devices shown in Fig. 2.22, the operating temperature of the LED ranges from -40 ℃ to over 100 ℃, while the extreme operating temperature of LDs is usually below 100 ℃, and such value of some special LDs is even lower than 60 ℃. Although the above discussion only bases on a few individual devices, the conclusions reflected are general truths, which is the fact that LED is more tolerant to the temperature than LD device. The reason for such difference is LD generate more heat during operating due to the high

current density. In fact, the limitation of junction temperautre of LED and LD is similar. The equation of the junction temperature[50] is shown in equation (2.1):

$$T_j = T_a + (P_D \times R_{ja}) \tag{2.1}$$

Here the T_j (℃) is the junction temperture of the semiconductor diode, T_a (℃) represents the ambient temperature for the package, and P_D (W) represents the power dissipation of the integrated circuit, and R_{ja} ($℃/W$) is the junction to ambient thermal resistance. Therefore, the junction temperature is directly affected by the ambient temperature. When the limite junction temperature of LED and LD is similar, LD generates more heat by itself because of higher current density. Consequently, the operating temperature range of the LD needs to be limited to a lower level to prevent the semiconductor junction temperature from becoming too high. This is the reason of higher temperature tolerance of LED.

In addition, the high temperature-sensitivity of LD is not only reflected in the operating temperature, but also on the wavelength shift. The centre wavelength of a LD is temperature-dependent, meaning the emitted wavelength will change when the temperature of the LD changes. The Fig. 2.23 shows the wavelength shift caused by temperature of a LD (PLPT5 450KA, Osram).[47] Under normal circumstances, the centre wavelength shift caused by temperature changes of LD is within a few nanometres. It should be mentioned that the peak wavelength of the LED will also shift due to the temperature changing, and temperature controlling is also important. However, unlike LD, the original spectrum of LED is relatively wide. Compared with the tens of nanometres FWHM value, the influence of a few nanometres centre wavelength shift caused by temperature will not such obvious. The FWHM value of LD is usually less than 1 nm, thus the effect of limiting the wavelength shift is particularly obvious.

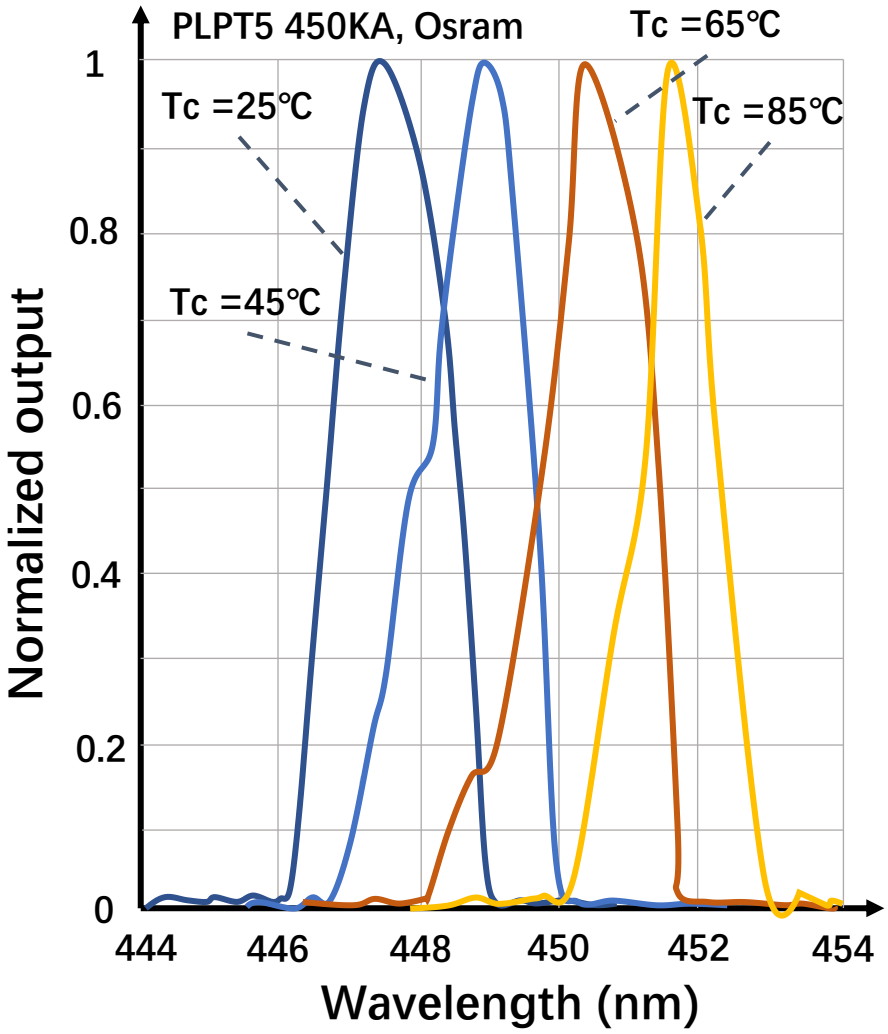

Fig. 2.23 Wavelength shift of typical LD

The difference in the temperature sensitivity of LEDs and LDs has been explained in the above discussion. In the application of OWPT, although such difference will not cause great difference in design or performance of two light sources, there are still several points worth discussing. The first is the limitation of the working environment between two light sources. Although in a normal environment, the ambient temperature is in the range of room temperature and not influence the light source performance, in some special application scenarios, such as the high temperature workshop of a factory, the ambient temperature will be really high of 40 ℃ or higher. Even if the ambient temperature does not exceed the specified

range in such scenario, the junction temperature is already close to the limit value for LD. The non-radiative recombination caused by the excessively high junction temperature will result in lower electro-optical efficiency and generate more heat. The heat generated will further reduce the performance of the light source and form a vicious circle. In addition, long-term working in a high temperature environment will greatly shorten the life of the semiconductor light source. Therefore, in such application scenario, the LED's higher tolerance to ambient temperature will be particularly important, and will show a higher performance than LD. The second discussion is the heat dissipation module of the OWPT system. Whether it is LD or LED, heat dissipation is critical. Problems caused by excessively high temperature such as non-radiative recombination, reduced electro-optical conversion efficiency, deteriorated beam quality, and shortened working lifetime of the light sources have been explained in the above discussion. For that reason, in practical applications, a heat dissipation module is often configured to ensure that the semiconductor light sources can work at an environment with relatively constant temperature. For low-power OWPT applications such as a few watts of output light intensity, usually a small-sized heat sink is sufficient for heat dissipation of whether LED or LD. However, in high-power OWPT applications with LED-array light source or the LD-array light source, the heat generation between the light sources will affect each other, making it more difficult to restrain the temperature. In this case, for the LED-based OWPT system, a small heat sink may be sufficient, while a large-dimension heat sink or an active cooling module such as a small fan might be necessary to be configured to ensure that the temperature is maintained within the operating temperature range for LD-based OWPT system. As a result, the light and simple configuration becomes an advantage of the LED-based OWPT system, and the LD-based OWPT system will lose portability feature due to the addition of an overweight heat sink module or an additional active cooling module. Accordingly, when discussing the portable OWPT system, the smaller heat sink module enables LED light sources to gain advantages in such application scenarios.

The products regulation is another important point that needs to discuss. It can be said that, as a light source for high-power applications such as the OWPT system, the biggest advantage of LEDs over LDs is relatively loose products regulation.

Moderate and high-power lasers are potentially hazardous because they can burn the retina of creature's eyes and even the skin. Thermal and photochemical effects are the main causes of the laser radiation damage. Due to the high coherence and ultra-small divergence of the laser beam, and also the convergence effect of the lens of an eye on the light beam, the laser beam will be concentrated into an extremely small irradiation spot on the retina of eye, thus even small power laser might cause damage to creatures' eye. On the other hand, for some of the high-power lasers, even the diffuse reflection from the surface has the possibility to harm the human's eye. A transient temperature increases of only about 10 ℃ can destroy retinal photoreceptor cells, and If the laser output is powerful enough, permanent damage can occur within a time that faster than a blink of eye. Therefore, it is difficult to rely on the body's own action and response to avoid the possible laser hazard.

The lasers with the wavelength in the range from the visible to near infrared (400-1400 nm) are highly dangerous to eyes due to light with such wavelength is barely absorbed by the cornea of eye, thus most of the power can reach the retina. The lasers with infrared wavelength are particularly hazardous, since the body's protective glare aversion response, which also referred to as the "blink reflex," is triggered only by visible light. Since the infrared wavelength is invisible, the protective glare aversion response cannot be triggered immediately when under the exposing to infrared lasers, people may not feel pain or notice immediate damage to their eyesight.[51]

The light with the wavelength of 1400 nm - 2100 nm will be greatly absorbed by the cornea, lens, aqueous and vitreous humors in the eye, so that the intensity of the light will be greatly reduced when it reaches the retina, so it is relatively safe. However, this security is only relative to other wavelengths. The absorption is not

unlimited. If the light power density is high enough, it will still cause harm to the human eye.

The Table 2.4 summarizes the various medical conditions caused by lasers at different wavelengths, not including injuries due to pulsed lasers.

Table 2.4 Medical conditions caused by lasers

Wavelength range	Pathological effect
180 – 315 nm	Photokeratitis (inflammation of the cornea, equivalent to sunburn)
315 – 400 nm	Photochemical cataract (clouding of the eye lens)
400 – 780 nm	Photochemical damage to the retina, retinal burn
780 – 1400 nm	Cataract, retinal burn
1400 – 3000 nm	Aqueous flare (protein in the aqueous humour), cataract, corneal burn
3000 – 10000 nm	Corneal burn

It is precisely because of the high risk of laser to the human body, in order to control the risk of injury, various jurisdictions, standards bodies, legislation, and government regulations define classes of laser according to the risks associated with them, and define required safety measures for people who may be exposed to those lasers depending on their power and wavelength. Such as European standard EN 207 (eye protection requirements),[52] European standard EN 208 (requirements for goggles for use during beam alignment)[53] and European standard EN 60825 (optical densities in extreme situations) of the European Community (EC), ANSI Z136 series of standards of the united states, Japan safety standards of laser products JIS C6802,[54] and international standard IEC 60825.

The Table. 2.5 lists the classes and description of laser products based on the IEC 60825-1 standard.

Table 2.5 Laser products classes of IEC 60825-1

Classes	Description
Class 1	Safe under all conditions of normal use
Class 1M	Safe for all conditions of use except when passed through magnifying optics
Class 2	Safe during normal use; the blink reflex of the eye will prevent damage. Usually up to 1 mW power
Class 2M	Safe because of the blink reflex, not viewed through optical instruments
Class 3R	Safe if handled carefully, with restricted beam viewing. Usually up to 5 mW
Class 3B	Hazardous if the eye is exposed directly, but diffuse reflections are not harmful.
Class 4	The highest and most dangerous class of laser, can burn the skin, or cause devastating and permanent eye damage as a result of direct, diffuse or indirect beam viewing.

It can be seen that the classes of laser products are not only based on the wavelength and total intensity output, but also related to the beam size and divergence angle. Although the total intensity output of a laser is very small, the beam converging on a small spot may still cause great harm to the human body. In the same way, even the intensity output of a laser is very high, but its optical path is isolated in an enclosure and will not be directly exposed to the user, then it is relatively safe. In short, the classes of laser products are based on the energy density (in W/cm^2 or J/cm^2) of a light source that exposing to the user and the possible hazard.

As for the LD-based OWPT system, in order to realize the effective wireless power transmission, the total intensity output of the laser will inevitably be higher,

and the divergence angle of the beam will also be small to achieve long-distance pointing. In addition, the basis of optical wireless power transmission is the direct line of sight, so it is impossible to seal the system together with the optical path. In other words, the laser-based OWPT system is highly dangerous to the human body, and it is not an exaggeration to classify it as the most dangerous laser product class. During the testing of high-power LD-based OWPT system in the laboratory, wearing protective safety goggle is a basic requirement for avoiding possible laser hazard.[55] After the commercialization of optical wireless power transmission technology, it is feasible to require technicians to wear protective safety goggle during operating OWPT system in non-daily applications, such as optical wireless power charging for factory equipment or various professional IoT devices. However, in daily home applications scenarios, it is obviously unrealistic to require the users to wear protective safety goggle during OWPT system running. In daily application scenarios, one of the advantages of OWPT technology is that it can provide long-distance power supply for devices anytime and anywhere without deliberately operating the system, and the requirement of wearing safety goggle is obviously in contradiction with the convenience feature of OWPT technology. Because of this, objects detection system and emergency brake systems are often indispensable in OWPT system of daily application.[56] The OWPT system needs to detect whether there are creatures approaching in the area near the light path during working, and urgently brake the light output before the creatures have the possibility to be directly exposed under the high-power light beam. The creatures here include not only humans, but also pets and other creatures. In addition, in OWPT applications where the intensity output is much higher, or the continuous irradiation time is longer, which may cause combustion of combustible materials or damage other objects at the target region, more complex safety systems are necessary. For example, the temperature at the receiving end is monitored in real time and the information is fed back to the transmitting end through a communication link, and the transmitter then performs adaptive intensity output adjustment or other measures based on the feedback information. It needs to be clarified that high-power LEDs are still potentially harmful to human eyes. When the wavelength is the same as well as the output

light intensity, the harmfulness of LED is not much different from LD. It is a fact that the divergence angle of LED is larger than LD because of the different light emitting principle, and the output will be slightly lower than LD. However, in the application of OWPT, in order to high directionality light beam, the LED is usually equipped with a beam control system and the divergence angle of the beam is minimized. Therefore, the LED-based OWPT system also has a very high energy density at the target distance, and such a high energy density is undoubtedly hazard if it irradiates on the human or other creatures. For that reason, same as the LD-based OWPT system, the use of the LED-based OWPT system also requires various safety measures. However, the difference from the LD-based OWPT system is that LEDs are not strictly regulated like lasers. As long as the security module is designed and installed based on the application scenarios, the LED-based OWPT system can be quickly commercialized and applied in Various scenes. On the other hand, the laser has severe classification and regulation. Some classes of lasers require strict safety modules even in industrial or scientific research environments, such a key switch and a safety interlock, not to mention the high-level safety measures in the application of such high-output lasers in daily life. Even with a complete safety system, the LD-based OWPT system cannot be quickly accepted and commercialized by the market as the LED-based OWPT system. It can be said that it is precisely because of the severe regulation of laser products that LED has become the only light source that can make OWPT system to be smoothly commercialized and spread in the near future. As the light source of OWPT system, this is the biggest advantage of LED compared to LD. Summarily, when discussing LEDs and LDs on the premise of OWPT system light source, the products regulation is a point that cannot be ignored and needs to be fully considered according to the situation.

2.2.4 Proper LED as light source of OWPT system

So far, LED and LD have been compared in detail, and LED has been proved to be an appropriate light source for OWPT system. In this section, the detailed characteristics of the LED as the light source for OWPT applications will be

discussed. The wavelength of the light source is a very important parameter. There are many types of existing light receiving devices, but most of them are used in communication and information technologies and cannot effectively convert optical energy into electrical energy, and relate discussion will detailly shown in the next section 2.3. The most appropriate and efficient candidate is photovoltaic cells, or refers as solar cells. Assuming that applying photovoltaic cell as intensity receiver in OWPT application, the choice of light source wavelength will greatly affect the photovoltaic conversion efficiency of the photovoltaic cell. Generally speaking, the wavelength of the light source should be as close as possible but slightly smaller than the wavelength corresponding to the bandgap of the photovoltaic cell in order to achieve high photovoltaic conversion efficiency. Therefore, the choice of LED wavelength must not only consider the performance of the LED itself, but also premeditate various factors of the photovoltaic cell. Basically, the wavelength of an LED has a certain relationship with its own efficiency. As shown in Fig. 2.21, the existing commercial LEDs have the highest efficiency in the blue wavelength range (about 400nm-450nm), followed by the near-infrared wavelength (780nm-1100nm) with above 40% efficiency. However, there is no photovoltaic cell in the commercial market can achieve a very high photovoltaic conversion efficiency for this wavelength currently. Thus, even if the LED itself has excellent efficiency in the blue wavelength range, such wavelength is not a good choice for OWPT applications at present. Nevertheless, as will be discussed in the next section 2.3, the theoretical maximum efficiency of photovoltaic cells in the case of monochromatic light increases as the light wavelength decreases. In other words, with the advancement of research in the field of photovoltaic cells, low-cost, high-efficiency short-wavelength photovoltaic cells are expected to be marketed and spread in the future. By then, the blue wavelength band can be used as the best wavelength choice for the LED in OWPT application, and greatly improve the overall efficiency of the OWPT system. At current stage, the near-infrared wavelength LED is the best light source choice. The near-infrared LED has an efficiency second only to the blue wavelength. Secondly, the existing common photovoltaic cells in the commercial market, such as Si solar cells, CIGS solar

cells, GaAs solar cells, etc., can achieve relatively high photovoltaic conversion efficiency with such wavelength. Therefore, the near-infrared wavelength is considered the best wavelength choice for the LED-based OWPT system at this stage. One characteristic of near infrared light is invisible. In the OWPT system installed with an object tracking module, the invisibility of infrared light is not a problem. Such type of OWPT system will detect the coordinates of the receiving terminal and automatically point the beam to the receiver, without the need for human aiming. On the contrary, because the invisible near-infrared light will not cause visual impact on surrounding organisms, it can be well applied in various daily home scenes. The OWPT system that not installed with tracking system needs to artificially aim the invisible beam at the receiving end, which is an issue that needs to be solved. The issue can be solved by installing a small laser pointer on the transmitting end, or add upconversion luminescent material on the receiving end to allow users to confirm the position of the light spot.[57] However, when the transmission distance is too long, the above two methods still cannot solve the issue of clearly identify the specific position of the light spot, so the application scenarios are subject to certain restrictions.

The two characteristics of LED divergence angle and light-emitting chip size need to be discussed together. The divergence angle of the LED determines the degree of divergence of the light beam. A beam with a large degree of divergence will quickly dissipate with the extension of the transmission distance, while a beam with a smaller divergence angle can be pointed to the target position even during long-distance transmission. Although in OWPT systems using LEDs as the light source, a beam control system is often designed and installed to reduce the divergence of the beam, but the divergence angle of the LED itself is also an important parameter. If the LED light source has a smaller divergence angle, then the beam control system (lens system) can avoid using a lens with a relatively large aperture to collect light energy, so the size of the system can be greatly reduced. Therefore, the divergence angle of the LED should be as small as possible.

On the other hand, the size of the light-emitting chip of the LED determines the irradiation spot size at the transmission distance to a certain extent. In the case of a certain transmission distance, the size of the irradiation spot formed after the beam passes through a set of lenses is proportional to the light-emitting area of the light source, such ratio is called transversal magnification. Thus, smaller the light-emitting chip size of the LED, the smaller the spot size can be achieved, as well as the smaller receiver. Although the transversal magnification can be changed by adjusting the parameters of the lens system, it will greatly increase the size of the lens system, correspondingly. Especially in the application of IoT-OWPT, the terminal size of the IoT is very small, so in order to adapt to devices of various sizes and reduce the cost of the receiver, the chip size of the LED light source should be sufficiently small.

However, the parameters of divergence angle and the size of light-emitting chip is closely related to each other. According to the etendue in non-imaging optics,[58][59][60] the relationship between the two parameters is described, and the formula is as follows:

$$\text{Etendue} = n^2 \int\int \cos(\theta) dA d\Omega \tag{2.2}$$

The n parameter is the refractive index of medium, dA is the infinitesimal surface element, $d\Omega$ is solid angle, at an angle θ with the normal. Etendue is a property of light in an optical system, which characterizes how "spread out" the light is in area and angle. Etendue never decreases in any optical system where optical power is conserved. From the source point of view, it is the product of the area of the source and the solid angle that the system's entrance pupil subtends as seen from the source. This means that under the condition of conservation of etendue value, the light source cannot achieve a very small light-emitting area and a very small divergence angle at the same time. When it is desired to reduce the divergence angle, the light-emitting area of the light source must be increased accordingly to ensure that the etendue remains unchanged, and vice versa. This relationship can not only apply to LED light sources, but also to laser light sources. Therefore, in the case that the LED light source cannot achieve the extremely

small divergence angle and the small light-emitting chip size at the same time, there is a trade-off between the two parameters.

Generally, an excessive LED divergence angle causes geometrical loss of light intensity, which can be solved by appropriately increasing the size of the lens aperture size. While if the size of the LED light-emitting chip is too large, the parameters of the entire lens system must be adjusted to reduce the transversal magnification value, which includes increasing the distance between the lenses and increasing the aperture size of the lens. Theoretically, for ensuring the same performance of the OWPT system, the increase of the LED divergence angle will increase the vertical length of the system, and this effect is one-dimensional. The enlarging of LED light-emitting chips will increase the vertical and horizontal dimensions of the system, and its impact is two-dimensional. From the perspective of system volume, the impact of a large light-emitting chip is far greater than the divergence angle. Moreover, as the transmission distance increases, the degree of system volume increase will be enlarged due to the large light-emitting chip, while the divergence angle does not have a similar impact. Therefore, compared to the divergence angle, ensuring the chip size of the LED is considered to be more priority.

The Fig. 2.24 shows several examples of high-power LEDs with relatively small divergence, and their corresponding IR images of irradiation.

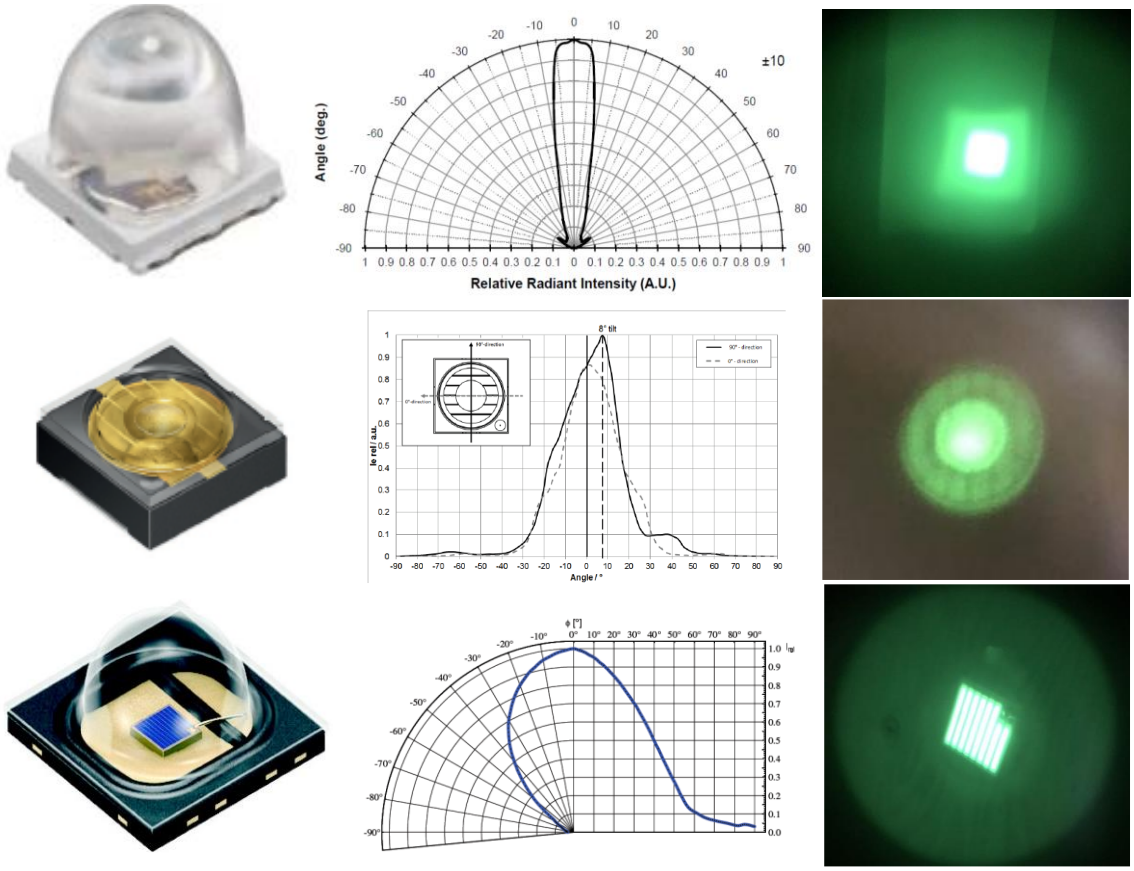

Fig. 2.24 Characteristics of divergence and corresponding irradiation spot of LEDs with different package lens (top: Ushio SMBB850DS-1100-02; mid: Osram, SFH-4786S; bottom: Osram, SFH-4703AS)

The pointed epoxy resin package LED (Ushio SMBB850DS-1100-02, 850 nm, ± 10°, 1400 mW, 1 mm × 1 mm chip) has relatively smallest divergence angle among all types of LEDs, but according to the etendue definition, the chip size will be slightly large, correspondingly. It is widely used in the applications of Infrared Illumination for Cameras and Machine Vision System field. While the issue of such LED is also obvious. First, the pointed epoxy resin package LED has a bullet-shaped package lens which is similar with designing of the edge-emitting LED that discussed in section 2.2.2. The package lens of this shape gives the LED a very small divergence angle and high directivity. However, the lens surface is not a perfectly curved surface. The front surface of the lens is a smooth curved surface but the side surface is flat. This design will cause a certain

light intensity leakage on the side and form an irregular weak irradiance area around the center irradiation spot at the target distance (as shown in Fig. 2.24). This will cause the receiver cannot fully collect the light intensity from the light source, hence decreasing system efficiency. More importantly, the center thickness of its bullet-shaped package lens is larger than that of other types of LEDs. Therefore, when the beam control system is installed, the LED light source cannot be close to the front surface of the collecting lens, which will increase the irradiation spot size at the target distance. The discussion of this point will be analyzed in detail in Chapter 3.

The metal reflective cavity package LED (Osram, SFH-4786S, 810 nm, ± 13°, 700 mW, 0.75 mm × 0.75 mm chip)[61] has a reflectorr inside of the package in order to achieve near collimation. This design sacrifices the total intensity output (smaller etendue value) to achieve a smaller divergence angle and light-emitting area at the same time. The metal reflective cavity package LED is used in access control / biometrics (IRIS, Scan, Vein scan) applications. If this kind of LED is used in OWPT system, there are several issues. The first is that the metal reflective cavity package LED is installed with a reflector in the package to collimate light with a large divergence angle, and also a micro lens is configured on the surface of LED to collimate light with a small divergence angle. Therefore, it can be seen from Fig. 2.24 that the intensity distribution is not uniform between the central area and the peripheral area of the irradiation. In the case of only a single photovoltaic cell configured at the receiving side, the unevenness of the irradiation will not cause any problems, while in the application where the receiver is composed of multiple photovoltaic cells in series, the uneven irradiation will cause inconsistent performance of different solar cell and thereby reduces the overall efficiency of the receiver. The second issue is that the irradiation spot of the metal reflective cavity package LED will be slightly enlarged due to the addition of the reflector in package, and also the shape of the irradiation spot will be round as the reflector. Considering that almost all photovoltaic cells in the market are regular rectangles, the shape of the irradiation spot does not match

the shape of the photovoltaic cell well, which will cause some of the area of the photovoltaic cell to be wasted.

The third type is a dome-type package LED (Osram, SFH-4703AS, 810 nm, ± 40°, 1040 mW, 0.75 mm × 0.75 mm chip),[62] which is a relatively common type of LED package. By designing the package lens, the divergence angle of the LED can be controlled within a certain range. It is widely used in a CCTV surveillance, eye tracking, safety systems and CCTV applications. Compared with the first two types of LEDs, the dome-type packaged LED has a larger divergence angle, but at the same time it has a smaller light-emitting chip size and higher intensity output, which has a very good balance in performance. In fact, a 0.75 mm × 0.75 mm light-emitting chip is almost the smallest size that a high-intensity LED can achieve. In addition, the irradiation spot of such type of LED is the same as the shape of the light-emitting chip, which is a regular rectangle with very clear edges, and can well match the shape of the photovoltaic cells. Therefore, the dome-type packaged LED is considered to be the best choice for the OWPT system light source.

Another thing to discuss is the electrodes pattern of the LED. The Fig. 2.25 shows two typical LED electrode designs. Usually, the top face of the chip is connected with a gold bonding wire to an electrode, and because the gold bonding wire is non-emitting component, the position of the gold bonding wire connection will affect the intensity distribution at the target distance. The gold bonding wire of the left LED in Fig. 2.25 is connected to the center position of the chip, so it can see that the middle of the corresponding irradiation spot is dark because of the low intensity. The connection position of the second type of LED is on the corner of the chip, so a corner corresponding to the irradiation spot is dark. The intensity distribution caused by the electrode pattern will greatly affect the performance of the receiver. In order to suppress the unstable output caused by possible tremor during operation, the irradiation spot will be slightly larger than the size of the receive. If the LED on the left side of Fig. 2.25 is applied as the light source, most of its light energy is distributed in the non-center position of the irradiation spot, thus a large part of the light energy is lost at receiving side. If the LED on the right

side of Fig. 2.25 applied, most of the light energy is concentrated in the center position of the irradiation. Thus, most of the intensity can be successfully collected by the receiver even if the irradiation is larger than the receiver. Therefore, the electrode pattern of the LED is also a point that needs attention. When choosing the LED light source in the OWPT system, in order to obtain the irradiation with the intensity concentrated at the center area, the LED with the gold bonding wire connected at the edge or corner position of the chip is an appropriate candidate.

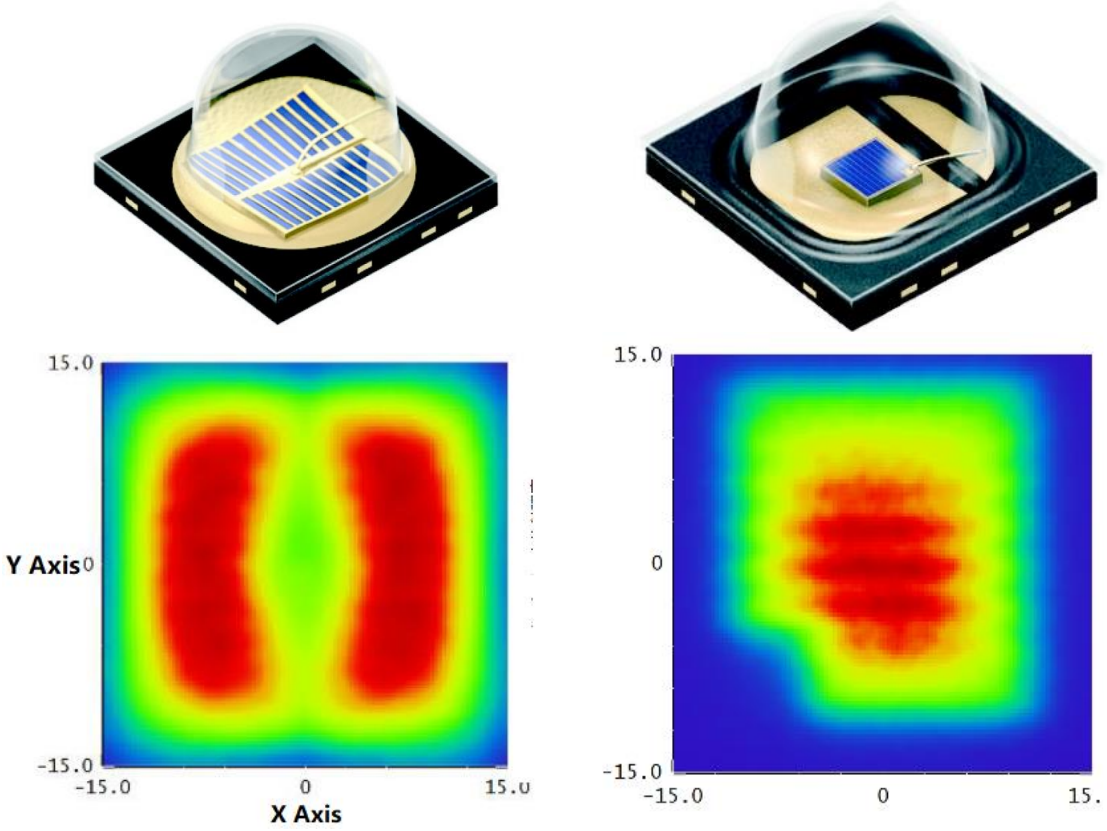

Fig. 2.25 Irradiation spot of LEDs with different grid electrode pattern (left: Osram, SFH-4715S; right: Osram, SFH-4703AS)

2.2.5 Summary of light source of OWPT system

In section 2.2, the existing typical light source types is investigated, and analyzed whether they have the necessary characteristics for OWPT applications, which

are easy beam forming, high intensity output, high conversion efficiency and monochromaticity. Thereby, it is concluded that semiconductor lasers and semiconductor LEDs are excellent light source candidates for the OWPT system. Then, the light emission principle, structure, material, spectrum and other characteristics of semiconductor laser and LED are investigated in detail in section 2.2.1 and section 2.2.2 respectively. In section 2.2.3, from the perspectives of intensity output, electro-optical conversion efficiency, monochromaticity, divergence angle, heat tolerance, and products regulation, a detailed comparison of the potential of semiconductor lasers and LEDs as light sources in the OWPT system is given. The conclusion that LED is slightly inferior to LD in divergence angle and output performance, but has a huge advantage in products regulation is obtained, proves the feasibility of LED as the light source of OWPT system. Finally, in section 2.2.4, the various parameters and designs of the LED are analyzed, and the most ideal characteristics of the LED as the light source of the OWPT system are discussed, which are wavelength in near-infrared band, as small as possible light-emitting chip size, sufficiently small divergence angle, dome-type package lens, and the electrode pattern of the gold bonding wire connected to the corner or edge of the chip.

2.3 Investigation of OWPT energy receivers

In optical wireless power transmission technology, in order to supply power to the load at the receiving side, a special receiving device is required to extract energy from the light beam and convert the optical energy into electrical energy. This is the photovoltaic conversion device. In addition to common photovoltaic cells, photovoltaic conversion devices also include photodiodes (PD),[63] avalanche photodiodes (APD),[64] and photomultiplier tube (PMT).[65] The Table 2.6 shows the categories and description of these devices. PD, APD, PMT and photovoltaic cells receive light as photons, and generate electrons to an external circuit to obtained electric current. However, except for photovoltaic cells, rest devices are belonged to optical detectors whose purpose is to detect light as "signal" and "information", and convert such information into electricity signal. In the case of

an optical detector, in order to extract the generated electrons, a voltage is need to apply on the device, and the optical detector can generate current according to the light intensity or voltage. Since power is provided by the product of current and voltage, not only current but also voltage generation is important. Thus, such devices cannot be used to provide sufficient power for the load. On the other hand, photovoltaic cells generate both stable current and voltage based on the received intensity, thus can be used as an ideal receiver in OWPT system.

Table 2.6 Typical optical energy receiver

Abbreviation	Device	Main features	Applications
SC	Solar Cell	Slow response, high efficiency	Power generation
PD	Photo Diode through magnifying optics	Fast response, low noise	Communication, measurement
APD	Avalanche Photo Diode	High sensitivity, fast response, low noise	Communication
PMT	PhotoMultiplier Tube	Ultra-high sensitivity, low noise	Measurement
OR	Optical Rectenna	efficiency, ultra-high-speed, small antenna required	Power generation

Besides of the photovoltaic devices mentioned above, there is another light receiving device named rectifying rectenna. A rectifying antenna is a device that combines an antenna function and a rectifying function, which was originally developed to receive microwaves with an antenna and rectify high-frequency current to extract direct current. A similar configuration can be considered for receiving optical energy.[66] However, light wave is a much higher frequency electromagnetic wave than microwaves. Since the rectifying antenna is

necessary to respond to high frequencies of light frequency (10-several 100 THz), it is not easy to realize. Nevertheless, rectifying antenna has the potential to become a candidate of OWPT receiver in the future.

From the above viewpoints and situations, photovoltaic cells are the appropriate choice as optical energy receiving devices of OWPT system.

2.3.1 Basic principle of solar cells

A solar cell (also known as a photovoltaic cell or PV cell) is defined as an electrical device that converts light energy into electrical energy through the photovoltaic effect. A solar cell is basically a p-n junction diode.

The constructure of photovoltaic cell is shown in Fig. 2.26. A very thin layer of p-type semiconductor is grown on a relatively thicker n-type semiconductor, then a few finer electrodes on the top of the p-type semiconductor layer is applied. Just below the p-type layer there is a p-n junction. Also, also a current collecting electrode at the bottom of the n-type layer is configured.

When light reaches the p-n junction, the light photons can enter in the junction through the very thin p-type layer. The light supplies sufficient energy as the form or photons to the junction, and then a number of electron-hole pairs are created. The free electrons and holes in the depletion region can quickly come to the n-type side and p-type side of the junction, respectively. Once, the newly created free electrons come to the n-type side, cannot further cross the junction because of barrier potential of the junction, as well as the holes come to the p-type side. As the concentration of electrons becomes higher in one side, and concentration of holes becomes more in another side, a voltage is created on the p-n junction. If a load is connected to the junction, a current is provided. This is the theory of photovoltaic effect, and the process of solar cells generating electricity is similar to the reversed process of LED generating light energy. The current generated by the solar cell is direct current, so no additional rectifier circuit is required. This is an advantage of the solar cell applied in the OWPT system.

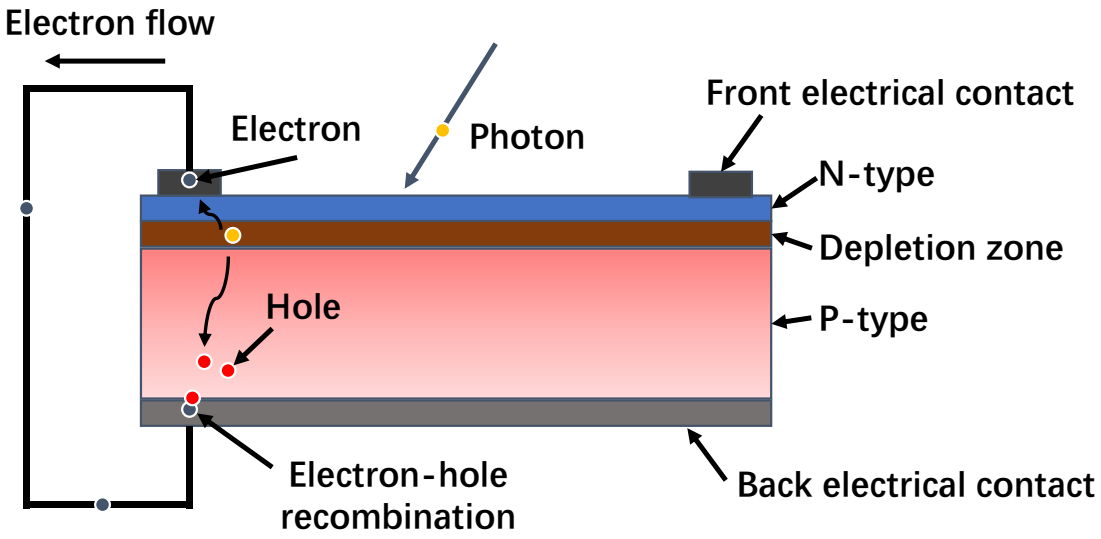

Fig. 2.26 Basic constructure of solar cell

The Fig. 2.27 shows the I-V (current-voltage) characteristics of solar cells. The open circuit voltage is the voltage measured by opening the terminals of the solar cell, and the short-circuit current is the current measured by short-circuiting the solar cell, and is approximately proportional to the amount of incident light intensity. The solar cell works at an operating point determined by the load characteristics (impedance) of the target circuit. In other words, the operating point is in the middle of the I-V characteristics from the short-circuit current to the open circuit voltage. If the solar cell can be operated at the optimum operating point, the maximum power can be obtained. Since the load differs depending on the circuit, and the optimum operating point also changes depending on the amount of incident light intensity, the MPPT (Maximum power point tracking) method is usually used. The value obtained by dividing the power at the optimum operating point by the product of the open circuit voltage and the short circuit current is called the fill factor (FF), and is one of the indexes showing the characteristics of the solar cell. The closer FF is to 1, the closer the curve of the I-V characteristic is to the rectangular side surrounded by the open circuit voltage and short-circuit current. This FF is mainly affected by the resistance and diode characteristics inside the solar cell, and it is generally in the range of 0.6-0.8.

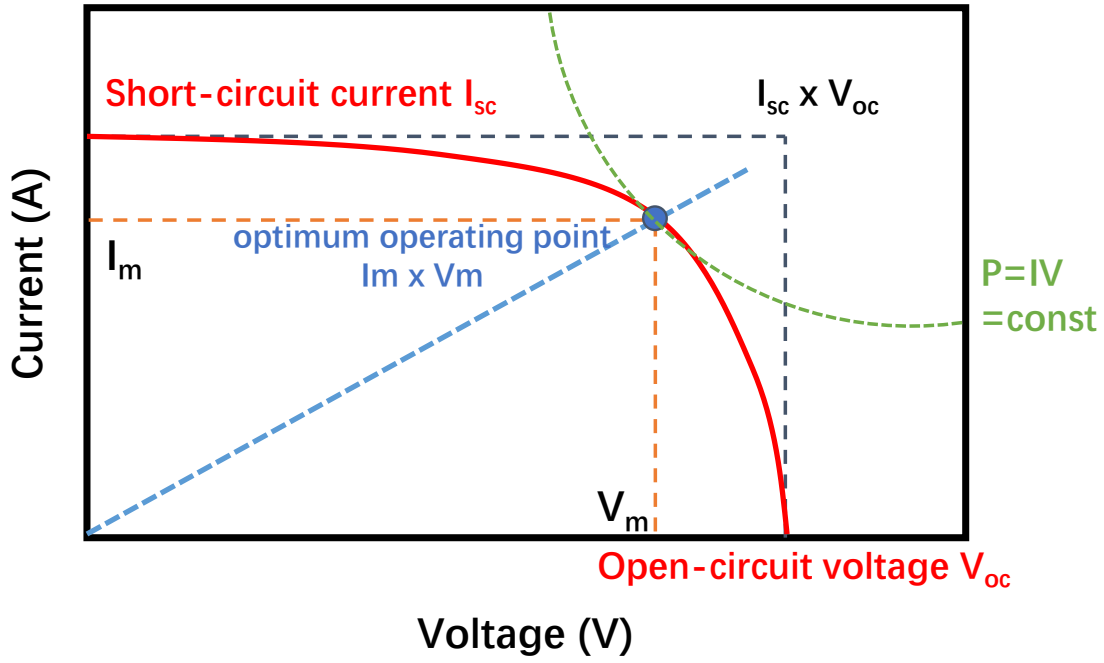

Fig. 2.27 Current-voltage characteristics of solar cells

2.3.2 Efficiency of solar cells

A solar cell is a device that converts the optical energy into electric power, and the photovoltaic conversion efficiency is the most important parameter. In this section, the detailed discussion of solar cell photovoltaic conversion efficiency will be shown.

Solar cells were originally developed for sunlight, as can be seen from its name "solar" cells. Sunlight has a very wide spectral width. Specifically, as shown in Fig. 2.28, the full width at half maximum of the spectrum is as wide as about 500 nm, and the peak intensity occurs near the wavelength of 500 nm. AM (air mass) means the amount of air which sunlight passes through. AM 0 is the condition that is not affect from the earth's atmosphere, and AM1.5 is the condition that the sunlight passes 1.5 times the thickness of the Earth's atmosphere layer. AM1.5 is often used as an index because it can be considered as a representative condition when viewed from the entire globe. The light intensity of the entire sunlight spectrum at AM1.5G condition is 1 kW/m^2 = 0.1W/cm^2, which is generally

referred as 1 sun condition. When sunlight is focused, several suns condition intensity can be obtained depending on the focusing magnification.

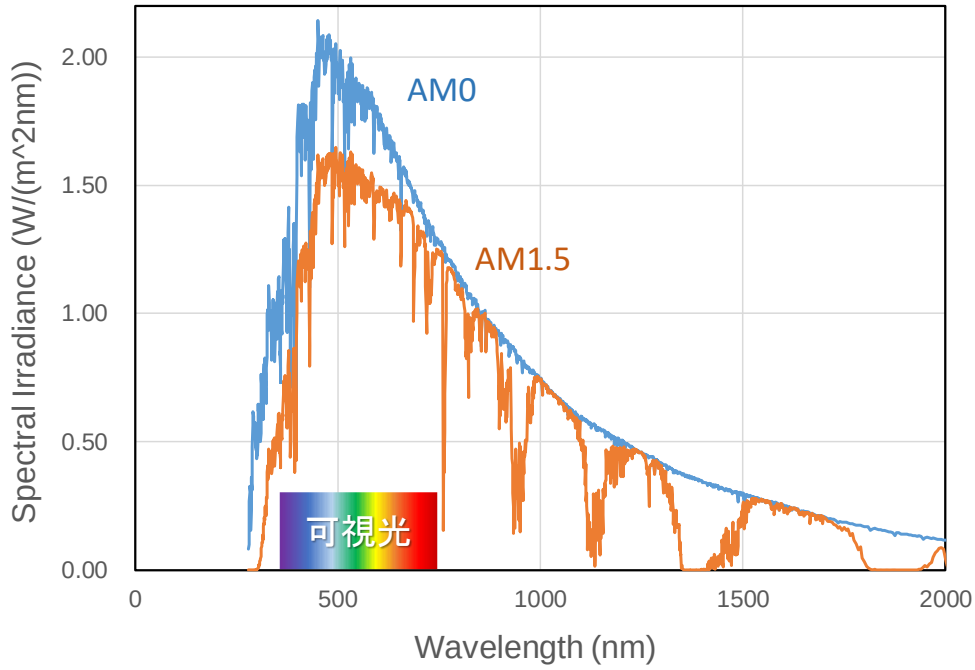

Fig. 2.28 Spectrum of sunlight

The solar cell can absorb the sunlight spectrum and convert the optical energy to electrical power. As shown in Fig. 2.29, the band gap refers to the energy difference between the top of the valence band and the bottom of the conduction band in solar cell. In order for an electron to jump from a valence band to a conduction band, it requires a specific minimum amount of energy for the transition, which is the photon energy in the condition of solar cell.

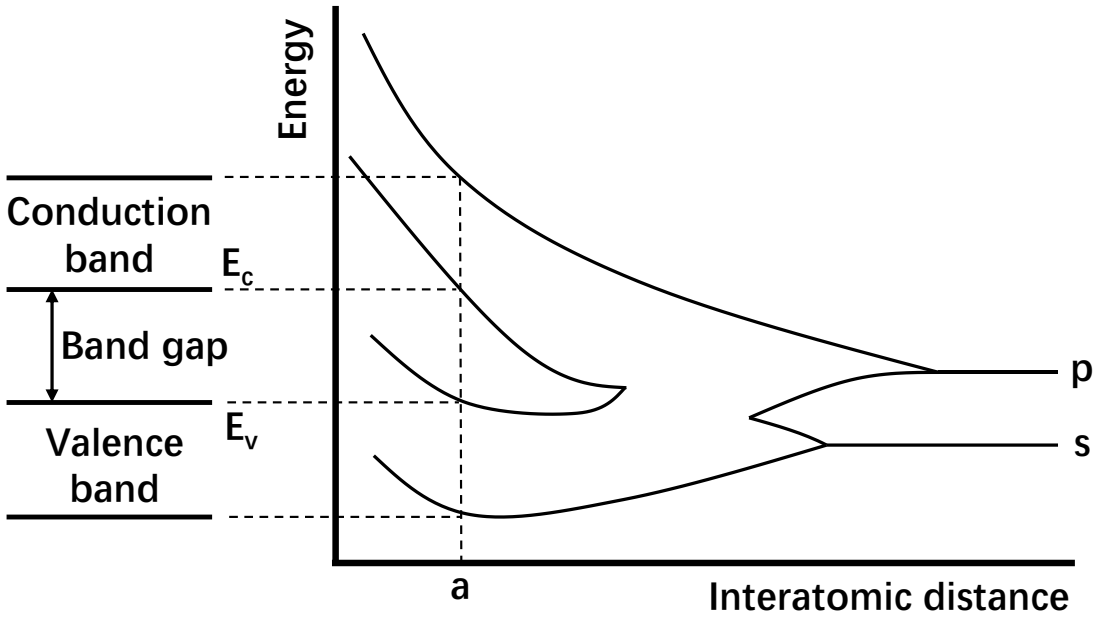

Fig. 2.29 Characteristics of solar cell band gap

Thus, as show in Fig. 2.29, the light with photon energy smaller than the band gap of the solar cell cannot be absorb due to the photon energy cannot support the transition of electron. On the other hand, light with photon energy larger than the bandgap can be absorbed, part of the light energy is lost as heat, and the shorter the wavelength of light, the greater the rate of loss. The relation between the band gap and the corresponding wavelength is shown in equation (2.3):

$$Eg = \frac{hc}{\lambda} \tag{2.3}$$

Here *Eg* is the band gap, *h* is the Planck's constant, λ is the wavelength and *c* are the velocity of light. Conclusively, light with a wavelength greater than the band gap of the solar cell cannot be absorbed, while light with a wavelength much smaller than the band gap causes low efficiency of the solar cell due to heat generation. Only light with a wavelength just slightly smaller than the band gap of the solar cell can be absorbed efficiently. This is the reason why solar cells are generally not very efficient under sunlight.

The Fig. 2.30 shows the timeline of research solar cell energy conversion efficiencies.[67] It can be seen that under the condition of 1 sun (AM1.5G), Si solar

cells and GaAs solar cells, which are core members of solar cells, exhibit high efficiency. This is because the band gap of Si solar cell and GaAs solar cell are 1.14 eV and 1.43 eV,[68] which are both close to the Shockley–Queisser limit, which is solar cells with a band gap of 1.34 eV can achieve the maximum theoretical efficiency.[69] This theory is only for the case of single-junction solar cells. Multi-junction solar cells can absorb multiple wavelengths of sunlight at the same time, so the efficiency is usually higher than that of single-junction solar. However, the multi-junction solar cell is not suitable candidate of OWPT system receiver due to the monochromatic light is used.

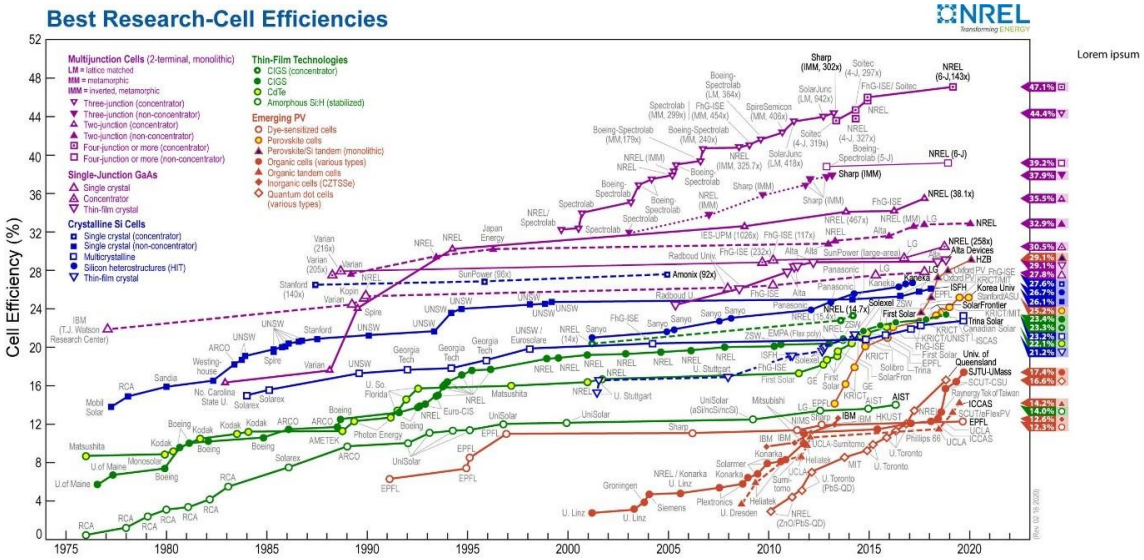

Fig. 2.30 The timeline of research solar cell energy conversion efficiencies

The above discussion is based on the sunlight with light intensity of one sun condition (AM1.5G). However, in the case of monochromatic light or condensed light, the efficiency of solar cells will be significantly improved.

In the case of sunlight, the radiant intensity is 0.1 W/cm^2 of 1 sun condition (AM1.5G), but the radiant intensity can be increased by condensing with a lens, then the efficiency of solar cell can be improved because of the higher carrier density. Such approach has two merits. The first is by condensing the light, the radiant intensity as well as the efficiency of the solar cell can be increased. The

second merit is the irradiation area is decrease, thus the cost can be decreased as well due to smaller size of solar cell.

The only possible issue is that more heat is generated when a high intensity light is incident on solar cell. The higher the temperature of the solar cell, the more likely non-radiative recombination occurs, then decrease the efficiency of solar cell. The characteristic of solar cell efficiency changing with the concentration ratio is shown in Fig. 2.31 In the Fig. 2.31, the degree of heat saturation differs depending on the material. This is because the difference in short-circuit current density causes a difference in Joule heat generation. InGaP / InGaAs / Ge cells have a high current density of JSC = 13 - 14 mA/cm^2, GaAs has a high current density of JSC = 30 mA/cm^2, and silicon has a high current density of JSC = 41 mA/cm^2.

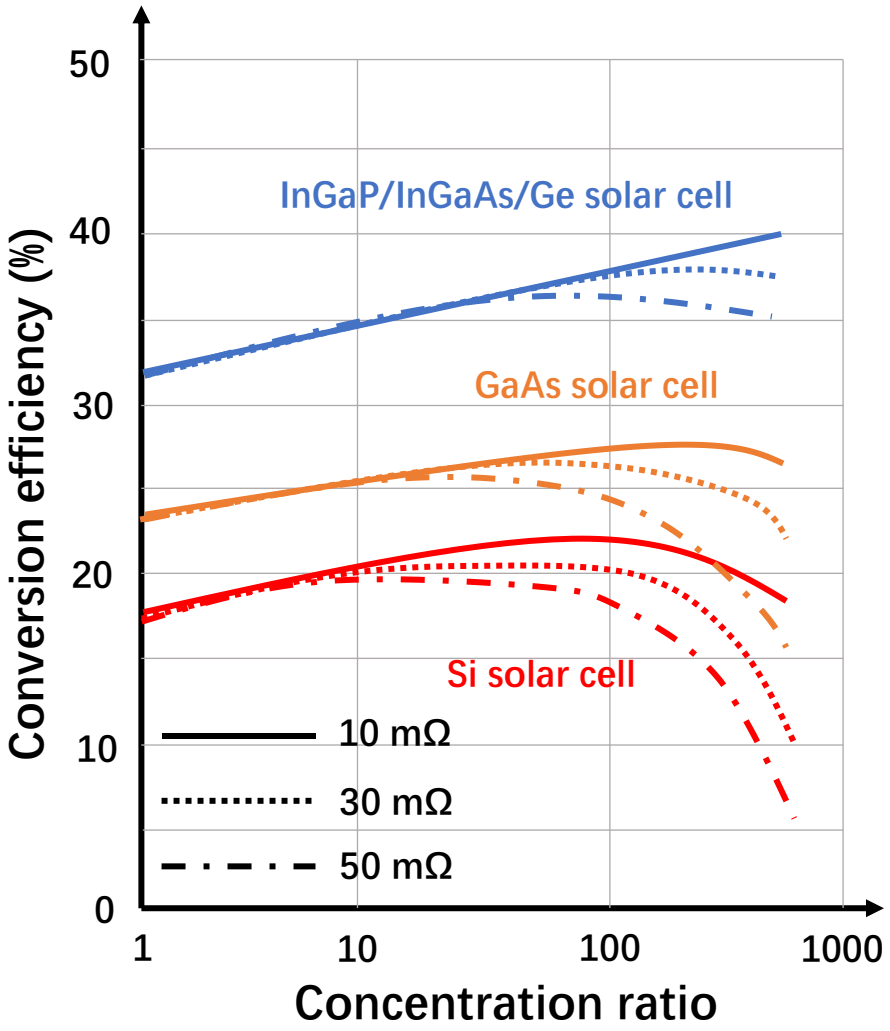

Fig. 2.31 The characteristic of solar cell efficiency with different concentration ratio

Therefore, considering the negative impact of the temperature on the solar cell, the heat dissipation is necessary at the solar cell side if the radiant intensity of the incident light is too high.

On the other hand, as mentioned in previous section, light with a wide spectrum cannot be effectively absorbed by solar cells, resulting in a decrease in the efficiency. On the contrary, the irradiation of monochromatic light with the wavelength close to the band gap of the solar cell can effectively prevent unnecessary energy from turning into heat. By doing so, even if the light intensity

is the same as 1 sun condition (AM1.5G), the solar cell's photovoltaic conversion efficiency can be greatly improved. As discussed in Section 2.2, both semiconductor lasers and LEDs can provide monochromatic light. The Fig. 2.32 shows the characteristic between solar cell efficiency and light wavelength.[70] Assuming that the band gap of the solar cell corresponds to the wavelength of light. Taking Si solar cells and GaAs solar cells for example, in the case of the sunlight with radiant intensity of 1 sun condition (0.1 W/cm^2), the corresponding efficiencies of Si solar cells and GaAs solar cells are about 15-25% and 20-30%, and the same radiant intensity of monochromatic light can obtain efficiencies of approximately 40% and 50%, respectively, which are nearly twice of sunlight. This is because monochromatic light irradiates the solar cell without generating ineffective heat energy, so light energy can be utilized to the maximum. In addition, it can be seen from the figure that the shorter the wavelength, the higher the maximum efficiency of the solar cell. This is because the photon energy of a short-wavelength photon is high under the same optical power, so the number of irradiated photons is small, which reduces the current density generated. However, the performance of existing solar cells in the short-wavelength region is still poor, but with the development of research, large-bandgap solar cells are expected to be used in OWPT systems.

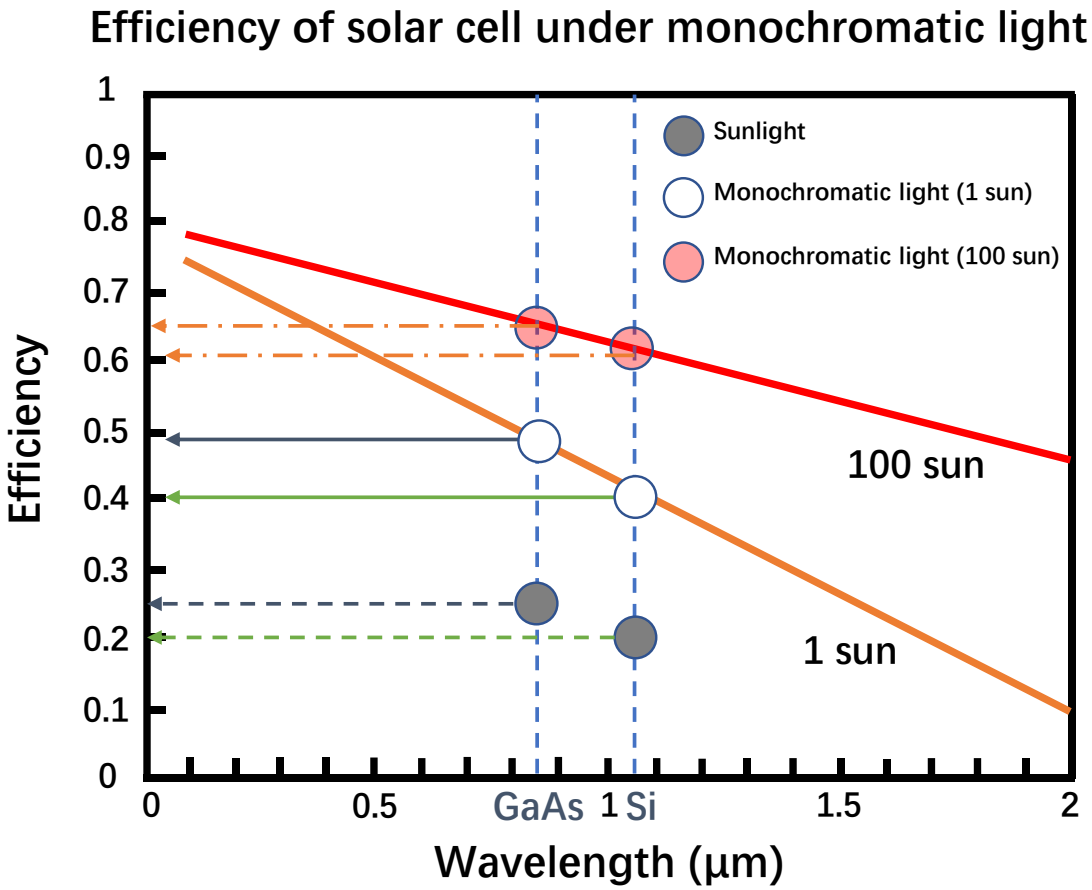

Fig. 2.32 Solar cell efficiency under monochromatic light

In summary, monochromatic light and condensed light are important factors to improve the photovoltaic conversion efficiency of solar cells, and are also the key reasons why the OWPT system can successfully provide sufficient power for remote devices. A simple calculation is shown below to evaluate the performance of the OWPT system under the condition of condensed monochromatic light. Usually 1 sun irradiance (AM1.5G) is used as a criterion. The radiant intensity of 1 sun condition is 0.1W/cm^2, which usually occurs at the time of the strongest daily solar radiation (2 pm). Taking into account the alternation of day and night and, for example, cloudy and rainy days, the irradiance is reduced, and the average sunlight radiant intensity in a whole day (24h) is around 1/3 sun irradiance. Even after the light beam propagation and divergence of the high-intensity LED or LD, the radiant intensity still has about 0.2W/cm^2 - 0.3W/cm^2,

which is 2-3 sun irradiance. If the light source array is used in OWPT system to enhance the total intensity output, the irradiance will increase several times on this basis. Therefore, it can be said that the OWPT system can provide 2-3 times irradiance of the average sunlight even just consider the light source itself. Moreover, as shown in Fig. 2.32, the efficiency of solar cells irradiated by concentrated monochromatic light is about 3 times that of sunlight. As a result, the power provided by the OWPT system is around 10 times that of sunlight under the same irradiation time. the above. Therefore, 60 minutes irradiated by the OWPT system can provide the same electric power as solar energy harvesting system operation a day (10h). The above discussion is based on the outdoor situation, while the advantages of the OWPT system are more obvious in the indoor scene. Indoor ambient light is generally provided by lighting equipment, and its irradiance is much weaker than sunlight, usually around 1/300 sun irradiance. In this case, the OWPT system can provide more than 1000 times irradiance compared to the indoor ambient light. Considering the corresponding PV conversion efficiency of the solar cell, the ordinary single-LED OWPT system provides 2000-5000 times power of the indoor ambient light, and the light source array OWPT system can even provide 10000-50000 times electric power of the ambient light. Thus, tens of seconds irradiated by the OWPT system can supply electric power same as several days or even one month of ambient light in such case. By concentrating monochromatic light to improve the photovoltaic conversion efficiency of solar cells, the OWPT system can be widely used as an efficient power supply technology in various application scenarios.

In addition, there are other ways to improve the efficiency of solar cells, such as making the solar cell to works in a low temperature environment,[71] optimizing the electrode design of the solar cell, or adding a light trapping layer on the surface of the solar cell.[72] These methods can usually only be applied to specific scenarios, or the efficiency improvement is not significant, or the cost cannot be controlled. They cannot be used as a general method to improve solar cell efficiency in OWPT applications, so they are not described in detail in this thesis.

2.3.3 Categories of solar cells

Solar cells are divided into single-junction solar cells and multi-junction solar cells according to the number of junctions. In the application of OWPT, the light source is not broad-spectrum sunlight but monochromatic light which can improve the photovoltaic conversion efficiency of solar cells. Therefore, this thesis only discusses single-junction solar cells. According to the different semiconductor materials, the band gap of solar cells is also different, so they show different corresponding absorption spectrum. As discussed in section 2.2.3, the photovoltaic conversion efficiency of a solar cell is closely related to the wavelength of the incident light, thus the selection of the light source and the solar cell of the OWPT system needs to be considered at the same time. Although LEDs have the highest efficiency in the short-wavelength band, solar cells are mainly designed for the sunlight, thereby the research on solar cells designed specifically for short-wavelength light such as blue and ultraviolet light advances slowly. In the near-infrared wavelength band, both LEDs and solar cells have higher efficiency, so the chose solar cells should have the band gap corresponds to the near-infrared wavelength band. Within this bandgap range, Si solar cells, CIGS solar cells and GaAs solar cells are taking as examples to compare the characteristics in OWPT application. The Table 2.7 listed these solar cells and their characteristics.

Table 2.7 Typical solar cells

Solar cell types	**Jsc@1-sun (mA/cm^2)**	**Features**	**Feasibility in OWPT**
Si	41	The most common solar cell, low cost but relatively low efficiency	△
CIGS	38	High current density, applicable less than 20-sun	△
GaAs	25-30	An excellent material in OWPT with high efficiency	○

The Si (silicon) solar cell is the most common and spread solar cell, and have been widely used in solar energy generation application. The band gap of Si solar cell is 1.14 eV. The research and development of Si solar cell is relatively mature, thus the cost of Si solar cell is cheapest. Whereas, the current density of solar cell is high, and high current density causes the Joule heat to be more easily generated, which increases the non-radiative recombination and reduces the photovoltaic conversion efficiency of the solar cell. Therefore, the efficiency of Si solar cell is relatively low. However, in large-scale OWPT applications, such as ultra-long distance (above kilometers) optical wireless power transmission, the irradiation spot size on the receiving side is very large, which requires a large number of solar cells to form an array to receive optical energy. Therefore, in such applications, the low-cost advantage of Si solar cells will be amplified, making it a candidate for the receiver of OWPT system.

The CIGS (copper indium gallium selenide) solar cell is a thin-film solar cell. The band gap of the CIGS solar cell can be adjusted within the range of 1.0 eV-1.7 eV by adjusting the ratio of Ga and In. The CIGS solar cell has a high current density similar to Si solar cell, thus it is considered to be applicable only the radiant intensity is moderate. Besides, the advantages of CIGS solar cells in terms of efficiency are not obvious enough compared with Si solar cells in OWPT application.

The band gap of GaAs (gallium arsenide) solar cell is 1.43 eV, which is perfectly corresponded to near-infrared wavelength. The short-circuit current density of GaAs solar cells is about 25 - 30 mA/cm^2, which is relatively low compared with Si solar cell and CIGS solar cell, thus makes it an excellent material that can perform higher efficiency. Besides, because Gallium is a by-product of the smelting of other metals, the GaAs cells are relatively insensitive to heat and it can keep high efficiency when temperature is high. Moreover, GaAs solar cells are usually thin films, so they have very light weight and flexibility. Although the cost of GaAs solar cell is relatively high, considering the application of OWPT always requires concentration of light beam which causes small irradiation spot, thus the required size of GaAs solar cell is also small and cost can be controlled.

In summary, GaAs solar cell is a very suitable choice for OWPT applications in current stage.

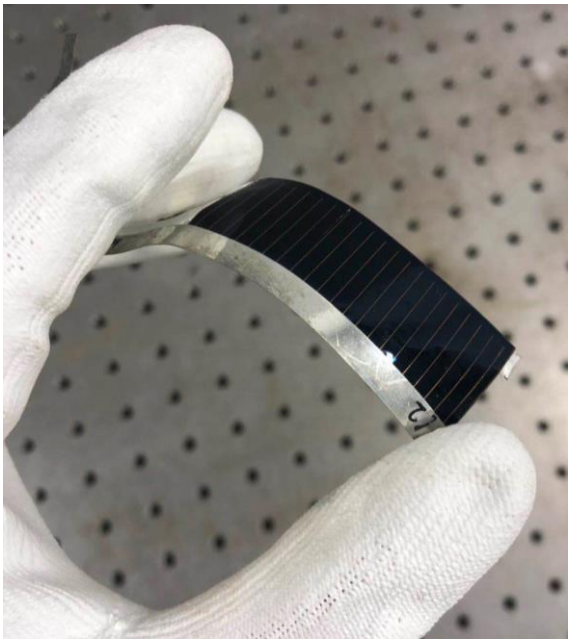

Fig. 2.33 Flexibility of GaAs solar cell

The solar cells listed in Table 2.7 are not the only ones that can work with near-infrared wavelength light. According to related reports,[73][74][75] there are also many solar cells with higher performance, but such solar cells are either still in the research stage and have not been commercialized, or the cost cannot be controlled. In fact, in terms of performance, cost, or dimension, GaAs solar cells is the most suitable choice for OWPT applications currently.

In addition, there are solar cells for short-wavelength light, such as PVK (perovskite) solar cells and GaInP (gallium indium phosphide) solar cells. However, they all have some problems more or less. For example, the absorption layer of a perovskite solar cell may be degraded under the irradiation of high intensity. GaInP solar cells have a lower current density and can withstand a high light intensity, but the thermal resistance of the material itself is too large. Therefore, considering the application scenarios of OWPT technology, they are

not suitable to be applied at this stage. However, it can be predicted that such solar cells have the potential to be used in OWPT systems in the future, and combined with high-efficiency LED light sources of short-wavelength, the overall efficiency of LED-based OWPT system can be greatly improved.

2.3.4 Summary of light energy receiver of OWPT system

At the beginning of section 2.3, various types of light energy receiving devices are discussed, and it was explained that solar cells are the only devices that can relatively efficiently convert optical energy into electrical energy at this stage. In section 2.3.1, the basic principles and properties of solar cells are introduced in detail. Considering that in OWPT applications, the photovoltaic conversion efficiency of solar cells is the most important parameter, then in section 2.3.2, the efficiency of solar cells and two methods of improving solar cell efficiency in OWPT applications are discussed, which are monochromatic light and intensity condensation. Besides, brief discussion of the OWPT performance that can be achieved by using such approaches is shown. Finally, in section 2.3.3, several types of solar cells correspond to the typical near-infrared wavelength range are compared. Through the characteristics of efficiency, thermal resistance, it is concluded that GaAs solar cells are the most suitable choice for OWPT system at this stage.

2.4 Optical elements in OWPT system

The beam control system is an essential part of the OWPT system. In order to point to a long-distance terminal, the light beam emitted by the OWPT system needs to be sharp enough to reduce the intensity lost by the divergence of the light beam through the long-distance propagation. Especially in the LED-based OWPT system, as discussed in section 2.2, in order to ensure that the light-emitting area is minimized, the divergence angle of the LED will be slightly large. Due to the spatially incoherence LEDs, beam collimation at a long distance is difficult. Therefore, the beam control system is far more important for the LED-based OWPT system. The beam control system can be configured as an array

antenna like microwave power transmission technology, but it is very difficult and the device size will be large. Fortunately, the light beam can be shaped and controlled simply by optical elements, which lens groups. Therefore, in this research, the lens group is used as a beam control system to rearrange the intensity distribution of the light source. The discussion of the relevant parameters of the beam control system of the LED-based OWPT system will be introduced in detail in Chapter 3. In this section, the proper lenses in the beam control system are mainly discussed.

2.4.1 The particularity of OWPT optical system

Optical systems can be divided into imaging optical systems and non-imaging optical systems. The most important factor that the general imaging optical systems care about is the imaging quality on the image plane. For example, the optical systems of cameras and microscopes will make the image at the image plane as clear as possible, and the shape and size of the image and the object are in scale, thus various information of the object can be reflected through the image. Another application of imaging optical system is lighting. For instance, as for various stage lighting or household lighting devices, although their purpose is not to produce a clear image at the target distance, it is necessary to make the light distribution as even as possible, so the concern is the high luminance and intensity even distribution of the image. Therefore, although the total intensity of such system might be very high, the irradiance at the target location is low (usually much lower than 1 sun irradiance).

Different from the above-mentioned imaging optical system, the task of OWPT beam control system is to rearrange the intensity and transmit it with high efficiency, and ensures the high radiant intensity at the receiving side. The image quality at the receiving end is not an important factor to OWPT application, while the high efficiency and high irradiance is the most important factors. Therefore, the beam control system of OWPT application belongs to the field of non-imaging optics.[76] As mentioned in the section 2.2, etendue is the most important parameter of OWPT beam control system. Therefore, the optical components in

the OWPT beam control system do not need to consider parameters such as spherical aberration, chromatic aberration, etc., but the parameters such as reflectance, absorptance, geometrical loss. In the design of the entire beam control system, the entire efficiency and transversal magnification of the optical system are the two most important parameters, which separately characterize the efficiency of the optical system, and the ratio of the irradiation spot size at the target transmission distance to the light-emitting area of the light source. Basically, each optical element will cause a certain degree of reflection and absorption of light intensity. Besides, the convex lens is generally used in the optical system of OWPT for beam convergence, the transversal magnification of which is greater than 1, thus for each additional lens used, the transversal magnification value of the entire optical system will increase. Based on these two reasons, the number of optical elements should be as small as possible in the OWPT beam control system to ensure the high transmission efficiency and small irradiation spot size. This is based on the particularity of the optical system applied by OWPT application.

2.4.2 Proper lens types of OWPT optical system

As mentioned above, because the divergence angle of the LED is large, and convex lenses can reduce the divergence of the beam, which makes convex lenses to be the main optical components in the OWPT system. Convex lenses are generally classified into biconvex lenses and plano-convex lenses. From the performance point of view, there is not much difference between the two in OWPT applications. However, both surfaces of the biconvex lens are curved, so the center thickness of the lens will be larger than plano-convex lens, as well as the weight. In a portable OWPT system, this is a factor need to be considered. In addition, the surface of the biconvex lens has curvature as shown in Fig. 2.34, the surface close to the light source cannot effectively collect the light rays from the light source due to the beam has a certain degree of divergence, thus makes a small part of the intensity loss. Compared with biconvex lens, one surface of a plano-convex lens is flat without any curvature. Therefore, the loss of light

intensity will be reduced if use the flat surface to receive the light beam. Therefore, the plano-convex lens is the main component of the OWPT optical system.

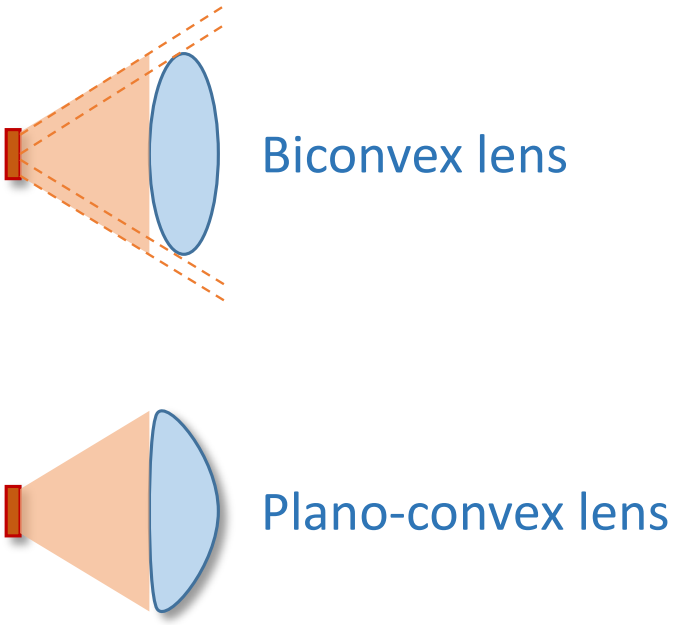

Fig. 2.34 The performance of the biconvex lens and plano-convex lens in LED-based OWPT system

In addition, there is aspheric lens which has very similar shape to plano-convex lens. Whereas, curved surface of the aspheric lens is not a standard spherical surface, but a freeform surface (FFS) that designed by controlling the curvature of each point on the curved surface.[77] The aspheric lens can more accurately control each component of the beam, which makes the light rays are refracted or reflected with different degrees, so aspheric lens can achieve better imaging than conventional lenses. In the field of imaging optics, aspheric lenses are one of the most important optical components. However, in the OWPT system which not require high-quality imaging, the functions of aspheric lenses and plano-convex lenses are almost the same, and the two can be substituted for each other.

Besides the two lenses mentioned above, there is another excellent lens option, which is the Fresnel lens. The Fresnel lens is a type of composite compact lens

which was originally designed for lighthouse. As the Fig. 2.35 shows, the Fresnel lens reduces the amount of material required compared to a conventional lens by dividing the lens into a set of concentric annular sections, and each annular section has same curvature. Thus, the design of Fresnel lens allows the construction of lenses of large aperture and short focal length without the mass and volume of material that would be required by a lens of conventional design.[78] A Fresnel lens can be made much thinner than a comparable conventional lens. Besides, the Fresnel lens can capture more oblique light from a light source.

Fresnel lens design allows a substantial reduction in thickness, at the expense of reducing the imaging quality of the lens, which makes Fresnel lens cannot be an ideal optical component in image optical system. However, in the non-imaging optical system such as OWPT system that not require imaging quality, the small thickness and weight make Fresnel lens a perfect candidate, especially the portable LED-based OWPT system.

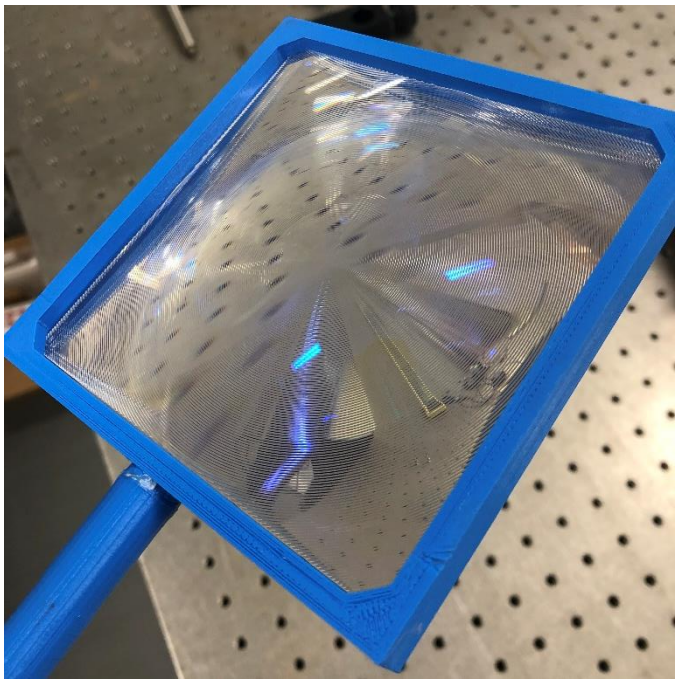

Fig. 2.35 The Fresnel lens with light weight and large aperture

2.4.3 The characteristics of lens

Generally, the focal length and aperture of the lens are the most important parameters in the OWPT system. As long as the focal length and aperture parameters are the same, plano-convex lens, aspheric lens or Fresnel lens with any material can almost achieve the same performance. The focal length of the lens affects the beam shaping effect of the optical system and other parameters such as the distance between the lenses, while the aperture of the lens affects the light collection efficiency of the lens. Therefore, as long as the lens apertures are sufficiently large, the high efficiency of the OWPT optical system can be realized. However, when designing the OWPT optical system, the parameters of each lens are not independent, but are interrelated and affect each other. For example, increasing the focal length of one lens to achieve higher radiant intensity at the target distance, but in turn may cause the aperture of the other lens to increase, thereby increasing the vertical dimension and weight of the entire system, then affecting the portability. Therefore, the parameters of each lens need to be carefully designed according to the needs of the OWPT applications. When designing an OWPT optical system, there is usually a balance between system performance and system efficiency. The system performance here includes factors such as the radiant intensity and system dimension, while the system efficiency usually refers to the efficiency of the optical system.

The material of the lens affects the reflectance, absorptivity and numerical aperture (NA) value of the lens. Generally, the light intensity absorption of single lens is small because of relatively small thickness. In order to minimize the value of the entire transversal magnification of the OWPT optical system, applying too many lenses is avoided. Therefore, the loss of light intensity caused by the absorption of the lens material is very small, usually only about a few percent. The light intensity loss caused by reflection on the lens surface is related to the incident angle of the beam, and the reflection loss of light component with a large incident angle is large. Considering the divergence angle of the LED light source is relatively large, the light lost due to reflection cannot be ignored. It is usually possible to reduce the reflection loss on the lens surface by adding AR (anti-reflection) coating to the lenses. An AR coating is a type of optical coating applied

to the surface of lenses and other optical elements to reduce reflection. The simplest interference AR coating consists of a single thin layer of transparent material. The typical AR coating is the quarter-wave layer AR coating, which provide no reflectance for the light with wavelength equal to four times of the coating's thickness. Therefore, the applying of such AR coating should be corresponded with the target wavelength.[79] The multi-layer interference AR coating for broad wavelength band is also possible, however it is complex and relatively expensive. Due to the emitted light of OWPT system is usually monochromatic, thus single-layer AR coating is sufficiently providing very low reflectivity of the lenses. By applying AR coating, the reflectivity of a single lens (two surfaces) can be usually reduced around 8%. Adding an AR coating to the optical components of the OWPT system is a low-cost method, but it can significantly reduce the light intensity loss. Therefore, it is necessary to configure AR coatings for all the optical components of the OWPT system, normally.

The numerical aperture (NA) of the optical element is another point need to be discussed. In the optical field, NA value describes the cone angular range of light that an optical element (lens) can collect. NA value is usually defined as:

$$NA = n \times \sin\theta \approx \frac{n \times D}{2f} \tag{2.4}$$

Here n is the refractive index of the lens working medium, θ is the half of the maximum cone angle when light enters the lens. And the NA is approximately equal to $\frac{n \times D}{2f}$. The D is the aperture size of the lens, and f is the focal length of the lens.[80]

It can be seen that NA defines the relationship between lens aperture and focal length. When the NA value and the aperture of the lens are constant, the focal length of the lens cannot be too small. In the OWPT system, the aperture of the optical element is generally larger to better collect the light beam and improve the system efficiency. Therefore, NA is a factor that limits the parameter design of optical components in some cases. Although by increasing the thickness of the lens, it is possible to achieve a smaller focal length under the same aperture. However, this approach may cause the mechanical dimensions of the lenses to

be mutually restricted and increase the weight of the equipment. From the equation (2.4), NA is also related to the material of the lens. By applying a material with a larger refractive index to increase the NA value of the lens, the focal length of the lens can be reduced while ensuring a certain aperture. Therefore, NA is a factor that must be considered when selecting lens materials. In some specific cases, it is necessary to choose a material with a larger refractive index to ensure that the lens can have both good aperture parameters and focal length parameters.

The Table 2.8 shows the common materials of the lenses.

Table 2.8 Typical materials of lens and corresponding parameters

Materials	Transmission range	Refraction Index	Reflection loss
BK7	350nm-2500nm	1.517	8.1%
PMMA	380nm-1000nm	1.492	8%
CaF2	130nm-1000nm	1.399	5.4%
MgF2	120nm-7000nm	1.413	5.7%
ZnSe	600nm-21000nm	2.403	29.1%
B270	290nm-2700nm	1.523	8.6%
S-LAH64	320nm-2400nm	1.788	16%

2.4.4 Summary of optical elements in OWPT system

In the section 2.4.1, the particularity of OWPT optical system is discussed. The difference between the OWPT optical system and normal image optical system is clarified. Then plano-convex lens, aspheric lens and Fresnel lens are the proper lens type for OWPT system is proved in section 2.4.2. Especially due to the light weight and small thinness of the Fresnel lens make it perfect candidate of lens for OWPT optical system. In the last section 2.4.3, the parameters of focal length, aperture size and material of lens is discussed. In conclusion, the focal length of the lens should be designed according to the specific applications. The

aperture of the lens should be sufficiently large to ensure the high efficiency of the optical system. The material of the lens has little effect under normal circumstances, and the loss caused by the light absorption is small, while the reflection loss can be reduced by adding AR coating on the lens surface. In special cases, in order to increase the NA value of the lens, a material with a larger refractive index should be selected.

Reference

[1] Seyedmahmoudian. M, Horan. B, Soon. T. Kok, Rahmani. R, Than Oo. A. Muang, Mekhilef. S, Stojcevski. A, "*State of the art artificial intelligence-based MPPT techniques for mitigating partial shading effects on PV systems – A review,*" Renewable and Sustainable Energy Reviews, 64, pp: 435–455, 2015.

[2] Dawei Liang and Joana Almeida, "*Highly efficient solar-pumped Nd:YAG laser,*" Opt. Express, 19, pp: 26399-26405, 2011.

[3] Hochstein. Peter A, "LED integrated heat sink", U.S. Patent No. 6, 517, 218, 11, 2003.

[4] Dian. F, John. Amirhossein Yousefi, and Sungjoon Lim, "*A practical study on Bluetooth Low Energy (BLE) throughput,*" 2018 IEEE 9th Annual Information Technology, Electronics and Mobile Communication Conference (IEMCON), IEEE, 2018.

[5] Bremner. S. P, M. Y. Levy, and C. Bo Honsberg, "*Analysis of tandem solar cell efficiencies under AM1. 5G spectrum using a rapid flux calculation method,*" Progress in photovoltaics: Research and Applications, 16 (**3**), pp: 225-233, 2008.

[6] https://en.wikipedia.org/wiki/Luminous_efficacy.

[7] Zhukov, Sergey, Andrei Iones, and Grigorij Kronin, "*An ambient light illumination model,*" Rendering Techniques' 98, Springer, Vienna, pp: 45-55, 1998.

[8] Alatawi. Abdullah, et al., "*High-power blue superluminescent diode for high CRI lighting and high-speed visible light communication,*" Optics express, 26 (**20**), pp: 26355-26364, 2018.

[9] Janassek. Patrick, Sébastien Blumenstein, and Wolfgang Elsäßer, "*Ghost spectroscopy with classical thermal light emitted by a superluminescent diode,*" Physical Review Applied, 9 (**2**), 2018.

[10] Rishinaramangalam. Ashwin K, et al., "*Nonpolar GaN-based superluminescent diode with 2.5 GHz modulation bandwidth,*" 2018 IEEE International Semiconductor Laser Conference (ISLC), IEEE, 2018.

[11] Kafar. Anna, et al., "*InAlGaN superluminescent diodes fabricated on patterned substrates: an alternative semiconductor broadband emitter,*" Photonics Research, 5 (**2**), pp: A30-A34, 2017.

[12] Miller. S. E; Li, Tingye, Marcatili. E. A. J, "*Part II: Devices and systems considerations,*" Proceedings of the IEEE, 61 (**12**), pp: 1726–1751, 1973.

[13] D. Kouznetsov, J.F. Bisson, K. Takaichi, K. Ueda, "*Single-mode solid-state laser with short wide unstable cavity,*" JOSA B. 22 (**8**), pp: 1605–1619, 2005.

[14] Forrest. Adam F, et al., "*High-power quantum-dot superluminescent tapered diode under CW operation,*" Optics Express, 27 (**8**), pp: 10981-10990, 2019.

[15] Zia. Nouman, et al., "*High-power single mode GaSb-based 2 μ m superluminescent diode with double-pass gain,*" Applied Physics Letters, 115 (**23**), pp: 231106, 2019.

[16] Aho. A. T, et al, "*High power GaInNAs superluminescent diodes emitting over 400 mW in the 1.2 μ m wavelength range,*" Applied Physics, Letters, 115 (**8**), pp: 081104, 2019.

[17] Larry A. Coldren, Scott W. Corzine, Milan L. Mashanovitch, "*Diode Lasers and Photonic Integrated Circuits,*" John Wiley & Sons, 2012.

[18] Jin. Ke, and Weiyang Zhou, "*Wireless laser power transmission: a review of recent progress,*" IEEE Transactions on Power Electronics, 34 (**4**), pp: 3842-3859, 2018.

[19] Kamiyama. Daisuke, Akira Yoneyama, and Motoharu Matsuura, "*Multichannel data signals and power transmission by power-over-fiber using a double-clad fiber,*" IEEE Photonics Technology Letters, 30 (**7**), pp: 646-649, 2018.

[20] Dirac. Paul Adrien Maurice, "*The Quantum Theory of the Emission and Absorption of Radiation,*" Proc. Roy. Soc, A114 (**767**), pp: 243–265, 1927.

[21] Einstein. A, "*Strahlungs-emission und -absorption nach der Quantentheorie,*" Verhandlungen der Deutschen Physikalischen Gesellschaft, 1916.

[22] Einstein. A, "*Zur Quantentheorie der Strahlung,*" Physikalische Zeitschrift, 18, pp: 121–128, 1917.

[23] Fabry. C, Perot. A, "*Theorie et applications d'une nouvelle methode de spectroscopie interferentielle,*" Ann. Chim. Phys, 16 (**7**), 1899.

[24] Perot. A, Fabry. C, "*On the Application of Interference Phenomena to the Solution of Various Problems of Spectroscopy and Metrology,*" Astrophysical Journal, 9, pp: 87, 1899.

[25] Chang-Hasnain, Connie J, "*Tunable vcsel,*" IEEE Journal of Selected Topics in Quantum Electronics, 6 (**6**), pp: 978-987, 2000.

[26] Hariyama. Tatsuo, et al., "*High-accuracy range-sensing system based on FMCW using low-cost VCSEL,*" Optics express, 26 (**7**), pp: 9285-9297, 2018.

[27] Haghighi. Nasibeh, Philip Moser, and James A. Lott, "*Power, bandwidth, and efficiency of single VCSELs and small VCSEL arrays,*" IEEE Journal of Selected Topics in Quantum Electronics, 25 (**6**), pp: 1-15, 2019.

[28] Chong. C. K, et al., "*Bragg reflectors,*" IEEE transactions on plasma science, 20 (**3**), pp: 393-402, 1992.

[29] Seurin. Jean-Francois, et al., "*Progress in high-power high-efficiency VCSEL arrays,*" Vertical-Cavity Surface-Emitting Lasers XIII, Vol. 7229, International Society for Optics and Photonics, 2009.

[30] N. Otake, E. Kojima, et al., "*High-pulsed-power (49W) vertical-cavity surface-emitting laser with five quantum wells by uniform current injection into large emitting area,*" IEICE ELEX, 8 (**2**), pp: 109-113, 2011.

[31] Thompson. George Horace Brooke, "*Physics of semiconductor laser devices,*" wi, 1980.

[32] Samuel. Ifor David Williams, and Graham Alexander Turnbull, "*Organic semiconductor lasers,*" Chemical reviews, 107 (**4**), pp: 1272-1295, 2007.

[33] Okon. Thomas M, Biard. James R, "*The First Practical LED,*" EdisonTechCenter.org. Edison Tech Center, 2015.

[34] Zheludev. Nikolay, "*The life and times of the LED—a 100-year history,*" Nature photonics, 1 (**4**), pp: 189-192, 2007.

[35] Nakamura. Shuji, Stephen Pearton, and Gerhard Fasol, "*The blue laser diode: the complete story,*" Springer Science & Business Media, 2000.

[36] Edwards. Kimberly D, "*Light Emitting Diodes,*" University of California at Irvine, pp: 2, 2019.

[37] Schubert. E. Fred, Thomas Gessmann, and Jong Kyu Kim, "*Light emitting diodes,*" Kirk‐Othmer Encyclopedia of Chemical Technology, 2000.

[38] Gupta. S. Dutta, and B. Jatothu, "*Fundamentals and applications of light-emitting diodes (LEDs) in in vitro plant growth and morphogenesis,*" Plant Biotechnology Reports, 7 (**3**), pp: 211-220, 2013.

[39] Michael W. Davidson, "*Fundamentals of Light-Emitting Diodes (LEDs),*" ZEISS.

[40] Ikeuchi. Katsushi, "*Lambertian Reflectance,*" Encyclopedia of Computer Vision, Springer, pp: 441–443, 2014.

[41] Kwan. A, Dudley. J, Lantz. E, "*Who really discovered Snell's law?,*" Physics World, 15 (**4**), pp: 64, 2002.

[42] Lee. Ya-Ju, et al., "*Enhancing the output power of GaN-based LEDs grown on wet-etched patterned sapphire substrates,*" IEEE Photonics Technology Letters, 18 (**10**), pp: 1152-1154, 2006.

[43] Leonard. Daniel L, et al., "*Polymerization efficiency of LED curing lights,*" Journal of Esthetic and Restorative Dentistry, 14 (**5**), pp: 286-295, 2002.

[44] Osram, KT DDLM31.13, datasheet.

[45] Osram, PLT5 520B, datasheet.

[46] Osram, LE B Q8WP, datasheet.

[47] Osram, PLPT5 450KA, datasheet.

[48] Osram, LE B Q7WP, datasheet.

[49] Osram, PLPT9 450LA_E, datasheet.

[50] Vassighi. Arman, Sachdev. Manoj, "*Thermal and Power Management of Integrated Circuits, Integrated Circuits and Systems,*" 2006.

[51] Rogov P.Yu, Knyazev M.A, Bespalov V.G, "*Research of linear and nonlinear processes at femtosecond laser radiation propagation in the medium simulating the human eye vitreous,*" Scientific and Technical Journal of Information Technologies, Mechanics and Optics, 15 (**5**), pp: 782–788, 2015.

[52] SS-EN 207:2017, (E) EUROPEAN STANDARD EN 207, "*Personal eye-protection equipment - Filters and eye-protectors against laser radiation (laser eye-protectors) (ICS 13.340.20),*" CEN-CENELEC Management Centre, 2017.

[53] Parker. S, "*Laser regulation and safety in general dental practice,*" British dental journal, 202 (**9**), pp: 523-532, 2007.

[54] "*Safety standards of laser product,*" Japanese industrial standards committee (JIS) Std. JIS C6802-002, 2018.

[55] Bhojani. Naeem, et al., "*Canadian Urological Association best practice report: Holmium: YAG laser eye safety,*" Canadian Urological Association Journal, 14 (**12**), pp: 380, 2020.

[56] Duncan. Kate J, "*Laser based power transmission: Component selection and laser hazard analysis,*" 2016 IEEE PELS Workshop on Emerging Technologies: Wireless Power Transfer (WoW), IEEE, 2016.

[57] Zhou. Jing, et al., "*Upconversion luminescent materials: advances and applications,*" Chemical reviews, 115 (**1**), pp: 395-465, 2015.

[58] Chaves. Julio, "*Introduction to Nonimaging Optics, Second Edition,*" CRC Press, 2015.

[59] Roland Winston, et al., "*Nonimaging Optics,*" Academic Press, 2004.

[60] Matthew S. Brennesholtz, Edward H. Stupp, "*Projection Displays,*" John Wiley & Sons Ltd, 2008.

[61] Osram, SFH-4786S, datasheet.

[62] Osram, SFH-4703AS, datasheet.

[63] Ito. Hiroshi, et al., "*High-speed and high-output InP-InGaAs unitraveling-carrier photodiodes,*" IEEE Journal of selected topics in quantum electronics, 10 (**4**), pp: 709-727, 2004.

[64] Capasso. Federico, "*Physics of avalanche photodiodes,*" Semiconductors and semimetals, 22, pp: 1-172, 1985.

[65] Abbasi. Rasha, et al., "*Calibration and characterization of the IceCube photomultiplier tube,*" Nuclear Instruments and Methods in Physics Research Section A: Accelerators, Spectrometers, Detectors and Associated Equipment, 618 (**1-3**), pp: 139-152, 2010.

[66] Sharma. Asha, et al., "*A carbon nanotube optical rectenna,*" Nature nanotechnology, 10 (**12**), pp: 1027-1032, 2015.

[67] Essig. Stephanie, Allebé. Christophe, Remo. Timothy, Geisz. John F, Steiner. Myles A, Horowitz. Kelsey, Barraud. Loris, Ward. J. Scott, Schnabel. Manuel, "*Raising the one-sun conversion efficiency of III–V/Si solar cells to 32.8% for two junctions and 35.9% for three junctions,*" Nature Energy, 2 (**9**), pp: 17144, 2017.

[68] Streetman. Ben G, Sanjay Banerjee, "*Solid State electronic Devices (5th ed.),*" New Jersey: Prentice Hall, pp: 524, 2000.

[69] S. Rühle, "*Tabulated values of the Shockley–Queisser limit for single junction solar cells,*" Solar Energy, 130, pp: 139–147, 2016.

[70] Tomoyuki Miyamoto, "*Optical Wireless Power Transmission —Toward the Creation of New Optical Application Fields—,*" IEICE TRANSACTIONS on Electronics c, J103-C (**5**), pp: 270-278, 2020.

[71] Lee. Young Il, et al., "*A low-temperature thin-film encapsulation for enhanced stability of a highly efficient perovskite solar cell,*" Advanced Energy Materials, 8 (**9**), 2018.

[72] Wang. Yang, et al., "*Diffraction-Grated Perovskite Induced Highly Efficient Solar Cells through Nanophotonic Light Trapping,*" Advanced Energy Materials, 8 (**12**), 2018.

[73] Li. Wanning, et al., "*A High-Efficiency Organic Solar Cell Enabled by the Strong Intramolecular Electron Push–Pull Effect of the Nonfullerene Acceptor,*" Advanced Materials, 30 (**16**), 2018.

[74] Yamamoto. Kenji, et al., "*High-efficiency heterojunction crystalline Si solar cells,*" Japanese Journal of Applied Physics, 57 (**8S3**), 2018.

[75] Yuan. Jun, et al, "*Single-junction organic solar cell with over 15% efficiency using fused-ring acceptor with electron-deficient core,*" Joule, 3 (**4**), pp: 1140-1151, 2019.

[76] Winston. Roland, Juan C. Miñano, and Pablo G. Benitez, "*Nonimaging optics,*" Elsevier, 2005.

[77] Zhenrong. Zheng, Hao Xiang, and Liu Xu, "*Freeform surface lens for LED uniform illumination,*" Applied optics, 48 (**35**), pp: 6627-6634, 2009.

[78] Leutz. Ralf, et al., "*Design of a nonimaging Fresnel lens for solar concentrators,*" Solar energy, 65 (**6**), pp: 379-387, 1999.

[79] Hemant Kumar Raut, V. Anand Ganesh, A. Sreekumaran Nairb, Seeram Ramakrishna, "*Anti-reflective coatings: A critical, in-depth review,*" Energy & Environmental Science, 4 (**10**), pp: 3779–3804, 2011.

[80] Greivenkamp. John E, "*Field Guide to Geometrical Optics,*" SPIE Field Guides, vol. FG01. SPIE, pp: 29, 2004.

Chapter 3 Configuration of portable LED-based OWPT system

In Chapter 2, the components in the OWPT system have been discussed in detail. So far, the basic configuration of the IoT-OWPT system with LED as the light source, solar cell as the optical energy receiving element, and lens group of the beam control system has been determined. In Fig. 3.1, the illustration schematic of the portable LED-based OWPT system for compact IoT is shown.

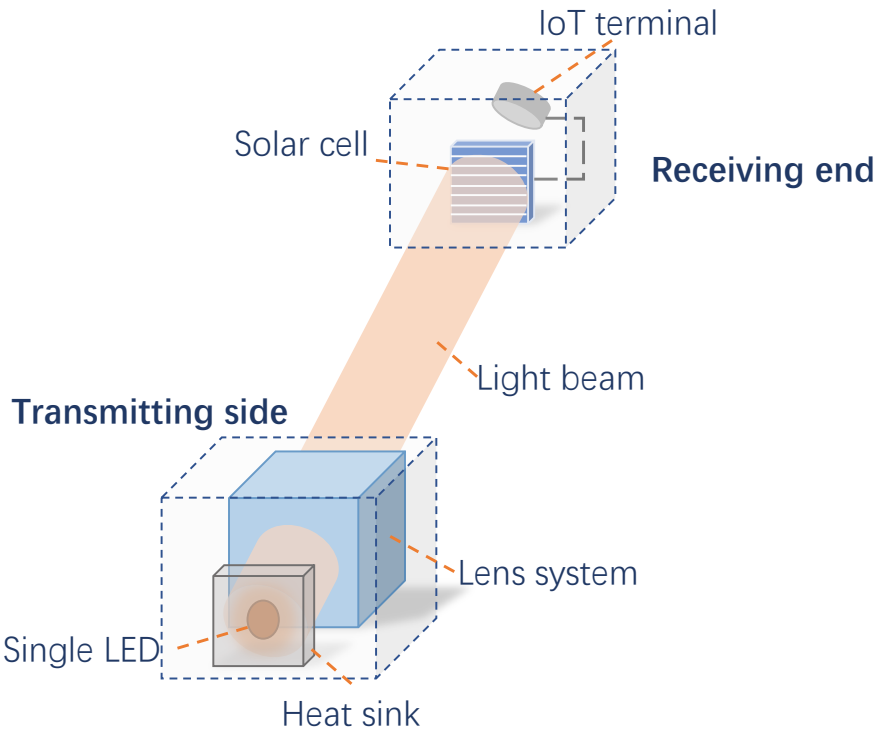

Fig. 3.1 The illustration schematic of the portable LED-based OWPT system for compact IoT

On the transmitting side, a portable OWPT transmitter is consisted with a single LED light source and a lens system. A small-dimension heat sink is usually necessary for heat dissipation and ensuring the LED always works at a relatively constant temperature. The material of the heat sink is usually aluminum or copper, which has a light mass. Considering that the LED has relatively excellent heat

resistance, a heat sink with side length of several centimeter is enough for the heat dissipation, thus it will hardly affect the portability of the OWPT transmitter. On the receiving side, solar cell is used as the optical energy receiving element. With a short transmission distance (up to 1 m), the irradiation spot can usually be controlled very small, so a single solar cell has enough area to receive light energy. In the case of a long transmission distance, the irradiation spot will become larger due to the light beam divergence, thus a solar cell array that multiple solar cells connected in series is usually applied as the receiver. In such case, the radiant intensity of the irradiation spot needs to be uniform enough to ensure that each solar cell has a high efficiency. The temperature of the receiving end is lower than the transmitting end, so a heat sink is usually unnecessary for the solar cell. In the cause of high-intensity OWPT system (LED array), the temperature at the receiving end may have an obvious impact on the efficiency of the solar cell. Besides, if the IoT terminal is not configured built-in battery, the component of light energy that higher than the terminal power consumption will be converted into heat energy on the surface of the solar cell and have a negative impact on the efficiency of the solar cell. In such application scenarios, a heat sink is considered to configure behind the solar cell. Solar cell can be directly connected to IoT terminals without any additional rectifier circuits. According to the requirements of the application, an MPPT module is sometimes configured between the solar cell and the IoT terminal to ensure that the load can always work at the optimum operating point.

In this chapter, the optical system of the LED-based OWPT system will be analyzed in detail. The links between various parameters in the optical system and their influence on the system performance will be discussed through mathematical models and simulations, and appropriate value ranges for each parameter will be provided.

3.1 Basic configuration of the LED-based OWPT lens system

The beam control system, or optical system, is the most critical part of the LED-based OWPT system. The optical system is composed of single or multiple

lenses with appropriate parameters. In OWPT applications, in order to accurately point the light beam to the receiver of the IoT terminal at a long distance, an optical system needs to be applied to rearrange the light intensity emitted from the LED and control the degree of divergence, so that the light energy will not dissipate greatly during the propagation of the light beam. On the other hand, the photovoltaic conversion efficiency of the solar cell as the receiver improves with the increase of the radiant intensity on the surface of the solar cell. Therefore, in order to increase the radiant intensity at the receiving end to improve the efficiency of the solar cell in the case of a certain total light source intensity, the optical system needs to make the size of irradiation spot to be small enough. Moreover, for avoiding the deterioration caused by overheating of a part area on the solar cell, the intensity distribution of the irradiation spot needs to be sufficiently uniform. Summarily, the optical system determines the efficiency and final output of the entire LED-based OWPT system. Therefore, each parameter of the optical system needs to be carefully designed and optimized multiple times according to application requirements.

According to the number of lens elements in the optical system, the optical system can be simply divided into the single-lens system, the double-lens system and the multi-lens system which is composed of more than two lenses. In Section 3.1, the three configurations of optical systems will be analyzed and compared in detail through mathematical models to determine the optimal optical system configuration for the LED-based OWPT system.

3.1.1 Single-lens optical system

Single-lens optical system is the simplest configuration. One lens is used to collect the light beam from the light source and transmits the intensity to the solar cell at the target distance. The illustration schematic of the single-lens optical system is shown in the Fig. 3.2.

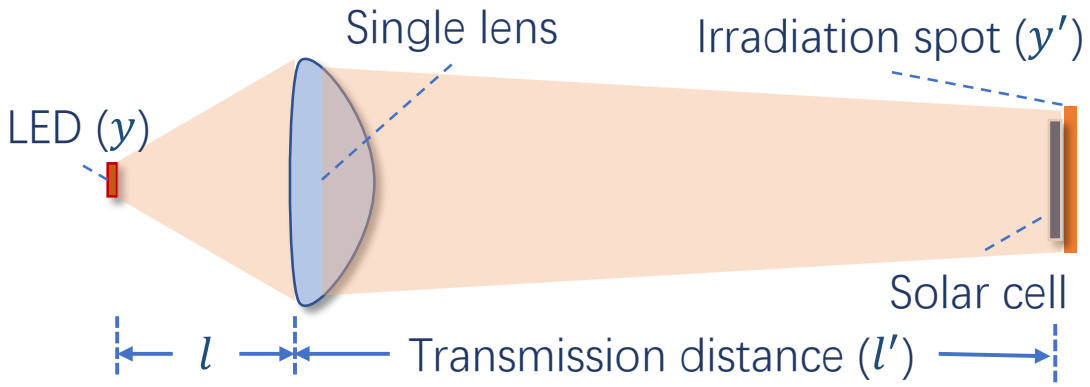

Fig. 3.2 The illustration schematic of the single-lens optical system

The single-lens optical system has several merits. First, the configuration of single-lens optical system is very simple, only one lens is applied to rearrange the light beam. Thus, it is easy to design and optimize due to the number of parameters is small. Besides, light weight and low cost is also an advantage of this configuration. Such single-lens optical system configuration is usually applied in the laser-based OWPT system. Due to the spatial coherence of the laser beam, the applying of one collimation lens to the laser light source can be sufficient to form a highly collimated beam, which can maintain a very small degree of divergence even in a long-distance propagation, thus achieving the effect of long-distance pointing. In addition, because the divergence angle of the beam emitted by the laser is small enough, the aperture of the collimation lens can be restrained to a small size, so that a highly compact system configuration can be realized. However, single-lens configuration has a fatal flaw in the application of LED-based OWPT technology. As discussed in section 3.1, a small irradiation spot is always desired in order to improve the photovoltaic conversion efficiency of the solar cell and also decrease the size receiver in the application of OWPT. Therefore, the transversal magnification of the entire optical system is far more important, which describes the ratio between the size of irradiation spot and the light emitting area. The definition of transversal magnification of optical system is shown in the equation (3.1):

$$\beta = \frac{y'}{y} = \beta_1 \times \beta_2 \times \beta_3 \times \beta_4 \times \ldots \times \beta_{\mathrm{n}} \tag{3.1}$$

The β value is the overall transversal magnification of the optical system, y' and y are the size of the irradiation spot and light emitting chip of the LED, respectively. The overall transversal magnification value is the product of the transversal magnification value of each optical element in the system, as shown in the equation (2.5). Thus, in a single-lens optical system, the overall transversal magnification value of the system can be approximately equal to the transversal magnification of the only lens, which is:

$$\beta = \beta_1 \tag{3.2}$$

Here β_1 is the transversal magnification value of the lens. It should be noted that, usually the LED itself has a package lens, which is also regarded as an optical component. When an accurate overall transversal magnification value of optical system is required, the package lens of LED should also be included into the calculation. However, due to the accurate parameters of LED package lens are difficult to obtain, and once a certain LED as the OWPT system light source is determined, the package lens will not affect the design of the OWPT optical system. Therefore, the package lens of LED is not considered into the calculation in this thesis.

The Fig. 3.3 shows the geometrical schematic diagram of light path of a single-lens optical system.

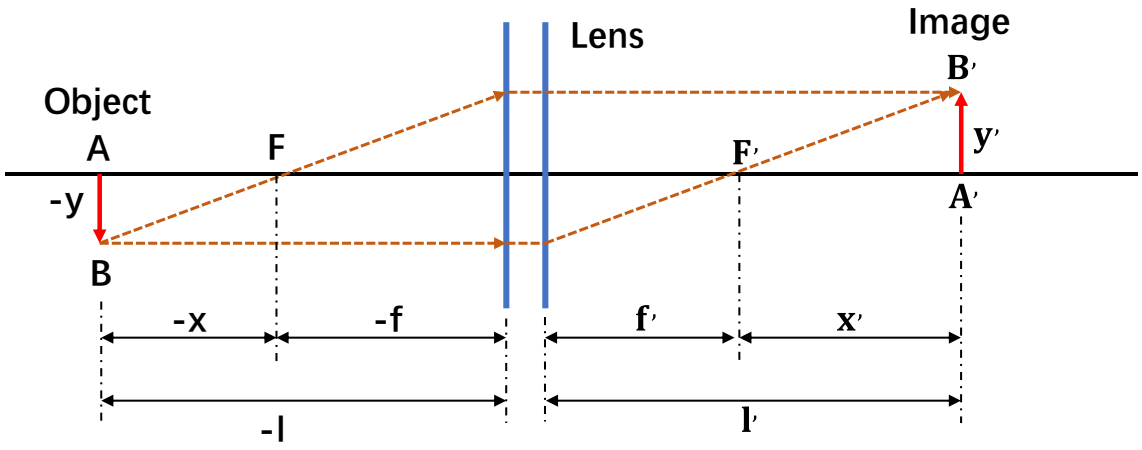

Fig. 3.3 The geometrical analysis of the single-lens optical system light path

The transversal magnification can be expressed in two forms, which are the form under the Newton's formula and under the Gaussian's formula.[1] Newton's formula is shown as:

$$xx' = ff' \tag{3.3}$$

Here x is the distance between the object (light source) and the back focal length of the lens, and x' is the distance between the image (irradiation spot) and the focal length of the lens, separately. While f is the back focal length of the lens, and f' is the focal length of the lens.

Thereby, according to a simple geometric relationship, the transversal magnification form under the Newton's formula can be described as the following equation (3.4):

$$\beta = \frac{y'}{y} = -\frac{x'}{f'} = -\frac{f}{x} \tag{3.4}$$

The Gaussian's formula is shown as:

$$\frac{f'}{l'} + \frac{f}{l} = 1 \tag{3.5}$$

The value of l' is the distance between the object and the rear surface of the lens, the l is the distance between the image and the front surface of the lens. The relation between the value of x, f and l can be simply obtained as:

$$l = x + f \tag{3.6}$$

Similarly,

$$l' = x' + f' \tag{3.7}$$

Thereby, the transversal magnification form under the Gaussian's formula is:

$$\beta = \frac{y'}{y} = -\frac{f}{f'} \times \frac{l'}{l} \tag{3.8}$$

According to the Lagrange invariant, the relationship between the value of the back focal length and the focal length of a lens can be derived as:

$$\frac{f'}{f} = -\frac{n'}{n} \tag{3.9}$$

In the above equation, n is the refractive index of the medium in the object space, while n' is the refractive index of the medium in the image space. Under normal circumstances, the medium in object space and image space are both air, thus it can be concluded that the back focal length and focal length of the lens are approximately equal, which is:

$$f' = -f \tag{3.10}$$

Hence, the overall transversal magnification of the single-lens optical configuration can be represented as:

$$\beta = \beta_1 = \frac{y'}{y} = \frac{l'}{l} \tag{3.11}$$

Therefore, the transversal magnification value of a single-lens optical system is directly related with the ration between the transmission distance and the distance between the LED and the lens. In the application scenario of OWPT, the target is transmitting power remotely through a relatively long distance, thus the value of l' is always large. While in order to achieve a sufficiently small irradiation spot, the transversal magnification value β should be small. Thus, without changing the transmission distance, the value of β can only be reduced by increasing the value of l', which is the distance between the LED and the lens. Whereas, due to the relatively large divergence angle of the LED, increasing the distance between the LED and the lens will cause large part of intensity lost on

the surface of lens and deteriorate the efficiency of the lens system. Enlarging the aperture size of the lens is one solution, but it will greatly increase the dimension of the system and cause the OWPT transmitter to lose its portability. For instance, the typical half divergence angle of a dome-type package LED is 40°, by simple geometric calculation, the radius of the lens aperture should be around 8.4 cm in order to collect the divergent LED beam when the distance between the LED and the lens is 10 cm, which means more than 16 cm diameter of the lens. At this size, the OWPT transmitter has been difficult to maintain portability. Moreover, the calculation shown above is only based on the half divergence angle of the LED, which means that there is still a large part of light intensity exists outside of such half divergence angle. In order to improve the efficiency of the optical system, the actual required lens aperture size will be much larger than the calculated value shown above. Therefore, the single-lens optical configuration is not suitable to be applied in the LED-based OWPT system due to the difficulty of obtaining a small irradiation spot and high efficiency of the optical system at the same time.

In general, single-lens optical configuration has the merits of simple configuration and light weight. It can be a perfect option of the optical system in the laser-based OWPT application. However, in the LED-based OWPT system, the performance of single-lens optical configuration will be poor due to the low efficiency or large irradiation spot caused by relatively large divergence angle of the LED light source.

3.1.2 Double-lens optical system

The double-lens optical system consists of two lenses. The first lens is a condenser lens, and the task of which is to efficiently collect the light beam emitted from the LED light source and reduce the degree of divergence of the light beam. Then an image lens will converge and focus the light beam that passed through the condenser lens at the designated transmission distance. Since the degree of divergence of light beam is decreased after being refracted

by the condenser lens, the aperture size of the image lens can be controlled. The Fig. 3.4 shows the illustration schematic of the double-lens optical system.

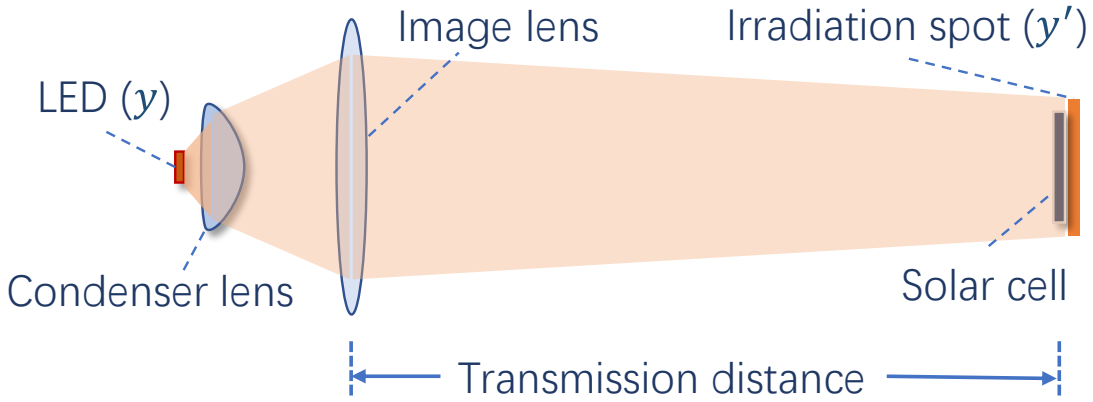

Fig. 3.4 The illustration schematic of the double-lens optical system

As shown in Fig. 3.4, the condenser lens can be closely installed after the LED light source, thus almost all the light emitted from the LED can be received by the optical system. The efficiency of the double-lens optical system is determined by the light condensing ability of the condenser lens and the aperture size of the image lens. Generally, the smaller the condenser lens limits the degree of beam divergence, the smaller the aperture of the image lens can be, and the dimension of the optical system can be minimized. However, the parameters of the condenser lens are not only influence the efficiency of the optical system, but also other performance such as transversal magnification of the optical system. Thereby, it is inappropriate to simply determine the parameters of the condenser lens only in order to reduce the aperture size of the image lens, the parameters of the lens need to be decided based on the performance of all aspects of the OWPT system. Because the condenser lens is generally placed close to the LED light source, the required lens aperture is generally small, so no matter plano-convex lens, aspheric lens or Fresnel lens can be used as the condenser lens in OWPT optical system. The image lens will be placed at a distance from the condenser lens, and because the light beam still has a certain degree of

divergence after being refracted by the condenser lens, the image lens needs to have a larger aperture size. Considering the large size of the image lens, the Fresnel lens is considered the most ideal choice as the image lens in the OWPT optical system. The thickness of the Fresnel lens is thin and the mass is small, so even a large aperture size can ensure a very light weight. Although the image quality of the Fresnel lens is poor, in non-imaging optical applications such as OWPT, the drawbacks of the Fresnel lens will not have any negative impact on the performance of the system.

The overall transversal magnification of the double-lens optical system is the product of the individual values of the transversal magnifications of the two lenses. Specifically, it is determined by the parameters and relative positions of the two lenses. Therefore, unlike the single-lens optical system, the transversal magnification of a double-lens optical system is determined by numinous parameters, and these parameters are not independent, but interacted. Hence, the overall transversal magnification value and efficiency of the double-lens optical system can be optimized by adjusting different parameters. In other words, the designing of the double-lens optical system is more flexible. The detailed analysis of the overall transversal magnification of the double-lens optical system will be provided in the section 3.2.

In summary, the designing a double-lens optical system is more flexible and changeable than the single-lens optical system. The efficiency and overall transversal magnification of the optical system are no longer determined by one or two parameters, but by the values and interaction of multiple parameters in the optical system. In other words, by optimizing the parameters of the optical system, the double-lens optical system can simultaneously obtain high efficiency and excellent performance. Moreover, the double-lens optical system only uses two optical elements, so it still has a good performance in terms of system weight and cost. Therefore, the double-lens configuration is an excellent candidate for the OWPT optical system.

3.1.3 Multi-lens optical system

Multi-lens optical systems generally consist of 3 or more optical elements. Such optical systems are mostly used in the field of imaging optics such as camera, telescope and microscope. In the field of imaging optics, if only a simple optical system is applied, aberration (spherical aberration, comatic aberration, field curvature, astigmatism, image distortion, chromatic aberration, and wavefront aberration) will inevitably occur on the image plane, thereby reducing the image quality. For example, when a single lens is used to image a wide beam, the central and edge rays cannot converge at the same point, so spherical aberration occurs. Besides, when broad-spectrum light (sunlight) passes through the lens and refracted, light of different wavelengths will have different degrees of refraction, so chromatic aberration will occur on the image surface. Therefore, in order to ensure the image quality, a multi-lens compound is usually used to gradually rearrange the light rays and achieve the effect of eliminating aberration. In addition, by changing the relative position of the lenses in the multi-lens optical system, a very precise zoom function can be achieved. These are the advantages of multi-lens optical system.

However, multi-lens optical system is not a suitable choice for OWPT application. First, the OWPT application do not require high image quality but high efficiency of optical power transmission. Thus, the multi-lens optical system is not able to maximize its advantages in OWPT applications. Secondly, the multi-lens optical system cannot further improve the efficiency of the optical system or achieve a smaller irradiation spot at the target distance on the basis of the double-lens optical system. In fact, according to the definition of etendue, under the condition of a certain transmission distance, the minimum size of the irradiation spot is not related with the number of lenses. As for the efficiency of the optical system, because the light will be lost due to the absorption of the material and the reflection on the lens surface when passing through the optical elements, the efficiency of the multi-lens optical system will be lower comparing with the double-lens optical system. In other words, the performance of the multi-optical lens system in OWPT applications is not as good as the double-lens optical system. Finally, because of applying more lenses, the weight and cost of multi-lens optical

systems are higher than single-lens or multi-lens optical systems. For OWPT applications that targeting to achieve miniaturization and portability, the portability of the multi-lens optical system is poor. In the OWPT application scenario, only in certain specific systems (such as the LED-array OWPT system introduced in Chapter 5), the multi-lens optical system will have its own unique advantages. This point will be discussed in detail in Chapter 5.

In summary, the multi-lens optical system has irreplaceable advantages in imaging optical applications. However, in the common scenes of OWPT application, the multi-lens optical configuration is not the best choice.

3.1.4 Summary of basic configuration of the LED-based OWPT lens system

In the section 3.1, according to the number of the optical elements, three kinds of optical system configurations are analyzed and compared based on the application of OWPT. The single-lens optical system has the simplest configuration. However, in order to obtain a sufficiently small irradiation spot at the target distance, the efficiency and size of the optical system will be greatly deteriorated. The multi-lens optical system has excellent imaging capabilities and is widely used in the field of imaging optics. However, such configuration cannot improve the two most critical performances in OWPT applications, which are system efficiency and irradiation spot size. On the contrary, due to the loss of light energy caused by the absorption and reflection of optical elements, the multi-lens optical system will reduce the system efficiency and increase the system weight. The double-lens optical system has a simple configuration second only to the single-lens optical system. Besides, the efficiency and performance of the system can be optimized by adjusting various parameters, which makes the design of the system very flexible. Compared with a single-lens optical system, a double-lens optical system can simultaneously achieve high efficiency, small irradiation spot size, and compact system dimension. When compared with multi-lens optical systems, double-lens optical systems have the advantages of higher efficiency, simpler design and lighter weight. Therefore, the double-lens optical configuration is considered to be the most suitable choice for OWPT system.

3.2 Parameters of the lens system

3.2.1 Theoretical analysis of irradiation spot size and related parameters

In the application of OWPT, the double-lens optical system that consists of a condenser lens and an image lens is believed as the optimal choice of the beam control system. Due to the typical property of LED divergence, a condenser lens is necessary to restrain the divergency in order to decrease the aperture of second lens and avoid optical energy leakage. The light beam is refracted when cross the condenser lens and its divergency angle is greatly restrained, and then been irradiated on target which at specific distance by an image lens. The analysis of the optical path is shown in Fig. 3.5.

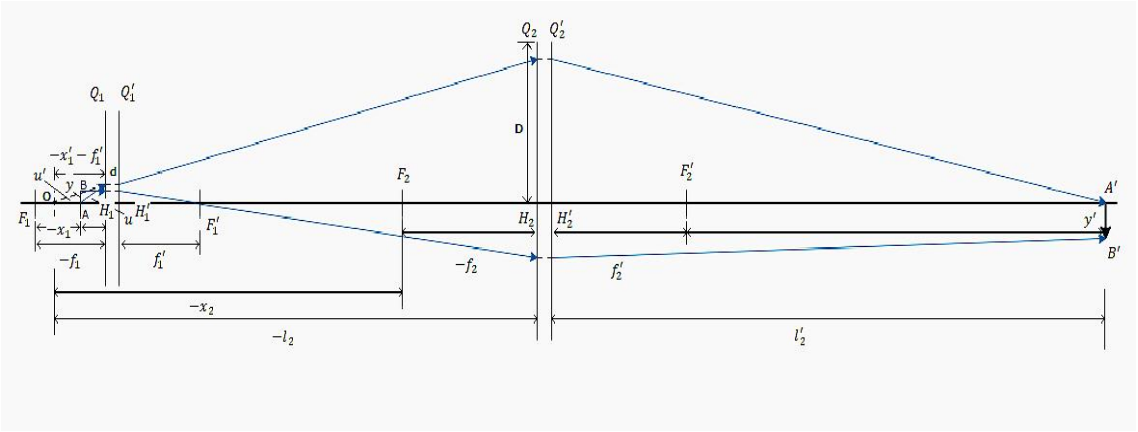

Fig. 3.5 The analysis of the LED-based OWPT system optical path

In the Fig. 3.5, AB is the half size of the LED light emitting chip, and $A'B'$ is the half size of the irradiation spot. The Q_1H_1 is the principal plane of the condenser lens, while the Q_2H_2 is the principal plane of the image lens. The light rays emitted from the light source located at AB will be refracted by the condenser lens and creating virtual image which located at *O* point. Based on the optical path model shown in Fig. 3.5, the overall transversal magnification of the double-lens optical system can be figured out:

$$\beta = \frac{y'}{y} = \beta_1\beta_2 = \frac{-f_1}{f_1'}\frac{l_1'}{l_1} \times \frac{-f_2}{f_2'}\frac{l_2'}{l_2} \tag{3.12}$$

Then according to the Gaussian's formula that shown in the equation (3.5) and the conclusion shown in equation (3.10) that the back focal length is roughly the same as focal length under the condition that the medium of object space and image space is the same, the overall transversal magnification of the optical system becomes to:

$$\beta = \frac{y'}{y} = \beta_1\beta_2 = \frac{l_2' f_2}{f_2'} \times \frac{1}{-l_1 + d\left(1 - \frac{-l_1}{f_1'}\right)} \tag{3.13}$$

As shown in equation (3.13), the overall transversal magnification value of the optical system is equal to the product of the transversal magnification value of individual optical elements in the system. Here l_2' refer to the target transmission distance, which is the length from the front surface of the image lens to the receiver of the OWPT system, and the values of f_2 and f_2' are the back focal length and focal length of the image lens, respectively. Besides, the l_1 value is the distance between the LED light emitting chip to the back surface of the condenser lens, and d is the distance between the two lenses. Finally, the f_1' value is the focal length of the condenser lens. It should be noted here the overall transversal magnification is not the accurate ratio between emitting area and irradiation size directly. In the definition of transversal magnification, only the parallel edge ray in paraxial region is considered, however in the situation discussed here, the edge ray still has divergence angle, which made the real ratio between emitting area and final irradiation size bigger than this value. Besides, the package lens of the LED also belongs to one of the optical components in the system, but didn't considered in the calculation. Therefore, the accurate size of the irradiation spot cannot be calculated directly by the LED chip size and the transversal magnification value calculated from equation (3.13). Nevertheless, the equation (3.13) can still reveal the relation between the transversal magnification of the optical system and other parameters.

In practical condition, the value of l_1 and l_2' is usually fixed. The value of l_2' equals to the transmission distance, and in the condition of practical application,

the transmission distance is always decided according to the requirement of the application. The l_1 is the distance between the LED light emitting chip and the back surface of the condenser lens. Generally, considering the divergence of the LED light beam, the value of l_1 should be as small as possible in order to avoid the intensity loss on the aperture of condenser lens. If the value of l_1 is large, the aperture size of the condenser lens should be increase as well to ensure the high efficiency of the lens system, which will enlarge the dimension and weight of the OWPT transmitter. Although according to the equation (3.13), a larger value of l_1 can obtain a smaller transversal magnification of the optical system, but the contribution is very little. On the contrary, because of the divergence of the LED beam, even a small increase in the value of l_1 will significantly affect the efficiency and size of the system. Therefore, the l_1 is always set as the possible smallest value. However, the limitation of the l_1 value exists, which is the size of the package lens of the LED. As discussed in the section 2.2.2, LED usually has an epoxy package lens for controlling the divergence angle of the light beam, and the shape of the package lens is different according to the application scenarios. The centre thickness of the package lens of a dome-type LED is usually around 4 mm, which is the limitation value of the l_1. This is also one of the reasons why pointed epoxy resin package LED is not suitable for use as light source in LED-based OWPT system. The bullet-shaped package lens has a large centre thickness, so the value of l_1 will also increase accordingly. Thus, based on the discussion shown above, the values of l_2' and l_1 are fixed in advance in the practical condition, and are not variables that can be modified at will when analysing the parameters of the OWPT optical system.

Moreover, according to the equation (3.10), the value of back focal length and focal length of a lens is roughly the same, thus the value of the function of $\frac{f_2}{f_2'}$ in the equation (3.13) can be seen as 1. Therefore, the remained parameters that will greatly influence the overall transversal magnification of the optical system are d value and f_1', which are the distance between the two lenses and the focal length of the condenser lens. In order to achieving small irradiation spot, the values of both d and f_1' should be sufficiently large. On the other hand, notice the

function of $\frac{-l_1}{f_1'}$ has the limited value, which is 0 when the value of f_1' closes to infinite. This is to say, under the condition that the distance between two lenses is decided, the overall transversal magnification of the optical system does have the smallest value if the focal length of the condenser lens is large enough. However, either increasing value of d or f_1' will enlarge the size of light beam that reaches the aperture of the image lens, which requires the aperture size of image lens to increase in order to receive the intensity as much as possible and realize high efficiency of the optical system. Consequently, the values of d and f_1' cannot be increased blindly, but need to be accurately analysed and decided for achieving a balance in the performance of the system efficiency, size of irradiation spot, and system dimension.

According to the equation (3.13), the graph of the relation between the overall transversal magnification of the optical system (β), the distance between two lenses (d), and the focal length of the condenser lens (f_1') can be plotted as Fig. 3.6. The value of l_1 is set as -4 mm, which is the minus value considered the size of LED's package lens, and value of l_2' is set to be 1000 mm, which means 1 m is set as a typical transmission distance.

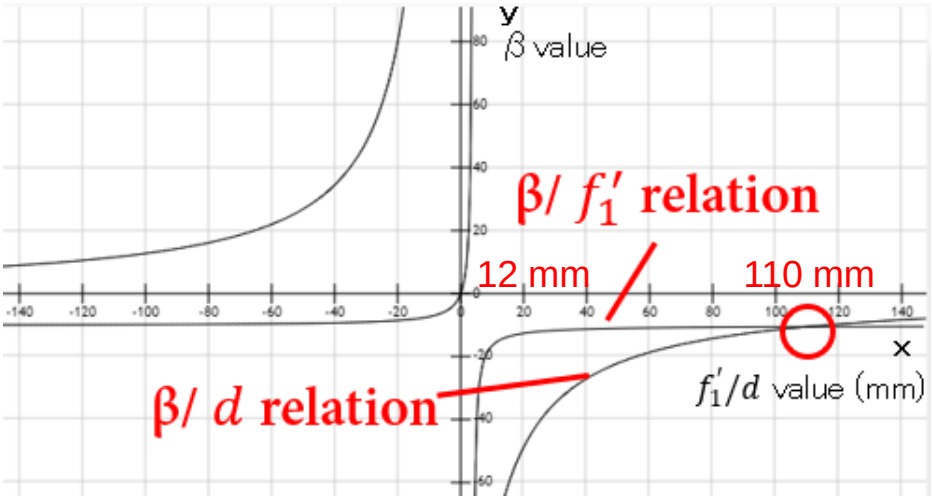

Fig. 3.6 The relation between the overall transversal magnification, d parameter and f_1' parameter of LED-based OWPT system

The Fig. 3.6 shows the relation graph of relation between β and d/f_1' value after fixing rest of parameters. Notice Fig. 3.6 shows two lines, which is the relation between β and d and the relation between β and f_1'. Whereas, the meaning of their x axis is different but with same unit. From Fig. 3.6, the turning point of β/f_1' relation is roughly at 12mm. If f_1' value is smaller than 12mm, the β value (irradiation size at target distance) will be rapidly increase. When f_1' value larger than 12mm, it will not largely influence the final irradiation size. On the other hand, the influence of d value on β is smoothly decreased when d value increasing. Increasing the distance between two lenses will greatly help to control the irradiation size at target distance. Comparing the transversal magnification value when the value of d equals 50 mm and 100 mm, the irradiation size can be cut in half. In other words, ensuring long enough lenses distance is the key to restrain the size of irradiation at target distance. The Table 3.1 shows the simulation results of the irradiation size based on different lenses distances. The value of f_1' is set as near infinite during the simulations, thus the data shown in Table 3.1 represents almost the smallest irradiation size that can be achieved with different d values.

Table 3.1 Limit irradiation size based on different lenses distance

Distance between two lenses (mm)	Irradiation size (mm×mm)
30	37×39
40	30×31
50	23×24
60	19×20
70	18×19
80	16×17
90	14×15

100	12×13
110	11×12

This table shows very important when designing portable LED-based OWPT system. It shows the limitation size of the irradiation spot in the condition of 1 m transmission distance. Although the data shown in Table 3.1 is only based on 1 m transmission distance, according to the equation (3.13), the overall transversal magnification value of the optical system is proportional to the transmission distance l_2', thus the value of irradiation size shown in Table 3.1 will also increases linearly with the extending of transmission distance. Conclusively, the Table 3.1 shows the guideline of how to balance transmitter dimension and receiver dimension.

Back to the discussion of Fig. 3.6, the cross point of the two lines occurs at 110mm, which lead out the conclusion that the influence of d value on β is larger than f_1' value before d value smaller than 110mm. However, after d value greater than 110mm, f_1' value becomes to the main parameter that decides final irradiation size at target distance. This is to say, as long as f_1' value larger than 12mm, if the irradiation size is larger than the requirement of application, one of the methods to decrease irradiation size is increasing d value to compensate the influence from f_1' value. The smallest irradiation size will occur when d value increase to 110mm, and after d value larger than 110mm, f_1' value becomes to the main factor. Thus, the irradiation will be very hard to decrease no matter how large the d value increase to. Summarily, the theoretical limitation of system performance (smallest irradiation size) can be achieved when d value equals to 110mm.

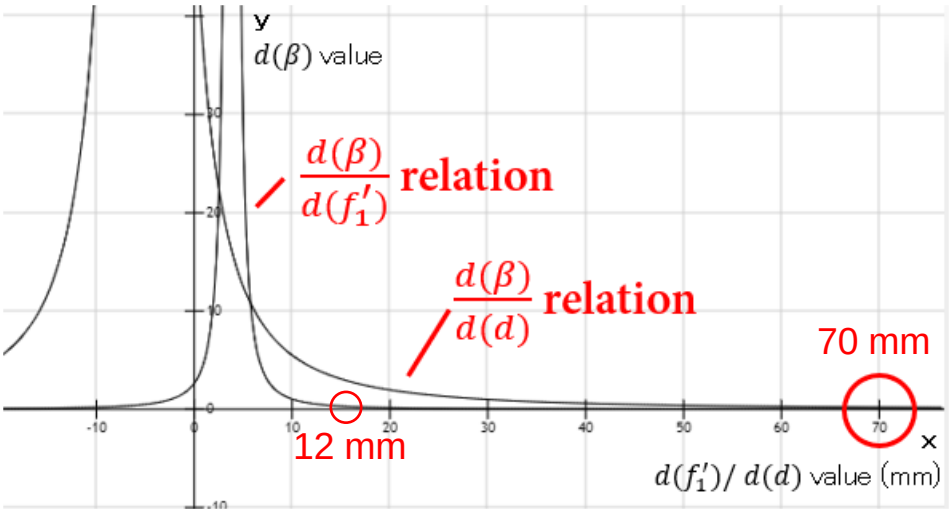

Fig. 3.7 The relation between β and differential of d/f_1' value

The Fig. 3.7 shows the relation between β and differential of d/f_1' value, which indicates the changing tendency of β when d/f_1' value changing. From Fig. 3.7, the changing of β/f_1' tends to be 0 when f_1' value larger than around 17mm. Combines with the result from Fig. 3.6, it's very easy to find that irradiation size will increase rapidly when f_1' value smaller than 12mm, and when f_1' value larger than 12mm but smaller than 17mm, irradiation size will also decrease, but the degree of changing becomes very small, which means in this range the f_1' value still affects final irradiation size but of a very small extent. While when f_1' value larger than 17mm, it will approximately not influence irradiation size anymore. On the other hand, the changing of β/d lasts to larger range. Due to the value of the two lines can never reach 0, thus a certain value can be used to indicate the "approximate 0", which means the parameters will almost have no influence on final performance. Combining the simulation results, when f_1' value larger than 17mm, it will almost have no influence on irradiation size, thus the y axis value when f_1' value equals to 17mm is set as "approximate 0" value. If apply this "approximate 0" on β/d curve, the point will occur when d value equals to 70mm. This is to say, when d value larger than 70mm, it will not obviously affect the final irradiation size. However, considering the same small influence from the f_1' value, d value can still to be used to compensate the impact from f_1' value and decrease

the irradiation size when d smaller than 110mm as discussed above. Generally, combining the results from Fig. 3.6 and Fig. 3.7, as long as the focal length f_1' of condenser lens is larger than 12mm and d value is in the range of 70mm to 110mm, the roughly same performance (irradiation size) can be ensured by modifying d and f_1' value. On the other hand, the irradiation spot size will not greatly change if the d value is larger than 70 mm, and if system length is wished to be smaller than 70mm, irradiation size must be increased, so as solar cell size.

On the other hand, the simulation data shown in Table 3.2 proves the conclusion that same irradiation spot size can be achieved by adjusting the value of d parameter and f_1' parameter as long as they are in the proper range. The simulation results were carried out using ZEMAX (ZEMAX LLC). The size of LED emitting chip is 0.75 mm × 0.75 mm. The simulation data shows the various configurations of optical system with different focal length of the condenser lens (f_1' parameter), and the distance between the two lenses (d parameter).

Table 3.2 Simulation results of portable LED-based OWPT system

f_1' (mm)	d (mm)	Irradiation size (mm×mm)
11	106	26×28
13	106	21×22
15	106	20×21
18	106	17×18
238	70	18×19

From Table 3.2, several configurations of OWPT system are simulated and shown. The first 4 configuration applies 106 mm d parameter and several different f_1' parameters, and it shows the changing tendency of the irradiation size when f_1' parameter increases. It can be found that when the value of d parameter fixed and f_1' parameter increasing from 11 mm to 18 mm, the irradiation size is keeping decreasing, especially from 11 mm to 13 mm, the decreasing of the

irradiation size is obvious, which proves the conclusion that 12 mm is the turning point of f_1' parameter in the viewpoint of irradiation size. The last row in Table 3.2 shows the simulation result of configuration with 70 mm d value, which is the theoretical smallest length based on the discussion shown above. As discussed, due to the influence from f_1' parameter on the irradiation spot size becomes small once its value beyond 17 mm, here the value of f_1' parameter has to be increased to 238 mm to compensate the negative influence on irradiation size from small d value. According to the data shown in Table 3.2, sufficiently small irradiation size can also be achieved as long as the focal length of the condenser lens is large enough, and these results demonstrate the conclusion that by adjusting the value of f_1' and d in the proper range, the same irradiation size at the target distance can be achieved by different optical system configurations.

3.2.2 Theoretical analysis of optical system dimension and related parameters

The discussion stated above is focused on the overall transversal magnification value of the optical system, while the dimension of the optical system is also a critical factor that needs to be considered. As it is discussed, either increasing value of d and f_1' will cause the enlarging of the image lens aperture size, and finally increasing the system dimension. Thus, the analysis on the aperture size of the image lens based on the changing of various parameters is also necessary.

Portable LED-based OWPT system is designed to be hold by human or robot. Compared to square shape, flashlight-like configuration that has relatively long length but small height is desired. Thus, decreasing system aperture without sacrificing performance is one important topic in this research.

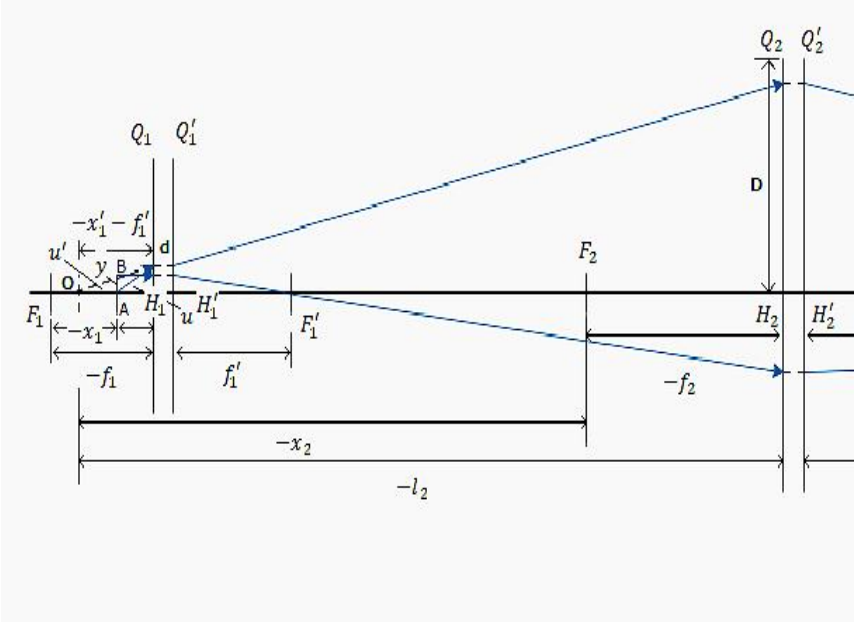

Fig. 3.8 Geometrical configuration of lens system in LED-based OWPT system

The Fig. 3.8 shows the geometrical designing of lens system in the portable LED-based OWPT system. It is easy to know from Fig. 3.8, vertical dimension (height) of the system is decided by aperture size of image lens, and its value is controlled by several parameters. Based on the geometrical configuration shown in Fig. 3.8 and Newton's formula, the mathematical representation of aperture size of image lens is shown in equation (3.14) as follow:

$$D = \frac{\tan(u)(f_1 - l_1)}{-f_1} \times \left(d + \frac{-l_1 \times f_1}{f_1 + l_1}\right) \tag{3.14}$$

Here D is the half aperture size of image lens, u is the half divergence angle of LED light source, f_1 indicates the back focal length of condenser lens, and l_1 is object distance, which is the distance between the LED emitting chip and the back surface of condenser lens. The value d is still the distance between two lenses. Although D value is controlled by many parameters, some of them can be fixed considering practical application situation. The u value can be set as 40°, which is almost the smallest half divergence angle of dome-type package LED which can be found in commercial market at present, and l_1 value can be set as

-4 due to the package lens of the LED. Hence, equation (3.14) can be transferred to equation (3.15) that shown below:

$$D = \frac{0.84(f_1+4)}{-f_1} \times \left(d + \frac{4f_1}{f_1-4}\right) \tag{3.15}$$

By setting such parameters, the aperture size of image lens is only related with back focal length of condenser lens and distance between two lenses, which is the value of f_1 and d value. Thus, the graph of the relation on aperture size between f_1 and d value can be drawn.

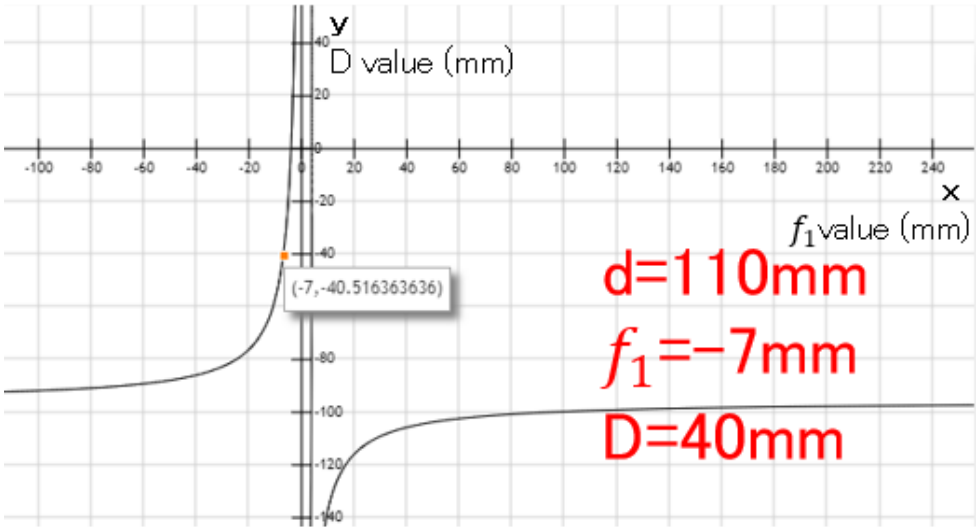

Fig. 3.9 The relation on aperture size between f_1 and d value (d=110 mm)

The Fig. 3.9 shows the relation between D value and f_1 value when d is set as 110 mm. From the Fig. 3.9, the turning point occurs roughly at -17 mm. When f_1 larger than -17mm, aperture size can be rapidly decreased with f_1 value increasing. For example, 40 mm half aperture size of image lens can be achieved if f_1 value set as -7 mm, and 20 mm half aperture size can be achieved if f_1 value set as -3 mm. However, as stated at previous discussion in this section, irradiation size will be largely increased if focal length or back focal length of condenser lens is smaller than 12 mm. So even such method can decrease aperture size, system performance (size of irradiation spot) will be sacrificed.

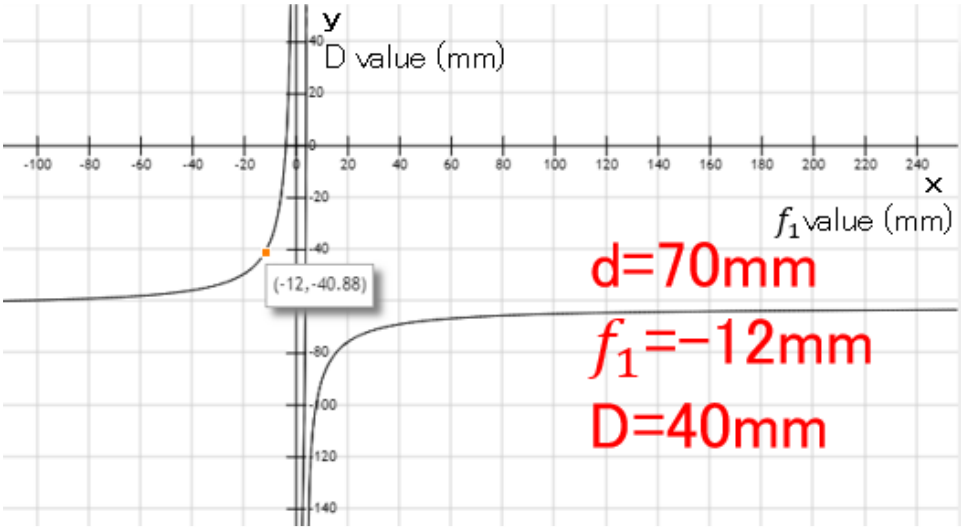

Fig. 3.10 The relation on aperture size between f_1 and d value (d=70 mm)

As shown in Fig. 3.10, if d value is decreased, image lens will be more closed to condenser lens, hence geometrical loss can be controlled and aperture size can be decreased. From Fig. 3.10, when d value decreased to 70 mm, -12 mm f_1 value can achieve 40 mm half aperture size of the image lens, which can avoid largely increasing irradiation size and deteriorating system performance. However, as discussed above, 70 mm for d value and 12 mm for f_1' value are almost smallest parameters that can be applied, and considering the back focal length and focal length of a lens is roughly equals to each other the when the medium of object space and image space is the same, then -12 mm is also the limitation value for f_1 parameter. If both d parameter and f_1 set as the minimum value, the irradiation spot size at the target distance will be larger than desired, as discussed. In fact, due to smaller irradiation spot size can enhance the radiant intensity of the irradiation, then improving the PV conversion efficiency of the solar cell, when designing the OWPT optical system, the one of the d or f_1 parameter will be appropriately increased for achieving a smaller spot size. Therefore, although 40 mm can be the theoretical smallest half aperture size of the image lens, a larger aperture image lens will be applied in practical. Besides, due to the analysis shown above is based on the 40° half divergence angle of the

LED light source. Concluding the fact that part of intensity exists beyond the half divergence angle of the light beam, and also the possible deviation between calculation and practical condition, hence 50 mm is believed as limitation value of the half aperture size of the image lens based on the analysis. Such value is also the limitation value of the half vertical dimension of the optical system.

On the other hand, increasing the value of d and f_1 can achieve very small irradiation size, while small values of d and f_1 are necessary for realizing small system dimension, which causes conflict in the aspects of system performance and system size. According to the analysis shown above, the value of d should be in the range of 70 mm-110 mm. When value of d closes to 70 mm, small system height can be achieved, while irradiation size will be enlarged, while value of d closes to 110 mm, irradiation size can be small but system height is sacrificed. Therefore, the value of d should be chosen the middle value in its range, which is around 90 mm. As for the value of f_1 parameter, it should be at least larger than 12 mm in order to ensure the small size of the irradiation, and the actual half aperture size of the image lens will be greater than 50 mm in this case. In fact, such size of aperture of the image lens is necessary. This necessity can be demonstrated not only by the above mathematical model, but also by the definition of etendue.

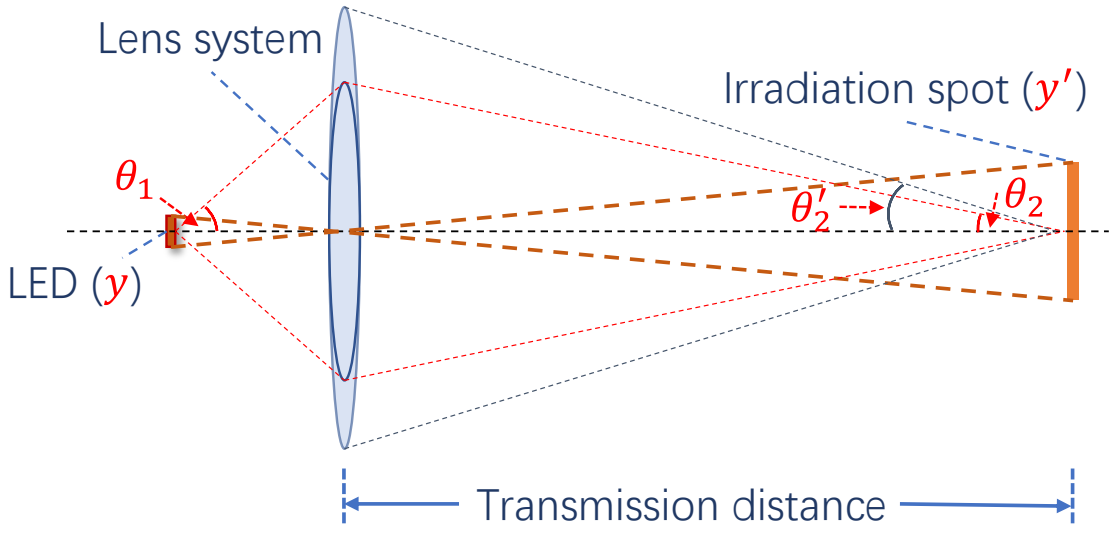

Fig. 3.11 Etendue analysis of LED-based OWPT system

The Fig. 3.11 shows the light path of a typical optical system. The size of the emitting area is y, and the size of the irradiation spot is y'. The cone angle of the emitted light beam is θ_1, which is only decided by the light source. The etendue of such system is decided by the LED light source, which is the product of the area of the source y and the solid angle θ_1 that the system's entrance pupil subtends as seen from the source. And from the viewpoint of receiver side, the value of etendue is the product of the irradiation size y' and the incident solid angle θ_2. According to the definition of the etendue that shown in the equation (2.2), the value of the etendue will never change during the prorogation of the light rays. Thus, in the condition that the etendue value is decided by the light source and the transmission distance is fixed, the incident solid angle at the receiver side needs to be increase if smaller irradiation area is desired. As shown in the Fig. 3.11, if the exit pupil of the lens system increases, the incident solid angle at the receiver side will increase from θ_2 to θ_2', which allows the irradiation size to be smaller. The exit pupil of the lens system is the beam size the emitted from the image lens, and this is the reason why the large size of aperture of the image lens is necessary to achieve a small irradiation spot. In fact, whether increasing the focal length (f_1' parameter) of the condenser lens or extending the distance between the two lenses (d parameter), the purpose is to increase the beam size on the image lens and increase the incident solid angle of the receiving end to reduce the irradiation spot size. Summarily, the small vertical dimension and the small irradiation size cannot be achieved at the same time due to the limits of system etendue value, and the balance between the system dimension and the size of irradiation spot need to be considered according to the requirement of the application scenarios.

Conclusively, the focal length of the condenser lens should be at least larger than 12 mm for avoiding too large irradiation spot, and the proper distance between the condenser lens and image lens should be in the range of 70 mm to 110 mm. In this cause, the half aperture size of the image lens is around 50 mm. Thus, the

shape of the OWPT transmitter is like a cube with around 100 mm side length. If the irradiation spot size needs to be smaller, under the condition that system size allows, the beam size on the imaging lens and the aperture size of the imaging lens should be increased. The beam size can be increased by extending the distance between the two lenses, but this method will increase the horizontal and vertical dimensions of the system at the same time. The same effect can also be achieved by increasing the focal length of the condenser lens. Although according to Fig. 3.11, the effect of this approach is not as obvious as enlarging the value of d parameter, such method will only cause an increase in the vertical size of the optical system without influencing the length of the system.

3.2.3 Theoretical analysis of optical system efficiency

As a power supply application, the efficiency of the optical system of the OWPT is a very important parameter. In the condition that the efficiency of the LED light source and solar cell is approximately fixed by current technology, the efficiency of the optical system decides how much power can be effectively transmitted to the load. Therefore, the optical system efficiency should be as high as possible. In fact, because the condenser lens is placed close to the light source, there is no significant loss of light energy on the condenser lens, so the efficiency of the optical system is almost only related to the aperture size of the image lens. In the case where the aperture size of the imaging lens is sufficiently large, the efficiency of the optical system can be sufficiently high. However, as a portable OWPT system, too large lens aperture will affect the portability of the system. As analyzed in Section 3.2.2, under the premise of ensuring that the irradiation spot size is small enough, the half aperture of 50 mm is the minimum value of the image lens, which is 100 mm of the entire aperture. In this case, the value of d parameter needs to be in the range of 70 mm to 110 mm. After determining the aperture of the image lens and the value of d parameter, under the premise of ensuring the efficiency of the optical system, the value of f_1' parameter should be increased as much as possible to increase the exit pupil on the image lens in order to reduce the size of the irradiation spot. According to the simulation data,

when the proper value of f_1' parameter is about 25 mm, the aperture value of the image lens ($2D$) and the distance between the two lenses (d) are both about 100 mm, which is a cubic shape. This configuration is considered an ideal shape that can realize the portability of the OWPT system.

The Fig. 3.12 shows the detailed relation between the system efficiency, d parameter and the aperture size of the image lens based on thousands of times of simulations. The OWPT system simulation model is carried out using ZEMAX (ZEMAX LLC). At the simulation, two main variable values are controlled, the distance between the two lenses (d value) and aperture size of image lens ($2D$). Due to the thickness values of the lenses applied in the optical system are usually several millimetres, thus the length of the system (horizontal dimension of optical system) can be seen as roughly equal to the distance between the two lenses (d value), and the height of the system (vertical dimension of the optical system) is exactly the same as the aperture size of image lens ($2D$). The focal length of the condenser lens (f_1' parameter) was set as 23.5 mm in the simulation model.

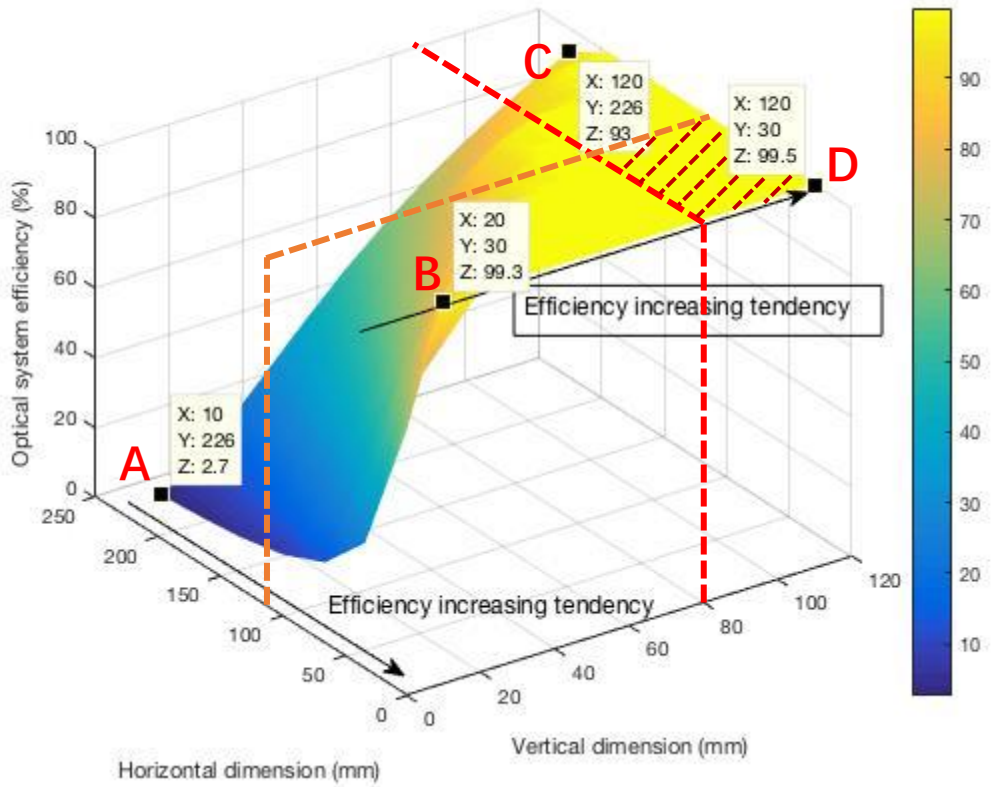

Fig. 3.12 Simulation results of the LED-based OWPT system

According to the Fig. 3.12, the optical system efficiency has two tendencies based on both horizontal and vertical dimension. Four typical points are listed in the Fig. 3.12. The detailed information of them is shown in Table 3.3.

Table 3.3 Typical points of optical system efficiency characteristic

Points	**Aperture size of image lens (mm)**	***d* value (mm)**	**Optical system efficiency**
A	10	226	2.7%
B	20	30	99.3%
C	120	226	93%
D	120	30	99.5%

On vertical direction, if compare the A and C point, the optical system efficiency will decrease with the aperture of image lens become smaller, and on horizontal direction, on the other hand, smaller d value can achieve higher efficiency, as the A and B point show. As for C and D point, even these two points has almost same efficiency, the irradiation size is greatly different at the same transmission distance according to the d value is largely different as discussed. Based on the analysis show in section 3.2.2 and section 3.2.3, if set the horizontal dimension of the optical system (d value) smaller than 110 mm, and the vertical dimension (aperture size of image lens) larger than 80 mm, the very high efficiency of the optical system can be achieved as the crossing area shown in Fig. 3.12.

The data shown in Fig. 3.12 represents the minimum d value and the maximum aperture size of the image lens that can achieve high efficiency of the optical system. The results are consistent with the conclusion of the theoretical analysis on the optical system parameters in Sections 3.2.2 and Section 3.2.3. In other words, in this section, the simulation results of the optical system with different parameters have verified the analysis conclusions of the previous optical system mathematical models.

3.2.4 Summary of analysis on the parameters of the lens system

In Section 3.2, through the discussion of three aspects, which are the irradiation spot size at target transmission distance, the dimension of the optical system and the efficiency of the optical system, a detailed analysis on the relationship of various parameters in the double-lens optical system is shown, and the effects of parameters on the performance of the LED-based OWPT system was discussed. By establishing the mathematical model of the optical system in Section 3.2.1 and Section 3.2.2, under the premise of ensuring the small enough irradiation spot size at the target distance and the high efficiency of the optical system, the ideal value range of the d parameter, the f_1' parameter, and the $2D$ parameter is provided. In summary, the distance between two the condenser lens and image lens should be in the range of 70 mm - 110 mm, and the focal length of the condenser lens should be at least larger than 12 mm, while the aperture size of

the image lens should be above 80 mm (the ideal value is 100 mm). In addition, based on the definition of etendue, it is concluded that the large size aperture of the image lens is the key factor to obtain a small irradiation spot. Finally, in Section 3.2.3, the correctness of the values of the parameters was verified by establishing a simulation model of the optical system and analyzing the system efficiency.

3.3 Ideal configuration of portable LED-based OWPT system

3.3.1 Simulation model and analysis of portable LED-based OWPT system

Based on the analysis of the optical system configuration and parameters shown in section 3.1 and section 3.2, the ideal optical system configuration of portable LED-based OWPT system is shown in the Fig. 3.13. A near-infrared LED with 810 nm wavelength is used as the light source of the OWPT system, an aspheric condenser lens with 23.5 mm focal length and 32.5 mm aperture and a Fresnel lens with 100 mm focal length and 100 mm aperture are applied as condenser lens and image lens, respectively. As discussed in section 2.4, the plano-convex lens, aspheric lens and Fresnel lens can achieve roughly same performance in the LED-based OWPT system, thus three kinds of lenses can all be used as condenser lens. While due to the large aperture size of the image lens, the Fresnel lens is the ideal candidate to be used as the image lens. The Fresnel lens allows the construction of large aperture with small mass and volume of lens. Imaging performance of a Fresnel lens is generally inferior to convex lens, but it can be used sufficiently for OWPT application. On the other hand, GaAs solar cell is applied as the optical energy receiver due to the high photovoltaic conversion efficiency with the near-infrared light and flexibility that discussed in section 2.3. The parameters of the optical components are all in the proper range of the value that discussed in the section 3.2.

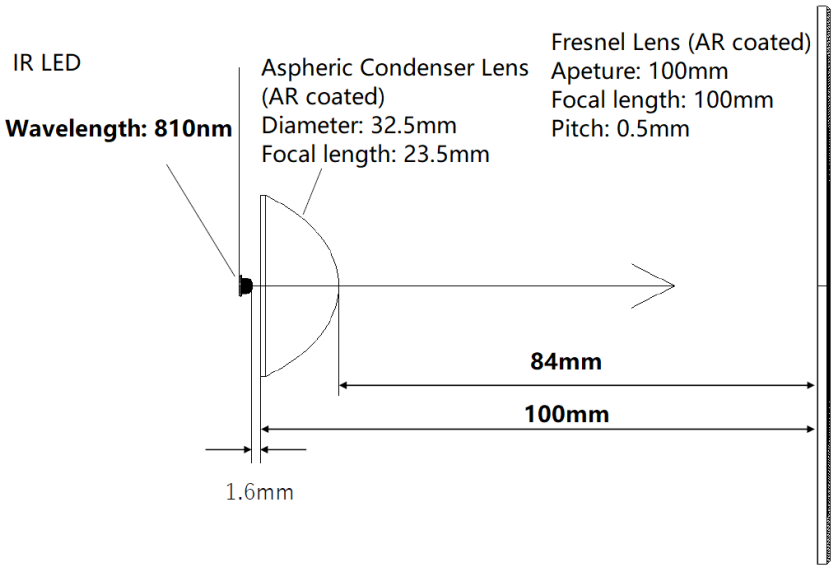

Fig. 3.13 The ideal optical system configuration of portable LED-based OWPT system

Besides, in order to be able to compare simulation and experimental data of the OWPT system, the components applied in the optical system are all commercially available, which means the parameters of the components might not be the most optimal value, but based on the proper range of the value and also whether it is available in the commercial market or not. For instance, considering the corresponding wavelength of the GaAs solar cell band gap is 870 nm, the LED with wavelength in the range of 820 nm – 860 nm will theoretically provide higher photovoltaic conversion efficiency of the GaAs solar cell than 810 nm wavelength near-infrared LED that shown in Fig. 3.13. Whereas, the near-infrared LEDs with wavelengths in this range may not be available in the commercial market, or the LED emitting chip size and package lens parameters are not ideal. For better understanding, the simulation results of irradiance map of two infrared LEDs are shown in Fig. 3.14. The LED (Osram, SFH 4715S) shown in Fig. 3.14 has a wavelength of 850 nm, which is more ideal combining with the band gap of GaAs solar cell. However, the gold bonding wire is installed at the center of the LED chip surface, which causes uneven irradiation at the target distance. More of the light intensity is concentrated in the edge area of the irradiation spot, which is unideal in OWPT application. The IR LED (Osram, SFH 4780S) shows in Fig.

3.14 has a small divergence angle (20°), while due to the structure of the reflective cup inside of the package, the irradiation spot is round shape, which will result in some areas of the solar cell being wasted in practical application due to the it unmatched the usual rectangular shape of the solar cell.

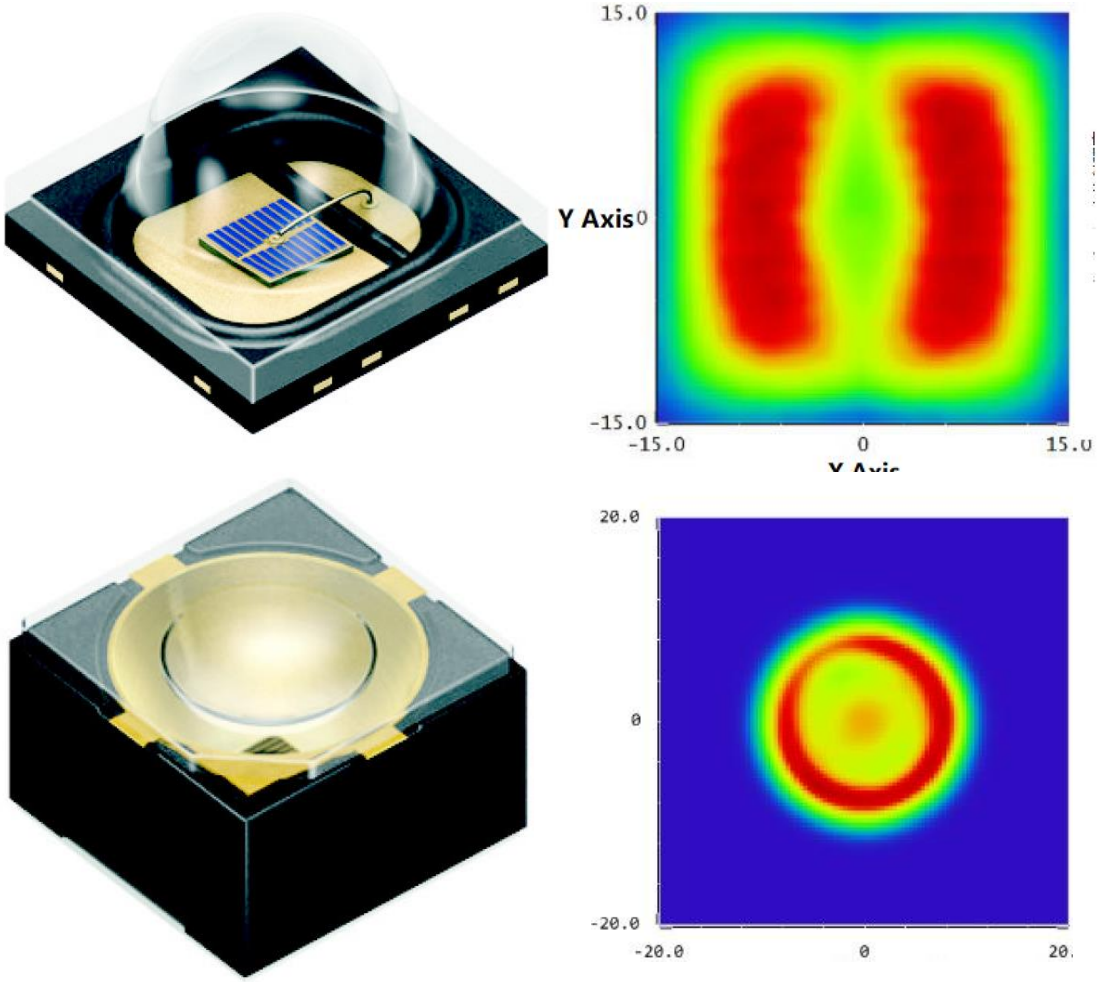

Fig. 3.14 Irradiance map of NIR LEDs with different constructures (top: Osram, SFH 4715S; bottom: Osram, SFH 4780S)

In the commercial market, a near-infrared LED with a wavelength of 810nm happens to have a more ideal design, so it was adopted in this research. In summary, the selection of the components in the research is not just based on the best parameters, but also concludes the other factors of the current available products.

The parameters shown in the Fig. 3.13 are designed for typical 1 m transmission distance. It should be noticed again that, due to the spatially incoherent, ideal collimation on LED is hard, thus a lens system for a specific transmission distance and irradiation size are indispensable. This is to say, if the transmission distance is changed, the parameters of the optical system need to be changed as well in order to focus the beam at proper distance.

According to the configuration shown in the Fig. 3.13, the simulation model based on ZEMAX (ZEMAX LLC) of the portable LED-based OWPT system is built for analyzing the characteristics and performance of the system. The simulation model has the exactly same parameters as the Fig. 3.13. The simulation optical model shown in the Fig. 3.15 contains a dome-type package NIR LED light source (1040 mW, 810 nm, ±40°, 0.75 mm × 0.75 mm chip), an aspheric condenser lens (32.5 mm diameter and 23.5 mm focal length, B270), Fresnel lens (100 mm aperture and 100 mm focal length, PMMA) and several regular detectors at different distances. Both aspheric condenser lens and Fresnel lens are AR coated for reducing the intensity loss caused by reflection on the lens surface. The data of IR LED model and aspheric condenser lens model is directly download from optical simulation library that provide from OSRAM company and SIGMAKOKI company. The Fresnel lens model data is not provided by the manufacturers, and the model used in simulation is prepared individually, thus the differences of results between simulation and experiment may appear. The transmission distance is set as 1000 mm in the simulation, which is a typical distance that can divide radiative power transmission technology and non-radiative power transmission technology.

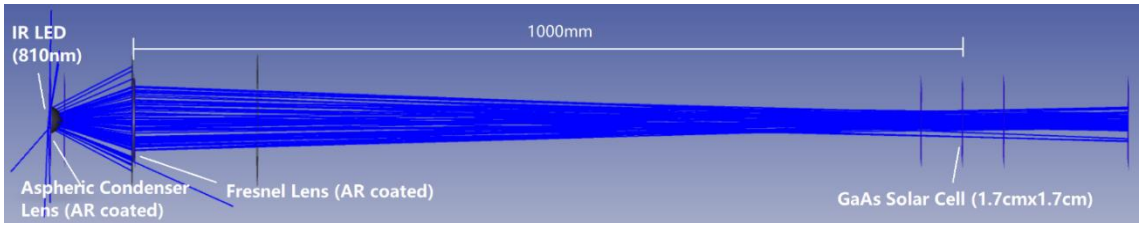

Fig. 3.15 Simulation model of portable LED-based OWPT system

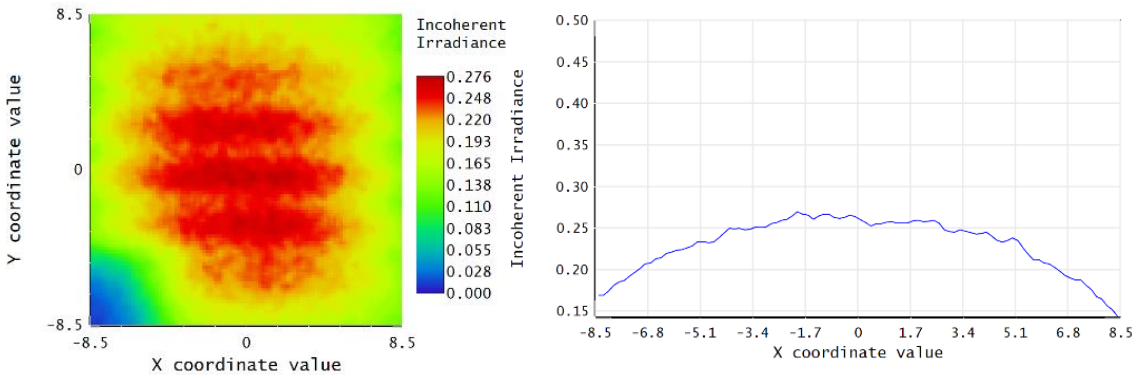

Fig. 3.16. (a) is the irradiance map, (b) is the cross section of row of intensity

The irradiance map and cross section of row of intensity is shown in the Fig. 3.16. The boundary of the irradiation is clear and the shape of the irradiation is an irregular rectangle. The size of the irradiation area is 2.1 cm × 2.3 cm. The electrode pattern on the LED chip surface creates a dark corner on irradiation area, resulting in a non-square irradiation, and it also influences the intensity homogeneity. At the receiver side, a detector with size of 1.7 cm × 1.7 cm plays the role as GaAs solar cell. There are two reasons for using such size of solar cell. First, the size of solar cell cannot be exactly the same as the irradiation area. It should be slightly smaller or larger than the irradiation area for avoiding the power fluctuation caused by possible tremor during the power transmission. Considering the possible condition that the optical energy receiver is composed of multiple solar cells in series, if the area of the irradiation spot is smaller than the size of the receiver, the tremor during power transmission will cause the unbalanced performance of the solar cells, thereby deteriorating the efficiency of the entire system. Therefore, a receiver with the size slightly smaller than the irradiation spot is the better choice. Although in this case, part of the light intensity cannot be received by the solar cell, such lost intensity is relatively low due to it locates at the edge area of the irradiation spot. Second, the shape of single piece GaAs solar cell that available in commercial market is almost not square but rectangle. In the experiment of this research, the size of a single piece GaAs solar cell is 5 cm × 1.7 cm. By covering the surface of the GaAs solar cell with opaque

material, a square receiver with 1.7 cm × 1.7 cm size can be obtained. Therefore, the detector in the simulation was also set as such size in order to compare with the data and results obtained from experiment. The average radiant intensity of the entire irradiation area is 178.1 mW/cm^2, and this value increases to 199.1 mW/cm^2 on the detector (solar cell), which is roughly twice of the sunlight irradiance (AM 1.5G). The curve in Fig. 3.16 (b) indicates that the intensity distribution on solar cell is relatively even and not gather at specific points, which is appropriate for energy conversion and heat dissipation on solar cell.

By installing a detector behind each surface of the optical components in the simulation model, the efficiency of different components in the optical system can be figured out. The data is shown in the Table. 3.4.

Table 3.4 Efficiency of different components in optical system (simulation)

Components	Intensity on surface (mW)	Efficiency
IR LED	1040	
AC lens (front surface)	1031	99.1%
AC lens (back surface)	1009	97.9%
Fresnel lens (front surface)	867.3	86.0%
Fresnel lens (back surface)	865.7	99.8%
Target distance (1000mm)	859.5	99.3%
On solar cell (1.7×1.7cm^2)	575.3	66.9%
Total efficiency		55.3%

According to the data shown in the Table. 3.4, the largest intensity lost occurs on the detector (solar cell). Due to the irradiation spot size is slightly larger than the detector applied in the simulation model, thus part of the intensity is lost due to

irradiated outside of the detector. However, such configuration is acceptable for compensating the negative impact from the possible tremor during the power transmission. In fact, in application scenarios where tremor does not occur, such as installing the OWPT system in a fixed position instead of being held by the operator, the size of the solar cell can be designed to be exactly the same as the irradiation spot size. In such case, the light intensity loss on the solar cell will be almost eliminated. This means that the receiving efficiency of solar cell will be close to 100%. It should be noticed that the discussion is only based on the condition that light beam is irradiated vertically on the solar cell, and the reflection on the surface of the solar cell is very small in such case. In the condition of oblique irradiation, the intensity lost cause by reflection on the surface of solar cell will increase with the tilt angle of irradiation. The discussion of oblique irradiation of OWPT system will be discussed in the later part of this section.

Without considering the receiving efficiency of the solar cell, the overall efficiency of the OWPT optical system itself is 83.2%, which is relatively high. The intensity lost on optical components is mainly due to reflection and light leakage. The intensity received by 1.7 cm × 1.7 cm size solar cell is 575.3 mW, and around 230 mW is available from the solar cell if 40% photovoltaic conversion efficiency assumed.[2] The total efficiency of the optical power transmission is 55.3%.

According to the data shown in Table. 3.4, around 3% of total intensity lost on the condenser lens, while 13.8% total intensity lost on Fresnel lens. The analysis of the intensity loss in the optical system is shown in the Fig. 3.17.

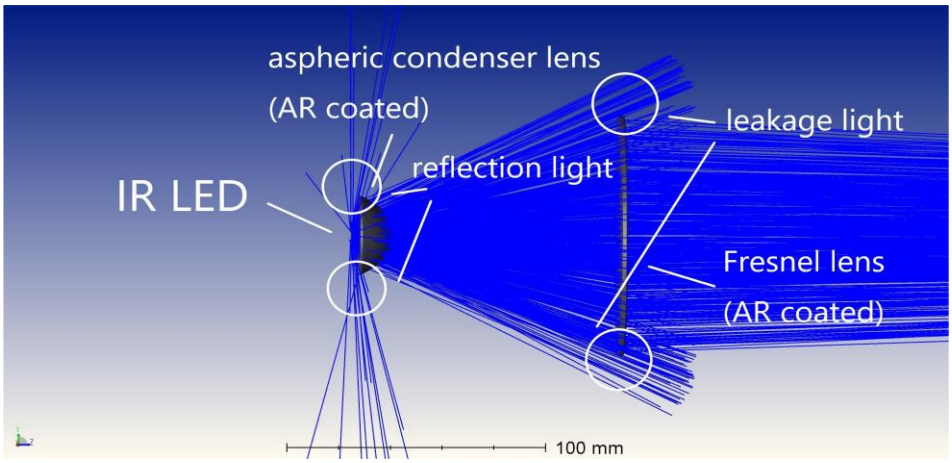

Fig. 3.17 Intensity loss analysis of optical system based on simulation model

As shown in the Fig. 3.17, the intensity loss on Fresnel lens is mainly due to the light rays leakage. As discussed in section 3.2, the aperture size of the image lens cannot be too large in order to achieve small dimension of the system. Because the distribution of the edge rays is relatively dispersed, if all the all rays are wished to be collected, the aperture of the image lens has to be increased a lot. Increasing the aperture of the image lens by around 1.5 times can increase its efficiency to over 95%. However, considering the PV conversion efficiency of solar cell, the final increase in electrical output of the system is only a dozen milliwatts. Therefore, it is believed that keeping the efficiency of the image lens around 85% can achieve a better balance between system performance and system dimension. Another method to enhance the efficiency of the Fresnel lens is decreasing the divergence angle of the LED light source. According to the calculation, the efficiency of the Fresnel lens can be increased to over 90% if the divergence angle of the LED light source is smaller than ±35.85. Whereas, such approach will decrease the exit pupil of the optical system, thus increasing the irradiation spot size, which is not desired in OWPT application.

On the other hand, there are two types of intensity loss on the aspheric condenser. The first is because although the LED package lens concentrates most of the light beam within a certain divergence angle, there is still a small amount of light intensity distribution outside such range. However, this part of the light intensity is very small, so it can be ignored in the OWPT application. The second is the intensity loss caused by reflection on the surface of aspherical condenser lens. All the lenses in the simulation model were applied AR coating, thus the intensity lost caused by the reflection on the aspheric condenser lens is only around 3% of total intensity. As discussed in section 2.4, the AR coating is very convenient and cheap to apply in the OWPT optical system due to the monochromaticity of the light source, thus it is necessary to apply AR coating to all optical components in the system generally. The discussion of the importance on reflection restrains and the difference of the lens performance between the conditions with and without AR coating is shown below.

According to the Fresnel Law, when the light beam strikes the interface of an optical medium, both reflection and refraction of the light will occur.[3] The relation between reflection coefficient and incidence angle is described by Fresnel Equation as follow:

$$R_s = \left[\frac{sin\,(\theta_t-\theta_i)}{sin\,(\theta_t+\theta_i)}\right]^2 = \left(\frac{n_1 cos\theta_i - n_2 cos\theta_t}{n_1 cos\theta_i + n_2 cos\theta_t}\right)^2 = \left[\frac{n_1 cos\theta_i - n_2\sqrt{1-(\frac{n_1}{n_2}sin\theta_i)^2}}{n_1 cos\theta_i + n_2\sqrt{1-(\frac{n_1}{n_2}sin\theta_i)^2}}\right]^2 \quad (3.16)$$

$$R_p = \left[\frac{tan\,(\theta_t-\theta_i)}{tan\,(\theta_t+\theta_i)}\right]^2 = \left(\frac{n_1 cos\theta_t - n_2 cos\theta_i}{n_1 cos\theta_t + n_2 cos\theta_i}\right)^2 = \left[\frac{n_1\sqrt{1-(\frac{n_1}{n_2}sin\theta_i)^2} - n_2 cos\theta_i}{n_1\sqrt{1-(\frac{n_1}{n_2}sin\theta_i)^2} + n_2 cos\theta_i}\right]^2 \quad (3.17)$$

Here the R_s is the reflectance for s-polarized light, R_p is the reflectance for p-polarized light. θ_i is the incidence angle and θ_t is the angle between normal and transmitted light. The n_1 and n_2 is the refractive indices of two mediums. The reflection loss is mainly on the aspheric condenser lens, thus here n_1 is 1 for air and n_2 is 1.523 for B270 material of the aspheric condenser lens applied in the optical system. As the unpolarized light, the effectively reflectivity can be described as the average value of two reflectivity:

$$R_{eff} = \frac{1}{2}(R_s + R_p) \quad (3.18)[4]$$

Based on the Fresnel Equation shows above, the characteristic of reflection coefficient on the front surface of the aspheric condenser lens based on light wave incidence angles is created by ZEMAX (ZEMAX LLC), which is shown as Fig. 3.18.

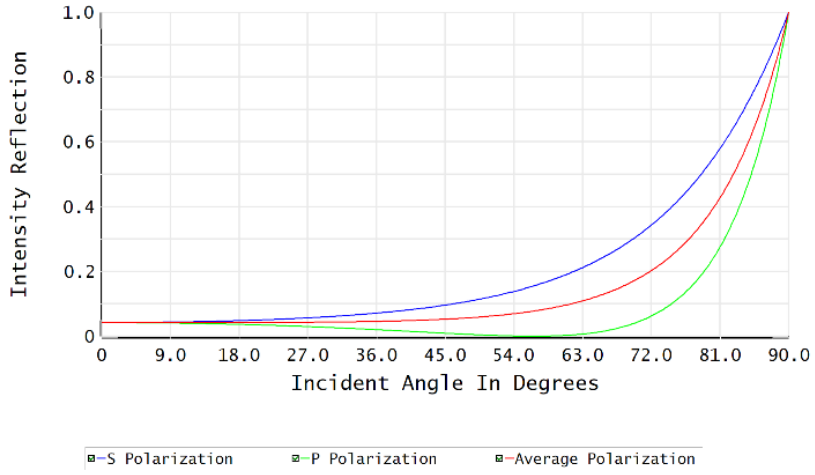

Fig. 3.18 Characteristic of intensity reflection based on incident angle on front surface of aspheric condenser lens (without AR coating)

As shown in Fig. 3.18, reflection coefficient is increasing with the incidence angle.[5] In the case of 40° which corresponds to the half divergence angle of the applied LED case, 4.8% intensity is reflected and lost. For reducing reflected intensity, AR coating is required. This type of optical coating can reduce reflection based on interference theory.

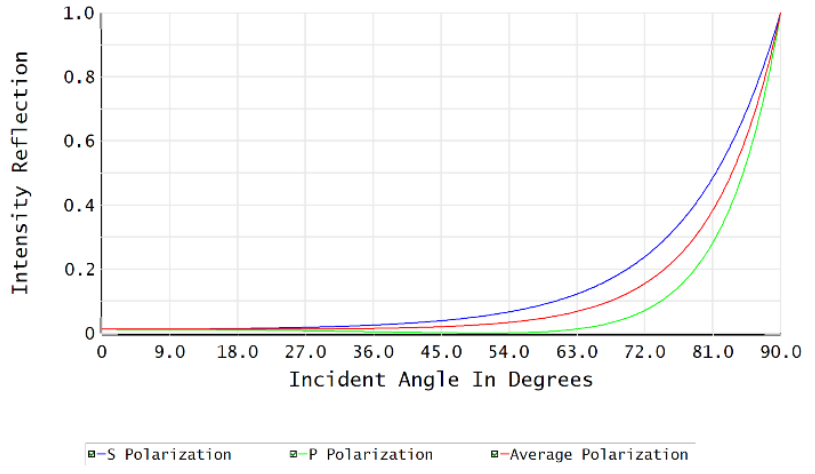

Fig. 3.19 Characteristic of intensity reflection based on incident angle on front surface of aspheric condenser lens (with AR coating)

The Fig. 3.19 is the characteristic of reflection coefficient on the front surface of

aspheric condenser lens with AR coating. The reflection intensity reduced to 1.66% at 40° incidence angle. In addition, reflection not only occurs on incident light at a large angle, but reflection loss occurs for all rays within the divergence angle range, including normal incident rays. Therefore, the actual intensity loss caused by reflection will be much larger than the data shown in the Fig. 3.18 and Fig. 3.19. According to the simulation results, applying AR-coated aspheric condenser lens will cause around 8% enhancement on lens efficiency comparing with the aspheric condenser lens without AR-coating. Therefore, applying AR-coating to the optical components in the system is an effective and easy way to restrain the intensity loss caused by reflection.

In summary, the analysis on the simulation model of the portable LED-based OWPT system shows high performance. The overall efficiency of the optical system shows more than 80% efficiency, and the intensity loss caused by reflection and light leakage is controlled to the minimum level. The irradiation spot with 2.1 cm × 2.3 cm size can be obtained at 1 m transmission distance away from the transmitter side. Such a small size allows a small receiver (solar cell) compatible with most IoT terminals to collect majority part of the transmitted intensity. The final electrical output from the solar cell is expected to be around 230 mW with 40% assumed photovoltaic conversion efficiency. The dimension of the OWPT transmitter is around 10 cm × 10 cm × 10 cm, which can achieve excellent portability.

3.3.2 Analysis on tolerant distance of portable LED-based OWPT system

Due to the spatially incoherent, ideal collimation on LED is hard, thus in OWPT system, a lens system for a specific transmission distance and irradiation size are indispensable. However, even non-target distance, effective power supplying is also possible in a certain range. This certain range which is not the target transmission distance but also able to transmit power effectively is defined as “tolerant distance” in this research. The tolerant distance can supply an easier-use environment when applying OWPT system. For example, tolerant distance can allow some deviation on transmission distance or deviation during manufacturing, and constrain negative effect caused by hand tremor during using

portable OWPT system in some degree. Thus, analyzing the tolerant distance of OWPT system is far more important.

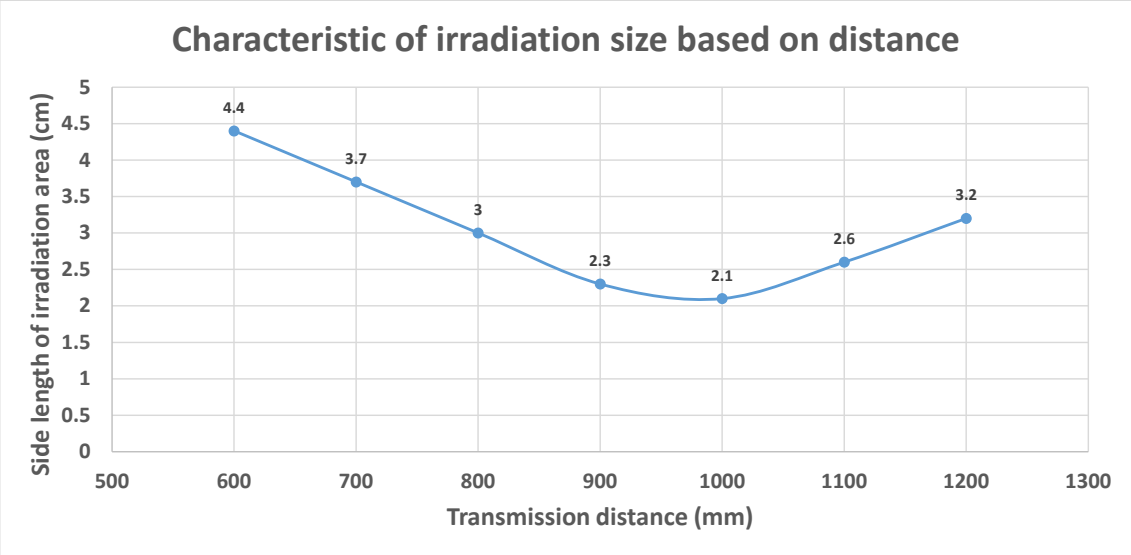

Fig. 3.20 Characteristic of irradiation size based on distance

The reason of the tolerant distance is the different irradiation size at different distance. The Fig. 3.20 shows the characteristic of irradiation size based on different distances. Because the LED-based OWPT system cannot collimate the LED beam over a long distance, the beam is always converged at the target distance to obtain a sufficiently small irradiation spot size. Therefore, the smallest irradiation spot size can be always achieved at the target distance. At the positions that in the nearby region of the target distance, the light beam has not been completely shaped and focused, thus the size of the light beam will be larger, so as the irradiation spot size. However, as long as the relative distance is short, the size of irradiation spot can still be considered small enough, hence the OWPT system can still supply power effectively in such range. The total range of such relative distance is defined as the tolerant distance in this research.

Based on the simulation and parameters of the optical system that shown in section 3.3.1, the intensity that received by the detectors installed at different distance is measured. These detectors are installed at the nearby region of the target transmission distance, specifically, at the places before and after the target

distance. In addition, considering that the beam size at each measurement distance is different, the side lengths of the detectors are set to 10 mm, 20 mm, 30 mm, and 40 mm, in order to better analysis the characteristics of the tolerant distance. The data obtained in the simulation is shown in the Fig. 3.21. Besides, for better analyzing the characteristics of the tolerant distance in the conditions of different transmission distances, simulation models of LED-based OWPT system for 2 m and 3 m transmission distance were also built, and the relative data was measured and arranged in Fig. 3.22 and Fig. 3.23, same as Fig. 3.21. For better comparing the characteristics of the tolerant distance in different transmission distance ranges, by adjusting the parameters of the optical system in the simulation model, the 2 m and 3 m OWPT systems was designed to be able to obtain the same irradiation as the 1 m OWPT system at their respective target distances, which is 2.1 cm $\times$ 2.3 cm irradiation spot. In other words, except the LED light source and the irradiation size at the target transmission distance, the other parameters of the three configurations such as the distance between the lenses, the lens aperture, and the lens focal length are all different. The data shown below is only for analyzing tolerant distance of LED-based OWPT system in different target transmission ranges. The x-axis in the Fig. 3.21 shows the relative position from the target transmission distance. For example, -100 mm means the position 100 mm before the target distance, which is 900 mm when the target distance is set as 1000 mm, and +100 mm means the measurement distance of 1100 mm. The y-axis shows the normalized total light intensity received by the detector. The value shows in the legend in graph is side length of detectors and targe transmission distance.

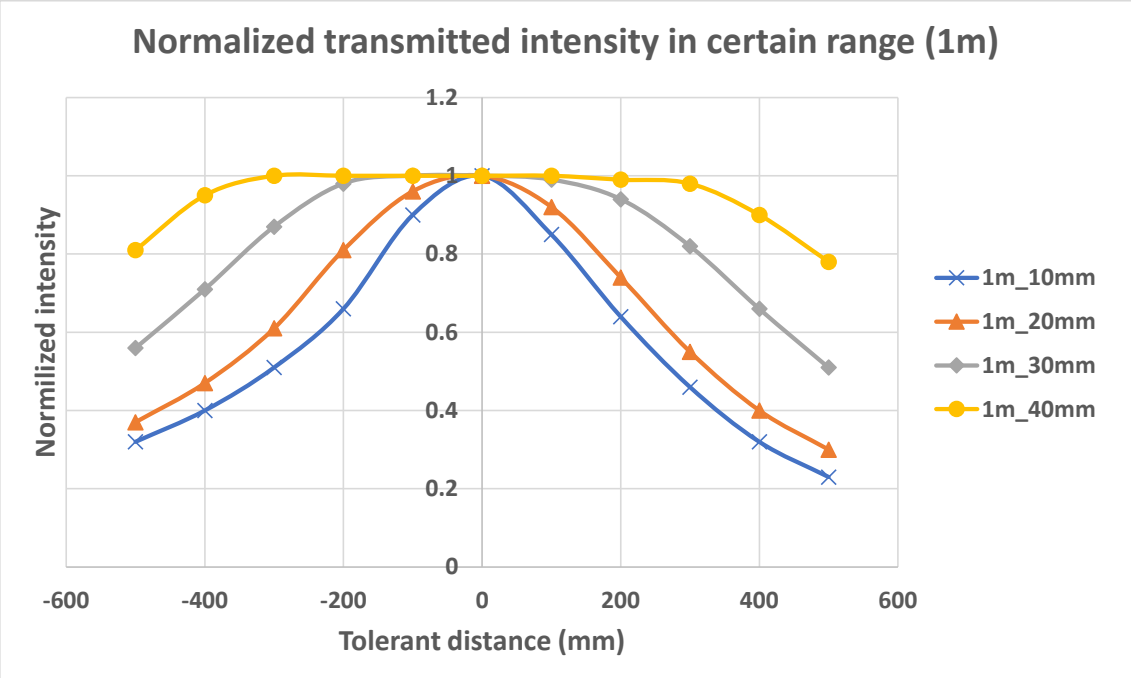

Fig. 3.21 Normalized transmitted intensity in 1m range with different size solar cell

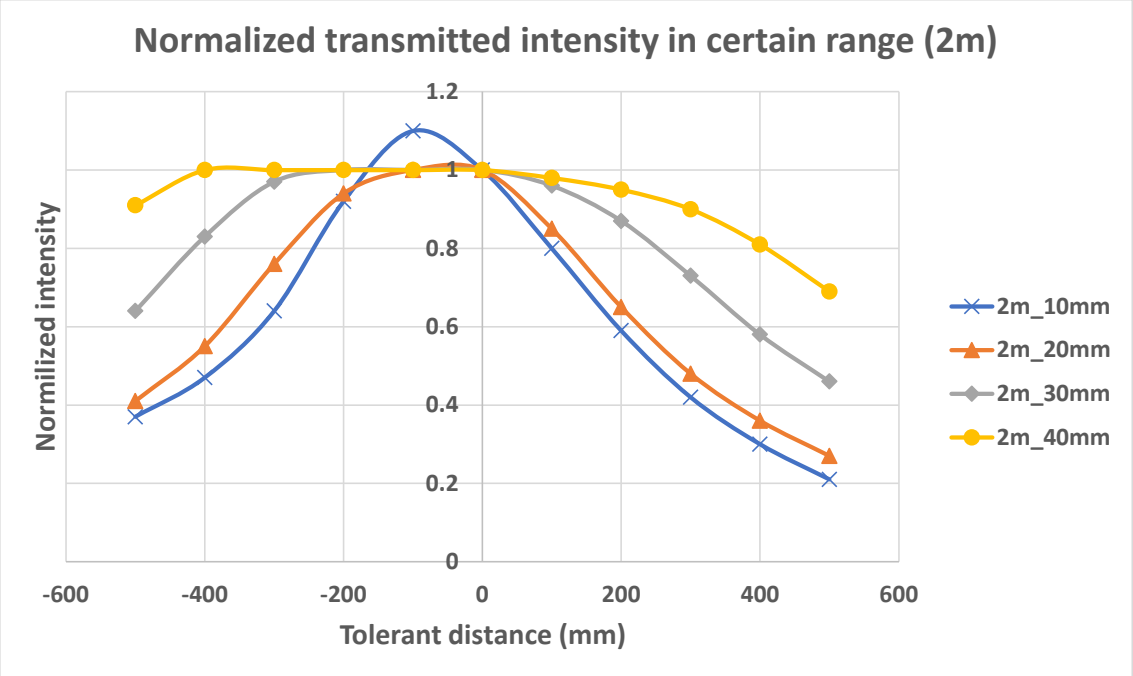

Fig. 3.22 Normalized transmitted intensity in 2m range with different size solar cell

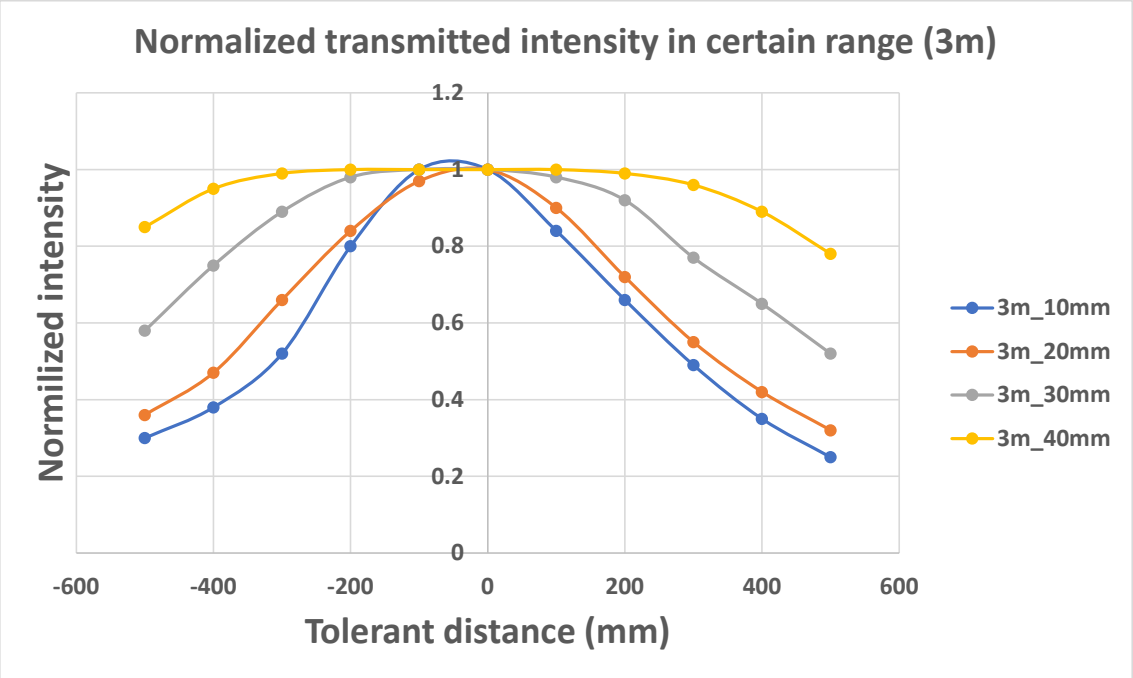

Fig. 3.23 Normalized transmitted intensity in 3m range with different size solar cell

From three figures, it's easy to see that transmission situations are very similar in three different distance range. When detectors are small, the transmitted intensity will be rapidly decreased when distance increased or decreased. With 10 mm × 10 mm solar cell, around 20% of intensity will be lost when relative distance increased to ±200 mm, and around 50% intensity will be lost with ±300 mm distance deviation. The decline tendency will be fast within nearby ±300 mm region and then goes to flat. When detector size is relatively large, then decline tendency tends to be small. For instance, when solar cell size increases to 20 mm × 20 mm, the system can still effectively transmit more than 60% intensity in the ±300 mm region, and this value increases to 80% when detector size enlarges to 30 mm × 30 mm. It is easy to understand that larger the receiver is, much intensity can be received, even the irradiation is not accurately focused. From the figures above, the tolerant distance of OWPT system is largely depends on solar cell size. Basically, for small terminals with small size of solar cell (smaller than 3 cm × 3 cm), more than 50% intensity can still be transmitted in ±500 mm

nearby region, and more than 70% intensity can be received in ±200 mm region. For OWPT system with slightly large size solar cell such as 4 cm × 4 cm or larger, more than 80% intensity is still available in ±500mm nearby region.

Another point that needs to be noticed is, because nearby region is not target transmission distance, thus the irradiation is not clearly imaged in such distance due to light beam cannot be accurately shape, which causes the irregular irradiation shape. Generally, from all the simulation data that shown in the figures above, in the nearby -300 mm and +100 mm region, irradiation can still be clearly imaged, and non-imaged in rest of region. Although the imaging quality is not the concern of the OWPT system, when analyzing the characteristics of the tolerant distance of the OWPT system, the imaged irradiation spot has a clear and regular boundary, thus the light intensity can be better received by the solar cell. Therefore, the OWPT system presents a feature that the received intensity in minus-region always more than plus-region with same relative distance. For example, in Fig.3.23, the 10 mm × 10 mm size detector can receive around 0.8 normalized available intensity at 2800 mm distance, while this value decreased to 0.66 at 3200 mm distance. This leads out a conclusion that OWPT system will be more tolerant in the nearby region that before the target distance than behind.

The electrical output power of the portable LED-based OWPT system is assumed around 230 mW in the discussion shown in section 3.3.1. As discussed in Section 2.1, the power output of 100 mW is used as the criterion for judging whether the OWPT system can effectively transmit power remotely. After including the PV conversion efficiency of the solar cell and other factors, the tolerant distance of the OWPT system is about -300 mm to +280 mm when the solar cell size is 10 mm × 10 mm. In the case of a solar cell size of 20 mm × 20 mm, the tolerant distance is -370 mm to +310 mm. When the size of the solar cell is above 30 mm × 30 mm, the tolerant distance beyond ±500 mm or more. The discussion about the tolerant distance of the OWPT system in this section is based on the irradiation spot size of 2.1 cm × 2.3 cm. Considering that the OWPT system configuration in Section 3.3.1 can almost achieve the smallest irradiation spot size at a transmission distance of 1 m, thus in practical applications that the

irradiation spot size larger than 2.1 cm × 2.3 cm, the tolerant distance of the portable LED-based OWPT system will be extended accordingly.

3.3.3 Analysis on oblique irradiation of portable LED-based OWPT system

The previous calculations, simulations and analysis are all discussed based on the condition that light beam is vertically irradiated on the solar cell. Whereas, the oblique irradiation is more common in the practical conditions. In OWPT applications, there are two biggest differences in oblique irradiation condition compared to the case of vertical irradiation condition. The first difference is that when the solar cell is irradiated obliquely, according to the Fresnel Equation, the reflection coefficient will increase accordingly due to the incident angle of light beam increases, so the light intensity loss due to reflection will also increase. The Fig. 3.24 shows the characteristic of the angle incidence performance of the typical single-junction GaAs solar cell (Advanced Technology Institute, LLC).[6]

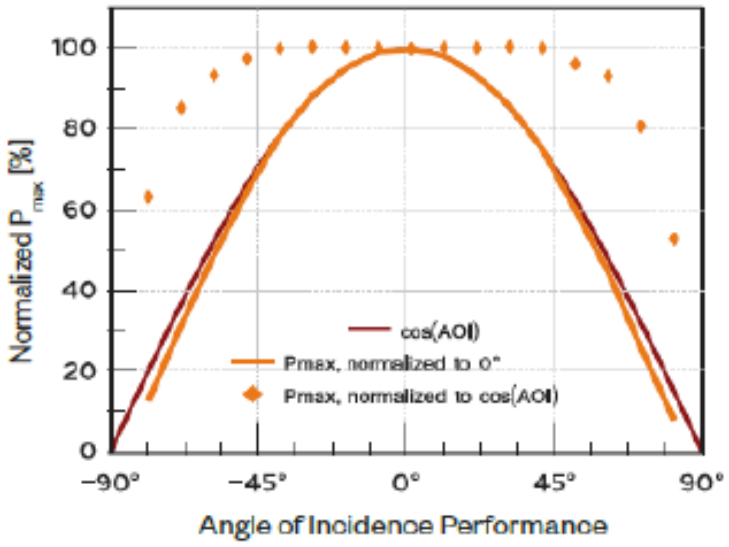

Fig. 3.24 The characteristic of the angle incidence performance of the typical single-junction GaAs solar cell (Advanced Technology Institute, LLC)

The second characteristic of oblique irradiation is that the irradiation spot will be deformed at the target transmission distance. The Fig. 3.25 shows the irradiation spot of the vertical irradiation and oblique irradiation (tilt 45° on x-plane).

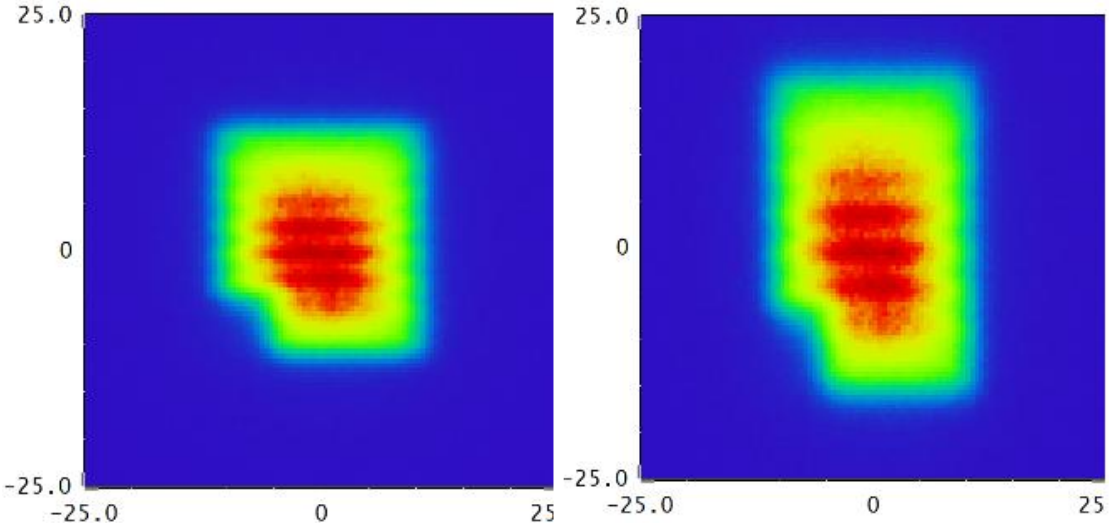

Fig. 3.25 Comparison of irradiation spot of vertical irradiation and oblique irradiation (tilt 45°)

It can be seen from Fig. 3.25 that the light spot formed under oblique irradiation is the oblique cut surface of the beam, so the shape of the light spot will be elongated in one direction and deformed. In the actual OWPT application, if the size of the solar cell is originally larger than the irradiation spot, the size of the irradiation spot formed under oblique irradiation might exceed the size of the solar cell in a certain direction, resulting in a loss of light intensity. On the other hand, when the size of the solar cell is smaller than the original irradiation spot, the size of irradiation spot formed by oblique irradiation increases to the deformation, which causes the radiant intensity of the light spot to decrease, and thus the performance of the OWPT system deteriorates.

The simulation of the portable LED-based OWPT system with oblique irradiation were held. The Fig. 3.26 shows the irradiance map of the irradiation spot from 0° to 80° tilt angle. Same as the simulation model in section 3.3.1, the size of the detectors is set as 17 cm × 17 cm in order to better comparing the results. Due to the detector in the simulation can only measure the received intensity without including the factor of reflection loss, the reflection coefficients based on the Fig. 3.24 were added in the model of detectors in the simulation. Thereby, the simulation results include both the reflection loss under oblique irradiation and

the geometric loss caused by the irradiation spot deformation.

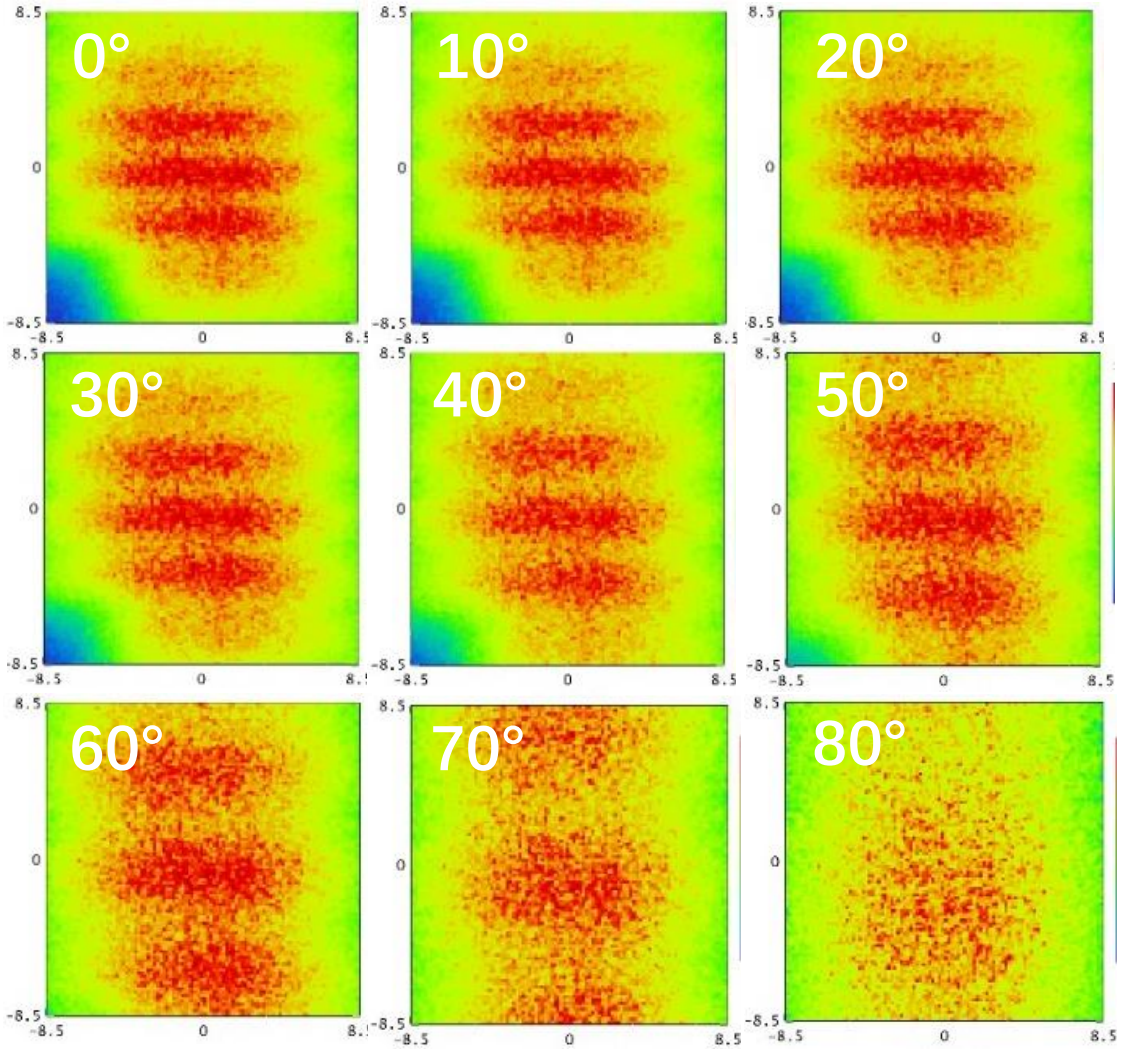

Fig. 3.26 Deformation of the irradiation spot under oblique irradiation

From the Fig. 3.26, the deformation degree of the irradiation spot becomes larger as the tilt angle increases. When the tilt angle is small, the deformation of the irradiation spot is not obvious. However, when the tilt angle increases to a certain degree (40°), the deformation process will be accelerated. Comparing the irradiance map under different tilt angle, it can be seen that as the tilt angle increases, the red area of the irradiation spot becomes more and more dispersed, which means the light intensity distribution becomes more and more dispersed as the irradiation spot stretches, and such dispersed intensity distribution

decreases the radiant intensity of the irradiation.

The characteristics of the normalized light intensity received by the detectors under oblique irradiation are shown in Fig. 3.27.

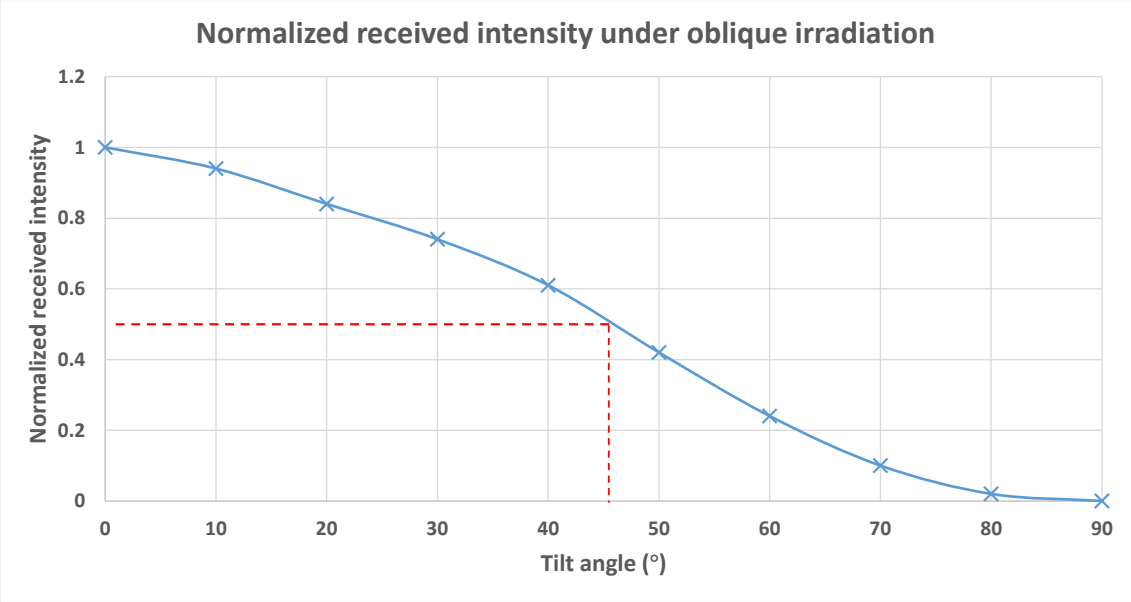

Fig. 3.27 The characteristics of the normalized light intensity received by the detectors under oblique irradiation

According to the data in Fig. 3.27, when the tilt angle is within 40°, the light intensity received by the detector drops smoothly. In this range tilt angle, the main reason for the decrease of received intensity is considered to be reflection loss caused by oblique irradiation. When the tilt angle exceeds 40°, the decline in the detector's received light intensity increases. In this tilt angle range, the reflection loss caused by the oblique irradiation and the geometric loss caused by the irradiation spot deformation increase at the same time, thus caused a large amount of light intensity loss on the detector.

The total received intensity under the condition of vertical irradiation (0°) is 575.3 mW in the simulation. Regarding the acceptable 50% total light intensity as the threshold for whether optical wireless power transmission can be carried out effectively, the maximum allowable tilt angle of the portable LED-based OWPT system is about 45°. Considering the factor of PV conversion efficiency of the

solar cell, the solar power output under such light intensity should be around 100mW, which meets the standard of minimum power output of the OWPT system that discussed in section 2.1. Therefore, based on the 45° maximum allowable tilt angle, the maximum transmission area of the OWPT system can be obtained.

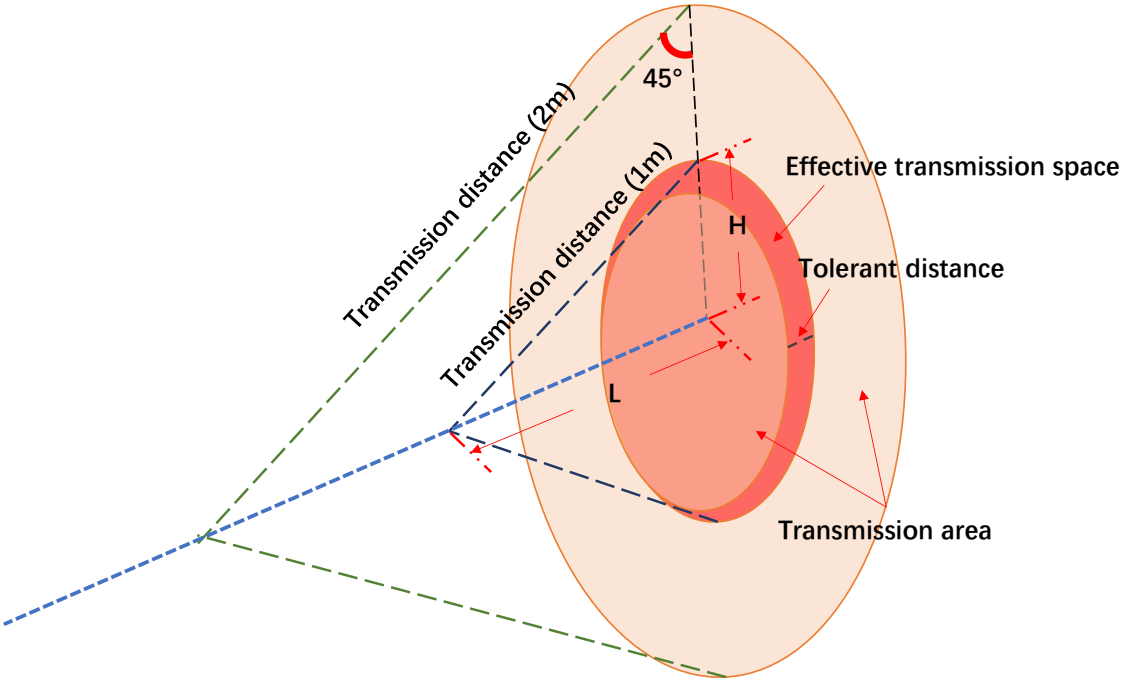

Fig. 3.28 The analysis of transmission area of LED-based OWPT system

The Fig. 3.28 shows the illustration schematic of oblique irradiation situation. Setting the 45° angle as the maximum tilt angle of the portable LED-based OWPT system according to the discussion above, the maximum transmission area of the portable LED-based OWPT system with a certain designed transmission distance can be figured out. The parameter L in the Fig. 3.28 is the maximum horizontal distance between the transmitter and the target load when using the OWPT system, and the parameter H represents the maximum installation height of the load in the vertical direction. The area Beyond the 45° tilt angle belongs to ineffective or less effective transmission region. Thereby, based on the designed transmission distance of the OWPT system and the maximum tilt angle of 45°, a circular area can be obtained. Calculating the length of the L parameter based on

the angle of 45°, it can be obtained that L is approximately equal to 0.88 times the designed transmission distance. According to the analysis of the tolerant distance of the portable LED-based OWPT system in Section 3.3.2, 0.88 times the designed transmission distance is still within the effective transmission distance range. Therefore, the entire circular transmission in the Fig. 3.28 belongs to the effective transmission area of the portable LED-based OWPT system. If the tolerant distance of the portable LED-based OWPT system is considered in the horizontal direction at the same time, a cylinder-like “effective transmission space” with the “effective transmission area” as the bottom surface and the “tolerant distance” as the thickness will be obtained, which is shown as the red space in the Fig. 3.28.

It is easy to understand that when the designed transmission distance increases, the effective transmission area, effective transmission space, and maximum installation height of the load will increase accordingly. The Fig. 3.29 shows the change trend of the effective transmission area and the maximum installation height of the load as the designed transmission distance of the portable LED-based OWPT system increases.

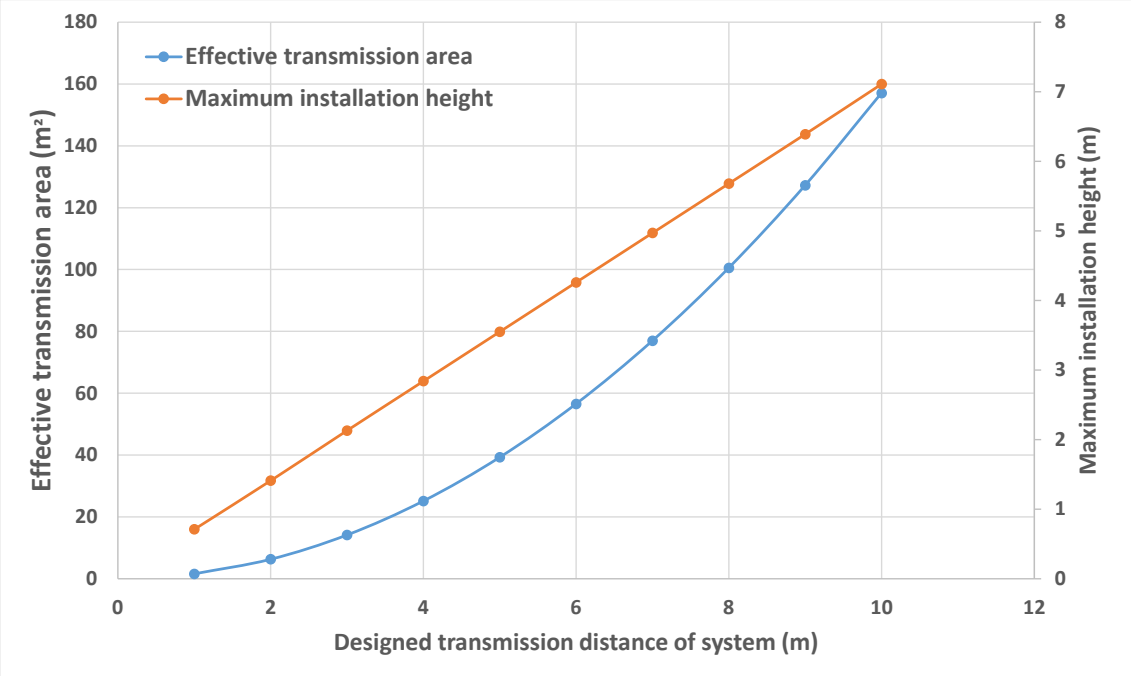

Fig. 3.29 Analysis of the effective transmission area and the maximum installation height of the load

According to the data shown in Fig. 3.29, the maximum installation height of the load increasing linearly when the designed transmission distance of the portable LED-based OWPT system enlarging, while the effective transmission area of the system will increase exponentially. Under the condition that the irradiation spot size at the target distance is designed as the same (2.1 cm × 2.3 cm), when the designed transmission distance of the LED-based OWPT system is greater than 3 m, the OWPT system will almost lose the portability due to the large dimension of optical system. Therefore, in this thesis that focusing on the research of the portable LED-based OWPT, the discussion of such long designed-distance LED-based OWPT system is not the main target. In fact, even if the designed transmission distance is 2 m or 3 m, the portability of the LED-based OWPT system is not good enough. However, it can be seen from the Fig. 3.29 that increasing the designed transmission distance of the LED-based OWPT system will greatly increase the effective transmission area of the system and the maximum installation height of the load, which is of great significance in practical applications. In the actual application, even though the portability of the LED-based OWPT system with a long designed-distance is not good enough, it can realize effective power transmission in a larger range, and also the installation position of the IoT terminal will be more flexible as well. Therefore, proper sacrifice of the irradiation spot size to reduce the dimension of the OWPT optical system with a longer designed-distance for realizing relatively good portability and a larger effective transmission range is also an important point that needs to be considered in practical applications.

3.3.4 Summary of the ideal configuration of portable LED-based OWPT system

In the section 3.3, the ideal configuration of the portable LED-based OWPT system is discussed. In the section 3.3.1, the simulation model of the portable LED-based OWPT system based on the ideal parameters of the optical system

that discussed in section 3.2 is shown. The analysis of the system performance including irradiation spot size, dimension of the system, efficiency of the system and transmitted intensity was discussed. Besides, the analysis of the reflection loss in the optical system is focused and researched. The tolerant distance of the portable LED-based OWPT system is presented in the section 3.3.2. The analysis is based on studying the normalized intensity that can be received by the detectors placed at the nearby region of the designed transmission distance, and three different transmission ranges were compared and discussed. Finally, in the section 3.3.3, the oblique irradiation of the portable LED-based OWPT system is analyzed. The characteristics of the intensity loss based on different tilt angle of irradiation is investigated, and 45° is set as the maximum tilt angle of irradiation based on 100 mW of the minimum transmission power standard of the OWPT system. Then, the characteristics of effective transmission area and maximum installation height of the load is researched based the maximum tilt angle of irradiation.

3.4 Mini-type LED-based OWPT system for short transmission distance

In the section 3.2 and section 3.3, the discussion about the LED-based OWPT system is almost based on the typical target transmission distance of 1 m. However, as a technology of transmitting power remotely, it is also very important to study the characteristics and performance of the LED-OWPT system in different transmission distance ranges. As discussed, the collimation of LED light beam over the entire transmission distance is very difficult due to the spatial incoherence of the LED light source. Thus, a system configuration for specific transmission distance is indispensable of LED-based OWPT system. For OWPT technology, the range below 1 m is defined as "short transmission distance", and the distance above 1 m can be defined as "long transmission distance". According to the discussion in Section 3.2, the dimension of the LED-OWPT system is proportional to the target transmission distance to some extent in order to ensure the size of the irradiation spot remains unchanged, which means that shorter the target transmission distance, the smaller the system size, and vice versa.

Therefore, it can be predicted that the size of the LED-based OWPT system can be miniature in application scenarios with short transmission distances (up to 1 m). In Section 3.4, the configuration, characteristics and performance of such mini-type LED-based OWPT system aimed at short transmission distance will be discussed and studied in detail.

3.4.1 The optical system configuration of mini-type LED-based OWPT system

Unlike the long power transmission such as several meters, the mini-type LED-based OWPT system is designed to aim at short range of transmission distance (shorter than 1 m). According to the equations shown in the section 3.1, the value of transversal magnification of optical system is linear with the designed transmission distance. That is to say, even if the exit pupil of the system is not enlarged as discussed in Section 3.2, the LED-based OWPT system aimed at short-distance can also achieve a small irradiation spot size, thus a "mini-size" LED-based OWPT very high portability can be obtained with.

The first discussion point of mini-type LED-based OWPT system is whether single-lens optical configuration is available or not. Due to the transmission distance is relatively short, the size of irradiation spot at the target transmission distance can be sufficiently small even the distance between the LED light source and image lens is short. Under this condition, the drawback of low efficiency of single-lens optical system might probably be eliminated. Therefore, the analysis on the feasibility of the mini-type LED-based OWPT system with single-lens optical configuration is necessary.

As discussed in the section 3.1, the overall transversal magnification of the single-lens optical system is the ratio between the transmission distance l' and the object distance l. Usually, the size of lens aperture of the mini-type LED-based OWPT system should be small enough (up to 5 cm). A device with such size can be carried around easily by human, so can be called “mini-type”. The Fig. 3.30 shows the characteristic of intensity that can be collected by the lens with 5 cm aperture with the object distance (distance between the LED light source and lens) increases of a single-lens optical system.

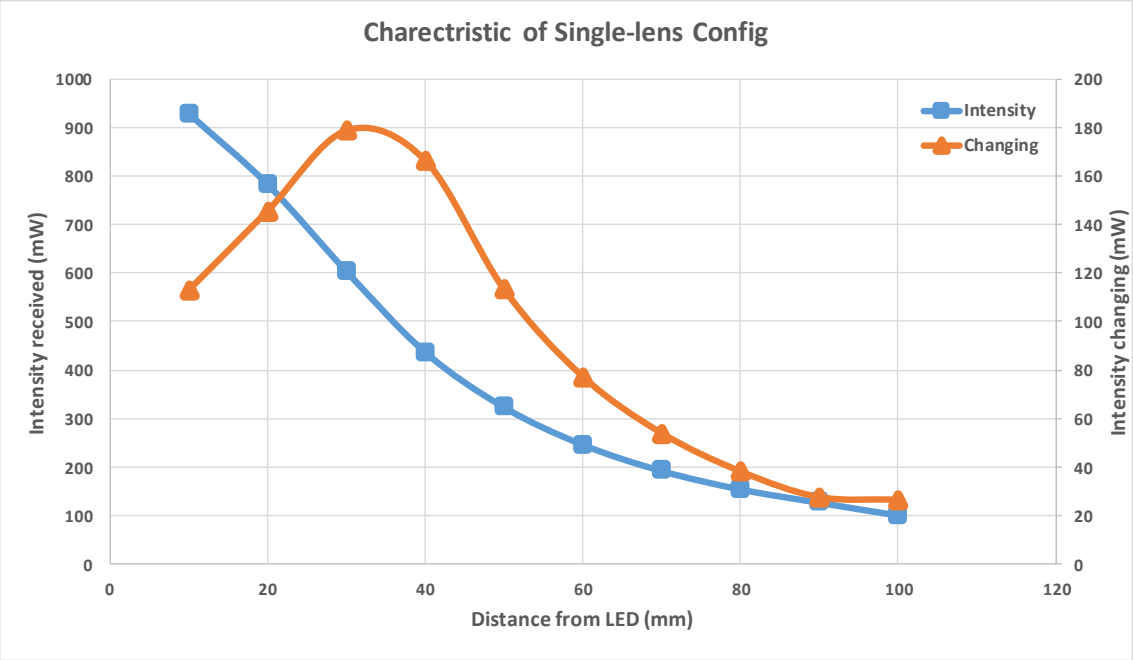

Fig. 3.30 The characteristic of the received intensity of single-lens mini-type LED-based OWPT system

According to the data shown in Fig. 3.30, when the distance between the LED light source and the lens is 10 mm to 50 mm, the light intensity collected by the lens has a rapid downward trend, especially in the range of 20 mm to 40 mm. For instance, as for the LED light source with total 1040 mW intensity, around 400 mW intensity will be lost when light source is 30 mm away from the lens. And if above 80% efficiency of the lens system is desired, the distance between the LED light source and the lens need to shorter than 20 mm. However, as discussed, the overall transversal magnification of the single-lens optical system equals the ratio between the transmission distance and object distance. As the same transversal magnification of the double-lens optical system shows in the section 3.3.1 as an example. The overall transversal magnification of the double-lens optical system shown in section 3.3.1 can be calculated as 13.6. On the other hand, if the same overall transversal magnification value wishes to be achieved by the single-lens optical system with 20 mm objective distance, the transmission distance of the system has to be smaller than 271 mm. This is to

say, the same size of irradiation spot of the OWPT system configuration shown in section 3.3.1 can be only achieved by a high-efficiency single-lens optical system when the transmission distance is short than 271 mm, which is not desired. As mentioned, due to the feature of the LED light source, a specific configuration LED-based OWPT is necessary for a certain transmission distance. In the long transmission distance range, considering the factor of tolerant distance, when the deviation between the actual transmission distance and the designed transmission distance is about 1 m, the configuration of the LED-based OWPT system needs to be redesigned to obtain higher power transmission efficiency over this distance. However, for the mini-type LED-based OWPT system that aimed at short range, the transmission range is inherently short (up to 1 m). If the system configuration needs to be redesigned every few hundred mm, the finance and labor costs will be too high. Therefore, an important feature of the mini-type LED-based OWPT system aimed at short distances is to achieve a proper irradiation spot size over the transmission range of 100 mm to 1000 mm. In other words, the effective transmission distance of the mini-type LED-based OWPT system needs to cover the transmission range from 100 mm to 1000 mm as much as possible. As for the single-lens optical system configuration, in order to ensure the high efficiency, the small irradiation spot size can only be achieved within a distance of 271 mm, which means that the system focuses the beam within a distance range of 271 mm, then at a longer distance, such as at the position in the range of 700 mm to 1000 mm, the size of irradiation spot can be expected to become very large. Conclusively, the mini-type LED-based OWPT system with single-lens optical configuration can only cover a very short distance range, it is thereby not an ideal candidate of the optical system configuration.

In summary, the performance of the single-lens configuration is still not satisfactory in the mini-type LED-based OWPT system. The configuration of the double-lens will still be used as the optical system of the mini-type LED-based OWPT system.

3.4.2 Analysis of parameters in mini-type LED-based OWPT system

As for the double-lens optical system, the first parameter that need to be decided

is the d value, which is the distance between two lenses. Although it can be seen from the equation (3.13) that larger d value can achieve smaller irradiation size. The balance between system dimension and irradiation size is far more important especially in mini-type LED-based OWPT system. The characteristic between d value, aperture size of the image lens, and system efficiency of double-lens optical system was figured out based on the simulation results. The data is shown in Table 3.5. The focal length of the condenser lens is set as 23.5 mm, and the data shown in the Table 3.5 is just for discussing the relation between the d value, aperture size of the image lens, and system efficiency.

Table 3.5 Characteristic of double-lens OWPT system

d / Aperture	30mm	63mm	95mm	128mm	161mm	194mm	226mm
20mm	65.70%	26.10%	13.20%	7.90%	5.20%	3.70%	2.70%
40mm	99.30%	62.60%	38.30%	25.20%	17.60%	12.90%	9.80%
60mm	99.50%	87.70%	61.30%	44.20%	32.70%	24.90%	19.50%
80mm	99.50%	99.90%	79.00%	60.90%	47.50%	37.60%	30.30%
100mm	99.50%	99.90%	83.20%	74.50%	60.60%	49.60%	41.00%

Due to the aiming of building mini-type OWPT system, the aperture of lens is limited to 50 mm. From the data shown in Table 3.5, with 50 mm aperture of the image lens, there will be around 20% intensity lost when d value increases to 60 mm. For achieving high efficiency of the system, it is believed range of d value need to be controlled from 30 mm to 50 mm based on 50 mm aperture. Noticed the data shown in Table 3.5 is based on certain parameters of the condenser lens, and the data will be changed if other parameters applied on the condenser lens. Based on the simulation results of mini-type LED-based OWPT system, the final efficiency of the system with 30 mm d value will be around 26% higher than the system with 50 mm d value. Considering in the short transmission range, the irradiation spot size is already relatively small comparing with long transmission

distance, thus the configuration of the mini-type LED-based OWPT system with smaller dimension and higher efficiency is more desired.

The relation between system overall transversal magnification and d value is shown in Fig. 3 31. The value of l_1 is set as -4, which is the minimum size of the LED package, as disused. Besides, considering the mini-type LED-based OWPT system has smaller d value, the focal length of the condenser lens can be appropriately increased to reduce the size of irradiation spot. Thus, the focal length of condenser lens is set as 50 mm in simulation, and the transmission distance is set as 400 mm, which is a typical transmission distance in short range. Such parameters show a common situation of the practical application of mini-type LED-based OWPT system for short transmission distance.

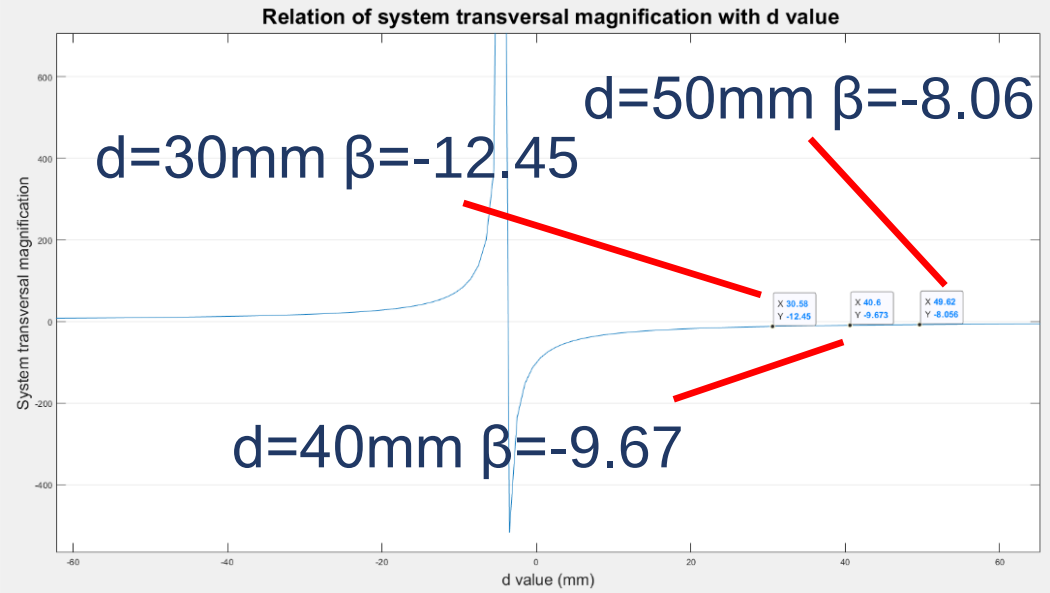

Fig. 3.31 The relation of system transversal magnification with d value

From data in the Fig. 3.31 which shows a very typical application situation of mini-type LED-based OWPT system, the changing of transversal magnification value is small after the d value beyond 20 mm. When the d value increases from 30 mm to 50 mm, the transversal magnification value is only changed from -12.45 to -8.06. Considering the irradiation sport size of the LED-based OWPT system in short-distance range is already small, such small coefficient difference cannot

lead out very obvious gain, while on the contrary, the efficiency will have around 26% decline. Thus, sacrificing a little bit performance on irradiation spot size but achieving higher efficiency is more proper method to enhance the overall performance or the mini-type LED-based OWPT system. From the Fig. 3.31, the value of d parameter should be at least larger than 20 mm but must be avoided too large. Therefore, 30 mm is considered as a proper value of d parameter in the mini-type LED-based OWPT system.

The second discussion is about the value of the focal length of the condenser lens, which is the f_1' parameter. As for the focal length of condenser lens, the fact that it largely influent overall transversal magnification value of the LED-based OWPT optical system has already been proved in section 3.2. In the section 3.2, the conclusion is large focal length of condenser lens will greatly decrease the size of the irradiation spot at target transmission distance. However, such conclusion slightly changed in the condition of mini-type LED-based OWPT system which focusing on transmitting power remotely to the IoT terminals installed in short-distance range. From equation (3.13) of the overall system transversal magnification of the double-lens optical system, it can be seen that the transmission distance l_2' is the first-order coefficient of other parameters, which means that the value of l_2' will influent the effect of other parameters on transversal magnification. In the mini-type LED-based OWPT system, the target transmission distance is short, which leads out the result that influence of the focal length of the condenser lens on the system transversal magnification to be small. Setting d value to be 30 mm based on the conclusion stated above and transmission distance is still 400 mm, the relation between the overall transversal magnification of the optical system and the value of f_1' parameter is shown in Fig. 3.32.

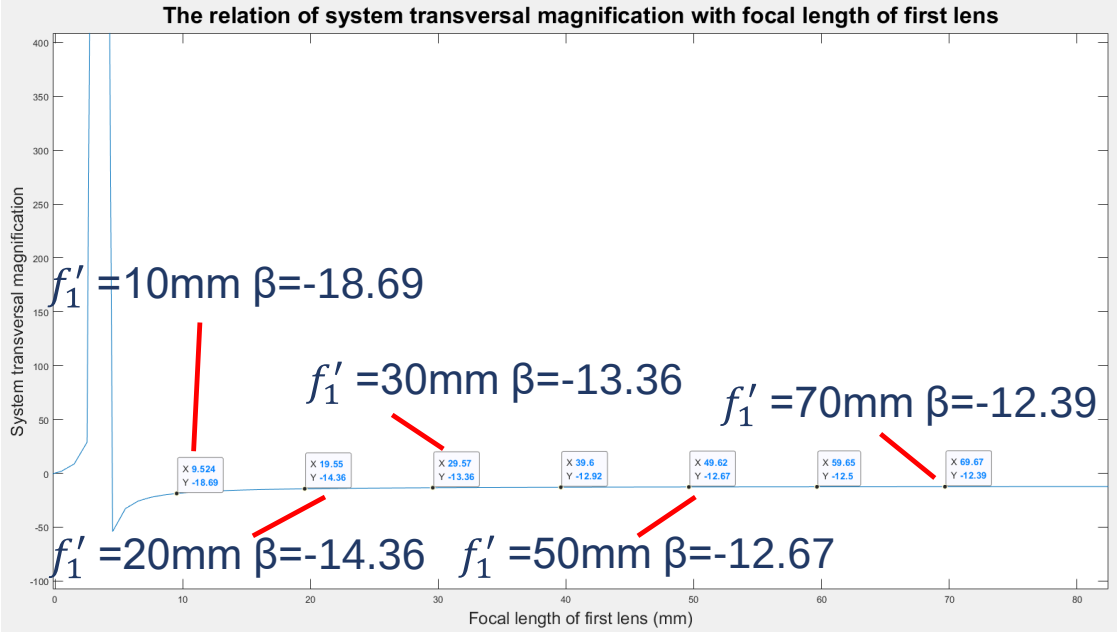

Fig. 3.32 The relation of system transversal magnification with f_1' value

From the data shown in Fig. 3.32, once the value of f_1' beyond 20 mm, the corresponded system transversal magnification value almost remains unchanged. When the value of f_1' parameter increases from 10 mm to 20 mm, the overall transversal magnification of the double-lens optical system changes from -18.7 to -14.4, while the value of f_1' parameter varies in the range from 20 mm to 70 mm, the corresponding value of system transversal magnification only changes from -14.4 to -12.4. For comparison, set the transmission distance to 1000 mm, such changing on overall transversal magnification value will be 2.5 times greater. This result proves the fact that, the value of the focal length of condenser lens is no longer the main factor that decides the irradiation spot size in the short-distance LED-based OWPT application, and only the transmission distance is the element that mainly determines the overall transversal magnification value of the optical system. However, in the viewpoint of system efficiency, the value of focal length of the condenser lens is still a critical factor. Therefore, the 20 mm is believed as a proper value of the f_1' parameter.

3.4.3 Three models of mini-type LED-based OWPT system for short transmission distance

As for the LED-based OWPT system configuration for relatively long transmission distance, a lens system configuration for specific transmission distance is necessary. However, the effective transmission distance of the mini-type LED-based OWPT system needs to cover the transmission range from 100 mm to 1000 mm as much as possible. In this section, three design ideas are proposed. The first designing is fixing the value of the d parameter while the f_2' value is variable. The d parameter is the distance between the two lenses distance and f_2' is the focal length of the image lens. The actual principle of this configuration is applying a focus tunable lens, such as liquid lens, as the image lens of double-lens optical system. The second configuration is fixing both value of d parameter and f_2' parameter, which is the same idea of designing of the configuration discussed in section 3.2. Third configuration is fixing the value of f_2' parameter while the d parameter is variable, which is the typical zooming lens system that the image lens is movable for changing the focal distance of the entire optical system. As the reason discussed above, the value of d parameter is set as 30 mm in all the configurations that the value of d parameter is immutable. The simulation data of first configuration (fixed value of d parameter/variable value of f_2' parameter) is shown in Table 3.6.

Table 3.6 Simulation results of fixed d value/variable f_2' value configuration (d=30mm, 50 mm aperture, f_1'=20mm)

Transmission distance(mm)	f_2' value (mm)	Irradiation size (mmxmm)	Lens system efficiency
100	34.0	6×6.5	88.4%
200	40.0	8×8.6	86.9%
300	43.0	12×13	86.5%
400	44.4	16×17	85.6%
500	45.5	20×22	85.5%

600	46.0	24×26	85.0%
700	46.7	28×30	85.0%
800	47.4	33×35	84.4%
900	47.7	37×40	84.4%
1000	47.9	40×43	84.1%

The Table 3.6 shows the best f_2' values in different transmission distances that can achieve smallest size of irradiation spot. In the simulation model, the focal length of the condenser lens is 20 mm, and the size of LED emitting chip is 0.75 mm × 0.75 mm. From the data shown in Table 3.6, due to the distance between the two lenses is small enough (d value of 30 mm), therefore the system can achieve above 80% efficiency no matter how the value of f_2' parameter changing. Besides, the changing on the value of the f_2' parameter tends to be very small when the transmission distance of the LED-based OWPT system above 200 mm, and irradiation spot size is linearly enlarged with the transmission distance increases. For instance, when the transmission distance of the system increases from 400 mm to 700 mm, the required value of f_2' parameter is just changed around 2 mm. This is to say, even in the first configuration (fixed value of d parameter/variable value of f_2' parameter) of the mini-type LED-based OWPT system for short-distance range that the value of f_2' parameter is variable, the value of f_2' parameter is almost remained unchanged in majority range of the transmission distance. Therefore, due to the value of f_2' parameter is almost unchanged, it is possible to choose a proper value of f_2' parameter that can cover majority region within 1000 mm transmission distance. Considering the focus tunable lens must be used if the value of f_2' parameter is hoped to be variable, which will largely increase the cost, therefore the more practical method is using a proper focal length lens which can cover majority region within 1000 mm transmission distance, which leads out the second configuration that the value of d parameter and f_2' parameter is fixed.

The Table 3.7 shows the simulation data of the second configuration of the mini-

type LED-based OWPT system for short-distance range.

Table 3.7 Simulation results of fixed d value/f_2' value configuration (d=30mm, 50 mm aperture, f_1'=20mm)

f_2'(mm) / L(mm)	34	40	43	44.4	45.5	46	46.7	47.4	47.7	47.9
100	6×6.5									
200		8×8.6								
300			12×13	17×18						
400				16×17	19×21	22×24	24×27			
500				22×24	20×22	23×25	24×26	30×32		
600					26×27	24×26	25×27	28×31	31×33	34×36
700					33×37	28×30	28×30	30×33	32×34	33×35
800						35×38	34×37	33×35	35×37	36×38
900						40×44	39×43	37×40	37×40	38×41
1000						48×53	46×49	42×45	41×44	40×43

In Table 3.7, all the blocks that crossed out is the relatively ineffective transmission distance, which means the beam cannot be proper focused at such range. Although the focused beam cannot be used as a basis for judging whether the LED-based OWPT system can effectively supply power, the shape of irradiation spot in such area is a circle with blurred edges with uneven intensity distribution, which results the lower photovoltaic conversion efficiency of the solar cell compared with accurately focused irradiation spot. Therefore, the focus range of the light spot can reflect the range of the effective transmission distance of the mini-type -LED-based OWPT system. From the data shown in Table 3.7, when value of f_2' parameter is very small (34 mm to 43 mm), the effective transmission distance is very limited, only around 100 mm range. When value of f_2' parameter

increased to 44.4 mm, the mini-type LED-based OWPT system can effectively transmit power with relatively small irradiation spot to the device locates at the distance from 300 mm to 500 mm. The image lens with 45.5mm focal length can cover the transmission distance region from 400 mm to 700 mm. The image lens with focal length of 46 mm to 47 mm lead outs the longest effective transmission distance, which can cover from 400 mm to 1000 mm. The image lens with smaller focal length will have a good performance in short-distance range, while the larger f_2' value image lens can achieve smaller irradiation spot in longer transmission distance from 500 mm to 1000 mm. As the results, the image lens with smaller than 44 mm focal length is considered not very suitable to be applied in this configuration due to too short effective transmission range. In the application with the requirement that the main target transmission distance is around 300 mm to 500 mm, the value of f_2' parameter can be set in the region from 44 mm to 45 mm. The image lens with the f_2' parameter of 46 mm to 47 mm can achieve around overall 600 mm effective transmission range, which is the longest distance according to the data shown in Table 3.7. Finally, if target transmission distance is at the end of 1000 mm region such as 700 mm to 1000 mm, then the value of f_2' parameter need to be set in the range from 47 mm to 48 mm in this configuration of mini-type LED-based OWPT system.

In order to extend the effective transmission distance range, a configuration with the fixed value of f_2' parameter but variable d parameter is cited as third configuration. In such configuration, the focal length of the both condenser lens and image lens is fixed, while the condenser lens is movable likes a zooming lens system, thus makes the value of d parameter is variable. From the data shown in the Table 3.7, the image lens with the f_2' parameter of 46 mm to 47 mm can achieve the longest effective transmission range, thus the value of f_2' parameter is set as 46 mm in the third configuration (fixed value of f_2' parameter/variable value of d parameter) of mini-type LED-based OWPT system for comparison. The simulation data is shown in Table 3.8.

Table 3.8 Simulation results of fixed f_2' value/variable d value configuration (50 mm aperture, f_1'=20mm, f_2'=46mm)

Transmission distance(mm)	d (mm)	Irradiation size (mmxmm)	Intensity transmitted (mW)
100	81.0	2×2.2	33.5%
200	43.0	7×7.5	70.2%
300	35.0	11×12	81.0%
400	32.0	16×17	84.5%
500	31.0	21×23	86.3%
600	30.0	24×26	87.5%
700	28.7	30×33	87.8%
800	28.0	35×38	88.1%
900	27.8	39×42	88.1%
1000	27.6	45×47	88.1%

From the data shown in Table 3.8, the third configuration can easily achieve long-range effective power transmission. According to the equation (3.3) of the Newton's formula, for imaging lenses, the object distance and the image distance are inversely proportional when the focal length is constant. Therefore, for the short transmission distance such as 100 mm, the image lens needs to be moved at very far position, thus the efficiency of optical system will be low. Specifically, around 65% total intensity is lost when the transmission distance is 100 mm. When transmission distance is in the range of 200 mm to 1000 mm, the changing of the value of d parameter changing becomes small, and efficiency of the lens system can be remained above 70%. Comparing with the second configuration (fixed value of d parameter and f_2' parameter) of mini-type LED-based OWPT system, the third configuration can achieve longer effective transmission distance range and smaller irradiation spot. Comparing the three kinds of configurations of mini-type LED-based OWPT system for short-distance range, the first configuration (fixed value of d parameter/variable value of f_2' parameter) has

relatively best performance on efficiency and size of irradiation spot, while the focus tunable lens is necessary to be used as image lens. The second configuration (fixed value of d parameter and f_2' parameter) has the simplest configuration. All the parameters of the optical system are decided in advanced, therefore the performance of the system is relatively poor. The focal length of the image lens should be determined based on the desired transmission distance. From the viewpoint of longest effective transmission range, the image lens with the f_2' parameter of 46 mm to 47 mm is the optimal option. In contrast, the third configuration (fixed value of f_2' parameter/variable value of d parameter) has the most balanced performance and flexible design. It does not need a focus tunable lens to achieve a long effective transmission distance range. Also, such zooming system is very easy to design and build in the mini-type LED-based OWPT system. Considering the good performance and simple configuration, the third configuration is believed to be the very talent choice applied in mini-type LED-based OWPT system for short distance range.

In order to better show the influence of the f_2' parameter on system performance and find out the best value of f_2' parameter in the third kind configuration of mini-type LED-based OWPT system, the comparison of the system with the image lens of 46 mm and 50 mm focal length in the aspects of efficiency of lens system and size of irradiation spot is shown in Fig. 3.33.

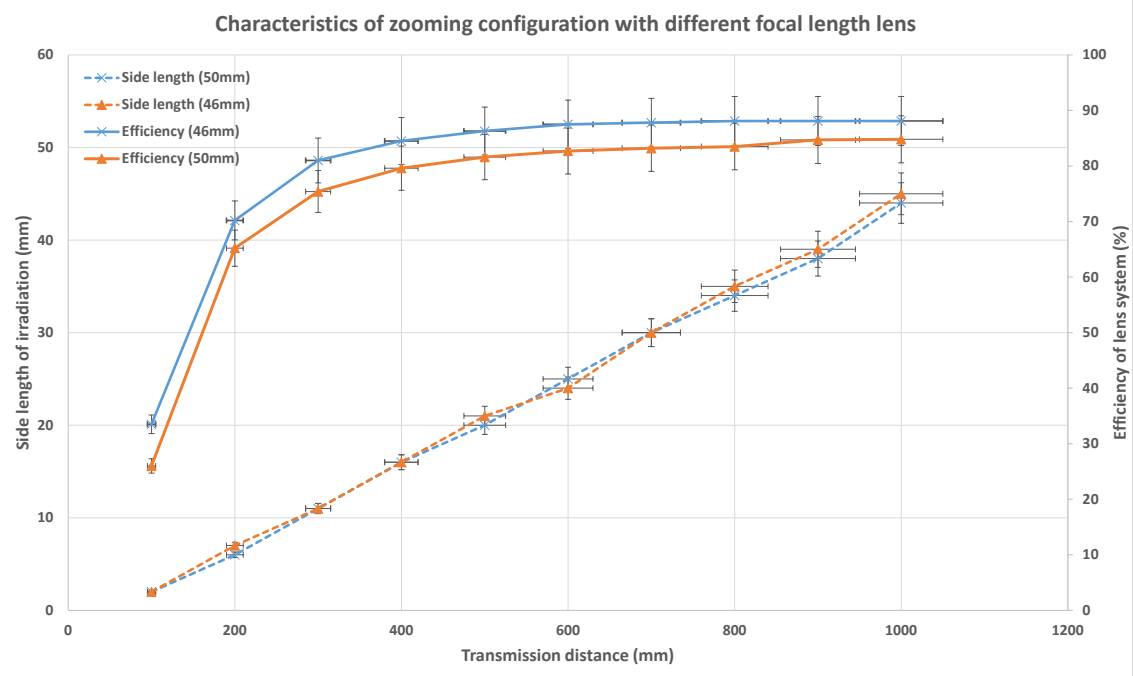

Fig. 3.33 The comparison of third configuration with 46mm and 50mm focal length lens

From the data shown in Fig. 3.33, the irradiation spot size of the system with 46 mm and 50 mm focal length image lens is almost the same. Considering the measurement error and possible tiny fluctuation during the power transmission, such small difference on the size of irradiation spot can be ignored. While for the efficiency of the optical system, the system with 46 mm focal length image lens can obviously achieve higher efficiency compared with 50 mm focal length image lens. By the simulation, the difference on the transmitted intensity is around 50mW. Therefore, increasing the focal length of the image lens cannot result a smaller size of the irradiation spot but deteriorate the efficiency of the lens system. Combining the results shown in Table 3.7, 46 mm is believed as a very proper focal length value of the image lens with 50 mm aperture in third configuration.

3.4.4 Summary of mini-type LED-based OWPT system for short distance range

In the section 3.4, the mini-type LED-based OWPT system for short distance range is analyzed in the aspects of basic lens system, parameters of the system

and different configurations. Due to the size of irradiation spot is inherently small in the short distance range, thus the dimension of the LED-based OWPT system for such range is small. Therefore, the analysis on the feasibility of the mini-type LED-based OWPT system with single-lens optical configuration is shown in section 3.4.1. By establishing a mathematical model of the optical system, and analyzing the system efficiency and overall transversal magnification of the system, it is proved that the double-lens optical system is still the most suitable configuration for the mini-type LED-based OWPT system for short distance range. According to the mathematical model, the parameters of the optical system are analyzed in detail in Section 3.4.2, and it is concluded that because of the feature of the mini-type LED-based OWPT system that focusing on short-distance range, the focal length of the condenser lens is no longer the main factor affecting the system irradiation spot size as long as the value of f_1' parameter is larger than 20 mm, and the optimal value of d parameter is 30 mm. Then in the section 3.4.3, from the viewpoint of as long as possible effective transmission distance, three kinds of configuration of the mini-type LED-based OWPT system is researched and compared based on the results of simulation. Conclusively, the first configuration (fixed value of d parameter/variable value of f_2' parameter) has relatively best performance on efficiency and size of irradiation spot, while the configuration is complex due to focus tunable lens is necessary. The second configuration (fixed value of d parameter and f_2' parameter) has the simplest configuration but relatively poor performance. The third configuration (fixed value of f_2' parameter/variable value of d parameter) has the most balanced performance and flexible design. The third configuration is believed to be the very potential choice applied in mini-type LED-based OWPT system for short distance range. The optimal parameters of the optical system in such configuration were figured out by simulation. Summarily, the 20 mm of f_1' parameter, 46 mm of f_2' parameter and 50 mm of lens aperture size is proved as proper value for the parameters in the optical system of mini-type LED-based OWPT system for short distance range. By applying such parameters in the optical system, the mini-type LED-based OWPT system can effectively transmit power in the range from 100

mm to 1000 mm with above 80% efficiency.

3.5 Large-size LED-based OWPT system for long-distance range

According to the discussion in Section 3.2, the dimension of the LED-OWPT system is proportional to the target transmission distance to some extent in order to ensure the size of the irradiation spot remains unchanged. Therefore, in order to achieve effective power transmission to the device installed at long distance, the dimension of the LED-based OWPT system has to enlarged. In the application of LED-OWPT system, the transmission distance longer than 1 m is defined as “long transmission distance”. In this section, the analysis of the large-size LED-based OWPT system for long transmission distance will be discussed.

3.5.1 The analysis of large-size LED-based OWPT system for long-distance range

In essence, the principle and design of the large-size LED-based OWPT system are exactly the same as the LED-based OWPT system for 1 m transmission distance that introduced in section 3.3. Similarly, the double-lens optical system is configured as the lens system in large-size LED-based OWPT system for long transmission distance. The only difference is because of the size of irradiation spot is proportional to the transmission distance, in order to transmit power effectively to the IoT terminal at long distance, the exit pupil of the LED-based OWPT system must be enlarged, which causes the value of d parameter (distance between two lenses) and the f_1' parameter (focal length of condenser lens) increasing as well. Therefore, the dimension of the system will be enlarged. Consequently, in this section, the structure and design of the large-size LED-based OWPT system are no longer discussed, and only the simulation results are used to analyze the optical component parameters and system dimensions of the LED-based OWPT system under long transmission distances.

The Fig. 3.34 shows the characteristic of irradiation size based on value of d and transmission distance by simulation results. The transmission distance is set from 1000 mm to 3000 mm. The simulation results were carried out using ZEMAX (ZEMAX LLC). The values of d parameter is selected from several typical value

that calculated from edge ray on image lens. In the simulation model, the f_1' was set as 23.5 mm and size of LED emitting chip is 0.75 mm × 0.75 mm, same as the parameters used in the simulation model shown in section 3.3.

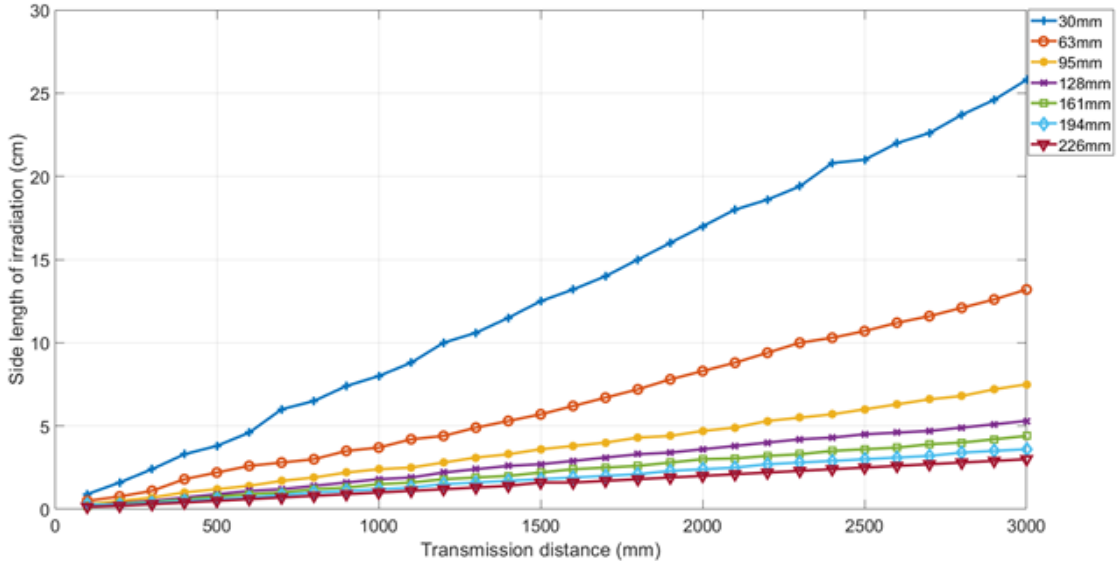

Fig. 3.34 The characteristic of irradiation size based on value of d and transmission distance by simulation

The Fig. 3.34 shows the size of irradiation spot with different transmission distance (100 mm – 3000 mm) and d values. The value of the focal length of the image lens is set according to the transmission distance. As discussed in section 3.2, the value of the image lens focal length will only determine the distance at which the light beam of the OWPT system is focused, and does not affect the size of the irradiation spot. Generally, the irradiation spot enlarging linearly with the transmission distance and decreasing with the d value increasing. As the Fig. 3.34 shows, the optical system with 30 mm d parameter has a rapidly climbing tendency on irradiation size while trend of 226 mm d parameter is flat and relatively steady. Comparing with tendency of different lines shown in the Fig. 3.34, it can be found that the irradiation sizes of the optical system with larger than 63 mm d parameter is not very different. For instance, even the value of d

parameter from 128 mm to 226 mm, which is almost doubled, the side length of the irradiation spot has only increased by less than 2 cm. While the increase of the irradiation spot between the configurations with 95 mm and 63 mm d parameter is much obvious. From the Fig.3.34, 70 mm d parameter is an important threshold value of the optical system that decides whether the small irradiation spot can be achieved or not, which fits the conclusion shown in section 3.2. Therefore, same as the conclusion shown in section 3.2, the 70 mm is the minimum value of d parameter. On the other hand, due to the size of irradiation spot is proportional with the transmission distance, in order to achieve small enough irradiation spot at the long transmission distance, the value of d parameter should be better larger than 130 mm in the LED-based OWPT system for long transmission distance. Even the relatively small irradiation spot can be achieved when d parameter larger than 70 mm, from the Fig. 3.34, the increasing tends to be ignorable only the value of d parameter larger than 128 mm. Therefore, 130 mm is believed as a proper value for the d parameter in the LED-based OWPT system for long transmission distance.

The Fig. 3.35 shows the characteristics of the lens system efficiency based on the different values of d parameter and the aperture size of the image lens. The data shows in the legend refers the different aperture size of the image lens.

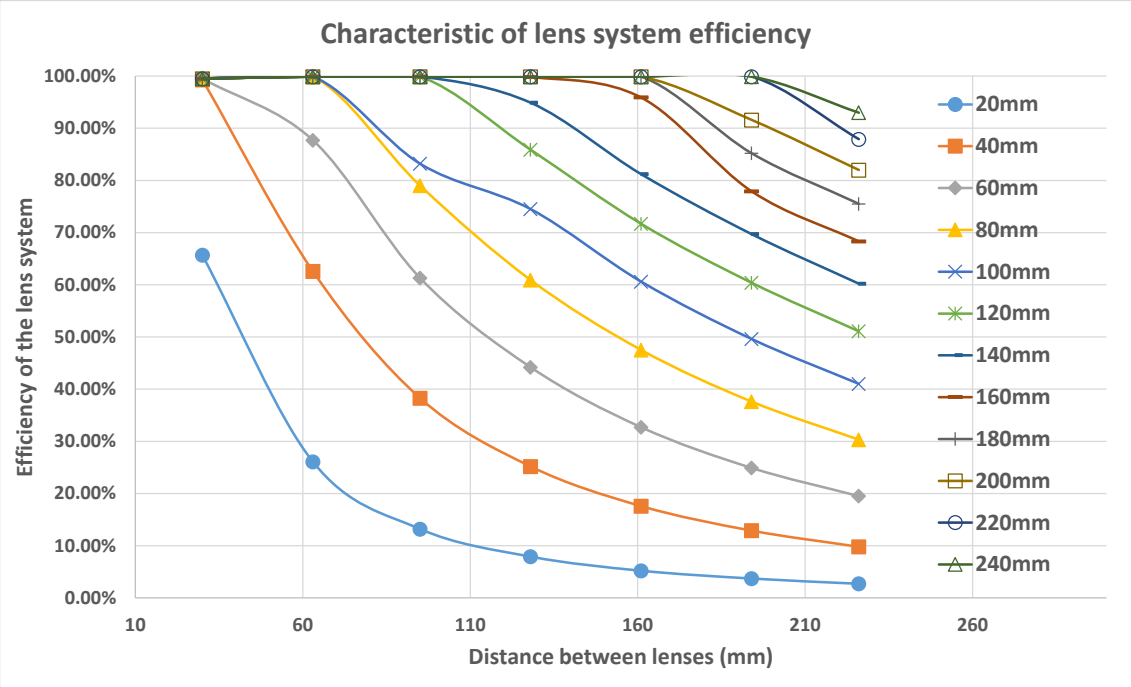

Fig. 3.35 The characteristics of the lens system efficiency based on the different values of d parameter and the aperture size of the image lens

According to the data shown in the Fig. 3.35, the efficiency of the optical system will decrease to varying degrees according to the aperture size of the image lens and the increase of the distance between the two lenses. When the aperture size of the image lens is not large enough, the efficiency of the lens system deteriorates rapidly with the increasing of the distance between the two lenses. As discussed above, the ideal value of d parameter should be larger than 128 mm in order to achieve a sufficiently small irradiation spot at long distance range. Based on such value of d parameter, the aperture size of the image lens should be at least larger than 120 mm if above 80% efficiency of the lens system is wished, and 140 mm size image lens is needed in order to achieve above than 90% lens system efficiency. Therefore, with 128 mm d parameter and 120 mm aperture of image lens, according to the Fig. 3.35, an irradiation spot with 4.6 cm side length can be obtained at 2 m transmission distance, and the side length of the irradiation spot increases to 5.1 cm when the transmission distance is 3 m. Under this case, the dimension of the LED-based OWPT system is around 13 cm × 12 cm × 12 cm. Such dimension is relatively large, but still can maintain a

certain portability. However, if the transmission distance is extended or required smaller irradiation spot, the dimension of the LED-based OWPT system will enlarged constantly. For instance, if the side length of the irradiation spot is required smaller than 3 cm at 3 m transmission distance, the value of d parameter must increase above 226 mm, and aperture size of the image lens need to larger than 200 mm for ensuring at least more than 80% efficiency of lens system. In this situation, the dimension of the LED-based OWPT system increases to 23 cm × 20 cm × 20 cm, and its portability will be almost difficult to maintain with such dimension. Conclusively, the size of 13 cm × 12 cm × 12 cm is considered to be the minimum size of an LED-based OWPT system which can achieve a small irradiation spot and high efficiency of the lens system.

3.5.2 Summary of the large-size LED-based OWPT system for long-distance range

In this section, the characteristics of the large-size LED-based OWPT system for long transmission distance is analyzed. Due to the target transmission distance is relatively long, the exit pupil of such LED-based OWPT system needs to enlarge in order to ensure a proper size of irradiation spot. Therefore, the dimension of the LED-based OWPT system for long transmission distance is relatively large. In the section 3.5.1, the characteristics of the irradiation size based on the transmission distance from 100 mm to 3000 mm and different value of d parameter is figured out by simulation. In order to achieve small irradiation spot at long distance, the value of d parameter should be large enough. From the simulation data, the value of d parameter must at least larger than 70 mm in order to guarantee the minimum performance of the LED-based OWPT system for long transmission distance. Besides, the ideal value of d parameter should be better larger than 128 mm for achieving sufficiently small irradiation spot at long transmission distance. Then, the efficiency of the lens system based on different value of d parameter is analyzed in Fig. 3.34. Based on the requirement that the value of d parameter should be larger than 128 mm, the proper size of the image lens aperture is figured out. For ensuring at least 80% efficiency of the lens system, the aperture size of the image lens must be larger than 120 mm, which

makes the dimension of the OWPT system to be 13 cm × 12 cm × 12 cm. With such configuration, the irradiation spot with around 5 cm side length can be obtained at 3 m transmission distance, the portability of the LED-based OWPT system can still be remained. Such dimension is the minimum requirement of the LED-based OWPT system for long transmission distance if the small irradiation spot and high efficiency of the lens system is wished. The actual parameters and dimension of the system is based on the requirement of the application. If longer transmission distance or smaller irradiation spot is required in the actual application, the dimension of the LED-based OWPT system needs to enlarge constantly. Therefore, the transmission distance of 3 m is considered as a threshold value of the portable LED-based OWPT system. When the transmission distance is greater than 3 m, at least one of the efficiency of the system, the size of the light spot and the portability of the LED-based OWPT system will inevitably be sacrificed.

Reference

[1] Keating. M, "*Lateral magnification–angular magnification relationship for a simple magnifier,*" American Journal of Physics. 48 (**3**), 214, 1980.

[2] Y. Ishida, T. Miyamoto, "*Study of 100 mW class optical wireless power transmission for compact IoT,*" the 78th JSAP, 2017.

[3] Yevick. D, Friese. T, Schmidt. F, "*A Comparison of Transparent Boundary Conditions for the Fresnel Equation,*" Journal of Computational Physics. 168 (**2**), 433, 2001.

[4] Craig Hoffman, Ronald Driggers, "*Encyclopedia of Optical and Photonic Engineering (2nd ed.),*" CRC Press, Chap. 72, p.1, 2015.

[5] Hecht. J, "*Fiber-optic measurements,*" Optics News. 13 (**4**),7, 1987.

[6] Advanced Technology Institute, LLC, single-junction GaAs solar cell, datasheet.

Chapter 4. Characteristics of single-LED OWPT system

The basic configuration and the detailed value of the parameters of the LED-based OWPT system is analyzed in chapter 3 based on the mathematical model and simulation results. By modeling the LED-based OWPT system and analyzing data such as size of irradiation spot, radiant intensity, intensity distribution and efficiency of the system, the predicted performance of the LED-based OWPT system is obtained. In Chapter 4, the LED-based OWPT system will be established in the laboratory, and the actual performance of the LED-based OWPT system will be verified through experiment data. By comparing the simulation data and experimental data, the real characteristics and performance of the LED-based OWPT system in practical applications are analyzed, and the reasons and solutions for the deviation between the experimental results and the simulation results will be discussed.

4.1 Experiment of portable LED-based OWPT system

4.1.1 Experiment setup of portable LED-based OWPT system

The experimental setup in this section corresponds to the conventional portable LED-based OWPT system with a transmission distance of 1 m that discussed in section 3.3. According to the configuration shows in section 3.3, the experimental setup of the proposed portable LED-based OWPT system was shown in Fig.4.1. The experiment setup is exactly the same as the configuration built in simulation model. A High-intensity near-infrared (NIR) LED (Osram SFH-4703AS, 810 nm, 1040 mW@1 A, 3.55 V, ± 40°, 0.75 mm × 0.75 mm chip) was applied as the light source of the OWPT system and a small-size heat sink was attached behind the NIR LED board with thermally conductive silicon grease for heat dissipation. An aspheric condenser lens (SIGMAKOKI, AGL-32.5-23.5P)[1] with 32.5 mm aperture and 23.5 mm focal length was used as condenser lens to restrain the divergence angle of the LED light beam, then a Fresnel lens ((NTKJ Co., Ltd., CF100)[2] with 100 mm aperture and 100 mm focal length was applied as the

image lens installed 84 mm behind the aspheric condenser lens to focus the light beam at the 1 m transmission distance. A single-junction GaAs solar cell (Advanced Technology Institute, LLC) was installed 1 m away from the transmitting side of the OWPT system as the receiver. The GaAs solar cell has an originally rectangular shape with 5 cm × 1.7 cm size, and the surface of the GaAs solar cell was covered with the opaque material to form a square receiver with 1.7 cm × 1.7 cm size.

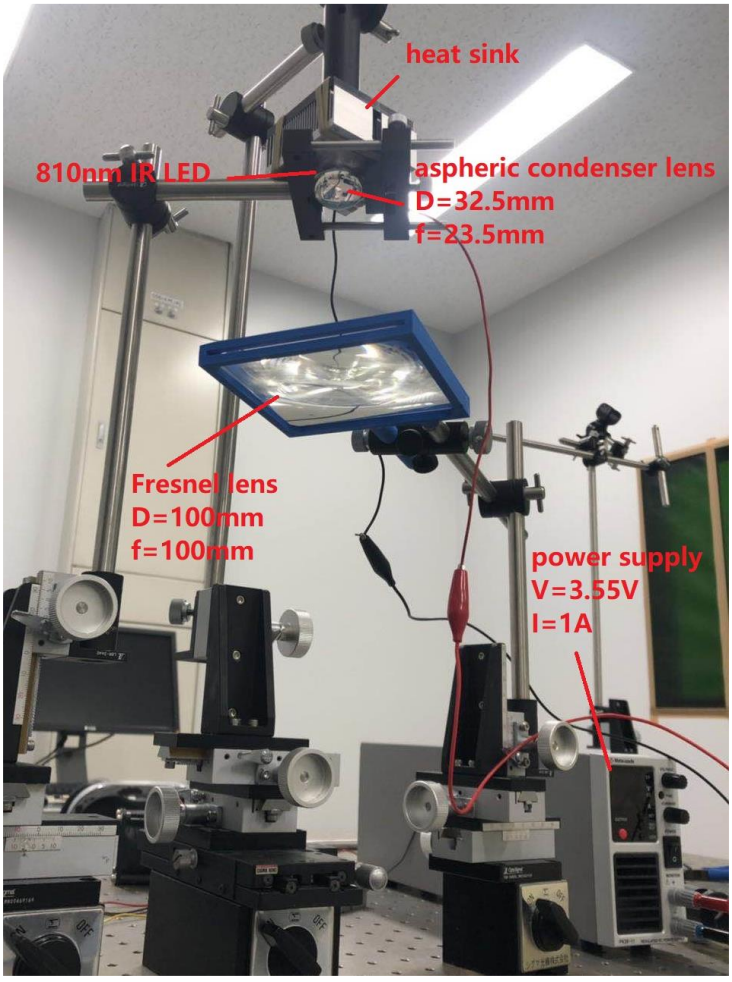

Fig. 4.1 The experimental setup of the portable LED-based OWPT system

4.1.2 Basic experiment of portable LED-based OWPT system

The IR image of the irradiation spot at target distance by the IR viewer is shown in Fig. 4.2.

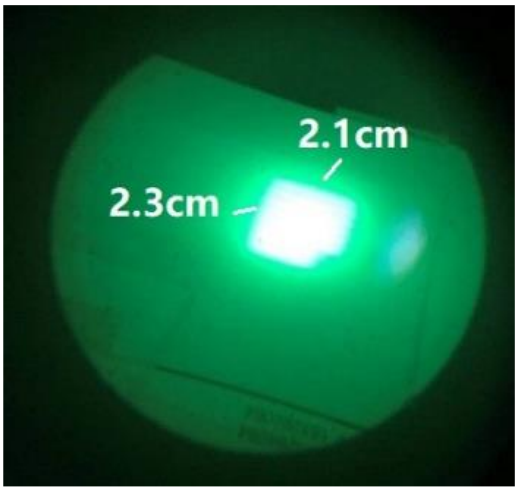

Fig. 4.2 The IR image of the irradiation spot at target distance

From the IR viewer, the size of the irradiation spot at the 1 m transmission distance is 2.1 cm × 2.3 cm, which is exactly the same as the simulation result. In the experiment, the intensity after lenses was measured, respectively, in order to show the efficiency of each optical component. The experimental results are shown in Table 4.1.

Table 4.1 Efficiency of different components in optical system (experiment)

Components	Intensity after (mW)	Efficiency
NIR LED	1020	98.1%
AC lens	1005	98.5%
Fresnel lens	792	78.6%
Target distance (1000 mm)	785	99.1%
On solar cell (1.7×1.7 cm^2)	537	68.4%
Total efficiency		51.6%

Compared with the simulation results shown in section 3.3, the efficiency of aspheric condenser lens is roughly the same in the experiment, while efficiency of Fresnel lens deteriorates a little. This difference can be explained as three

factors. The first reason is the divergence angle of NIR LED is larger than the ideal condition that shown in simulation model. The simulation model shows the relatively regular performance of the LED light source, while the actual divergence of the LED will be more dispersed and irregulating due to the error caused during the manufacturing. he second reason is the different effective aperture compared with the one that used in calculation and simulation in the research. The effective aperture used in calculation and simulation is obtained by the following equation when diameter is beyond 50 mm:

$$\boldsymbol{D_{eff} = D_m - 2} \tag{4.1}$$

It is possible that the difference is caused by smaller actual effective aperture of the Fresnel lens used in experiment. In addition, as the third reason, the company that manufactured the Fresnel lens does not provide an official simulation model, thereby the simulation model of the Fresnel lens is built individually according to the parameters shown in the datasheet in this thesis, and it might have difference from actual component characteristic.

Comparing with the simulation results, in experimental situation, less intensity was lost due to the size mismatching between irradiation size and solar cell size. The total intensity emitted from the LED light source is 1020 mW, which is slightly lower than the output shown in datasheet, and totally 785 mW intensity is transmitted with 77.0% lens system efficiency and focused on a 2.1 cm × 2.3 cm area at 1 m distance, while 537 mW intensity received by solar cell with 68.4% collecting efficiency, which is slightly different from simulation result. This difference is considered as uneven intensity distribution on actual irradiance. Compared with the simulation result shown in Fig. 3.15, the actual distribution might not be such even, and more intensity is focused at the center part.

The total efficiency of optical system was 77.0% without considering the intensity loss on the surface of the solar cell, and the optical energy transmission efficiency is 51.6% if consider the intensity loss on solar cell. The final electrical output from the GaAs solar cell was 223.9 mW with 41.7% photovoltaic conversion efficiency of the GaAs solar cell. The overall optical-electrical efficiency of the system was 21.9%, and considering the power consumption of the NIR LED was 3.55W under

operation condition of 3.55V and 1A, the overall efficiency of the entire LED-based OWPT system was calculated as 6.3%.

The tolerant distance of the portable LED-based OWPT system is also confirmed by the experiment data. The GaAs solar cell with 1.7 cm × 1.7 cm size was installed every 100 mm from the distance of 600 mm to 1300 mm to measure the received intensity, output from solar cell and the photovoltaic efficiency of the solar cell. The Fig. 4.3 shows such data from the results of simulation and experiment. Compared with the simulation, the intensity received by the solar cell is almost the same as well as the output power in the experiment. If consider 100 mW as the required minimum output of the portable LED-based OWPT system that can effectively supply power, the transmission range from 700 mm to 1200 mm can be seen as the tolerant distance. In such range, above 100 mW power can be provided to the IoT terminals.

Besides, the photovoltaic conversion efficiency of the GaAs solar cell differs at different transmission distance due to the changing of the radiant intensity, and the peak efficiency of 41.7% was measured at the 1 m transmission distance because smallest irradiation spot size and highest radiant intensity can be obtained at target transmission distance. Obviously, higher photovoltaic conversion efficiency of the solar cell can be achieved in the nearby distance before the target transmission distance than behind, and the reason is stated in the section 3.3.2. The received intensity in minus-region always more than plus-region with same relative distance of the portable LED-based OWPT system due to the irradiation of the light beam is easier to image in minus-region. Thus, higher photovoltaic conversion efficiency of the solar cell is available in the nearby distance before the target transmission distance due to higher radiant intensity.

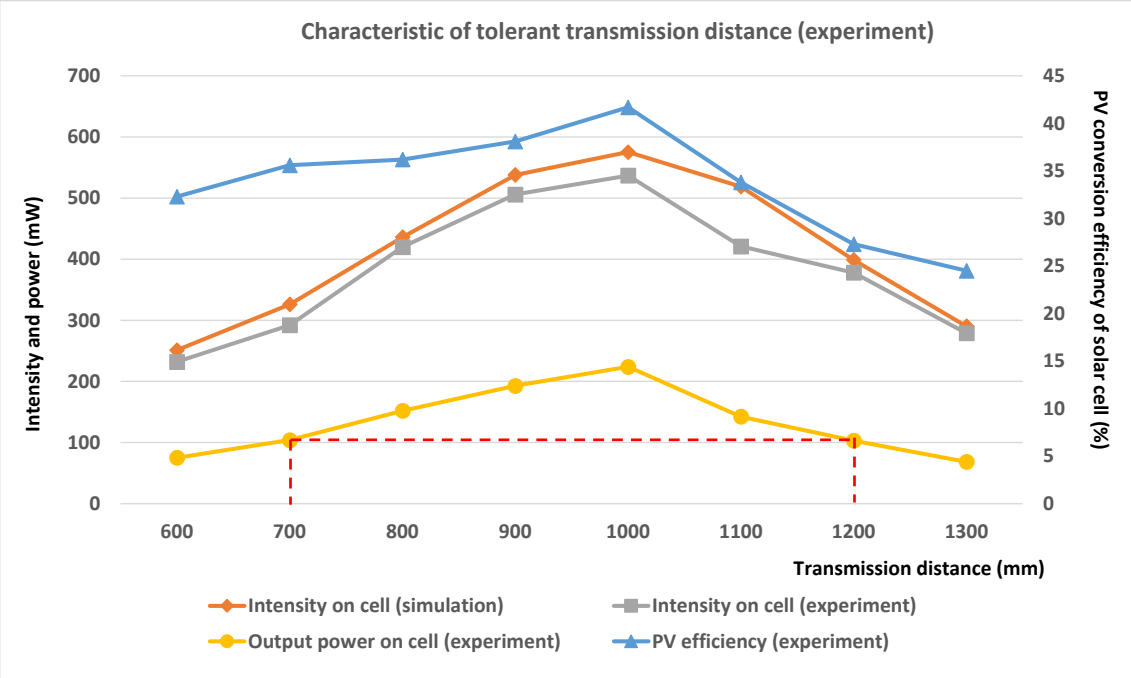

Fig. 4.3 The characteristics of tolerant transmission distance by experiment

4.1.3 Modularization of the portable LED-based OWPT system

The LED-based OWPT system is aimed to be used as a portable device, thus the modularization of the proposed LED-based OWPT system and the analysis on the corresponding performance is necessary. To clarify the difference and issues in comparison from experiment prototype configuration of the LED-based OWPT system, modularized system was prepared and characterized. As shown in Fig. 4.4, square-box LED-based OWPT system module for 1 m transmission distance was designed and made. The module consists of an NIR LED with heat sink, condenser lens, and Fresnel lens, and the parameters of the optical components are exactly the same with the configuration shown section 4.1.1. In addition, a lens frame (blue component in Fig. 4.4) is prepared for the Fresnel lens in order to easily installing and correcting lens' spatial coordinates deviation. The final size of the OWPT system module is 116 mm × 116 mm × 132 mm after considering the thickness of heat sink, lens frame and case, and the weight of the entire modularized portable LED-based OWPT system was measured as 620 g. Such dimension can easily achieve good portability of the LED-based OWPT system. The modularization was achieved by 3D printer and the case draw plan was made

by AutoCAD (Autodesk, Inc.).

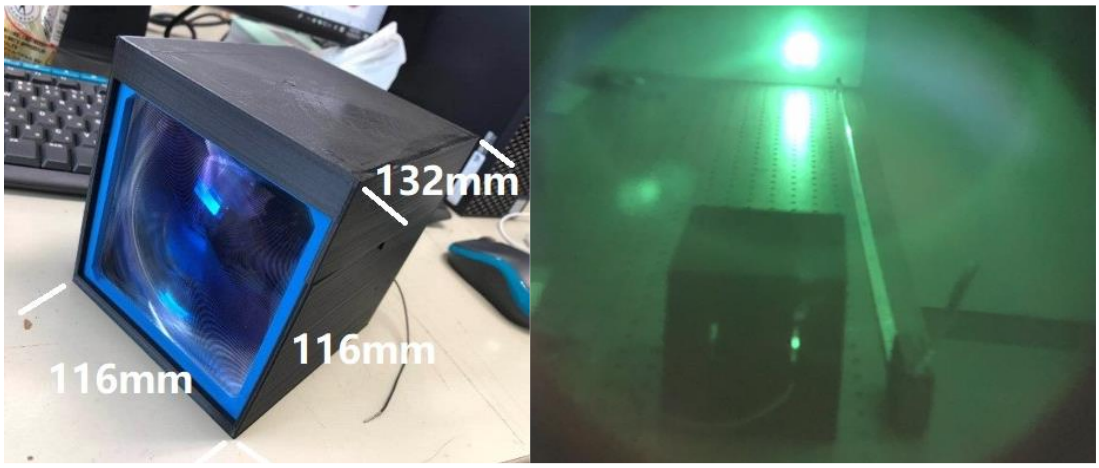

Fig. 4.4 The modularized LED-based OWPT system

The power transmission experiment with a fabricated module was held. Since the configuration of the modularized LED-OWPT system is exactly the same with the non-modularized system, the performance of both systems such as irradiation spot size and efficiency of the lens system is similar, while the final output of the modularized LED-based OWPT system is 10% - 20% lower than the non-modularized condition. The causes are considered as following two points. One is problem of heat dissipation of the LED in sealed case, and another is the deviation during module fabrication that causes the inaccurate parameters of the lens system. By manufacture the module with high precision and good heat dissipation, the module of LED-based OWPT system will be easily operated with designed performance.

4.1.4 Thermal analysis of portable LED-based OWPT system

Operating temperature is an important factor which decides the OWPT system performance and possible working environment. As the statement shown in section 2.2.3, the heat resistance feature is another advantage of using LED as the light source of OWPT system comparing with laser. The characteristics of the permissible forward current based on different ambient temperature of the high-intensity NIR LED (Osram SFH-4703AS) applied in the experiment is shown in

Fig.4.5. The data is obtained from the datasheet of the LED product from the official website.

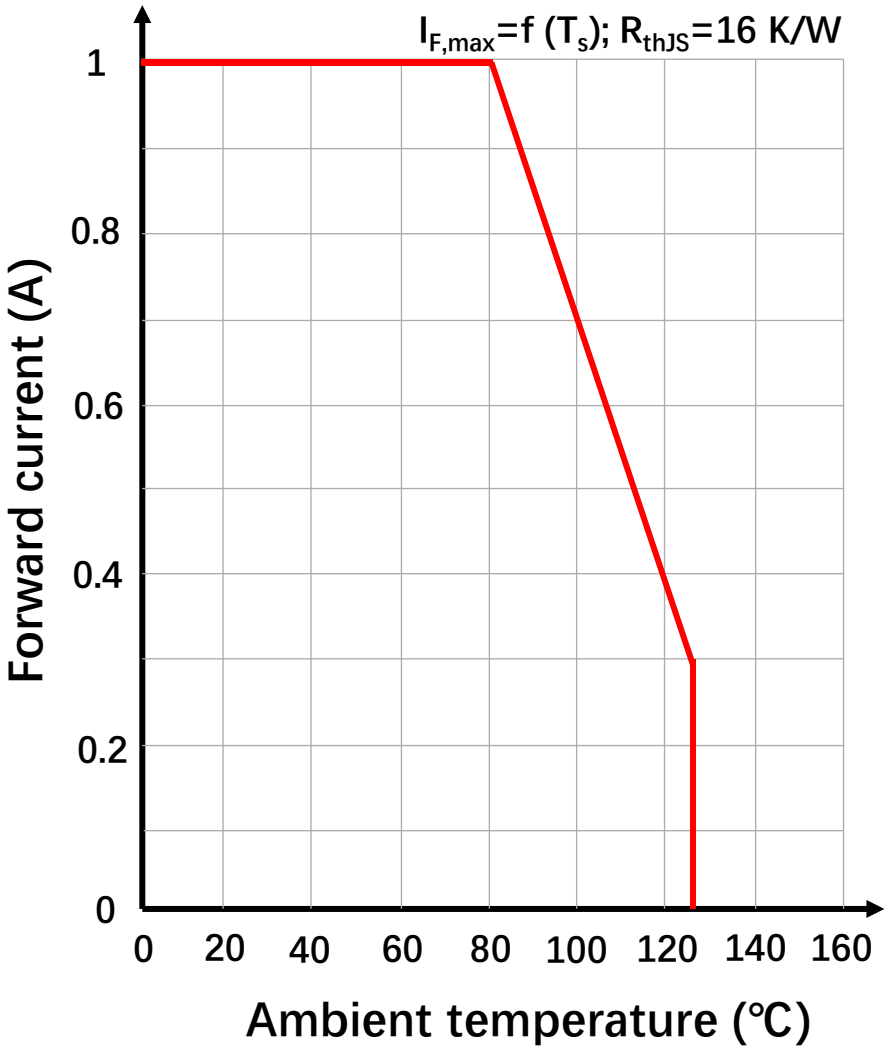

Fig. 4.5 The permissible forward current of NIR LED (Osram SFH-4703AS)

From the datasheet of the LED product, the proper operating temperature range is from -40°C to 125°C. Based on the permissible operating temperature of this range, the thermal analysis of the portable LED-based OWPT system was held in the experiment. The temperature at both transmitting side and receiving side was measured. The thermal analysis experiment setup is shown in the Fig. 4.6, and the thermal image at transmitting side and receiving side is shown in Fig. 4.7.

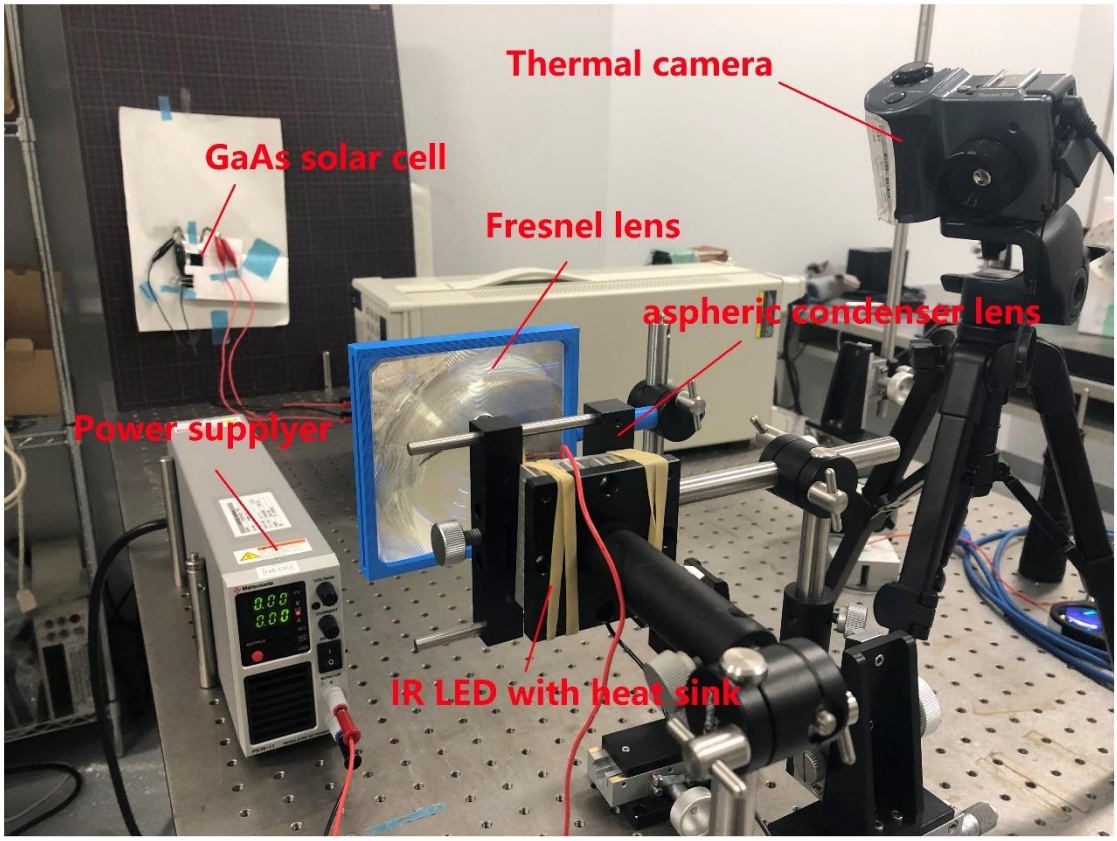

Fig. 4.6 The experiment setup of thermal analysis of LED-based OWPT system

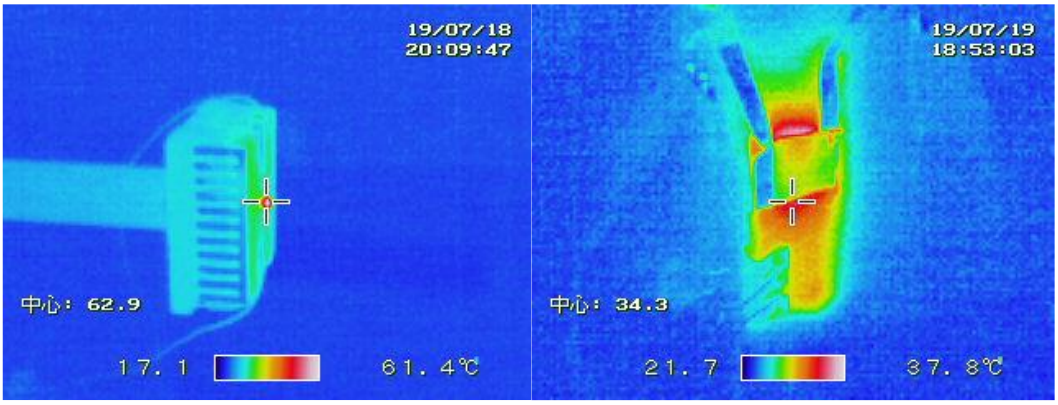

Fig. 4.7 Ambient temperature of LED chip and solar cell during operating

From the Fig. 4.7 of the light source side, the heat is concentrated in the center of the transmitting side, and such temperature can be approximately seen as junction temperature of the LED. While at the solar cell side, the heat is distributed

uniformly on the surface of the solar cell. With the simple heat dissipation measures as small heat sink with thermal grease, the temperature of LED chip can be controlled around 60°C during operation, which is much lower than the maximum junction temperature (145°C). The ambient temperature was measured around 27°C in such condition, which is in the range of permissible ambient temperature. And for the solar cell side, the temperature is around 34°C under the irradiation of the high-intensity beam and will not change extremely with prolonged exposure time. At this condition, the thermal environment at both sides is in the range of available operating temperature. For the IR LED that applied here, it can provide steady output in the range of 0°C to 78°C, as shown in Fig. 4.5. While for the single-junction GaAs solar cell (Advanced Technology Institute, LLC), without considering passivation on layer of the surface, the output will have -0.095% deterioration with 1°C ambient temperature change from the information shown in datasheet. According to experiment data, the temperature of solar cell surface will have around 10°C difference after dozens of minuets operating. Thus, the deterioration on solar cell output should only have around 1% decline.

According to the data obtained from several times experiments, the relation between temperature on LED and solar cell and the output of both prototype LED-based OWPT system and modularized LED-based OWPT system is shown in Fig. 4.8.

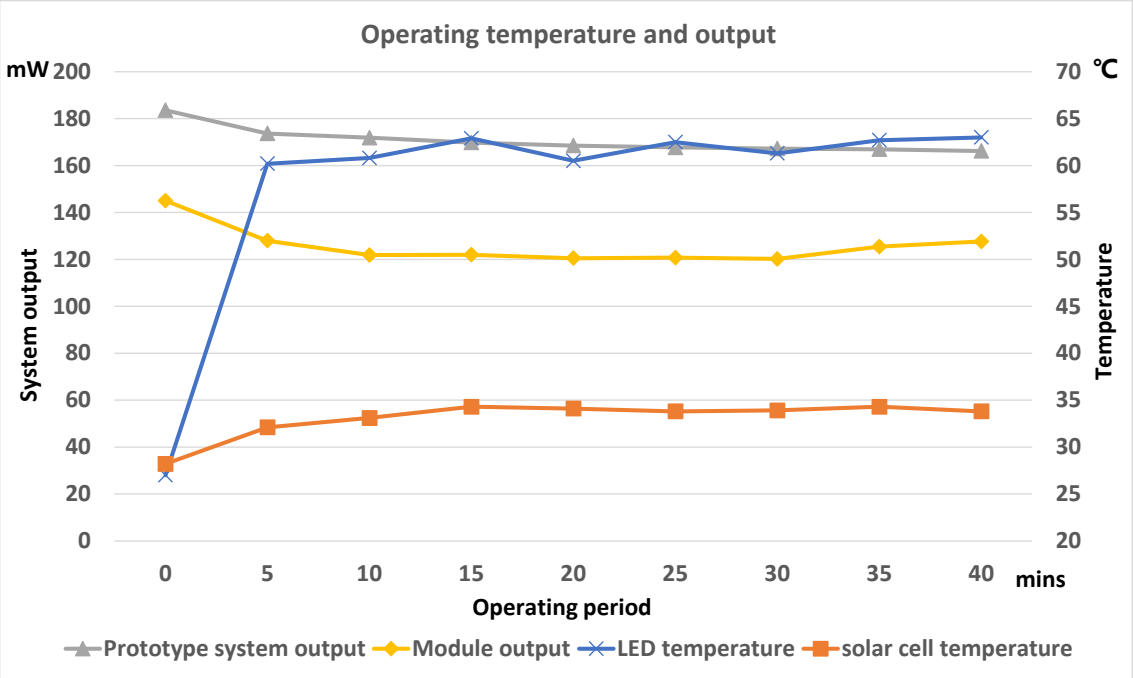

Fig. 4.8 Characteristic of the system output and operating temperature based on continuous operation period

As the Fig. 4.8 shows, within 5 mins' operation period, the temperature of both IR LED and sola cell will have an obvious climbing and then trend to be steady. Correspondingly, the output of the LED-based OWPT system will decrease. In the first 5 mins operation, the temperature on LED side climbed from room temperature (27°C) to 60.2°C, while the temperature on the surface of the solar cell increased from 27°C to 32.1°C. The output of the prototype LED-based OWPT system decreased from 184 mW to 174 mW after the first 5 mins working, which caused 5.4% deterioration on overall output of the system. The output of the prototype LED-based OWPT system decreased to 166 mW after 40 mins continually operation, which means 9.8% output deterioration in total. Such deterioration is due to the declining efficiency on both LED and solar cell that caused by increasing temperature. As for the modularized LED-based OWPT system, the output power is decreased from 145 mW to 128 mW after 40 mins operation, which has 11.7% output deterioration, and such output deterioration is slightly higher comparing with prototype LED-based OWPT system. The reason

is considered as poor heat dissipation due to the sealed enclosure of the modularization. On the receiving side, the solar cell temperature increase tendency is relatively steady, which just climbed from 27°C to 32°C at the first 5 mins, and to 34°C after 40 mins irradiation. Therefore, although the long-term operation of the LED-based OWPT system leads to an increase in temperature, the degradation of solar cell efficiency has caused a decrease in system output to a certain extent, considering the temperature increase on transmitting side is much severer, the main reason of the system output deterioration is believed to be the efficiency decrease on LED.

Conclusively, although the output deterioration of the LED-based OWPT system caused by increasing temperature is unavoidable, such deterioration is below 10% after long-term operation, which is not such severe. Moreover, considering the operation time of LED-based OWPT system is in seconds or several minutes when charging most of the IoT terminals, performance deterioration will be much lower in short-term operation, which is around 5% generally. In spite of the experiment setup might be slightly different from the practical application condition, and thermal condition of practical application should be slightly different, the performance deterioration caused by thermal reason is believed only around 5% in general. Thus, the simple heat sink with thermal grease heat dissipation configuration is considered to be enough for the LED-based OWPT system, which also can save space and weight for the portability of the system.

4.1.5 Summary of the experiment of portable LED-based OWPT system

In the section 4.1, the experiment of the portable LED-based OWPT system was held. The experiment setup is shown in the section 4.1.1. The components adopted in the experiment have exactly the same parameters. A high-intensity NIR LED was used as the light source of the OWPT system, and a small size heat sink was attached behind the LED for heat dissipation. An aspheric condenser lens and a Fresnel lens were applied as the condenser lens and image lens in the optical system, respectively. Finally, a single-junction GaAs solar cell was installed 1 m away from the transmitting side as the optical energy receiver. Then, the results and analysis of the basic experiment of portable LED-based

OWPT system were shown in the section 4.1.2. As a result, the irradiation spot with 2.1 cm × 2.3 cm size was observed at the 1 m transmission distance. The lens system efficiency was measured as 77%, and the efficiency of each optical component and the reasons of the intensity loss on was analyzed. The output from the solar cell was measured as 223.9 mW with 41.7% photovoltaic conversion efficiency of the solar cell. The overall efficiency of the portable LED-based OWPT system was 6.3%. Besides, the tolerant distance of the portable LED-based OWPT system was confirmed by experiment. By comparing the experiment and simulation results of the power transmission, the transmission range from 700 mm to 1200 mm was confirmed as tolerant distance, which is agreed with the simulation results. In such range, above 100 mW power can be provided to the IoT terminals. In the section 4.1.3, the modularized portable LED-based OWPT system was shown. The module was designed by AutoCAD and fabricated by 3D printer. The entire size of the modularized portable LED-based OWPT system is 116 mm × 116 mm × 132 mm, which maintains good portability. The output of the such modularized LED-based OWPT system had a small degree of deterioration than the non-modularized system, and the possible reasons were also clarified. In the section 4.1.4, the thermal analysis of the portable LED-based OWPT system was discussed. The temperature of both LED side and solar cell size was measured by a thermal camera, and the characteristics of the portable LED-based OWPT system output fluctuation with the increasing operation term and device temperature was analyzed. As a result, the temperature climbing on both LED side and solar cell side are concentrated in the first 5 mins operation, and the deterioration of the system performance caused by such temperature climbing was small. Even after 40 minutes of continuous operation, the decline of the system output is only around 10%. Besides, the thermal analysis of the modularized LED-based OWPT system was also processed, and the output deterioration was slightly higher than the non-modularized system, and the reason is considered as poor heat dissipation due to the sealed enclosure of the modularization. In general, the factor of temperature on both transmitting and receiving side will not greatly impact the performance of the LED-based OWPT system even after long-term operation.

Therefore, simple heat sink with thermal grease is proved to be enough for heat dissipation of the LED-based OWPT system.

4.2 Experiment of mini-type LED-based OWPT system for short-distance range

4.2.1 Experiment setup and data analysis of mini-type LED-based OWPT system for short-distance range

In the section 3.4, the basic configuration of the mini-type LED-based OWPT system for short-distance range was discussed. Three kinds of configurations were analyzed and compared, and the configuration with a movable image lens (fixed value of f_2' parameter/variable value of d parameter) was proved to has the most balanced performance and flexible design. Besides, the best parameters of the optical components in such configuration were figured out based on the mathematic model and simulation results. Specifically, the condenser lens with 20 mm focal length and 50 mm aperture and an image lens with 46 mm focal length and 50 mm aperture are the ideal optical elements for the lens system of the mini-type LED-based OWPT system, and the distance between the two lenses is variable. Whereas, due to the lack of lenses with suitable parameters in the experiment, the lenses with similar parameters were applied. The condenser lens applied in the experiment has 30 mm focal length and 15 mm aperture, and the image lens has 50 mm focal length and 50 mm diameter. All the optical components are AR coated for reducing the intensity loss caused by reflection. The experiment setup and the IR image of the irradiation spot is shown in Fig. 4.9. It can be seen from the Fig. 4.9 that the mini-type LED-based OWPT system has very compact dimension, and the size of the system is smaller than 5 cm × 5 cm × 5 cm in most cases, and such small size provide good portability to the system.

For better comparing the results, the simulation model with same parameters of the optical system was established, and the simulation and experiment data of the mini-type LED-based OWPT system is shown in the Fig. 4.10. The output data from the simulation was calculated based on the received intensity at target

distance and assumed 40% photovoltaic conversion efficiency of the solar cell. In the experiment, the focused light beam was achieved by varying the position of the image lens when transmission distance changes.

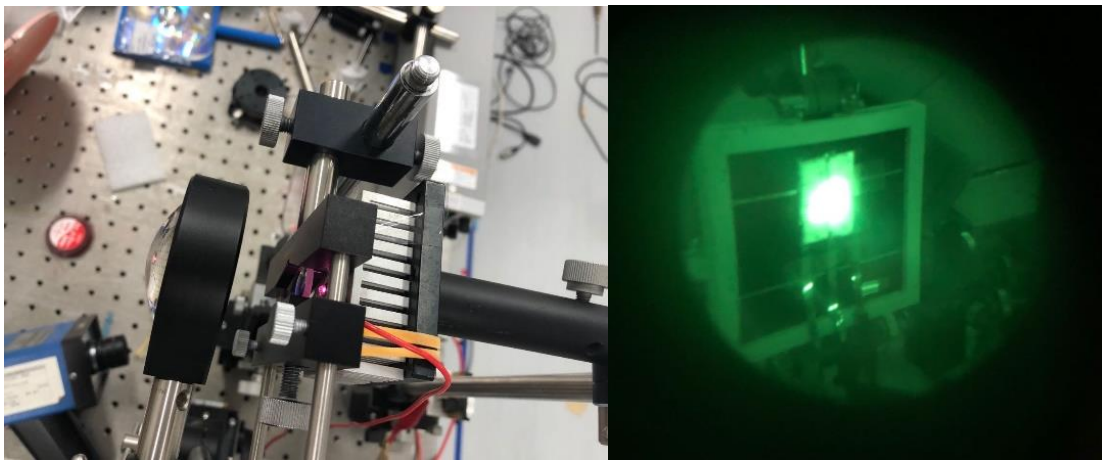

Fig. 4.9 The experiment setup and irradiation IR image of mini-type LED-based OWPT system

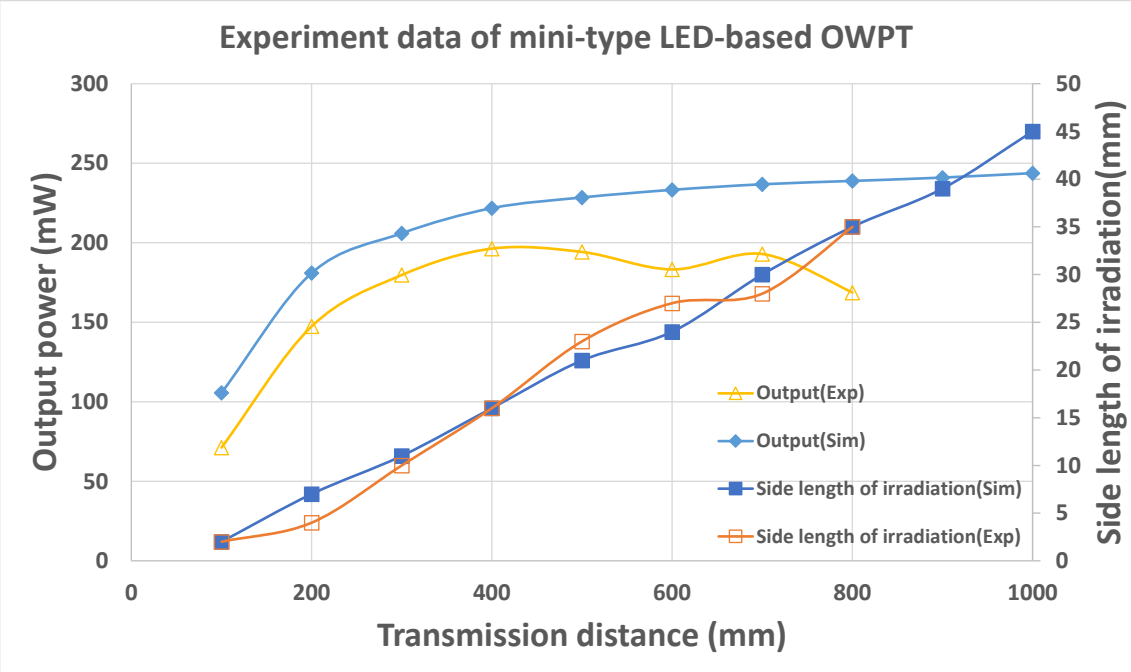

Fig. 4.10 Comparison of simulation and experiment data of mini-type LED-based OWPT system

From the data shown in the Fig. 4.10, the side length of the irradiation measured in simulation and experiment is almost the same, and it is approximately increasing linearly with the transmission distance extending. The irradiation spot with smaller than 3 cm side length can be achieved in the transmission range of 100 mm to 780 mm, which covers majority region in 1 m range. The largest irradiation spot occurred at 1 m distance, which has an irradiation spot with 4.4 cm side length. As for the output of the system, the results obtained from experiment is slightly lower than simulation. Besides, in order to focus the light beam at extremely close position, the image lens should be moved to very far position and thus caused large part of intensity lost. While in the range that transmission distance larger than 200 mm, the intensity loss becomes small and effective power transmission is possible. Therefore, the effective optical power transmission is believed to be available of the mini-type LED-based OWPT system with such configuration in the range of 200 mm to 1000 mm. The peak output power can be achieved at 400 mm position then slightly declines with the transmission distance extending in the experiment, the tendency is a little bit different from the simulation results. The reason can be explained as follow. With the transmission distance increases, the efficiency of the lens system is enhanced due to the image lens is more and more close to the condenser lens and thus decreased the intensity loss. On the other hand, the size of irradiation spot will enlarge when transmission distance increases, which causes lower radiant intensity on the surface of the solar cell as well as the photovoltaic conversion efficiency. Therefore, the peak output should be achieved at the middle position in the range of 1 m transmission distance, where high efficiency of both lens system and solar cell is available. In the simulation, however, the photovoltaic conversion efficiency of the solar cell is assumed to be 40% no matter the transmission distance, thus the highest output will be obtained at the end of the transmission distance range due to efficiency of the lens system is increased with the transmission distance.

Conclusively, the configuration and performance of mini-type LED-based OWPT system is confirmed by comparing the results of simulation and experiment. The

system will achieve peak output power at the middle position in the transmission range, and the effective power transmission can be realized in the range of 200 mm to 1000 mm with small size irradiation spot. Besides, due to the optical elements with optimal parameters were not used in the experiment, the better performance of the mini-type LED-based OWPT system is expectable if optima lenses are applied.

4.2.2 Summary of the experiment of mini-type LED-based OWPT system for short-distance range

Based on the configuration and parameters that shown in section 3.4, the experiment setup of the mini-type LED-based OWPT system was prepared and shown in the section 4.2.1. The optical system of the mini-type LED-based OWPT system adopts the double-lens configuration, and the aperture of both condenser lens and image lens is sufficiently small. The position of the image lens is movable, which leads out a zoom system and allows the target transmission distance to be variable. The dimension of the system is smaller than 5 cm × 5 cm × 5 cm in most cases, thus it is easy and convenient to be carried. Based on the experiment results, the effective power transmission range is 200 mm to 1000 mm, and the irradiation spot with smaller than 3 cm side length can be obtain from 100 mm to 780 mm. The highest output power of the mini-type LED-based OWPT system can be achieve at 400 mm distance, which is around 200 mW. The tendency of the output data in experiment is slightly different from simulation, and the result is concluded as the variable photovoltaic conversion efficiency of the solar cell according to the transmission distance. Through analysis, it is concluded that the peak output of the mini-type LED-based OWPT system with such zoom lens system always appears in the middle of the transmission range.

4.3 Experiment of Large-size LED-based OWPT system for long transmission distance

The basic configuration and principles of the large-side LED-based OWPT system from long-distance range was discussed in the section 3.5, and the

performance and characteristics of such system will be confirmed by the experiment in this section. Since the configuration and components of the large-size LED-based OWPT system are exactly the same with the portable LED-based OWPT system for 1 m transmission distance that shown in the section 3.3, except for the parameters of the Fresnel lens and transmission distance, the components in the experiment and the experiment setup are almost the same.

4.3.1 Experiment setup and data analysis of large-size LED-based OWPT system for long-distance range

The experiment setup of the large-size LED-based OWPT system is shown in Fig. 4.11. Same as the experiment of portable LED-based OWPT system, a High-intensity near-infrared (NIR) LED (Osram SFH-4703AS, 810 nm, 1040 mW@1 A, 3.55 V, ± 40°, 0.75 mm × 0.75 mm chip) was applied as the light source, and a single-junction GaAs solar cell (Advanced Technology Institute, LLC) with 1.7×1.7 cm^2 size was adopted as the receiver that installed from 1 m to 3 m away from the transmitting side. An aspheric condenser lens (SIGMAKOKI, AGL-32.5-23.5P) with 32.5 mm aperture and 23.5 mm focal length was used as condenser lens. As for the image lens, totally 11 kinds of Fresnel lenses with different parameters were applied in the experiment, separately, for confirming the characteristics of the large-size LED-based OWPT system for long-distance range. The AR-coating were applied on all the optical components used in the experiment.

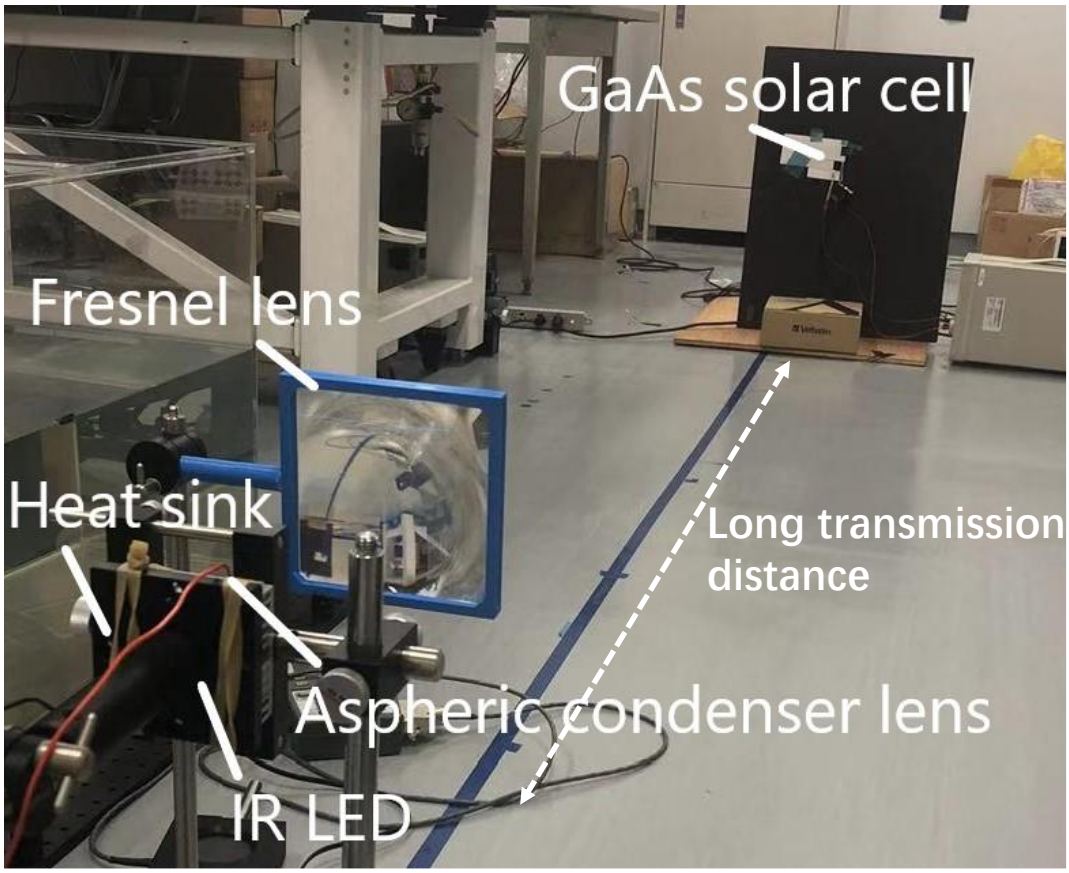

Fig. 4.11 Experimental setup of large-size LED-based OWPT system for long-distance range

Part of the experiment results of the large-size LED-based OWPT system is shown in the Table 4.2 for better showing the full information of performance and revealing the relation between multiple parameters. The value of the focal length and aperture size is the parameters of the different Fresnel lenses that used in the experiment.

Table 4.2 Experiment data of large-size LED-based OWPT system

Focal length (mm)	60	90	110	200	200	200
Aperture (mm)	60	60	60	60	100	210
Size (L×H×W) (mm)	55× 60×60	93× 60×60	115× 60×60	236× 100×100	236× 210×210	236× 210×210

Efficiency		62.50%	52.30%	31.50%	9.40%	22.50%	61.90%
1 m	Irradiation size (cm)	4.5×4.8	2.6×2.8	1.8×2.3	1.5×1.7	1.5×1.7	1.5×1.7
	Output (mW)	78.4	110.8	91.6	37.8	98.4	260
2 m	Irradiation size (cm)	9×9.4	5×5.4	4.5×4.8	2.3×2.6	2.3×2.6	2.3×2.6
	Output (mW)	15.8	32.1	26.7	23.5	65.1	200.5
3 m	Irradiation size (cm)	13.7×14	8×8.4	6.5×7.2	3.6×3.8	3.6×3.8	3.6×3.8
	Output (mW)	6.7	13.6	11.7	12.7	32.5	107.5

As the data shown in the Table 4.2, the system dimension, efficiency of the lens system, the irradiation spot size and output corresponding to different transmission distances is clarified based on the Fresnel lenses with different value of focal length and aperture size. The value of system size shown in the Table 4.2 refers the conditions of 3 m transmission distance, which is the largest dimension among the transmission distance from 1 m to 3 m. The first four columns in the Table 4.2 shows the Fresnel lenses with different focal length but same aperture size. As the conclusion shown in section 3.2, the focal length of the image lens is based on the d value (distance between the condenser lens and image lens) and the transmission distance. Once the focal length of the image lens is fixed, the d value needs to vary in order to focus the light beam at different transmission distance. Therefore, as the data shown in Table 4.2, the d value as well as the dimension of the system increased when the focal length of the Fresnel lens enlarged. For the Fresnel lens with 200 mm focal length, small irradiation spot with 3.6 cm × 3.8 cm size can be achieved even at 3 m distance,

and the value of d parameter needs to increase to 236 mm in order to accurately focus. However, due to the aperture size is only 60 mm, large part of intensity lost on the Fresnel lens and cause low efficiency of the lens system and undesirable output. In fact, the lens system can only have 9.4% efficiency with such configuration, and the output is extremely low. Thus, the aperture size of the Fresnel lens must increase to ensure the high efficiency of the lens system. As a result, for the LED-based OWPT system, when the transmission distance increases, if it is desired to keep the irradiation spot size small, the value of d parameter needs to be increased to ensure the size of the exit pupil of the lens system. On the other hand, when the value of d parameter is large, in order to ensure the efficiency of the optical system, the aperture of the image lens must be increased accordingly. Therefore, in the application scenario of long transmission distance, the size of the LED-based OWPT system will inevitably be larger. From the conclusion shown in the section 3.5, larger than 128 mm of the d parameter and bigger than 120 mm aperture of the image lens is necessary for the LED-based OWPT system for long-distance range. Therefore, the system with the Fresnel lenses of 100 mm and 210 mm aperture were also experimented, separately. The experiment results are shown in the last two columns in the Table 4.2. The value of the d parameter of both configurations is 236 mm, which satisfies the requirement that value of the d parameter must be greater than 128mm. As a result, when the value of the d parameter is 236 mm, and the aperture size of the Fresnel lens is 210 mm, more than 200 mW output power is available from 1 m to 2 m range, and above 100 mW output power can be achieved by the LED-based OWPT system in the entire range of 1 m to 3 m, which meets the requirement effective power transmission of LED-based OWPT system. In this case, the dimension of the system becomes 236 mm × 210 mm × 210 mm, which still retains a certain portability.

The Fig. 4.12 shows the characteristics of output power with different transmission distance based on the experiment results of the total of 11 Fresnel lenses with different focal length and aperture size. In the Fig. 4.12, the f value is the focal length of Fresnel lens, and D is the diameter of Fresnel lens aperture.

At lens system side, the efficiency will improve with aperture increasing, and at solar cell side, due to a part of intensity was irradiated outside of solar cell, and longer d value with larger focal length will cause smaller irradiation size, thus less geometrical loss happened. Besides, with radiant intensity increasing, higher PV conversion efficiency is predictable. From the data shown in Fig. 4.12, the system with the Fresnel lens of 200 mm focal length and 210 mm aperture shows the best performance, while the system with the Fresnel lens of 150 mm focal length and 100 mm aperture also shows relatively good output. This is because such configuration meets the all parameters requirement of the large-size LED-based OWPT system for long-distance range, except for the relatively small aperture size. If larger aperture Fresnel lens is applied, the higher output power is expectable at the distance range beyond 2 m. On the other hand, the dimension of the large-size LED-based OWPT system is almost four times than the LED-based OWPT system for 1 m transmission distance that shown in section 3.3. Although it is still retaining a certain portability, such dimension might be a drawback in some applications scenarios. Thus, increasing solar cell size is another simple but effective method to achieve high power and restrain system dimension at the same time, if it is allowed by the requirement of the applications. For instance, from the data shown in Table. 4.2, If the irradiation spot with maximum 10 cm side length at 3 m transmission distance can be accepted, the Fresnel lens with 90 mm focal length and 100 mm aperture is sufficient to achieve power transmission in long-distance range with high efficiency, and the system dimension will be controlled to be smaller than 100 mm × 100 mm × 100 mm, with high degree of portability.

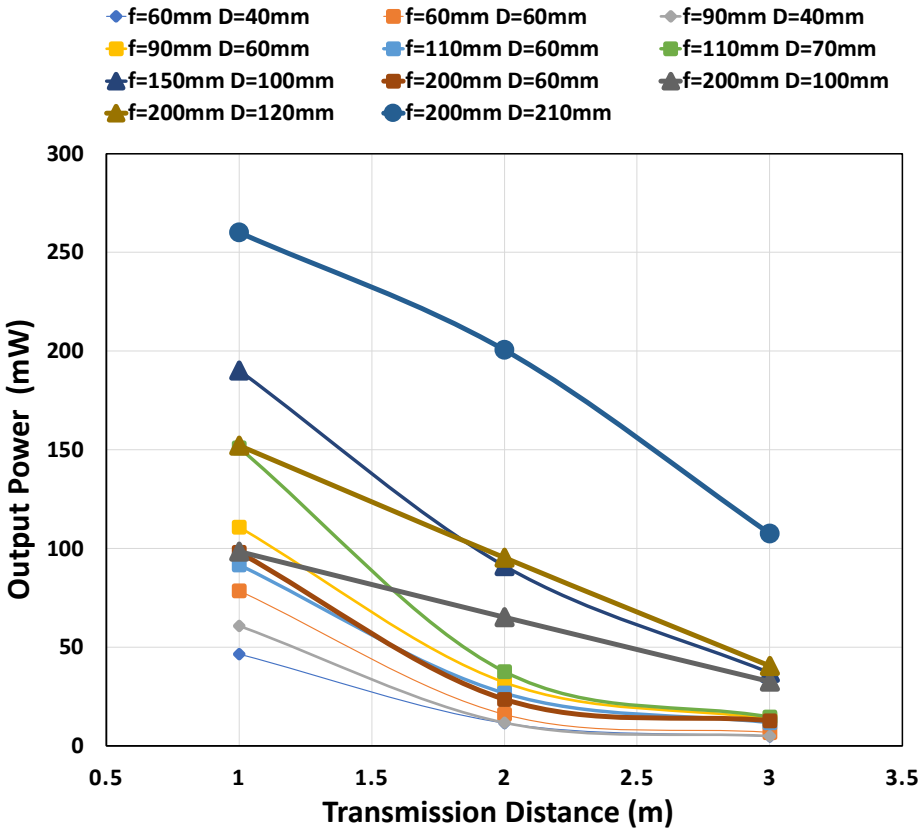

Fig. 4.12 Experimental results of large-size LED-based OWPT system

4.3.2 Summary of the experiment of Large-size LED-based OWPT system for long transmission distance

The experiment of the large-size LED-based OWPT system for the long-distance range was discussed in the section 4.3. In the experiment, the performance of the system in the distance range from 1 m to 3 m was confirmed by applying totally 11 Fresnel lenses with different focal length and aperture size. The ideal parameters of the optical system of the large-size LED OWPT system were confirmed by comparing the obtained experiment results with the simulation results that discussed in the section 3.5. As a result, the focal length of the image lens in the optical system must larger than 128 mm and the aperture size of the image lens should be at least bigger than 120 mm for ensuring the high performance of the LED-based OWPT system for long-distance range. The highest output was achieved by the LED-based OWPT system with a 200 mm focal length and 210 mm aperture size image lens in the experiment. Such

configuration can realize above 200 mW output power from the solar cell in the range from 1 m to 2 m transmission distance, and above 100 mW output power in the range from 2 m to 3 m, which makes the effective power transmission range to be 1 m to 3 m of the LED-based OWPT system. In such case, the dimension of the LED-based OWPT system is 236 mm × 210 mm × 210 mm, which still retains a certain portability.

4.4 Experiment of unideal irradiation conditions of the LED-based OWPT system

The experiments that discussed in the section 4.1, section 4.2 and section 4.3 are all under the ideal irradiation condition, whereas under the practical condition of the application, plenty of undesired conditions might be happened, and thus causes deteriorations on the final performance of the LED-based OWPT system. Researching and figuring out the performance and the characteristics of the portable LED-based OWPT system under such unideal irradiation conditions is a critical topic in this research. By studying the characteristics of the portable LED-based OWPT system under unideal conditions, it is possible to predict the performance of the system in different working conditions of practical applications, and also able to achieve better performance through the optimization of system parameters. At the same time, if it is not possible to eliminate or reduce the degradation of system performance by optimizing system parameters, then it is necessary to consider installing related sub-modules for the system to suppress the degradation of system performance under unideal conditions. As the portable power supplying device for the compact IoT terminals, there are usually two kinds of unideal irradiation conditions that happens normally. The first one is the oblique irradiation. In the all experiments shown in the previous sections in chapter 4 were held under the condition of vertical irradiation, therefore the intensity loss caused by the reflection at the surface of the solar cell was minimum level. However, in the scenarios of practical application, it is difficult to avoid the inclination of incident light. In other word, the intensity loss caused by reflection at the receiving side will be larger in practical applications will be larger comparing

the experiment scenarios. The second unideal irradiation condition is the irradiation with tremor. One of the application scenarios of the portable LED-based OWPT system is that the transmitter of the system is held by the user and supplies power wirelessly to the remote IoT terminals. During this process, the oscillation of the system final output caused by the tremor of the user's hand is inevitable. It can be expected that the characteristics of the final output of the portable LED-based OWPT system in this case will be different from the output under ideal conditions. In summary, studying the characteristics of the portable LED-based OWPT system performance under the unideal conditions and analyzing the difference between the performance of the portable LED-based OWPT system under ideal and unideal conditions is of instructive significance for the application of the OWPT system. Therefore, the experiment of the portable LED-based OWPT system under the unideal irradiation conditions of oblique irradiation and irradiation with tremor will be held and analyzed in the section 4.4.1 and section 4.4.2, respectively.

4.4.1 Experiment of the portable LED-based OWPT system under oblique irradiation

In the section 3.3.3, the analysis of the portable LED-based OWPT system under oblique irradiation was discussed based on the simulation results. By considering the two critical factors under the oblique irradiation, which are different reflection coefficient at the surface of the solar cell and the deformation of the irradiation spot, the characteristics of the received intensity on the solar cell was figured out based on different incident angle of the light beam. As a result, the portable LED-based OWPT system can provide above 50% of the total intensity to the receiving end installed at 1 m distance with smaller than 45° tilt angle of the incident light beam. Under such condition, above 100 mW is expected to be obtained from the solar cell. In the section 4.4.1, the experiment of the portable LED-based OWPT system under oblique irradiation will be discussed and the experiment results will be compared with the simulation results and analyze the characteristics of the portable LED-based OWPT system under oblique irradiation condition.

In the experiment of the oblique irradiation, the applied components of the portable LED-based OWPT system were exactly the same as the experiment setup shown in section 4.1.1. A High-intensity near-infrared (NIR) LED (Osram SFH-4703AS, 810 nm, 1040 mW@1 A, 3.55 V, ± 40°, 0.75 mm × 0.75 mm chip) was applied as the light source with a small-size heat sink attached behind and an aspheric condenser lens (SIGMAKOKI, AGL-32.5-23.5P) and a Fresnel lens ((NTKJ Co., Ltd., CF100) were applied as the condenser lens and image lens, separately. The distance between the two lenses was set as 84 mm, and a single-junction GaAs solar cell (Advanced Technology Institute, LLC) with 1.7 cm × 1.7 cm size was used as the receiver and installed 1 m away from the transmitting side.

In the experiment, the incident angle on the receiving side was increased from 0° to 90° at intervals of 10°. Three experiments were performed for each incident angle, and the average value of the output from the solar cell was taken as the final output of the system at such incident angle. Finally, normalize all the data to better study the characteristics of the portable LED-based OWPT system under oblique irradiation. The Fig. 4.13 shows the experiment results of the portable LED-based OWPT system with the incident angle from 0° to 90°. The y-axis shows the normalized output of the system under the oblique irradiation, and x-axis shows the incident angle. Besides, the simulation results were also sorted out and shown in the Fig. 4.13. Unlike the experiment results, the y-axis of the simulation data is not the output from the solar cell but the received normalized intensity on the surface of the solar cell. Considering the photovoltaic conversion efficiency of the solar cell is based on the radiant intensity on solar cell, the final output and the received intensity of the solar cell are not directly proportional, and the ratio should be a variable. However, considering that the radiant intensity of the solar cell surface does not change much in such case, the final output can be approximately regarded as roughly proportional to the received intensity of the solar cell. Therefore, it can be considered that Fig. 4.13 reflects the characteristics of the portable LED-based OWPT system performance under oblique irradiation condition in the simulation the experimental.

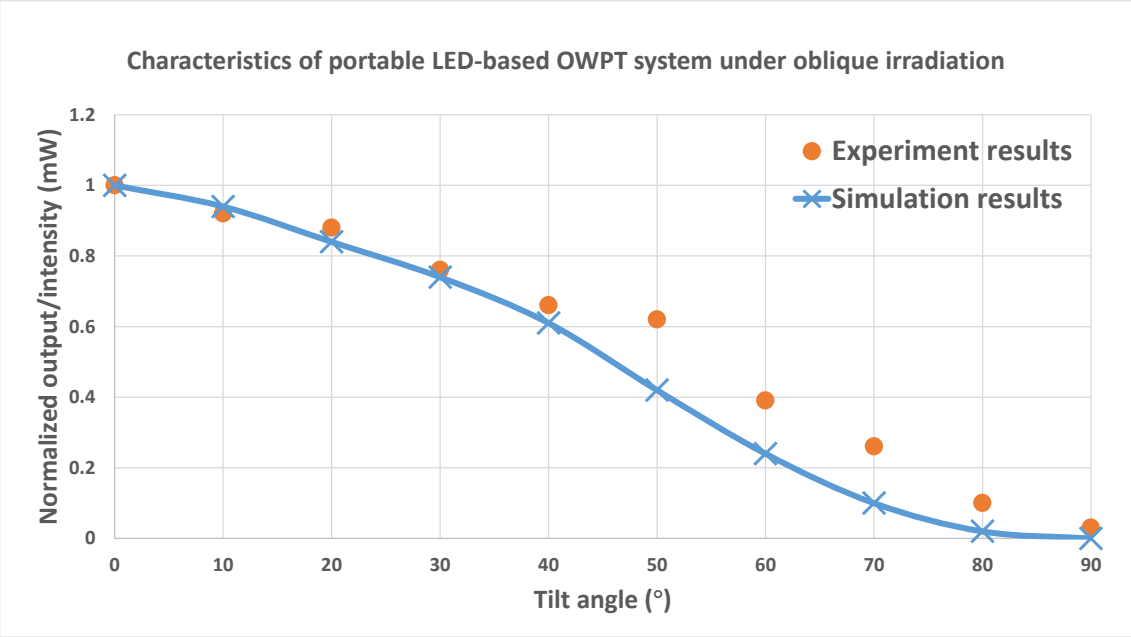

Fig. 4.13 The experiment results of portable LED-based OWPT system under oblique irradiation

In the Fig. 4.13, the blue curve shows the normalized received intensity of the solar cell with different tile angle of the incident light beam, and the orange dot shows the experiment results of the normalized output power from the solar cell. With the tilt angle of the incident light beam increasing, the performance of the portable LED-based OWPT system declines continuously. As discussed in section 3.3.3, the deterioration of the system performance is attributed to two reasons, which are the reflection loss on the solar cell surface and the geometrical loss due to the deformation of the irradiation spot. The case of 0° tilt angle indicates the light beam is vertical irradiated at the surface of the solar cell, which is the ideal irradiation condition. While the tilt angle of 90° means the surface of the solar cell parallels with the propagation direction of the incident light beam, and the intensity of the light beam can barely receive by the solar cell in such case. Comparing experimental data and simulation data, the overall trend of the two is similar. In both cases, the system performance drops steadily in the oblique irradiation angle range of 0° to 40°, then accelerates down in the range

of 40° to 70°, and finally tends to be gentle in the tilt angle range of 70° to 90°. From the data shown in Fig. 4.13, when the tilt angle is in the range of 0° to 40°, the experimental data and the simulation data agrees perfectly. However, in the range of 40° to 90°, the performance of the system measured in the experiment is slightly higher than the simulation results. Except for the measurement error in the experiment, the main reason can be considered to be the different reflection coefficient on the surface of the solar cell in experiment and simulation. As discussed in Section 3.3.3, the solar cell model does not exist in the simulation software, thus the detector module is used to simulate the solar cell function and measure the received intensity. However, the detector module does not have a reflection coefficient on its surface, so according to the characteristic of the angle incidence performance of the solar cell shown in official datasheet, the reflection coefficient of different incident angle is added on the detector module. When integrating the characteristics of the angular incidence performance of the solar cell, due to the relatively fuzz parameters shown on the official datasheet, only a few special discrete points can be selected to simulate the reflection characteristics of the solar cell. Thereby, it is highly possible that the reflection characteristics of the solar cell in the simulation is slightly different to the practical situation. However, from a general point of view, such small deviation will not make much difference in the analysis of system performance. In general, the experimental data and simulation data are almost in agreement, and the simulation conclusion is confirmed by the experiment data, which is that the portable LED-based OWPT system can transmit above 50% of the total intensity to the solar cell with smaller than around 45° tilt angle, and such tilt angle can be regarded as a threshold for judging whether the portable LED-based OWPT system can achieve effective power transmission.

4.4.2 Experiment of the portable LED-based OWPT system under irradiation with tremor

Tremor is an involuntary, with a certain rhythm, muscle contraction and relaxation, and cannot be controlled autonomously.[3] The tremor most often occurs on hand,

so when the OWPT system is held and operated by the user, the tremor of the user's hand during the operation will affect the performance of the portable LED-based OWPT system. Moreover, the degree of tremor is usually related to physical exhaustion, which means that as the user holds the portable LED-based OWPT system and keeps the hand and arm still for remote power supply, as the power supply time increases, the degree of tremor will increase correspondingly. The tremor of the user's hand will cause the OWPT's transmitter to shake slightly, which will cause the irradiation spot at the target transmission distance to shift. The displacement of the irradiation spot will cause fluctuation of the intensity received by the solar cell, which will eventually cause the oscillation of output power from the solar cell and thus worsening the portable LED-based OWPT system performance. For power transmission systems like OWPT system, stable output power is an important requirement, so the analyzing the characteristics of the portable LED-based OWPT system under the irradiation with tremor and discussing the method of suppressing the negative influence of tremor is essential.

From the viewpoint of the OWPT system, the tremor is combined with panning direction and angular direction. The Fig. 4.14 shows the tremor in the panning direction during 20 s fixed posture. It can be seen that the tremor in panning direction is only in the range of ±1 mm. As for the performance of the OWPT system, the output fluctuation caused by the tremor in lateral direction is not sever. The tremor in panning direction will only cause a corresponding degree displacement of the irradiation spot at the target distance, no matter how long the transmission distance is. From the Fig. 4.14, the tremor in panning direction is only ±1 mm in the 20 s fixed posture, so the corresponding displacement of the irradiation spot at the target distance will be also about ±1 mm. As discussed in the previous sections, the size of the solar cell is not perfectly matched the size of the irradiation spot but slightly smaller, thus the received intensity of the solar cell will almost unchanged even the tremor in panning direction happens. Although the tremor will be severe with the operation time extending, considering the charging time of the IoT terminals by the portable LED-based OWPT system

is almost within dozens of seconds or minuets, the negative impact of the panning direction tremor on the final performance of the system can be ignored.

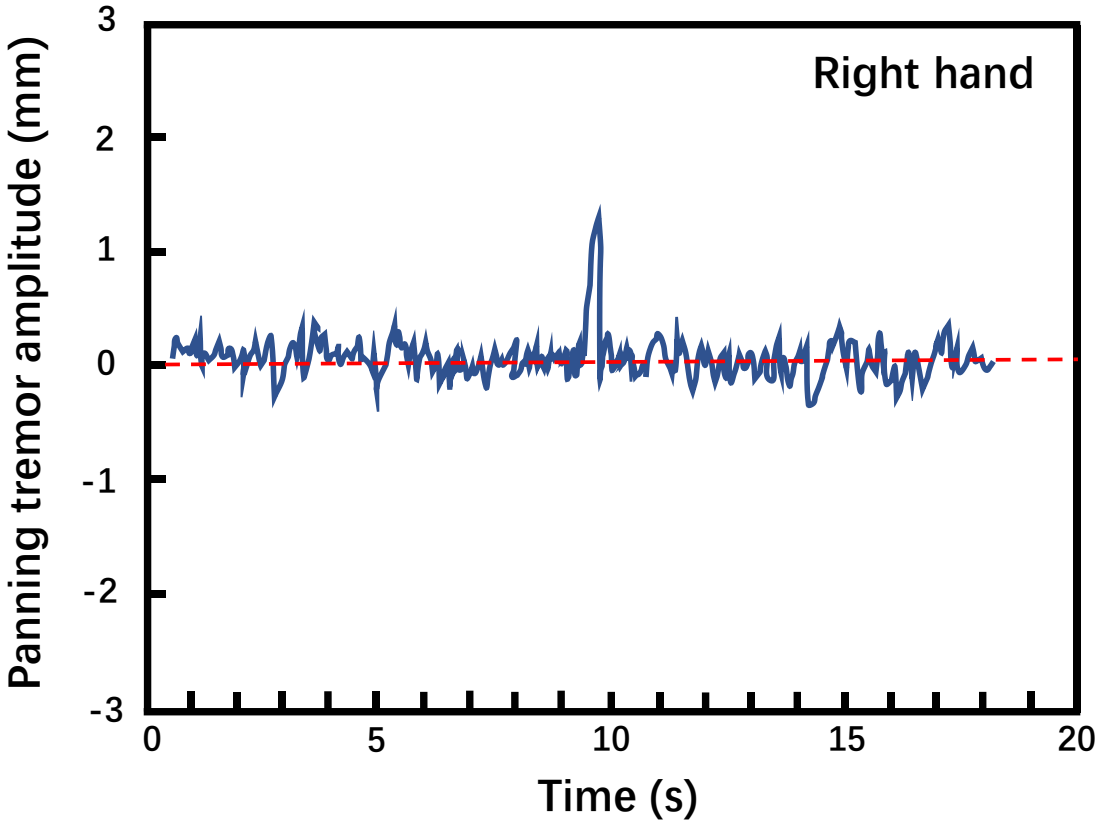

Fig. 4.14 Tremor in panning direction with fixed posture[4]

On the other hand, the tremor in angular direction is much more severe issue in the application of the portable LED-based OWPT system. The Fig. 4.15 shows the tremor in angular direction during 60s fixed posture by experiment. From the data shown in the Fig. 4.15, the angular change is in the range of ±5° during the 60s fixed posture. Unlike the tremor in panning direction, the degree of displacement of the irradiation spot caused by the tremor in angular direction is proportional with the transmission distance. For instance, in conditions of 100 mm transmission distance, every 1° of the angular tremor will cause 1.7 mm displacement of the irradiation spot at the target distance. Considering the transmission distance of the portable LED-based OWPT system is usually much

larger, thus every 1° of the angular tremor will cause 17 mm displacement of the irradiation spot at the 1 m distance, 35 mm displacement of the irradiation spot at 2 m distance, and 52 mm displacement at 3 m distance. In the case of 5° tremor in angular direction, the displacement of the irradiation spot increases to 87 mm at 1 m distance, 175 mm at 2 m distance and 262 mm at 3 m distance. Considering the size of the irradiation spot of the portable LED-based OWPT system is designed to be very small, usually with the side length shorter than 5 cm, so such a large degree of displacement of the irradiation spot will greatly degrade the output power of the system. Even a situation where the irradiation spot completely deviates from the position of the solar cell may occur, resulting in no output at all from the solar cell. Thus, suppression the tremor in angular direction is far more necessary.

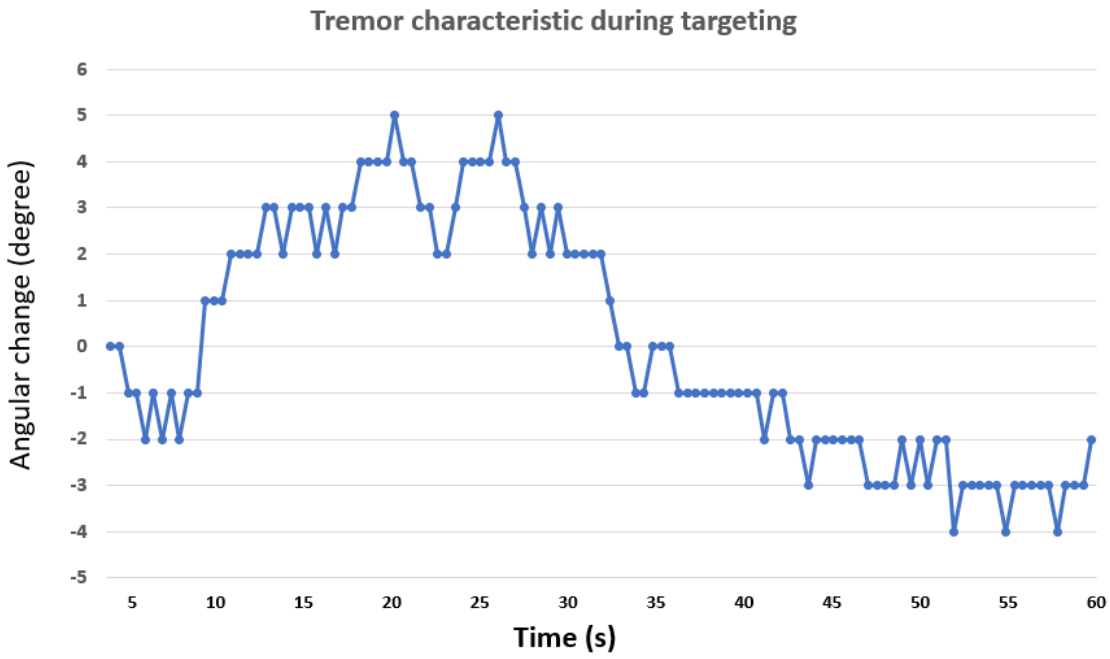

Fig. 4.15 Tremor in angular direction with fixed posture

The experiment of the portable LED-based OWPT system under the irradiation with tremor was held. The Fig. 4.16 shows the experiment setup of the tremor irradiation. As the Fig. 4.16 shows, the modularized LED-based OWPT system

was used in the experiment for process the tremor irradiation. The optical components that used in the experiment were exactly the same as the experiment configuration shown in the section 4.1.3. The operator held the modularized LED-based OWPT system in the right hand and the IR viewer in the left hand, and the single-junction GaAs solar cell with 17 mm × 17 mm was installed at 1 m away from the transmitting side. During the experiment, the operator fixed the posture and kept aiming the solar cell through the IR view, like the normal condition of operating the LED-based OWPT system. The normalized output from the solar cell was measured during 3 mins continuous operation. Besides, considering that the tremor is proportional to the weight of the device, by adding a load with different weight to the modularized LED-based OWPT system, the experiment data of the original modularized LED-based OWPT system (620 g), the system with a 100 g load of weight (720 g), the system with a 200 g load of weight (820 g) and the system with a 300 g load of weight (920 g) was measured, separately. The experiment data of the characteristics of normalized output under irradiation with tremor is shown in the Fig. 4.17.

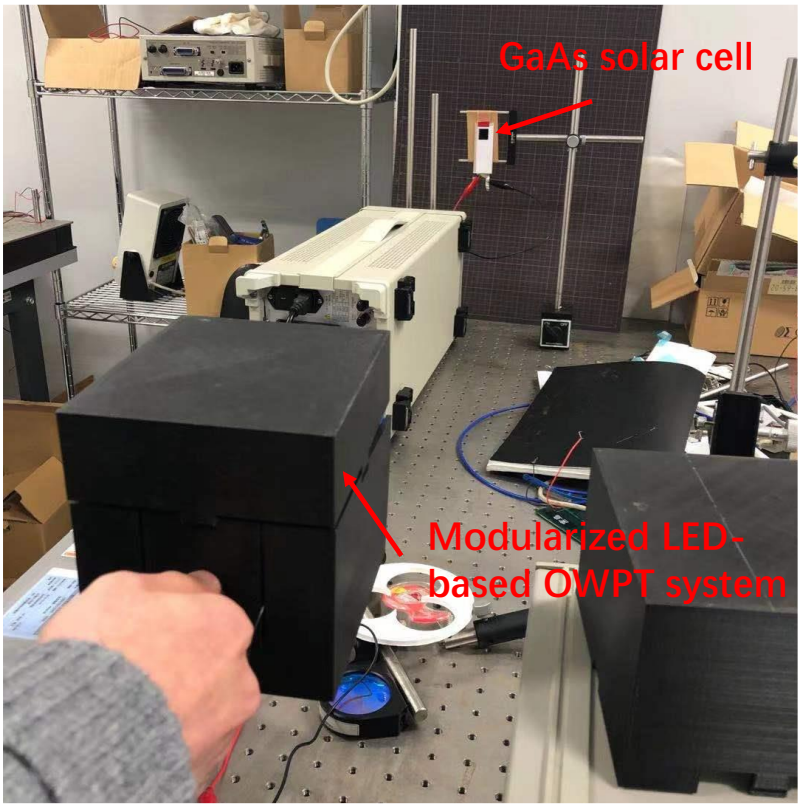

Fig. 4.16 Experiment setup of portable LED-based OWPT system with tremor

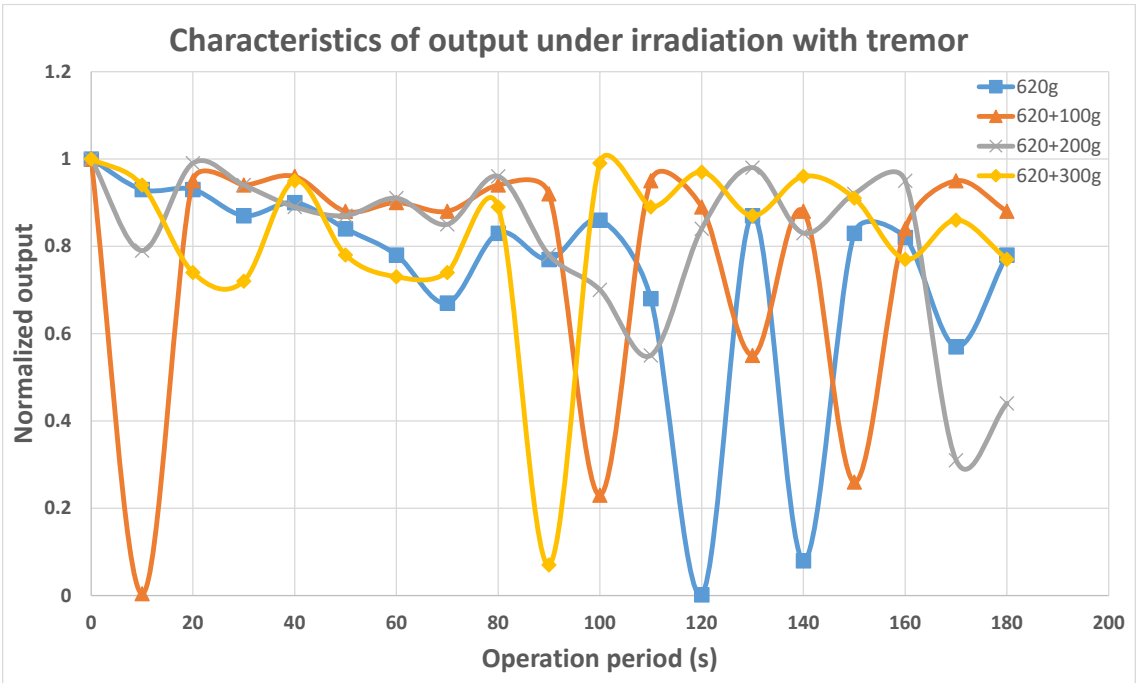

Fig. 4.17 Experiment results of portable LED-based OWPT system output under irradiation with tremor

From the experiment results shown in the Fig. 4.17, the output of the LED-based OWPT system will fluctuated during the operation, which is caused by the tremor during irradiating the solar cell. Such tremor is combined with the tremor in both panning direction and angular direction. Since the size of the solar cell (21 mm × 23 mm) is similar with that of the irradiation spot (17 mm × 17 mm), the tremor when holding the portable LED-based OWPT system will cause the displacement of the irradiation spot and thus makes part of the irradiation spot outside of the solar cell surface, thus lead out the fluctuation of the output from the solar cell. According to the experiment data, with the prolongation of the operation time, the tremor of the human body will increase because of keeping the posture for a long time, thus the fluctuation of the system output will be more obvious accordingly. It can be seen from the Fig. 4.17, in the range of 0 s to 80 s, the output of the system can still be relatively steady, while the fluctuation of the system output becomes very large when the operation period beyond 80 s. On the other hand, apart from a few special experimental data, when the weight of the system increases, the fluctuation of the system output caused by tremor becomes more obvious and frequent. This is because the tremor of the human body is directly proportional to the weight of the device. The heavier the weight of the device, the greater the amplitude and frequency of the tremor. Regarding the original modularized portable LED-based OWPT system that with 620 g weight, the output of the system can remain stable till more than 100 s continuously operating, while the obvious decline occurred after 80s continuously operating of the system with a 300 g load. Besides, when the weight of the device increases, some obvious output drop caused by tremor will also occur when continuously operating system in a short period of time, such as the experiment results of the system with 300 g load (yellow curve) in the Fig. 4.17.

From the analysis of the LED-based OWPT system under the irradiation with tremor, the performance of the system will be greatly impacted by the tremor of

the human body, and such negative influence becomes sever with the weight of the device enhanced and the continuous operation period extended. Thus, suppressing the negative of the tremor during the operating the portable LED-based OWPT system is far more important.

As discussed, the tremor of the human hand during the operation of LED-based OWPT system can be divided into panning and angular directions, and angular tremor has a greater impact on the performance of the LED-based OWPT system. Generally, the negative effects of tremor can be suppressed by adding a microelectromechanical system (MEMS) with a gyroscope to the optical components of the lens system.[5] However, such an adaptive system requires a complicated design and relatively high cost, and the dimension of the system will inevitably increase. More importantly, the MEMS with gyroscope can effectively suppress the tremor in the panning direction, but the tremor in the angular direction is still difficult to effectively control. Thereby, optimization of installing an electrical stabilizer with the LED-based OWPT system will be an easier and more flexible approach. Usually, stabilizer has multiple directions to compensate, while the compensation on the tilting and panning direction are the main targets for the LED-based OWPT application. The compensation of both the panning and tilting direction is for the angular direction tremor during operating the system. The technology of similar MEMS-based stabilizers has been very mature and has been widely used in the field of the PTZ camera (pan–tilt–zoom camera) of mobile phone or drone. The required degree of freedom of the stabilizer specially for the LED-based OWPT system is panning and tilting direction only, thus the configuration of the stabilizer is relatively simple, and the dimension and the cost can be well controlled as well.

The optimization of the relative size of the irradiation spot and solar cell can suppress the negative impacts of the panning direction tremor, while the MEMS-based stabilizer can effectively compensate the tremor in angular direction. The combination of both optimizations can effectively restrain the fluctuation of the system output caused by tremor during the LED-based OWPT system operation, and provide stable power for the IoT load.

On the other hand, applying the function of beam scanning in the LED-based OWPT system is also another possible solution for suppressing the negative impacts from tremor, which needs specially designed light sources array with control chip or steering system. Another easy approach is enhancing the total output of the portable LED-based OWPT system and reducing the operation time. By doing so, the tremor of the users' hand can be suppressed at the minimum level, which will increase the performance of the portable LED-based OWPT system, reversely.

4.4.3 Summary of the unideal irradiation conditions of the LED-based OWPT system

Discussing the characteristics of the portable LED-based OWPT system under unideal irradiation conditions can better analyze the performance of the system in real applications. In the section 4.4, the unideal irradiation conditions of the LED-based OWPT system were analyzed and discussed. The characteristics of the portable LED-based OWPT system under the oblique irradiation was studied by simulation results already in the section 3.3.3. The experiment of the portable LED-based OWPT system was discussed and the experiment data was shown in the section 4.4.1. In the experiment, the incident angle on the receiving side was increased from 0° to 90° at intervals of 10°, and the characteristics of the portable LED-based OWPT system with different incident angle light beam was obtained and then compared with the simulation results. In general, the experimental data and simulation data are almost in agreement, and the simulation conclusion is confirmed by the experiment data, which is that the portable LED-based OWPT system can transmit above 50% of the total intensity to the solar cell with smaller than around 45° tilt angle, and such tilt angle can be regarded as a threshold for judging whether the portable LED-based OWPT system can achieve effective power transmission.

In the section 4.4.2, the discussion of the portable LED-based OWPT system under the irradiation with tremor was shown. From the viewpoint of the OWPT system, the tremor can be divided into lateral direction and angular direction. By

maintaining a fixed posture for a period of time, the negative of tremor on the performance of portable LED-based OWPT system was measured in experiment. From the experiment data, after short-term (0 s to 80 s) continuous operating, the output of the system can still be relatively steady, while the fluctuation of the system output becomes very large when the operation period beyond 80 s. Besides, when the weight of the device increasing, the fluctuation of the system output caused by tremor is obviously strengthened, and there may be a significant output decline in short-term continuous operation when the weight of devices increased to around 1 Kg.

Reference

[1] SIGMAKOKI, AGL-32.5-23.5P, datasheet.

[2] NTKJ Co., Ltd., CF100, datasheet.

[3] Chen. Wei, Hopfner. Franziska, Becktepe. Jos Steffen, Deuschl. Günther, "*Rest tremor revisited: Parkinson's disease and other disorders,*" Translational Neurodegeneration, 6 (**1**), pp: 16, 2017.

[4] Elble. Rodger J, "*Tremor,*" Neuro-geriatrics, Springer, Cham, pp: 311-326, 2017.

[5] Clarke P, "*Smart MEMS microphones market emerges,*" EE News Analog, 2016.

Chapter 5. LED-array OWPT system for high output power

As a power system, the output power is a very important factor to measure the performance of the OWPT system. The higher output power not only allows the OWPT system to provide remote power supply for more types of loads, but also shortens the single operation time, which greatly increases the convenience and functionality of the OWPT system. The highest possible output power of the OWPT system is determined by the output of the light source. In the case of the LED-based OWPT system, the highest output power of the system is determined by the output intensity of the LED. Although high-intensity LEDs are gradually being marketed at current stage, the total output of a single LED chip is still extremely limited. The highest radiant intensity of the LED in the current commercial market is around 1 W/mm^2, and the size of the LED chip needs to be enlarged if high output is required. Generally, there are two methods to enhance the total output of the single LED, which are enlarging the size of the LED chip or integrating multiple chips into a single LED module. However, both of them will enlarge the emitting area of the light source and thereby increase the size of the irradiation spot at the target transmission distance. Therefore, arraying multiple LEDs as LED array and re-distributing the intensity from different LEDs to be an entire irradiation spot is the only way to enhance the total output of the LED-based OWPT system while not greatly increase the size of the irradiation spot at the target distance.

In the chapter 5, the designing and the configurations of the LED-array OWPT system will be analyzed, and the characteristics of the LED-array OWPT system will be discussed based on both simulation and experiment data.

5.1 Analysis of the array method

5.1.1 Conventional method of array

The LED chip can be seen as a Lambertian object, after first-order lens packaging, radiation will be restrained in a certain angle and distribution. If LEDs are arrayed, corresponded light rays from different LEDs will have same divergence angle. As

shown in the Fig. 5.1, in case of applying a single image lens, such same angle rays will be emitted at different curvature radius points on lens. Thus, beams will not be overlapped but separated, and radiant intensity on the surface of the solar cell will be not improved.

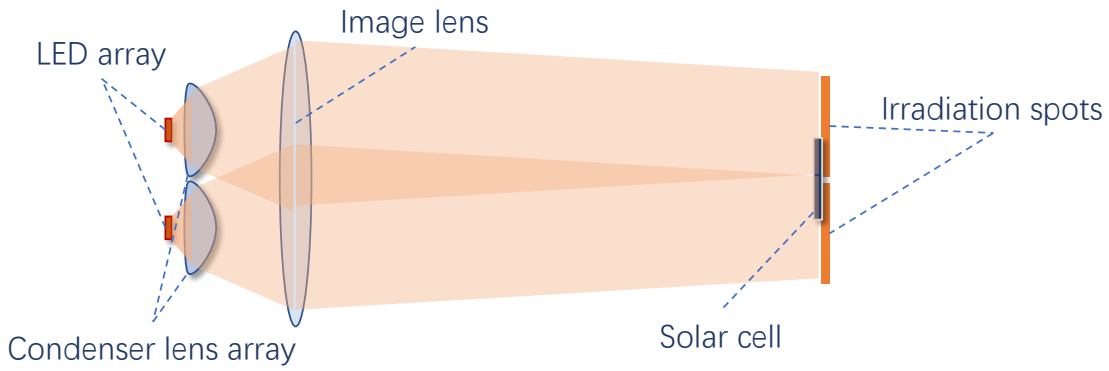

Fig. 5.1 The schematic diagram of LED-based OWPT system with multiple LEDs

In order to improve the amount of intensity that can be received by the solar cell, the irradiation spots from different LEDs should be focused at the same area and overlapped to each other, thus the idea of the configuration designing of the LED-array OWPT system need to be changed. The most conventional and simplest method is applying same lens-set for each LED and then tilting optical axis, as shown in the Fig. 5.2. By doing so, the irradiation spots from different LEDs can be easily focused on the position of the solar cell. However, due to such configuration needs apply same lens-set for each LED light source, thus multiple image lenses are necessary to be used in the optical system. As discussed in the section 3.2, from the viewpoint of the etendue of the entire system, the exit pupil of the optical system needs to be large enough for obtaining a small irradiation spot at the target distance, therefore the aperture size of the image lens should be sufficiently large. In the case of the LED-array OWPT system, since multiple image lenses are used in the optical system that shown in Fig. 5.2, the large size aperture of the image lenses will largely limit arraying compact level of the system.

In another word, although such configuration is simple to design, the dimension of the entire system will be too large. Moreover, with the number of the LEDs increasing, the size of the system will be rapidly enlarged, and soon loss the capability of portability.

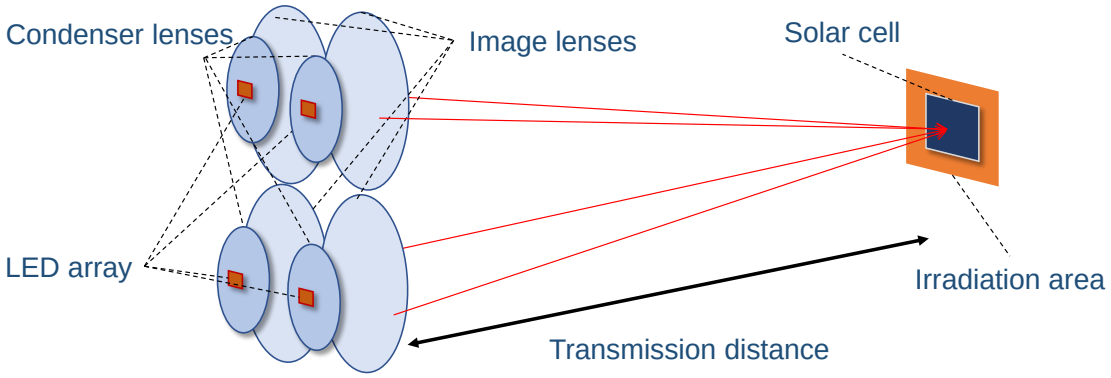

Fig. 5.2 The schematic diagram of conventional array method

5.1.2 Novel method of array

In order to rearrange the intensity from different LEDs and make their irradiation spots overlapped, a novel method of arraying the LEDs in the OWPT system is proposed. Due to the spatially incoherent of LED, collimation the LED on whole transmission distance is very difficult, however, approximate collimation in a very short distance is not so difficult. The novel method of arraying the LEDs in the OWPT system is shown in the Fig. 5.3. The collimations lenses are applied to each LED light source, and the light beams from different LEDs will be collimated by the lens set. After collimation, the light rays from all LEDs are parallelly emitted on the image lens without divergence. Therefore, just one image lens can rearrange intensity distribution and thus make the irradiation spots from different LEDs to be overlapped.

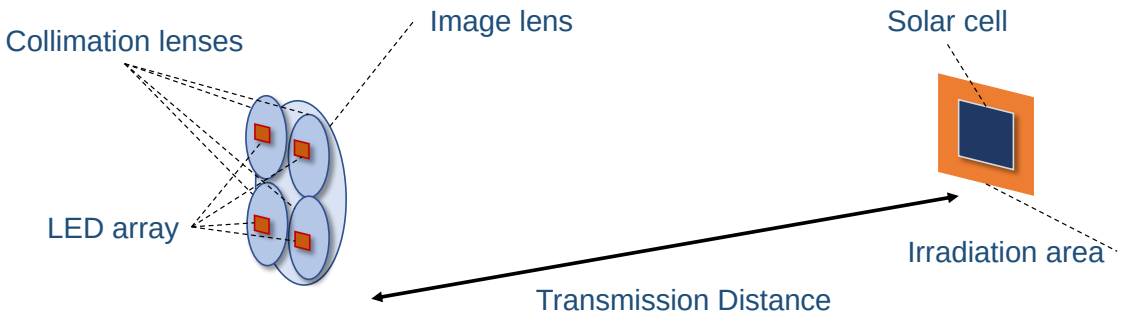

Fig. 5.3 The schematic diagram of novel array method

As for such configuration, due to only one image lens is used in the system, thus the aperture size of collimation lens becomes the factor that limiting compact level. Considering the aperture size of the collimation lens is much smaller than the image lens, multiple LED light sources and collimation lenses can be arrayed under the certain aperture size of the image lens. As a result, compact level of the LED-array OWPT system can be largely increased, and system vertical height (exit pupil of the system) can be deceased a lot as well. Moreover, since all the light beam before the image lens is collimated and roughly has no divergence, the value of d parameter, which is the distance between the collimation lens and image lens, will no longer impact the final irradiation spot size. In other word, the size of the irradiation spot at the target distance will not change no matter the value of the d parameter. Thus, the image lens can be closely placed after collimation lens, which allows horizontal length of system to be largely compressed. In fact, comparing with the configuration of the portable LED-based OWPT system that shown in the section 3.3, the horizontal length of the system can be decreased around 60% with such array configuration. Summarily, comparing with the conventional array method, the novel array method of the LED-array OWPT system proposed in this section allows the much greater number of LED light sources to be arrayed under the certain height of the system, which largely improved the compact level. Besides, the system length can be shortened by more than half because of the light beam is parallel before the image lens. Therefore, the entire dimension of the LED-array OWPT system can

be greatly compressed while the degree of integration of the LED light source has risen.

5.1.3 Summary of the array method for LED-array OWPT system

The array method of the LED-array OWPT system is discussed in the section 5.1. The conventional array method of the optical system is applying same lens-set for each LED light source and then tilting the optical axis, thus makes the irradiation spots from different LEDs overlapped. Whereas, the large-size aperture of the image lens will largely decrease the compact level of the LED array, and the large dimension of the system will also cause the loss the portability. In the section 5.1.2, a novel array method of the LED-array OWPT system is proposed. In such configuration, collimation lenses are used behind the LED light sources and refract the LED light beam to be parallel, then a single image lens can be applied to rearrange intensity distribution and make the irradiation spots to be overlapped. Since only one image lens is used in the system, the vertical dimension of such configuration is only a fraction of the system of conventional array method. Besides, the image lens can be placed closely behind the collimation lens, therefore the system length can be shortened by more than half. Conclusively, the novel method of array can realize the great compression of the system dimension while the degree of the integration of the LED light sources can be improved.

5.2 The configuration of the LED-array OWPT system

5.2.1 Single-set collimation lenses configuration of LED-array OWPT system

According to the novel array method of the LED-array OWPT system that discussed in the section 5.1, the configuration of the LED-array OWPT system is shown as the Fig. 5.4. In the system, multiple LEDs are used as the light sources, and a condenser lens is applied to each LED as the collimation lens, and one image lens is adopted and installed closely behind the set of collimation lenses.

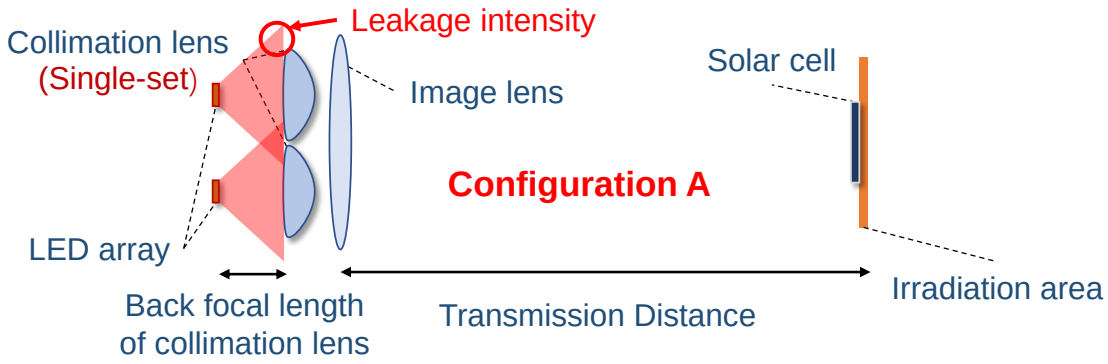

Fig. 5.4 The single-set collimation lenses configuration of LED-array OWPT system

As the configuration shown in the Fig. 5.4, one set of collimation lenses is used to collimate and then an image lens can be closely installed after collimation lens. For simplicity, the single-set collimation lenses configuration of the LED-array OWPT system is referred as “configuration A” in this thesis. Since the distance between the collimation lenses and the image lens is very short, the intensity loss between the collimation lenses and image lens will be very small and can be ignored. On the other side, in order to get collimation correctly, the LED array needs to be placed at the back-focus point of collimation lens. According to the theory of the etendue of the entire system, the exit pupil of the optical system needs to be sufficiently large for achieving small irradiation spot at the target transmission distance. In the case of the LED-array OWPT system, it means the beams size on the image lens should be large enough. Because the beam size on the image lens is the sum of the beam sizes of all collimation lenses in the LED-array OWPT system, and the beam size of the collimation lens is proportional to the aperture size of the collimation lens. Therefore, in order to obtain a smaller irradiation spot at the targe distance, the aperture of the collimation lens needs to be large enough. On the other hand, according to the principle of the NA (Numerical Aperture) value of the optical element that discussed in the section 2.4, the NA value of the lens will limit the focal length of the lens under the certain size of the aperture. In other word, when the NA value

and the aperture of the lens are constant, the focal length of the lens cannot be too small. Although by applying a material with a larger refractive index or increasing the thickness of the lens can slightly increase the NA value of the lens, the improvement will not be obviously. Therefore, in order to obtain a small irradiation spot at the target distance, the aperture size of the collimation lenses needs to be sufficiently large, while the focal length of the collimation lens cannot be reduced with the limitation of the NA value under to the condition of large size aperture. Due to the NA value of most lens is slightly larger than 1, as a fact, the focal length of the collimation lens cannot be much smaller than the value of the aperture size. As a result, the focal length of the collimation lens applied in the configuration shown in the Fig. 5.4 is generally large, and due to the LED array needs to be placed at the back-focus point of collimation lens in order to achieve collimation, the distance between the LED array and the collimation lens will inevitably be large. For this reason, as shown in the Fig. 5.4, the intensity loss between the LED array and the collimation lenses will be slightly large, then reduce the efficiency of the lens system accordingly. On the other hand, because the aperture of the collimation lens is fully utilized in configuration A, the exit pupil of the system is thereby large, hence that the irradiation spot size at the target distance will be small. In summary, simple and light configuration and small irradiation spot is the merits of the single-set collimation lenses configuration (configuration A) of LED-array OWPT system.

5.2.2 Double-set collimation lenses configuration of LED-array OWPT system

In order to solve such issue, another kind of configuration is shown in Fig. 5.5. In this configuration, two sets of collimation lenses are applied in the optical system, and collimation is finished by two set of lenses in two steps. For simplicity, the double-set collimation lenses configuration of the LED-array OWPT system is referred as “configuration B” in this thesis. The light source can be closely placed near the surface of first collimation lens set, and then modifying the distance between two sets of collimation lenses to collimate correctly. By doing so, the geometrical loss between light source and collimation lens can be largely

declined, and lens system efficiency will be increased accordingly. On the other hand, the exit pupil of the configuration B will be smaller than that of configuration A due to the divergence of the light beam has been constrained twice before the image lens. Therefore, in the same situation, the irradiation spot size at the target distance of configuration B will be slightly enlarged compared with configuration A.

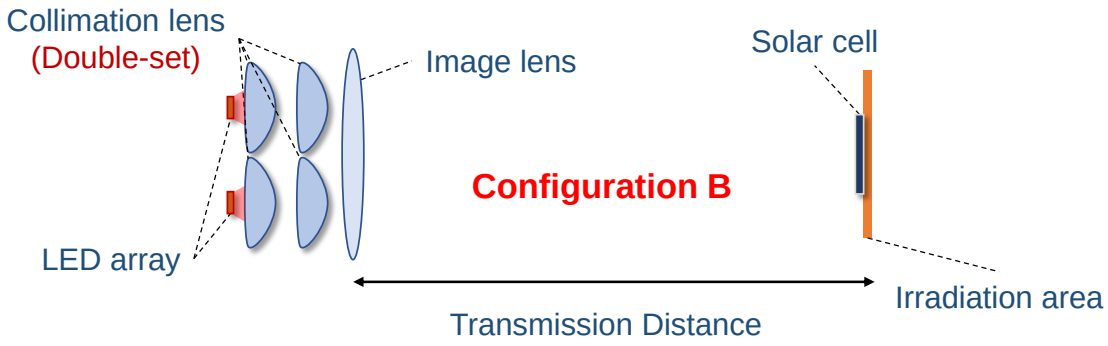

Fig. 5.5 The double-set collimation lenses configuration of LED-array OWPT system

Summarily, single-set collimation lenses configuration has simple configuration, smaller irradiation spot size but decreased efficiency, and double-set collimation lenses configuration has slightly complicated configuration, larger irradiation spot size but relatively high efficiency. Both configurations have their individual advantages and adapt to different applications and working environment.

5.2.3 Summary of the configuration of the LED-array OWPT system

In the section 5.2, two kinds of the configuration of the LED-array OWPT system are shown and compared. In the single-set collimation lenses configuration (configuration A) of the LED-array OWPT system, one set of collimation lenses is used behind the LED-array to finish the collimation. According to the principle of etendue, the aperture size of the collimation lens should be large enough for achieving small irradiation size at the target distance, while the value of the focal

length of the collimation lens has to be similar with the value of aperture due to the limitation of the NA value, which means the value of the collimation focal length cannot be very small. As a result, the LED-array will be placed at the back-focus point of the collimation lens in order to collimate correctly, and due to the value of the back focal length is relatively large, the intensity loss between the LED-array and the collimation lenses is slightly large. In summary, simple and light configuration and small irradiation spot is the merits of the configuration A of LED-array OWPT system, while the efficiency of the lens system is relatively low. In order to solve such issue, the double-set collimation lenses configuration (configuration B) of the LED-array OWPT system is proposed in the section 5.2.2. In the configuration B, two sets of collimation lenses are applied in the optical system, and the collimation is finished by two steps. The first-set of collimation lenses can be closely installed behind the LED-array, thus the intensity loss between the LED-array and the collimation lenses can be largely controlled. The second-set of collimation lens is installed at a certain distance from the first-set collimation lenses, and the distance between two sets of collimation lenses is determined by the focal length of the collimation lenses. Comparing with the configuration A, due to the intensity loss between the LED-array and the collimation lenses is greatly reduced, the overall efficiency of the configuration B can be improved. On the other hand, the exit pupil of the system is decreased due to the divergence of the light beam is reduced when it passes through the first-set collimation lenses, thus the irradiation spot size of configuration B at target transmission distance will be slightly larger.

5.3 Simulation of the LED-array OWPT system

5.3.1 Analysis of the simulation results of the LED-array OWPT system

In order to figure out the characteristics of the LED-array OWPT system, the simulation model of the two kinds of configurations of the LED-array OWPT system is established. The simulation results were carried out using ZEMAX (ZEMAX LLC). The examples of the simulation model of the LED-array OWPT

system are shown in the Fig. 5.6.

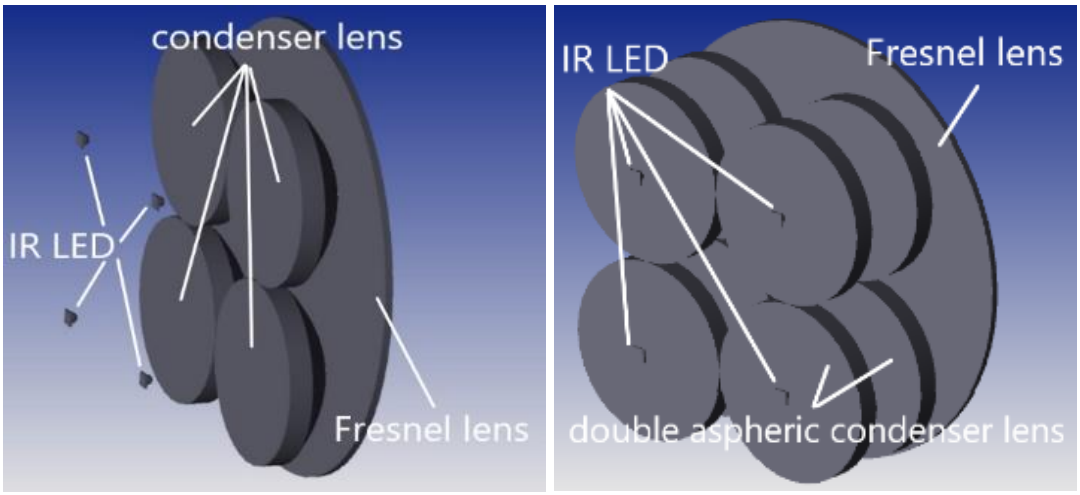

Fig. 5.6 The simulation model of two configurations for LED-array OWPT system

In the simulation, the model of light source is the same as the simulation model shown in section 3.3, which is the official simulation model of Osram SFH-4703AS NIR LED (1040 mW, 810 nm, ±40°, 0.75 mm × 0.75 mm chip). As the discussion of the etendue, the exit pupil of the system should be sufficiently large for achieving small irradiation spot size at target transmission distance, thus the focal length of the collimation lenses (condenser lenses) cannot be small, and the aperture size has to be increased accordingly. Therefore, the simulation model of all collimation lenses applied has 50 mm aperture and 50 mm focal length. In order to completely restore the parameters of the simulation model in the experiment, the material of the condenser lens is set as typical B270. Considering the relatively large number of condenser lenses that applied in the LED-array OWPT system, especially the double-set collimation lenses configuration, the condenser lens with a larger refractive index material is optimal, such as S-LAH64. The thickness of the lens with larger refractive index material will be smaller, thus the weight of the entire system can be reduced. Due to the collimated light beam, the focal length of the image lens should be set as the exactly same value of target transmission distance. In the simulation, the transmission distance is set

as the typical 1 m, thereby the focal length of the image lens should be 1000 mm. The aperture size of the image lens is decided by the overall beam size of the collimation light beam, and such size of the beam is determined by the number of light sources in the LED array. Conclusively, a Fresnel lens with 1000 mm focal length and material of PMMA is applied, and the aperture size of the Fresnel lens is changed with the number of LEDs. Several detector modules of different sizes are set up at a transmission distance of 1 m to measure the total intensity that solar cells of different sizes can receive. In the simulation model of configuration A, the distance between the LED-array and collimation lenses is 41 mm, which is the same value of the back focal length of the collimation lens, and the Fresnel lens is closely installed after the collimation lenses. On the other hand, in the simulation model of configuration B, the first-set of collimation lenses is placed 4 mm behind the LED-array, which is the package size of the LED module, and the distance between the two sets of collimation lenses is 22.6 mm. With such parameters, the light beam can be collimated correctly after two sets of collimation lenses.

The Fig. 5.7 shows the simulation results of the received intensity of two kinds of LED-array configurations with different number of LEDs based on different side length of the solar cell at 1 m transmission distance, and the simulation data of single-LED OWPT system that stated in the section 3.3 is also included in the Fig. 5.7 in order to better analyze the characteristics of the LED-array OWPT system.

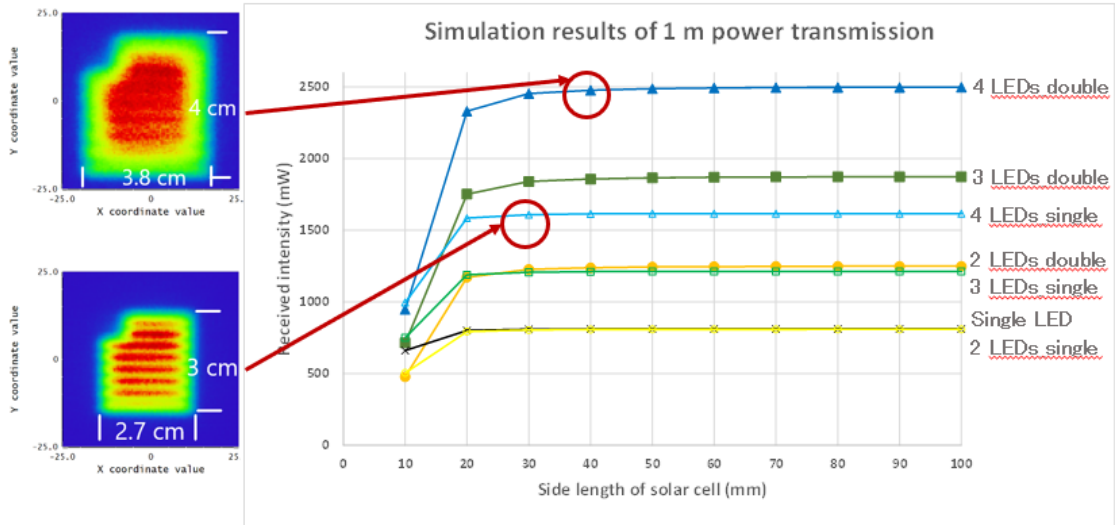

Fig. 5.7 The simulation results of the LED-array OWPT system with two configurations

The irradiance map of the two configurations of the LED-array OWPT system is shown at the left side of the Fig. 5.7. The size of the irradiation spot of the single-set collimation lenses configuration (configuration A) is 2.7 cm × 3 cm at 1 m distance, and double-set collimation lenses configuration (configuration B) has an irradiation spot with 3.8 cm × 4 cm size. It should be mentioned that the irradiation size of the system is decided by individual lens set of each light source, thus the final irradiation size of both configurations will not change no matter how many LEDs are applied. Specifically, irradiation size of the single-set collimation lenses configurations and the double-set collimation lenses configuration will always be 2.7 cm × 3 cm and 3.8 cm × 4 cm at 1 m transmission distance as long as the parameters of the optical components unchanged.

The top blue line shown in Fig. 5.7 refers the performance of the 4-LED OWPT system with configuration B, which can achieve around 2500 mW intensity when side length of solar cell size is larger than 4 cm. Because the irradiation size of configuration B is 3.8 cm × 4 cm, when side length of solar cell is smaller than 4 cm, part of intensity will be irradiated out of solar cell and be lost. Then the 3-LED OWPT system with configuration B can achieve around 1800 mW maximumly. On the other side, 4-LED OWPT system with configuration A can achieve around maximumly 1600 mW intensity, the lower intensity amount is caused by its lower lens system efficiency that discussed above. However, full intensity can be obtained with smaller solar cell (side length of 3 cm) of configuration A due to the smaller size of irradiation spot. The 2-LED OWPT system with configuration B and the 3-LED OWPT system with configuration A can transmit roughly same full intensity, which is around 1400 mW, and the 2-LED OWPT system with configuration A gets similar amount of intensity with single-LED OWPT system from the data shown in Fig. 5.7, which is about 860 mW. However, due to the irradiation spot size of the single-LED OWPT system at 1 m distance is 2.1 cm × 2.3 cm, which is smaller than the size of LED-array OWPT system with

configuration A, thus, the fact that the final output power of the 2-LED OWPT system with configuration A will be lower than that of single-LED OWPT system can be anticipated. Another very important conclusion is, if 4-LED OWPT system with configuration A is applied, 2500 mW intensity is available at 1 m target distance. According to simulation data, the average irradiance of 4-LED OWPT system with configuration B is higher than that of single-LED OWPT system, which means the photovoltaic conversion efficiency of 4-LED OWPT system with configuration B is higher as well. Since the experiment data of photovoltaic conversion efficiency of solar cell that shown in section 4.1 is around 42%, the actual photovoltaic conversion efficiency of the solar cell in the experiment of 4-LED OWPT system with configuration B should be larger than 42% as well. Thus, above 1 W output power of 4-LED OWPT system with configuration B is expected.

5.3.2 Summary of the simulation of the LED-array OWPT system

In the section 5.3, the analysis based on the simulation results of the two kinds of configurations of the LED-array OWPT system is shown and discussed. The number of arrayed LEDs is set from 2 to 4 in the simulation model, and the results of the two kinds of configurations are analyzed and compared with the single LED OWPT system, respectively. As a result, the irradiation size of the configuration A is 2.7 cm × 3 cm at 1 m distance, while the size of the irradiation spot increases to 3.8 cm × 4 cm at 1 m distance in configuration B. The lens system efficiency of the configuration A and configuration B is around 39% and 60%, separately. The highest intensity received at the target distance is around 2500 mW by configuration B with 4-LED array. By assuming around 40% photovoltaic conversion efficiency of the solar cell, above 1 W output power can be obtained by the LED-OWPT system with such configuration.

5.4 Characteristics of the LED-array OWPT system

5.4.1 Basic experiment and data analysis

In order to confirm simulation results and better analyse the characteristics of the LED-array OWPT system, the experiments of the LED-array OWPT system with

two different configurations were held. Totally four experiments were processed and the corresponding results were analysed, which are the 2-LED and 3-LED array OWPT system with configuration A and the 2-LED and 3-LED array OWPT system with configuration B, respectively.

Firstly, the experiment results and analysis of the 2-LED and 3-LED array OWPT system with configuration A will be discussed.

The Fig. 5.8 and Fig. 5.9 shows the experiment setup of the 2-LED and 3-LED array OWPT system with configuration A, separately. The Fig. 5.10 shows IR images of irradiation spot at the solar cell distance. Since the irradiation shape is not regular rectangle, the irradiation size is defined as size of a rectangular area that can just cover the entire irradiation.

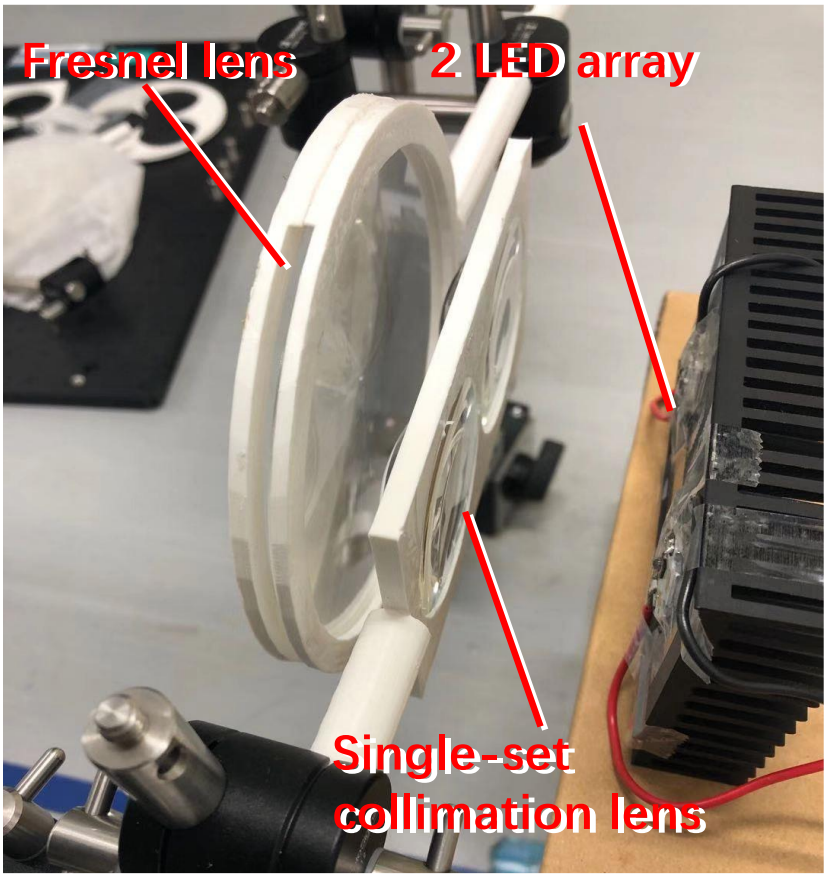

Fig. 5.8 The experiment setup of 2-LED array OWPT system (configuration A)

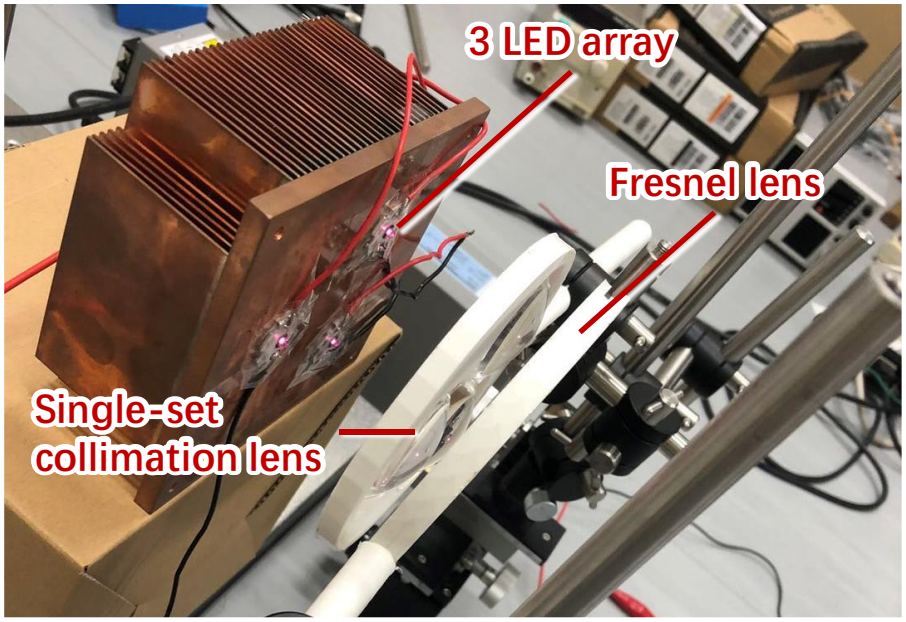

Fig. 5.9 The experiment setup of 3-LED array OWPT system (configuration A)

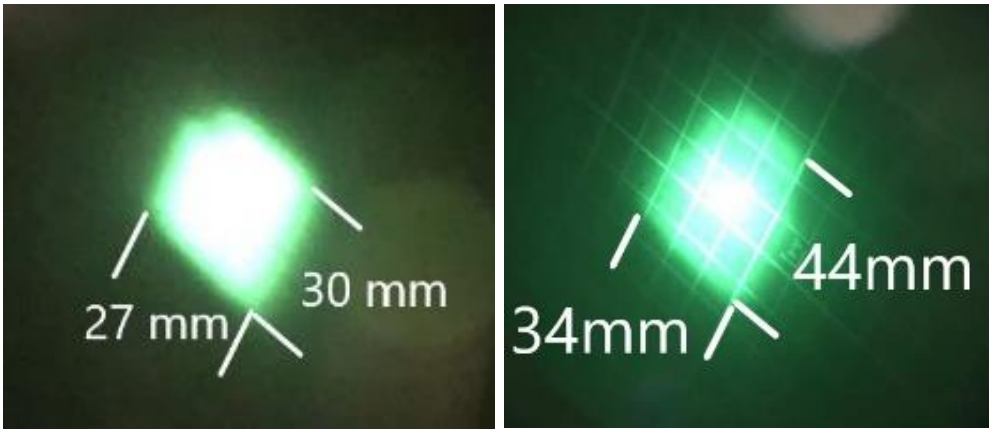

Fig. 5.10 IR image of irradiation spot of 2-LED array (left) and 3-LED array (right) OWPT system in experiment (configuration A).

Same as the LED used in the experiment of portable LED-based OWPT system shown in the section 4.1, multiple high-intensity NIR LEDs (Osram SFH-4703AS, 810 nm, 1040 mW@1 A, 3.55 V, ± 40°, 0.75 mm × 0.75 mm chip) were used to form the LED array as the light source in the experiment of the LED-array OWPT system. In the experiment of the LED-array OWPT system with configuration A,

one set of the aspheric condenser lenses with a 50 mm aperture and a 50 mm focal length (SIGMAKOKI, AGL-50-50P) were used as collimation lenses. The optical components applied in the experiment are all not AR coated. Due to the limitation of the mech aperture size of the collimation lenses, the two NIR LEDs were arrayed side by side with 50 mm distance in the 2-LED OWPT array system. While in the 3-LED array OWPT system, the 3 NIR LEDs were arrayed as equilateral triangle pattern, and the distance between each two LEDs was still 50 mm. Such pattern can achieve the most compact arrangement. The Fig. 5.11 shows the array pattern of the 3-LED array.

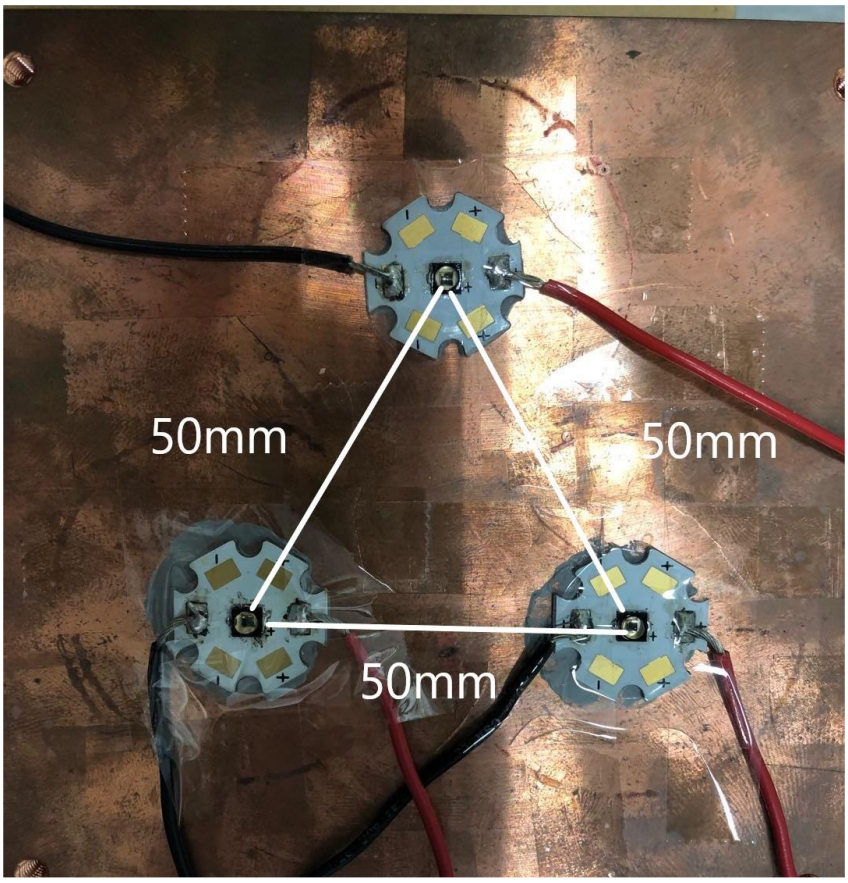

Fig. 5.11 The array pattern of the 3-LED array OWPT system

The aperture size of the image lens should be at least larger than the beam size of the collimated light beam for ensuring the high efficiency of the image lens. By

simple geometric calculations according to the arrangement of LED light sources, it can be figured out that the aperture size of the image lens in the 2-LED array OWPT system should be larger than 100 mm, while such value increases to 108 mm in the 3-LED array OWPT system. Therefore, the aperture size of the image lens was decided as 120 mm in order to effectively collect the intensity. Besides, the transmission distance was set 1 m in the experiment, thus a Fresnel lens (NTKJ Co., Ltd., CF1000) with 1 m focal length and 120 mm aperture diameter was used as the image lens to transmit intensity to the solar cell. In this experiment, no AR-coating was applied to lenses. Two pieces of single-junction GaAs solar cells (Advanced Technology Institute, LLC) with size of 17 mm × 50 mm were series connected to form an optical energy receiver with a 34 mm × 50 mm size. The results of both the simulation and the experiment are shown in Table 5.1 for comparison.

Table 5.1 Experiment results of configuration A (2 and 3 LEDs array**)**

	Sim. (2-LED)	Exp. (2-LED)	Sim. (3-LED)	Exp. (3-LED)
Irradiation size (mm×mm)	26×30	27×30	26×30	34×44
Intensity on solar cell (mW)	808	560	1189	850
Lens system efficiency (%)	38.9	26.9	38.1	27.2
Output from solar cell (mW)		196		316
PV conversion efficiency (%)		34.9		37.2

In all the experiments in this research, the intensity obtained at the target position or solar cell is measured by an intensity meter with a round shape detector with a diameter of 50 mm. Theoretically, the LED-array OWPT systems with configuration A will have the same irradiation size and lens system efficiency no matter how many LEDs installed.

From Table 5.1, the measured irradiation size of the 2-LED array OWPT system was very similar with the simulation result, which was around 27 mm × 30 mm. However, the irradiation size of the 3-LED array OWPT system measured in experiment was slightly larger than the simulation result. This difference is caused by alignment deviation in the experiment. The deviation will be easily happened when aligning the optical axis of different optical components in the experiment of the LED-array OWPT system, and such deviation will finally cause the displacement of the irradiation spots from different LED light sources at the target transmission distance. Suppressing the alignment deviation is one of the key targets when operating the LED-array OWPT system. The discussion about the issue of the alignment deviation of the LED-array OWPT system will be presented in detail in the section of 5.4.2 later. The received intensity of the solar cell measured in the experiment is not agreement with the simulation results. This can be explained by many uncertain elements in experiment such as increase of junction temperature of LED light source, the smaller effective aperture size of the applied lens, or the low accuracy of the intensity meter used in the experiment. The lens system efficiency can be calculated out around 38% in simulation and 27% in experiment. The intensity loss in the LED-array OWPT system with configuration A mainly occurs between the LED array and the collimation lenses as discussed. The output of the 2-LED array OWPT system measured from the solar cell was 196 mW, and 316 mW of the 3-LED array OWPT system. Compared with the experimental results of 223.9 mW output power of the single-LED OWPT system shown in the section 4.1, the output of the 2-LED array OWPT system is even lower. This result is consistent with the prediction based on the analysis of simulation results which stated in the section 5.3.1. A part of the performance degradation is caused by irradiance reduction due to lens loss and larger irradiation area. The output of the 3-LED array OWPT system is increased to about 1.5 times higher than that of single-LED OWPT system, and it means that the overall efficiency of the 3-LED array OWPT system with configuration A is deteriorated to about half comparing with the single-LED OWPT system. Essentially, irradiance reduction leads to lower photovoltaic conversion efficiency. However, as the photovoltaic conversion efficiency value shows in Table 5.1, with

the number of LEDs increased, the irradiance on the surface of the solar cell strengthened, and thus the photovoltaic conversion efficiency increased from 34.9% of the 2-LED array OWPT system to 37.2% the of 3-LED array OWPT system. By calculation, the radiant intensity of the 2-LED array OWPT system with configuration A is 69mW/cm2, which is about 0.7 times of sunlight irradiance (AM1.5G), and the radiant intensity of the 3-LED array OWPT system with configuration A will be 105mW/cm2 if no alignment deviation happens, which makes the radiant intensity to be around 1.05 times of AM1.5G. Therefore, the LED-array OWPT with configuration A can still provide a high output with high photovoltaic conversion efficiency if the number of LEDs is large enough.

Then, the experiment of the LED-array OWPT system with configuration B will be discussed. Same as the experiment of configuration A, the experiment of the configuration B with 2-LED and 3-LED array was held. The experimental setups of the 2-LED and 3-LED array OWPT system with configuration B are shown in Fig. 5.12 and Fig. 5.13, respectively.

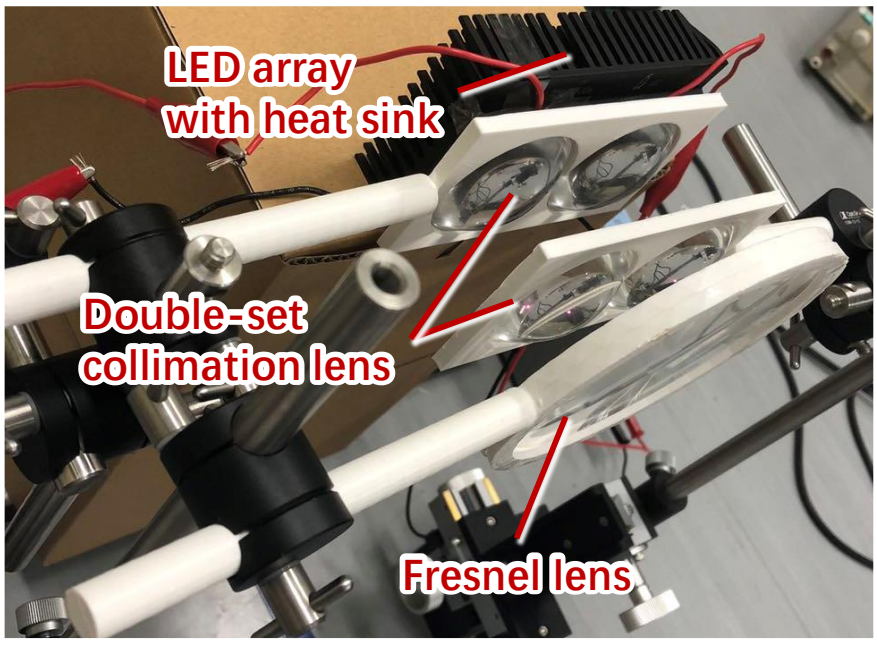

Fig. 5.12 The experiment setup of 2-LED array OWPT system (configuration B)

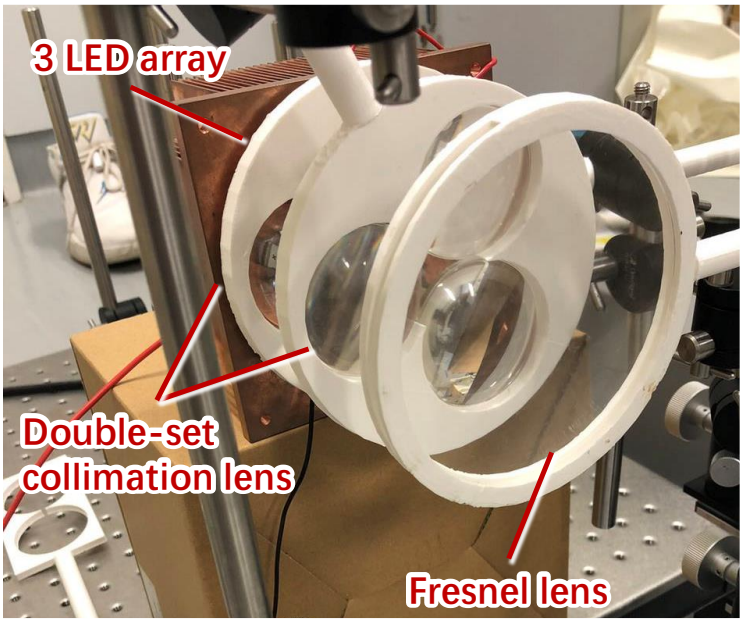

Fig. 5.13 The experiment setup of 2-LED array OWPT system (configuration B)

Same as the arrangement of the LEDs in the experiment of configuration A, the two NIR LEDs were arrayed side by side with 50 mm distance in 2-LED array, and in the 3 LEDs array, the 3 LEDs were arrayed as equilateral triangle pattern with 50 mm distance between each two LEDs. Two sets of collimation lenses applied to the system. The first set was closely installed after the LED array, and the second set was placed with a certain distance from the first set, and a Fresnel lens was closely behind the second set of collimation lenses as the image lens. A 34 mm × 50 mm size optical energy receiver that consists of two series connected GaAs solar cell is placed at 1 m away from the transmitting side. The all parameters of the components applied in the experiment of configuration B is exactly the same as the experiment of configuration A that shown in previous paragraph. The Fig. 5.14 shows IR images of the two systems' irradiation spot. Also, the results of both the simulation and the experiment are shown in Table 5. 2.

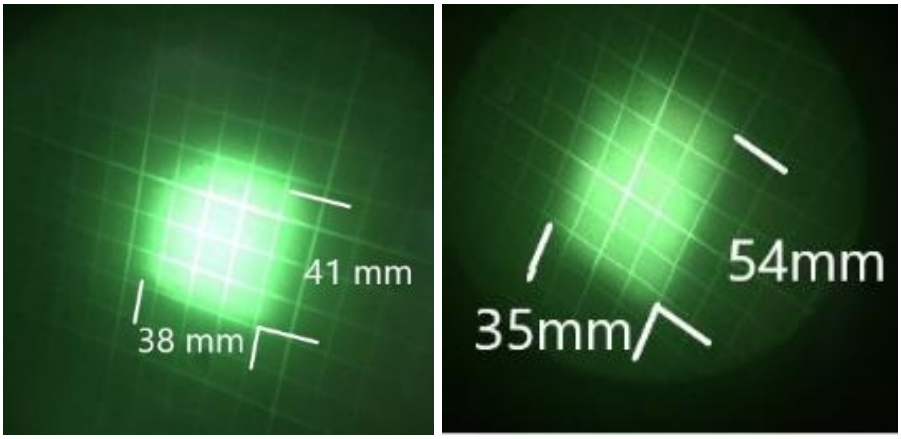

Fig. 5.14 IR image of irradiation spot of 2-LED array (left) and 3-LED array (right) OWPT system in experiment (configuration B).

Table 5.2 Experiment results of configuration B (2 and 3 LEDs array**)**

The brackets show the correct estimation

	Sim. (2-LED)	Exp. (2-LED)	Sim. (3-LED)	Exp. (3-LED)
Irradiation size (mm×mm)	38×41	38×41	38×41	35×54
Intensity on solar cell (mW)	1244	780	1784	960 (1080)
Lens system efficiency (%)	59.8	37.5	57.2	30.8 (35.2)
Output from solar cell (mW)		268		380

Same as the experiment results of configuration A, the irradiation spot size of the 2-LED array OWPT system measured in the experiment is agreed with the simulation result, while the irradiation spot size of the 3-LED array OWPT system in the experiment was larger than the simulation result. Besides, the irradiation spot of 3-LED array OWPT system with configuration B in the Fig. 5.14 shows very blurred boundary if compare with other IR images of the irradiation spot. The reason is still attributed as alignment deviation. With numbers of LEDs increasing, accurately align the optical axis of all the optical components becomes harder,

thus the deviation of the optical axis alignment appears more frequently and obvious displacement of final irradiation occurs. Comparing with configuration A, the lens system efficiency of configuration B increased to around 37%. The main loss occurs between the two sets of collimation lenses. As discussed in the section 5.2, the focal length of the condenser lenses (collimation lenses) should be large to ensure the proper size of the exit pupil of the system, while the distance between the two sets of collimation lenses in configuration B is proportional to the focal length of the collimation lenses. Thereby, the distance between the two sets of collimation lenses will be slightly large and cause part of the intensity lost. By applying collimation lenses with a shorter focal length, the distance between the two sets of collimation lenses can be shorten and the lens system efficiency can be increased. Conversely, the irradiation size will increase and a part of system performance will be sacrificed. Besides, increasing the aperture size of the second-set of collimation lenses can also easily improve the overall efficiency of the lens system, while the system height has to increase accordingly.

As discussed in section 5.2, the irradiation size of configuration B will slightly increase comparing with that of configuration A. Due to the size of the receiver applied in the experiment is 34 mm × 50 mm, comparing the size of the irradiation spot of the 3-LED array OWPT system with configuration B shown in the Fig. 5.14, one of the sides of the solar cell (50 mm) is slightly shorter than the side length of the irradiation spot (54 mm) at the targe distance in the experiment, the accurate amount of intensity that received by the solar cell is difficult to measured and troublesome of the PV conversion efficiency calculation. Therefore, discussion of the photovoltaic conversion efficiency of the solar cell is omitted in Table 5.2. The final output measured from the solar cell is 268 mW for 2-LED and 380 mW for 3-LEDs array OWPT system with configuration B, which is the highest record that achieved in the portable LED-based OWPT ever. Regarding the lens system efficiency shown in Table 5.2, the value of the 3-LED array OWPT system with configuration B is only 30.8%, which is much lower than the 2-LED configuration. Whereas, when the aperture size of the image lens is sufficient

large, the efficiency of the lens system should be consistent no matter how many LED light sources are used in the array. Thus, the value of the lens system efficiency of the 3-LED array OWPT system with configuration B that shown in the Table 5.2 seems unreasonable. The reason can be attributed as a part of intensity cannot be measured correctly by the intensity meter because the detector of the intensity meter is a round plate with 50 mm diameter, which is smaller than one of the side lengths of the irradiation size of the 3-LED array OWPT system with configuration B in this experiment. By estimation based on data from Table 5.1 and Table 5.2, the accurate intensity at the target position should be around 1080 mW, and the lens system efficiency can be calculated as 35.2% based on this value. The estimated value is shown in brackets of Table 5.2. The radiant intensity of the 2-LED and 3-LED array OWPT system with configuration B can be figured out based on the experiment data shown in Table 5.2, which is around 50 mW/cm^2 and 69 mW/cm^2. Such radiant intensity approximately equals to 0.5 times and 0.7 times of sunlight radiance. Although, the photovoltaic conversion efficiency of configuration B is not shown in the Table 5.2 due to the difficulty of measurement, by the theoretical analysis based on the radiant intensity of the irradiation spot, it should be relatively lower compared with the experiment value of configuration A when the number of the LEDs is the same. Comparing the experimental results of the two configurations, configuration B can achieve higher output power than configuration A when the number of LEDs is small. In spite of the larger irradiation spot size and lower photovoltaic conversion efficiency of configuration B, more intensity can be transmitted to the target distance with high efficiency of the lens system. On the other hand, it can be predictable that the PV conversion efficiency of configuration A might be high enough to compensate its drawback on total transmitted intensity if the number of LEDs beyond a certain value, and the final output can be close to or even exceed the output of configuration B which has the same number of LEDs. With the number of LEDs keeping increasing, the photovoltaic conversion efficiency of the solar cell in both configurations will reach the theoretical limitation value, and then configuration B will still have higher output power amount.

5.4.2 Alignment deviation analysis of the LED-array OWPT system

As discussed in the previous section, the alignment deviation is one of the biggest issues in the experiment of LED-array OWPT system. The core factor that the novel array method proposed in this thesis can rearrange the light intensity and make the irradiation spot from different LED light sources overlapped at the target transmission distance is based on the accurate collimation of the light beam before the image lens. Therefore, the optical axis of the optical components in the LED-array OWPT system need to be precisely aligned. Any deviation occurs during optical components aligning will cause the displacement of the irradiation spot at the target distance, which means the irradiation spots from different LED light sources cannot be perfectly overlapped and cause the boundaries of the irradiation spot blurred, thus the entire size of the irradiation area will increase while the radian intensity of the irradiation spot will decrease, reversely. For final manufacturing of commercial products, um-class accuracy can be applied if critically required. For example, when coupling a laser to a single-mode optical fibre, the accuracy is about 1 um because the fibre core diameter is around 10 um. On the other hand, an accuracy of about 10 um is easier than optical fibre, and an accuracy of about 0.1 mm is sufficiently usable in industrial products. However, at current experiment as initial temporal consideration, the lens holder is made by 3D printer, and the accuracy of the 3D printer is hard to guarantee. 1 mm or 2 mm deviation during the printing is normal. Therefore, it is difficult to completely suppress the displacement of the irradiation spot and performance drop caused by the misalignment in the experiment. In the Fig. 5.15, a specific example of the misalignment of the optical components in the LED-array OWPT system is shown.

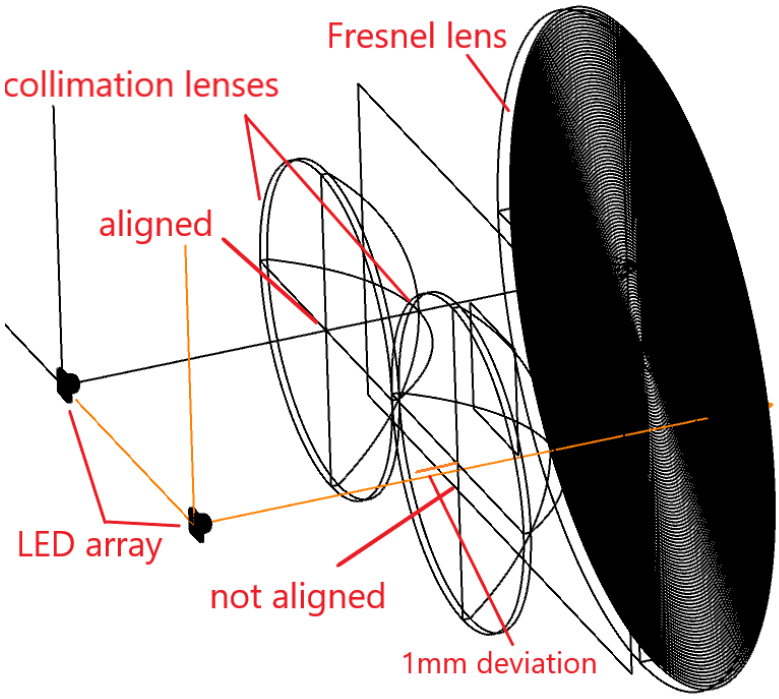

Fig. 5.15 Schematic illustration of alignment deviation in LED-array OWPT system

The Fig. 5.15 shows the schematic illustration of alignment deviation of LED-array OWPT system. From Fig. 5.15, the LED at left is accurately aimed the centre point of collimation lens, but 1 mm deviation exists between the right LED and the corresponding collimation lens, and this deviation makes the collimation lens not aligned with LED. Such small deviation will cause displacement of final irradiation and cause irradiance from different LEDs not correctly overlapped. The Fig. 5.16 shows the irradiation spot displacement caused by 1 mm alignment deviation of 2-LED array OWPT system with configuration in simulation and experiment, respectively. It can be seen from Fig. 5.16, even the position deviation is only 1 mm on one of the collimation lenses, the displacement of irradiation spot at 1 m transmission distance already becomes very obvious. Once the displacement of the irradiation spot occurs, only part of irradiation area overlapped, and the entire size of the irradiation area will greatly be enlarged,

while the radiant intensity of the irradiation will reduce, then deteriorates the photovoltaic conversion efficiency of solar cell.

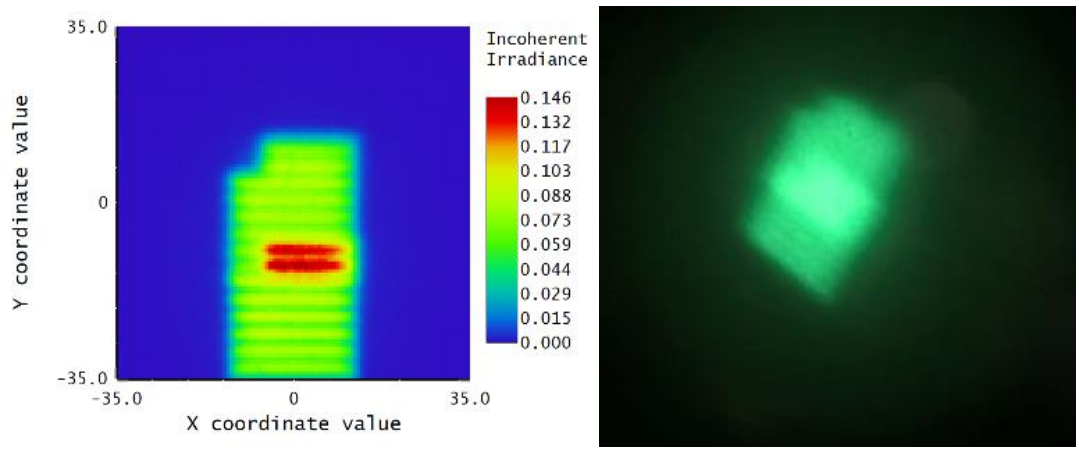

Fig. 5.16 Displacement of irradiation caused by alignment deviation (left: simulation; right: experiment)

The Fig. 5.17 shows the detailed analysis of alignment deviation of 2-LED array OWPT system with configuration A and 1 m transmission distance based on simulation model. Basically, 0.1 mm deviation between light source and condenser lens will cause 2 mm displacement on final irradiation, and 1 mm deviation will cause 20 mm displacement, accordingly. Considering the size of the irradiation spot at target distance of such system is 27 mm × 30 mm, just 1 mm deviation will largely deteriorate system performance. There are two important points in Fig. 5.17. First one is when alignment deviation increased to 0.7 mm, the overlap rate will decrease to 50%, which means half of the irradiation spot from different LEDs is separated and the size of the irradiation area will be double. Another point is when alignment deviation increases to 1.3 mm, irradiation displacement will become 27 mm, which means irradiation spots from two LEDs are completely separated and no overlap region at all. As for the application that the irradiation spot has similar designed size with the solar cell, the alignment deviation needs to be controlled at least smaller than 0.3 mm to

ensure around 77% overlapped region based on analysis, which is still within acceptable range.

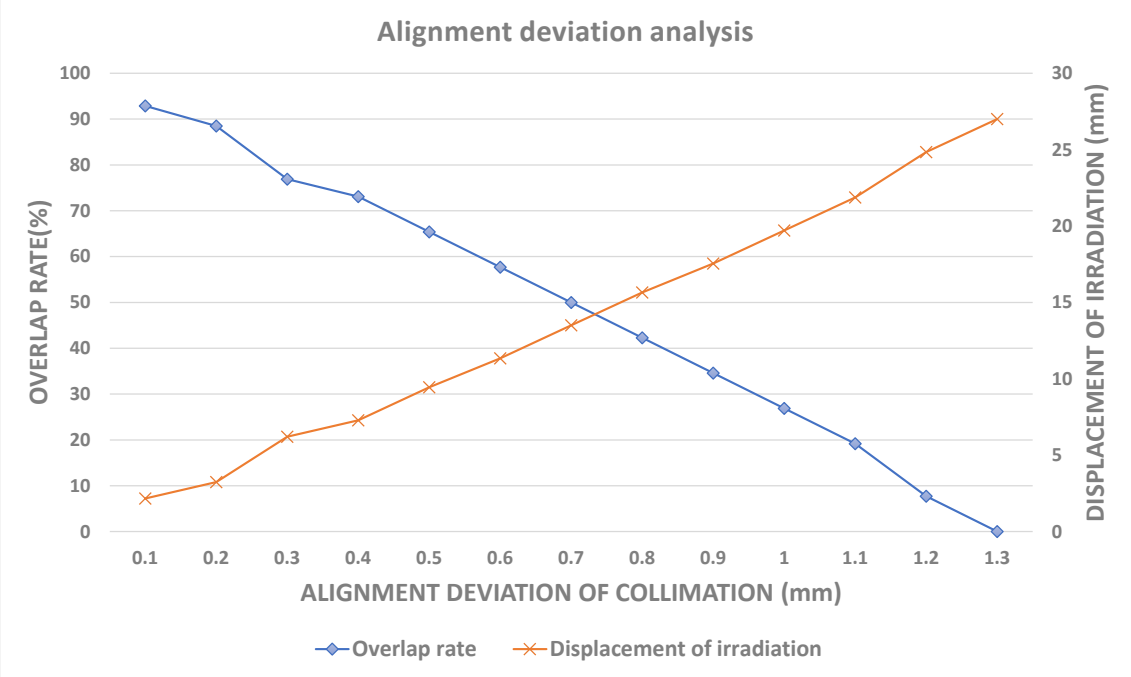

Fig. 5.17 Analysis of alignment deviation and corresponding irradiation spot displacement in LED-array OWPT system

As for the LED-array OWPT system with configuration B, the alignment deviation is harder to restrain due to the number of the optical components increase a lot, and displacement of final irradiation spot will be larger. Also, if transmission distance increased, irradiation displacement will also increase with roughly linear relation. Hence, longer the transmission is, or more lenses are applied in the system, more serious displacement will be. What's more, not only the alignment deviation on panning direction will cause the displacement of the irradiation spot at target distance, but also the deviation on pitching and rolling direction. The Fig. 5.18 shows the deviation that might happen on different directions.

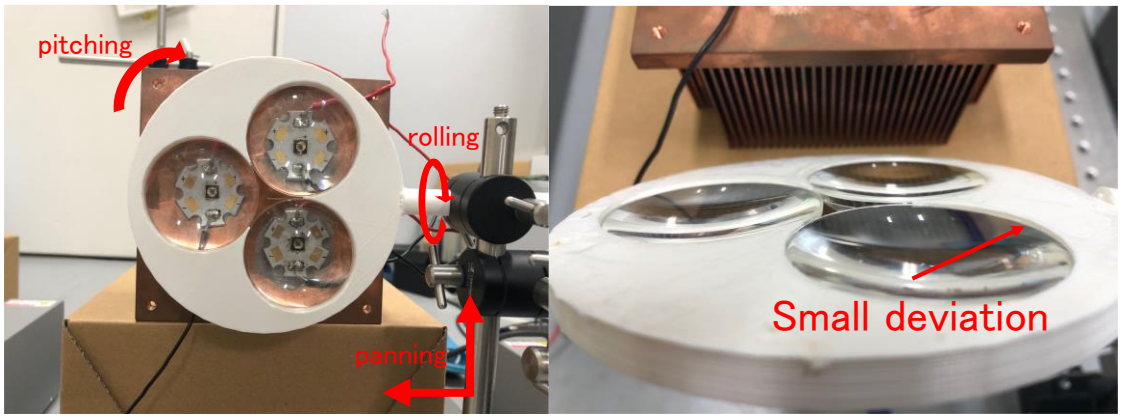

Fig. 5.18 The causes of alignment deviation in LED-array OWPT system

As the Fig. 5.18 shows, due to the different degree of freedom of the lens holder, the alignment deviation of the optical components might happen on panning, pitching and rolling direction. Moreover, due to the manufacturing error of the lens holder during printing, the inability of the lens holder and the lens to fit perfectly will also causes the deviations. All such deviation will cause the misalignment of the optical axis of the optical components, and thus makes the irradiation spot displacement at the target transmission distance. Therefore, the suppression of the alignment deviation is hard in the prototype experiment, and the displacement of irradiation spot caused by misalignment of the optical components will deteriorate the radian intensity, then declines photovoltaic conversion efficiency of solar cell. Besides, much more intensity will be lost on the surface of the solar cell due to enlarged size of irradiation spot. Thus, high accuracy needs to be ensured during designing and manufacturing. It should be mentioned that, the displacement of the irradiation spot caused by optical components misalignment will also happen in the cause of single-LED OWPT system. However, due to only one light source are used in the system, the misalignment of the optical components will cause the displacement of the only irradiation spot, while the size and the radiant intensity of the irradiation spot at the target transmission distance will unchanged. As a result, it only needs to modify the aiming direction of the OWPT system and then the power transmission can be processed normally. Therefore, although the displacement of the irradiation spot caused by

misalignment of the optical components also existed in the cause of single-LED OWPT system, its negative impact is far less than that of the LED-array OWPT system.

5.4.3 Summary of the characteristics of the LED-array OWPT system

In the section 5.4, the characteristics of the LED-array OWPT system with two kinds of configurations is studied and discussed based on the experiment results. The practical dimension of LED-array OWPT system with the two configurations is a cylinder with a diameter of 120 mm as the base and a length of 43 mm, and the volume of which is even smaller than the single-LED OWPT system. Thus, the LED-array OWPT system can easily achieve good portability. In the experiment, the data from totally four configurations of the LED-array OWPT system, which are the configuration A with 2-LED array, the configuration A with 3-LED array, the configuration B with 2-LED array, and the configuration B with 3-LED array, were obtained and then compared with the simulation results. As a result, the irradiation spot size measured from experiment of 2-LED array system is agreed with the simulation results, while in the experiment of 3-LED array system, the irradiation spot size is slightly larger than the simulation data. The reason is attributed as the displacement of the irradiation spot caused by alignment deviation of the optical components. The efficiency of the lens system of the configuration A and configuration B is around 27% and 37% respectively, and such value is slightly lower than the simulation results. As for the output power with 1 m transmission distance, the configuration A with 2-LED array can achieve 196 mW, the configuration A with 3-LED array can achieve 316 mW, the configuration B with 2-LED array can achieve 268 mW, and the configuration B with 3-LED array can achieve 380 mW, separately. Due to the higher efficiency of the lens system, configuration B of the LED-array OWPT system can realize higher output power from the long distance, and the 380 mW output power is the highest record of portable LED-based OWPT system ever. The analysis of the alignment deviation of the optical components during the experiment of the LED-array OWPT system is also a necessary point. According to the simulation and

experiment data of the characteristics of the displacement based on alignment deviation, in the configuration A, 0.1 mm deviation between light source and condenser lens will cause 2 mm displacement on final irradiation, and 1 mm deviation will cause 20 mm displacement. Considering the size of the irradiation spot is small, alignment deviation needs to be controlled at least smaller than 0.3 mm in configuration A. On the other hand, due to more lenses are used in the configuration B, the negative impact caused by alignment deviation will be much sever, thus the aligning of the optical components should be more accurately compared with configuration A. The difficulty of eliminating the alignment deviation enhances with the increase of the number of LEDs applied in the system. Moreover, the alignment deviation of the optical components is not only in panning direction, but also caused by pitching and rolling of the optical components. Therefore, elimination of the alignment deviation of the LED-array OWPT system is a very critical target when design and manufacture.

Chapter 6. Future prospect of the portable LED-based OWPT system for the compact IoT

The LED-based OWPT system has its unique advantages and can be foreseen to be used in various fields in the near future. However, the research of LED-based OWPT system still needs a lot of accumulation. From the performance of the system itself, the total output and total efficiency of the LED-based OWPT system are closely related to the research progress of the LED light source and the solar cell. At current stage, the performance of the LED-based OWPT system still has a lot of room for improvement. Such potential is not only manifested in the advancement of the research on light source and solar cell in the near future, but also reflected in the fact that there is no special design of the various components for OWPT applications in the market currently. The limitation on the light source side is generally manifested as the need for optimization and functionalization specially for the OWPT technology. Among the productized LEDs, high-efficiency LEDs are generally concentrated in the near-infrared band (700 nm-1100 nm), and their efficiency can reach 40%-50%. In the short wavelength range, most LEDs are designed for lighting purposes, and their light-emitting chip sizes and divergence angles are generally large, so even if the efficiency is high enough, it is not suitable for OWPT system. Using short-wavelength light as the transmission medium, because the energy of a single photon is large, lower heat production can be achieved on the solar cell side. In addition, according to the Rayleigh criterion, short-wavelength light can be focused in a smaller area than long-wavelength light. Therefore, the development of high-efficiency and high-output short-wavelength LED light sources is of great significance to OWPT applications. In addition, the research on LEDs with the relatively safe 1500 nm - 2100 nm long-wavelength for human eyes and the improvement of the efficiency and output are also crucial for OWPT applications. The efficiency of LED light sources is expected to reach 80% in the near future, and the performance of LED-based OWPT will be greatly improved by then. In addition to the efficiency of the LED itself, designing the package lens of LED especially for OWPT applications is also very important. For example, by

optimizing the microstructure of the LED module to reduce the total reflection loss inside the package lens. These LED light sources specially designed and developed for OWPT applications can greatly enhance the flexibility and diversification of the design of OWPT system.

On the other hand, in terms of solar cells, the characteristics of solar cells is not easy to further improve due to the performance of existing solar cells is already close to the theoretical limit. Therefore, the optimization of solar cells in the future should focus on the development of solar cells suitable for short wavelengths or long wavelengths (1500 nm-2100 nm) that are safe for human eyes. On the other hand, even if the photovoltaic conversion efficiency of solar cells is close to the theoretical limit currently, there are some ways to further optimize the efficiency. Research reports have shown that by optimizing the number, orientation and pattern of grid electrodes on the surface of solar cells, the efficiency of solar cells under monochromatic light can be improved. Especially under high radiant intensity light, the improvement of the efficiency is more obvious. Besides, the applying a light trapping layer on the surface of the solar cell can reduce the reflection loss and enhance the collection efficiency of the solar cell, which is considered to be effective in improving the system efficiency in the practical applications where the oblique irradiation is very common. Therefore, in the near future, the solar cell used in the OWPT system can be a solar cell specifically designed for OWPT applications instead of the conventional solar cell that used to receive sunlight. Such type of solar cell has a specially optimized grid electrode pattern or film layer, which can achieve maximum efficiency in OWPT applications. In addition, improving the heat dissipation of solar cells and reducing costs are key factors for the widespread promotion of the OWPT application in the future. At present, the optimal type of the solar cell applied in the OWPT system is GaAs solar cell. Compared with the most common Si solar cells, the cost of GaAs solar cells is still relatively high. Although in the LED-based OWPT system, since the size of light irradiation spot is designed to be small, the size of the solar cell required for a single load is small as well. However, considering the rapid increase in the number of IoT terminals in a certain space in the future, the total number

of solar cells required is also very large. Therefore, the suppression of the cost of solar cells is related to whether the OWPT system can be widely used as a popular wireless power supply method. On the other, the development of optical antennas might also be expected to become the receiver of the future OWPT system. In general, for the LED-based OWPT system, its characteristics are closely related to the research progress in the field of LED light sources. Because the relatively short transmission distance (less than 10 m), the requests for beam quality are not large, thus requirements for the progressing of LED light sources are relatively simple. The efficiency of LED light sources is expected to be greatly improved in a short time, while smaller chips and higher intensity density can also be achieved. Considering the improvement of the LED characteristics in the near future and the theoretical efficiency limit value of the solar cell, the LED-based OWPT system is expected to achieve a performance increase of several to tens of times in the near future. The single-LED OWPT system can achieve 1 watt to several watts output power, while the LED-array OWPT system can realize output of more than tens of watts. At the same time, while the total efficiency and total output of the LED-based OWPT system are improved, the device dimension can also be reduced according to demand. In addition, research on the sub-modules of the OWPT system, such as the visualization of near-infrared irradiation spot, object detection system, transmitter-receiver communication system, emergency brake system, etc., can improve the functionality of the LED-based OWPT system and expand its application scenarios.

Chapter 7. Conclusion

As a wireless power transmission technology, the OWPT system has great potential in various application scenarios. Especially for the growing field of IoT devices, the unique long-distance transmission, simple configuration, portable size, and no noise interference of the OWPT system can greatly reduce the cost of labor and money caused by wiring, traditional contact charging or battery replacement and realize simple and fast remote power supply. Therefore, the OWPT technology can improve the function and performance of IoT devices and extend the operating time as well. At current stage, the research on the OWPT system, especially the LED-based OWPT system is still at the initial stage. No research report has systematically studied and analyzed the mathematical model, component selection, system design, system characteristics and potential of the LED-based OWPT system. In this thesis, the systematic research and analysis of the portable LED-based OWPT system for the compact IoT terminals is presented. The results achieved in this research is concluded as follows.

1. **Investigating the components of LED-based OWPT system, and proposing the proper selections of the components based on their characteristics in LED-based OWPT system.**

The existing typical light source types is investigated, and analyzed whether they have the necessary characteristics for OWPT applications, which are easy beam forming, high intensity output, high conversion efficiency and monochromaticity. As a result, LED is proved to be an excellent light source of OWPT system. From the perspectives of intensity output, wavelength, divergence angle, grid electrode pattern, package design, and uniformity of distribution, various parameters and designs of the LED are analyzed, and the most ideal characteristics of the LED as the light source of the OWPT system are discussed, which are wavelength in near-infrared band, as small as possible light-emitting chip size, sufficiently small divergence angle, dome-type package lens, and the electrode pattern of the gold bonding wire connected to the corner or edge of the chip. Regarding the optical energy receiving devices, the single-junction GaAs solar cell is the most suitable

choice for OWPT system at current stage. The plano-convex lens, aspheric lens and Fresnel lens are the proper optical components for OWPT system. The AR coating is necessary of the lenses to reduce reflection loss. The material of the lens has little effect under normal circumstances, but in special cases, a material with a larger refractive index is appropriate in order to increase the NA value of the lens.

2. The basic configuration design of the portable LED-based OWPT system for compact IoT.

The double-lens optical system can simultaneously achieve high efficiency, small irradiation spot size, and compact system dimension by adjusting various parameters, which makes it to be the most suitable choice for OWPT system. By establishing the mathematical model of the optical system, the ideal value range of the parameters of the optical system for LED-based OWPT system is provided. In summary, the distance between two the condenser lens and image lens should be in the range of 70 mm - 110 mm, and the focal length of the condenser lens should be at least larger than 12 mm, while the aperture size of the image lens should be above 80 mm (the ideal value is 100 mm). The simulation results of the portable LED-based OWPT system are obtained. As a result, 575.3 mW intensity can be transmitted and form an irradiation spot with 2.1 cm × 2.3 cm at 1 m distance with 83.2% efficiency of the optical system. The average radiant intensity on the 1.7 cm × 1.7 cm size solar cell is 199.1 mW/cm^2, which is around twice of sunlight irradiance (AM1.5G). The tolerant distance of the portable LED-based OWPT system is confirmed as -370 mm to +310 mm, and 45° is set as the maximum tilt angle of irradiation based on 100 mW of the minimum transmission power standard of the OWPT system. The mini-type LED-based OWPT system for short distance range is analyzed. The configuration with movable image lens (fixed value of f_2' parameter/variable value of d parameter) is proved to be the optimal choice of lens system. The 20 mm focal length of condenser lens, 46 mm focal length of image lens and 50 mm of both lenses' aperture is proved as proper value for the parameters. The mini-type LED-based OWPT system can effectively

transmit power in the range from 100 mm to 1000 mm with above 80% efficiency. Regarding the large-size LED-based OWPT system for long transmission distance, the minimum dimension of the system is around 13 cm × 12 cm × 12 cm. The irradiation spot with around 5 cm side length can be obtained at 3 m transmission distance, the portability of the LED-based OWPT system can still be remained.

3. Characteristics analysis of the single-LED OWPT system with different configurations and application scenarios.

The characteristics of the LED-based OWPT system is confirmed by experiment. As a result, the irradiation spot with 2.1 cm × 2.3 cm size was observed at the 1 m transmission distance. The lens system efficiency was measured as 77%, and the output from the solar cell was measured as 223.9 mW with 41.7% photovoltaic conversion efficiency of the solar cell. The overall efficiency of the portable LED-based OWPT system was 6.3%. Besides, the transmission range from 700 mm to 1200 mm was confirmed as tolerant distance in experiment, which is agreed with the simulation results. In addition, the experiment of the modularized portable LED-based OWPT system was shown. The entire size of the modularized portable LED-based OWPT system is 116 mm × 116 mm × 132 mm. The thermal analysis of the portable LED-based OWPT system was analyzed by experiment. As a result, the temperature climbing on both LED side and solar cell side are concentrated in the first 5 mins operation, and the deterioration of the system performance caused by such temperature climbing was small. After 40 minutes of continuous operation, the decline of the system output is only around 10%. According to the experiment data of thermal analysis, simple heat sink with thermal grease is proved to be enough for heat dissipation of the portable LED-based OWPT system. The experiment of the mini-type LED-based OWPT system for short-distance range was processed. The dimension of the system is smaller than 5 cm × 5 cm × 5 cm in most cases, and the effective power transmission range of the system is 200 mm to 1000 mm. Besides, the irradiation spot with smaller than 3 cm side length can be obtain from 100 mm to

780 mm. The highest output power of the mini-type LED-based OWPT system can be achieve at 400 mm distance, which is around 200 mW. The experiment results of the large-size LED-based OWPT system for the long-distance range was obtained. The highest output was achieved by the LED-based OWPT system with a 200 mm focal length and 210 mm aperture size Fresnel lens in the experiment. Such configuration can realize above 200 mW output power from the solar cell in the range from 1 m to 2 m transmission distance, and above 100 mW output power in the range from 2 m to 3 m, which makes the effective power transmission range to be 1 m to 3 m of the LED-based OWPT system. The dimension of the system is 236 mm × 210 mm × 210 mm. Besides, the unideal irradiation conditions of the LED-based OWPT system were analyzed and discussed. Firstly, the characteristics of the portable LED-based OWPT system under the oblique irradiation was confirmed based on the experiment data. In general, the portable LED-based OWPT system can transmit above 50% of the total intensity to the solar cell with smaller than around 45° tilt angle, and such tilt angle can be regarded as a threshold for judging whether the portable LED-based OWPT system can achieve effective power transmission. Secondly, the characteristics of the portable LED-based OWPT system under the irradiation with tremor was confirmed based on the experiment data. From the experiment data, after short-term (0 s to 80 s) continuous operating, the output of the system can still be relatively steady, while the fluctuation of the system output becomes very large when the operation period beyond 80 s. Besides, when the weight of the device increasing, the fluctuation of the system output caused by tremor is obviously strengthened, and there may be a significant output decline in short-term continuous operation when the weight of devices increased to around 1 Kg.

4. Design and characteristics analysis of the LED-array OWPT system for achieving high output power.

In this research, a novel array method of the LED-array OWPT system is proposed, which can realize the great compression of the system dimension while the degree of the integration of the LED light sources can be improved. Two kinds

of the configuration of the LED-array OWPT system are designed. As a result, the single-set collimation lenses configuration (configuration A) can realize simple and light configuration and small irradiation spot, while the efficiency of the lens system is relatively low. The double-set collimation lenses configuration (configuration B) can improve the overall efficiency of the lens system, while the irradiation spot size will slightly increase. Based on the simulation results, the irradiation size of the configuration A is 2.7 cm × 3 cm at 1 m distance, while the size of the irradiation spot increases to 3.8 cm × 4 cm at 1 m distance in configuration B. The lens system efficiency of the configuration A and configuration B is around 39% and 60%, separately. The highest intensity received at the target distance is around 2500 mW by configuration B with 4-LED array. The practical dimension of LED-array OWPT system with the two configurations is a cylinder with a diameter of 120 mm as the base and a length of 43 mm. In the experiment, the irradiation spot size measured from experiment is almost agreed with the simulation results. The efficiency of the lens system of the configuration A and configuration B is around 27% and 37%, respectively. The highest output power at 1 m transmission distance can be achieved by the configuration B with 3-LED array, which is 380 mW. The analysis of the alignment deviation of the LED-array OWPT system was processed. As a result, the alignment deviation needs to be controlled at least smaller than 0.3 mm in the LED-array OWPT system.

5. Future prospect of the portable LED-based OWPT system for compact IoT.

From the performance of the system itself, the total output and total efficiency of the LED-based OWPT system are closely related to the research progress of the LED light source and the solar cell. The limitation on the light source side is generally manifested as the need for optimization and functionalization specially for the OWPT technology. The development of high-efficiency and high-output short-wavelength LED light sources is of great significance to OWPT applications. In addition, the research on LEDs with the relatively safe 1500 nm-2100 nm long-

wavelength for human eyes and the improvement of the efficiency and output are also crucial for OWPT applications. The efficiency of LED light sources is expected to reach 80% in the near future, and the performance of LED-based OWPT will be greatly improved by then. In addition to the efficiency of the LED itself, designing the package lens of LED specially for OWPT applications is also very important. As for the solar cells, the characteristics of solar cells is not easy to further improve due to the performance of existing solar cells is already close to the theoretical limit. Therefore, the optimization of solar cells in the future should focus on the development of solar cells suitable for short wavelengths or long wavelengths (1500 nm-2100 nm) that are safe for human eyes. In addition, improving the heat dissipation of solar cells and reducing costs are key factors for the widespread promotion of the OWPT application in the future. In general, considering the improvement of the LED characteristics in the near future and the theoretical efficiency limit value of the solar cell, the LED-based OWPT system is expected to achieve a performance increase of several to tens of times in the near future. The single-LED OWPT system can achieve 1 watt to several watts output power, while the LED-array OWPT system can realize output of more than tens of watts. At the same time, while the total efficiency and total output of the LED-based OWPT system are improved, the device dimension can also be reduced according to demand, and effective power transmission to longer distance becomes possible.

Conclusively, the portable LED-based OWPT system was realized by integrating the characteristics of semiconductor light sources, photovoltaic cells and optical components based on the property of optical wireless power transmission technology. Such system has a relatively simple configuration and portable size, which can conveniently realize effective long-distance power supply for electronics such as IoT terminals. This thesis has guiding significance not only for the general public but also for researcher and developers in application areas who may use the optical wireless power transmission technology, as well as specialists in various functional elements and devices that will make up this technology.

Acknowledgement

First of all, I am very grateful to my supervisor, Prof. Miyamoto, who have provided me selfless help in the past 3 years during the doctoral course, not only in the aspect of study and research, but also in the daily life. Secondly, I want to show my appreciation to all the students in the Koyama. Uenohara. Miyamoto Lab who helped me during the research. I thank Dr. Mori of Yamashita Denso Corporation for discussion of basic of lens design and Mr. Y. Ishida for preparation of basic experimental configuration. I also want to show my gratitude to Prof. Koyama, Prof. Uenohara, Prof. Tokuda, Prof. Maruyama and Prof. Miyamoto for the examination and comments of my doctoral dissertation. Last my thanks would go to my beloved family for their continuous support and encouragement.

List of publications and papers

Publications and papers

Published journal papers:

1. Yuhuan Zhou and Tomoyuki Miyamoto, "*200 mW-class LED-based optical wireless power transmission for compact IoT,*" Jpn. J. Appl. Phys., vol. 58, SJJC04, 2019.
2. Yuhuan Zhou and Tomoyuki Miyamoto, "*400 mW class high output power from LED-array optical wireless power transmission system for compact IoT,*" IEICE Electronics Express (ELEX), 17.20200405, 2020.
3. Yuhuan Zhou and Tomoyuki Miyamoto, "*Characterization of the portable LED-based OWPT system for compact IoT,*" (to be submitted).

International Conferences:

1. Yuhuan Zhou and Tomoyuki Miyamoto, "*Over 100mW class optical wireless power transmission for compact IoT,*" 23rd Microoptics Conf. (MOC2018), J-5, Taipei, Taiwan, Oct. 2018 (Oral).
2. Yuhuan Zhou and Tomoyuki Miyamoto, "*LED-based high power optical wireless power transmission for compact IoT,*" The 1st Optical Wireless and Fiber Power Transmission Conf. (OWPT2019), S2-06, Yokohama, Apr. 2019 (Oral).
3. Yuhuan Zhou and Tomoyuki Miyamoto, "*Optimized LED-based optical wireless power transmission system configuration for compact IoT,*" 24rd Microoptics Conf. (MOC2019), P-29, Toyama Nov. 2019 (Poster).
4. Yuhuan Zhou and Tomoyuki Miyamoto, "*Design of LED-based optical wireless power transmission for long distance operation and increased output power,*" The 2nd Optical Wireless and Fiber Power Transmission Conf. (OWPT2020), OWPT3-04, Yokohama, Apr. 2020 (Oral, only distribution of abstract due to COVID-19).

5. Yuhuan Zhou, Mingzhi Zhao and Tomoyuki Miyamoto, "*Optimization of dimension and output power of the portable LED-based OWPT system for compact IoT,*" The 3rd Optical Wireless and Fiber Power Transmission Conf. (OWPT2021), Online, Apr. 2021 (Oral).

Domestic conferences:

1. Yuhuan Zhou and Tomoyuki Miyamoto, "*Above 130mW class optical wireless power transmission for compact IoT,*" The 79th JSAP Autumn Meeting, Nagoya, 18p-232-13, Sep. 2018 (Oral).
2. Yuhuan Zhou and Tomoyuki Miyamoto, "*LED-based above 200mW optical wireless power transmission for compact IoT,*" The 66th JSAP Spring Meeting, Tokyo, 11p-W611-5, Mar. 2019 (Oral).
3. Yuhuan Zhou and Tomoyuki Miyamoto, "*Optimization of LED-based optical wireless power transmission for compact IoT,*" The 80th JSAP Autumn Meeting, Sapporo, 19p-E204-7, Sep. 2019 (Oral).
4. Yuhuan Zhou and Tomoyuki Miyamoto, "*LED-based optical wireless power transmission system for long distance operation,*" The 67th JSAP Spring Meeting, 15p-B410-8, Tokyo, Mar. 2020 (Oral, only distribution of abstract due to COVID-19).
5. Yuhuan Zhou and Tomoyuki Miyamoto, "*Research on LED-array optical wireless power transmission system designing,*" The 67th JSAP Spring Meeting, 15p-B410-9, Tokyo, Mar. 2020 (Oral, only distribution of abstract due to COVID-19).
6. Yuhuan Zhou and Tomoyuki Miyamoto, "*Designing of LED-array optical wireless power transmission system,*" The 81th JSAP Autumn Meeting, Online, 9a-Z13-9, Sep. 2020 (Oral).
7. Yuhuan Zhou and Tomoyuki Miyamoto, "*LED-based portable optical wireless power transmission system for compact IoT with high performance,*" 電気学会 光・量子デバイス研究会, Online, Oct. 2020 (Oral).

8. Yuhuan Zhou, Mingzhi Zhao and Tomoyuki Miyamoto, "*Experimental Characteristics of LED-array Based Increased Power Optical Wireless Power Transmission System for Compact IoT,*" The 68th JSAP Spring Meeting, Online, 2021 (oral) (to be presented).
9. Mingzhi Zhao, Yuhuan Zhou and Tomoyuki Miyamoto, "*Numerical design for size reduction in light source module of LED-OWPT system,*" The 68th JSAP Spring Meeting, Online, 2021 (oral) (to be presented).

Symposia:

1. Yuhuan Zhou, "*Optical wireless power transmission for compact IoT above 130mW class,*" The 41th Int. Symp. on Optical Comm., Yamanashi, P3-16, Aug. 2018 (Poster).
2. Yuhuan Zhou and Tomoyuki Miyamoto, "*Optical wireless power transmission for compact IoT,*" International Day of Light Symp., Tokyo, Jun. 2019 (Poster).
3. Yuhuan Zhou and Tomoyuki Miyamoto, "*Optical wireless power transmission for compact IoT over 130mW,*" The 42th Int. Symp. on Optical Comm., Yamanashi, P-3-31, Aug. 2019 (Poster).

Articles of specialized books:

Tomoyuki Miyamoto and Yuhuan Zhou, "*小型 IoT 向けの LED を用いた光無線給電,*" 光技術コンタクト（日本オプトメカトロニクス協会発行）, vol. 57, no. 6, pp. 32-38, 2019.

Award:

OWPT2019 Student Paper Award, Apr. 2019.

令和 3 年度電気学会技術委員会奨励賞

Appendix

Slides of Doctoral Final Defense

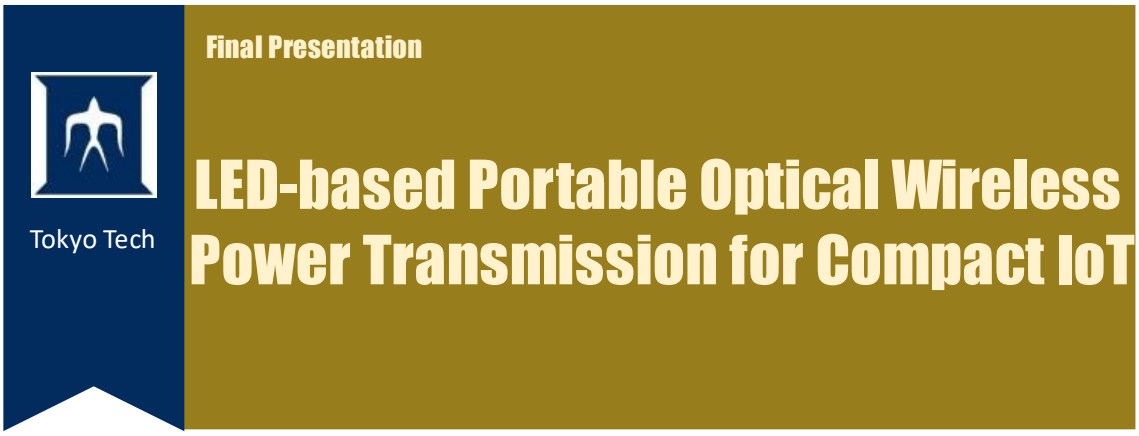

Yuhuan Zhou

18D10456

Electrical and Electronic Engineering

Tomoyuki Miyamoto Lab

2021/02/08

Part. 1

Brief Report of Doctoral Dissertation

Chap.1 Introduction

IoT (Internet of Things): explosive growth in various application fields and is estimated over 125 billion in next 10 years

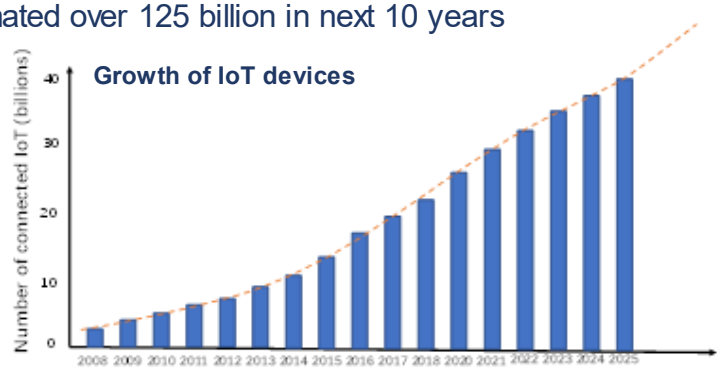

Power supply issue:

- Wiring (Part of fixed position applications): requests laying work, laying space and wires maintenance
- Battery (Part of fixed position and all movable applications): limits devices performance, requests replacement

Optical Wireless Power Transmission (OWPT):

- High power
- Long transmission distance
- Small size
- Simple configuration
- No noise
- Wireless

3

Chap.1 Conception of OWPT

Optical wireless power transmission (OWPT) technology: energy is propagating as the light wave , and be received and conversed into electrical power on photovoltaic cells at remote position

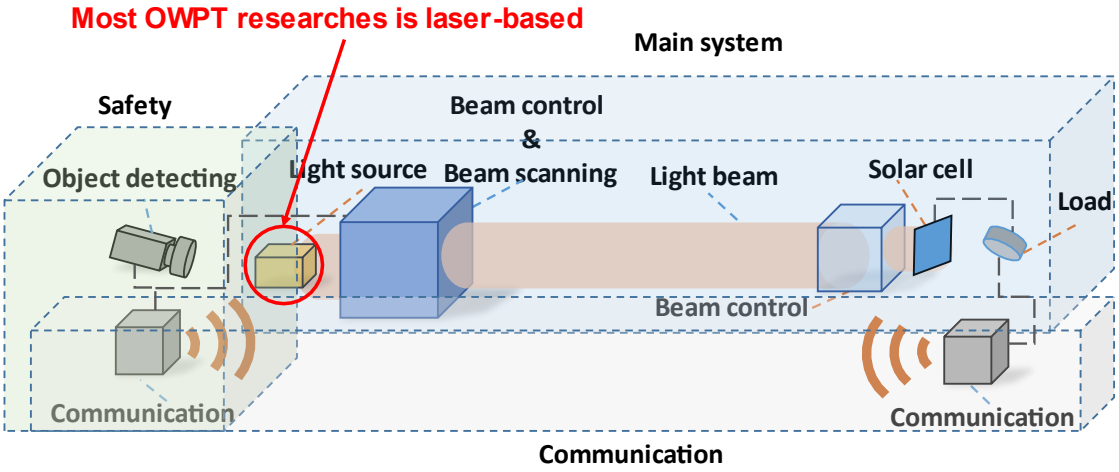

Schematic diagram of OWPT system

4

Chap.2 LED vs Laser

The main comparison between LED and LD as the light source of OWPT system

Light source	LED	LD
Monochromaticity	Sufficiently high	Extremely high
Irradiance/efficiency	High	High
Operating temperature	High	Intermediate
Heat dissipation system	Simple system is enough	High-performance system required
Directionality	Intermediate	Extremely high
Product dimension	Extremely small	Extremely small
Product regulation	Loose	Severe

LED is an ideal choice as the light source of OWPT system

5

Chap.2 Components of LED-based OWPT

Requirements of LED:

- NIR wavelength
- High efficiency and power
- Even and clear distribution
- Small irradiation
- Small divergence

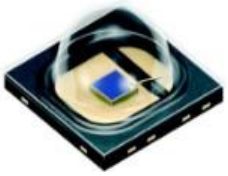

(Osram, SFH 4073AS)

- **Surface-emitting LED**
- **Dome-type package lens**
- **Gold bonding wire connects at the edge or corner of the chip**
- **NIR wavelength**

Solar cell

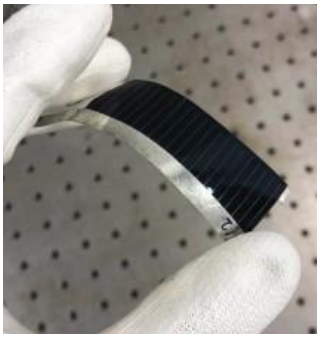

Single-junction GaAs
(Advanced Technology Institute, LLC.)

Optical components

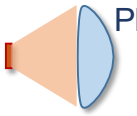

Plano-convex lens
Or
Aspheric lens

Fresnel lens :

- poor capability of image
- small mass, thickness and weight (d=100mm, f=200mm, glass lens: t=15mm, 200 g; Fresnel lens: t=2mm, 20g)

Chap.3 Design of Lens System

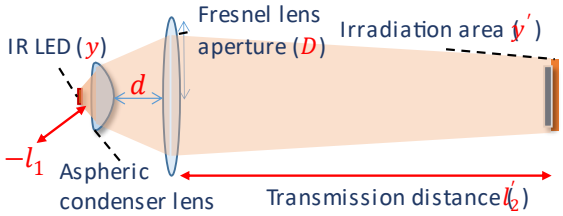

Double-lens configuration

1000 **Transmission distance**

$$\beta = \frac{y'}{y} = \beta_1\,\beta_2 = \frac{l_2'}{f_2'} \times \frac{1}{-l_1 + d\left(1 - \frac{-l_1}{f_1}\right)}$$

LED position -4

Typical 1 m transmission distance

- The focal length of the condenser lens (f_1') and length of system (d) are the key parameters to decide the size of irradiation (increasing exit pupil)
- The balance of system dimension and size of irradiation is critical
- The f_1' needs larger than 12 mm
- The d should be in the range of 70 mm-110mm
- In such condition, the size of irradiation is around 20mm x 20mm

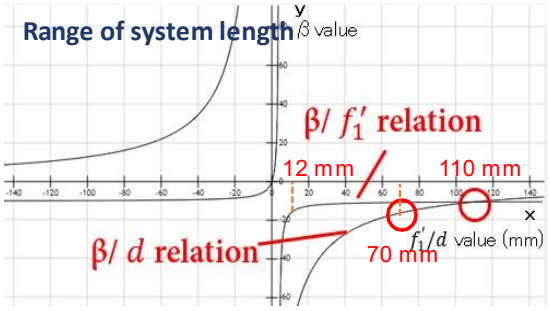

Chap.3 Design of Lens System

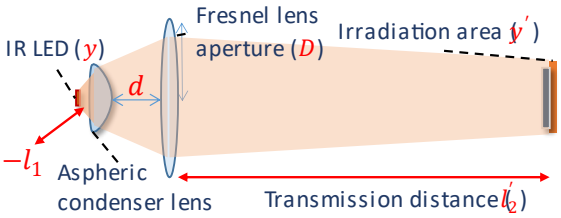

$$D = \frac{\tan(u)(f_1 - x_1)}{-f_1} \times (d + \frac{-x_1 \times f_1}{f_1 + x_1})$$

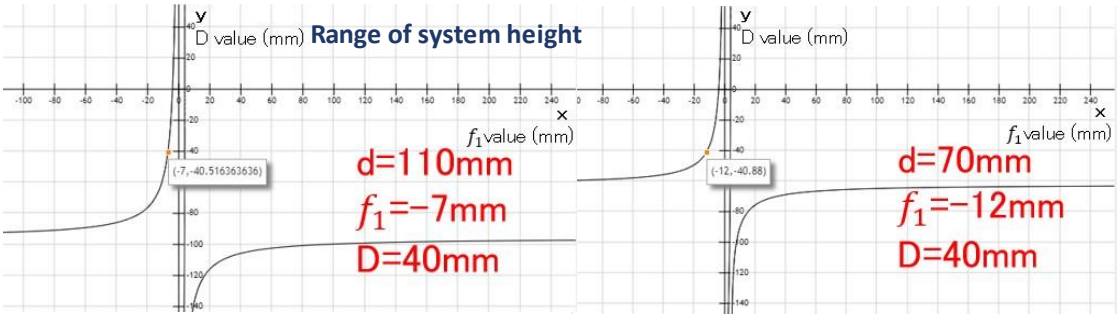

- The aperture of Fresnel lens (D) is the key parameters to decide system efficiency
- The D needs larger than 80 mm (80 mm – 110 mm appropriate)

8

Chap.4 Simulation and Experiment of Single-LED OWPT

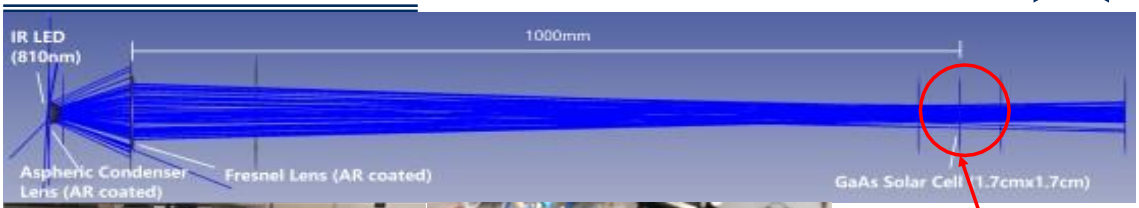

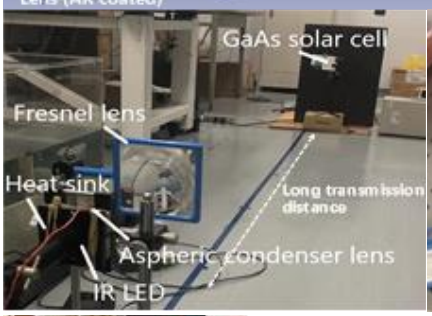

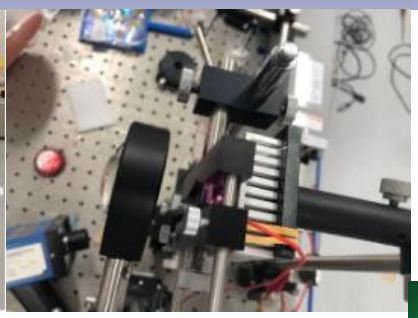

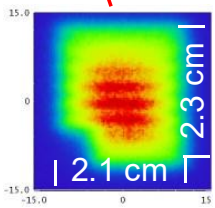

Experiment setup

Modularization of OWPT system

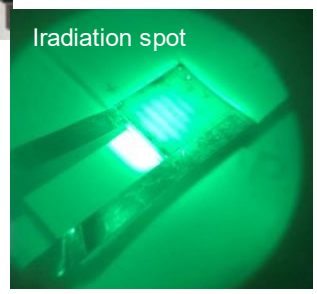

Chap.4 Simulation and Experiment of Single-LED OWPT

Experiment results of LED-based OWPT

Distance	Up to 1m	1m	2-3m
Irradiation (cm^2)	Average 2.3x2.3	2.1x2.3	Average 3x3
Dimension (cm^3)	Average 4x3x3	9.8x10x10	~23.6x21x21
Light utilization Efficiency	~48%	51.6%	~48%
Output	~200 mW	224 mW	~200 mW

Irradiance≒
500-3000x ambient light

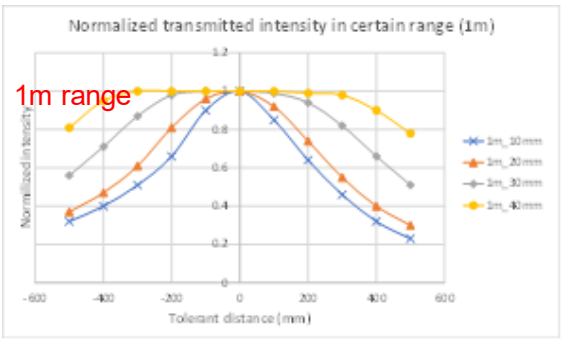

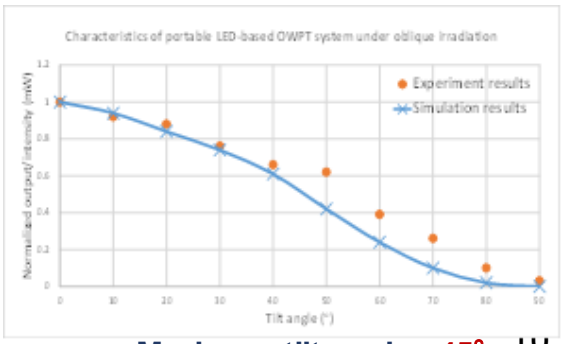

Tolerant distance: -300mm - +100mm

Maximum tilt angle: 45°

Chap.5 LED-array OWPT Configuration

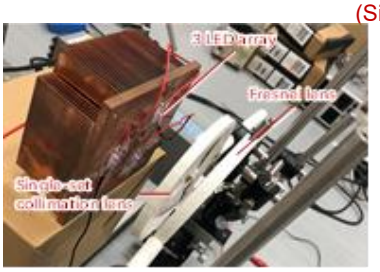

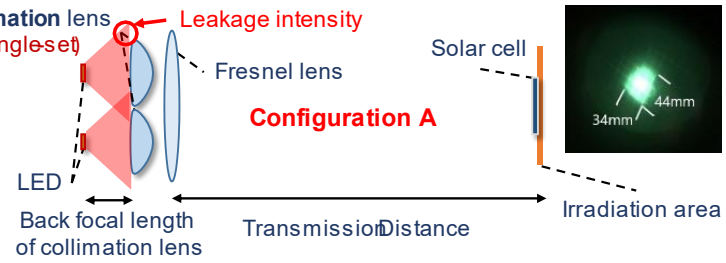

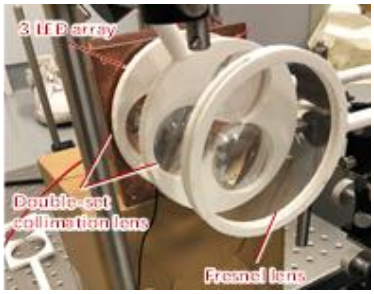

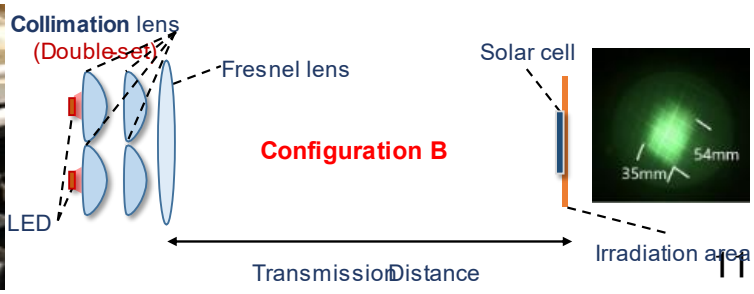

Chap.5 Experiment Results of LED-array OWPT

	Configuration A		Configuration B	
	2 LEDs	3 LEDs	2 LEDs	3 LEDs
Irradiation size (mm × mm)	27 × 30	34 × 44	38 × 41	35 × 54
Intensity on solar cell (mW)	560	850	780	960 (1080)
Lens system efficiency (%)	26.9	27.2	37.5	30.8 (35.2)
Output from solar cell (mW)	196	316	268	380 (389)

2-LED config. A= 215-1300x ambient light
3-LED config. A= 322-2000x ambient light

2-LED config. B= 153-930x ambient light
3-LED config. B= 215-1300x ambient light

Alignment requirement

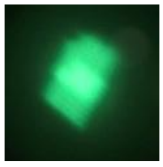

Alignment deviation ≤ 0.3mm
Overlap: 77%
Displacement: 6mm

12

Chap.7 Conclusion

1. The characteristics of single LED -based OWPT system for compact IoT

1. Portable LED-OWPT system is achieved (dimension < 10 cm × 10 cm × 10 cm, weight <700g).
2. Small receiver is realized (< 2 cm × 2 cm).
3. Above 100 mW output is obtained in 100 mm - 3 m.
4. At 1 m distance, 224 mW output power is available. (5 00-3000x ambient light).
5. Tolerance distance of LED -based OWPT is nearby -300mm and +100mm region, confirmed by simulation and experiment
6. Maximum tilt angle of the LED -based OWPT system is 45° .

2. The characteristics of LED -array OWPT system for compact IoT

1. 380 mW by LED-array OWPT with 1 m transmission distance is achieved. This is the highest output of LED -based OWPT with sufficiently small solar cell size. (200-1000x ambient light).
2. The misalignment of the optical components should be suppressed at least smaller than 0.3 mm for ensuring high performance.

13

Part. 2

Questions in Doctoral Dissertation Presentation

Part. 2 Q&A

Q: In LED-array OWPT system, about config. A and config. B, which one is better? (from Prof. Uenohara)

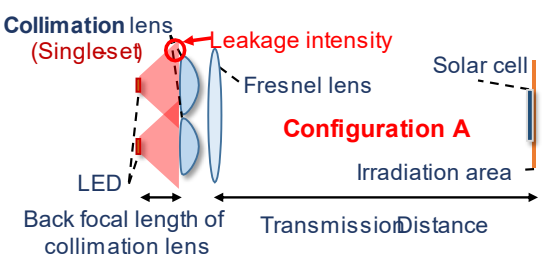

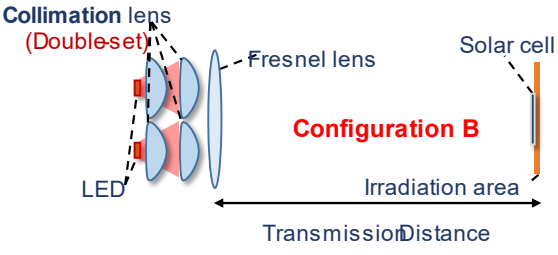

Main differences:

- Size of irradiation → etendue → Exit pupil (focal length of the collimation lens)
- System efficiency → Exit pupil (focal length of the collimation lens)
- System efficiency → Aperture of the collimation lens

15

Part. 2 Q&A

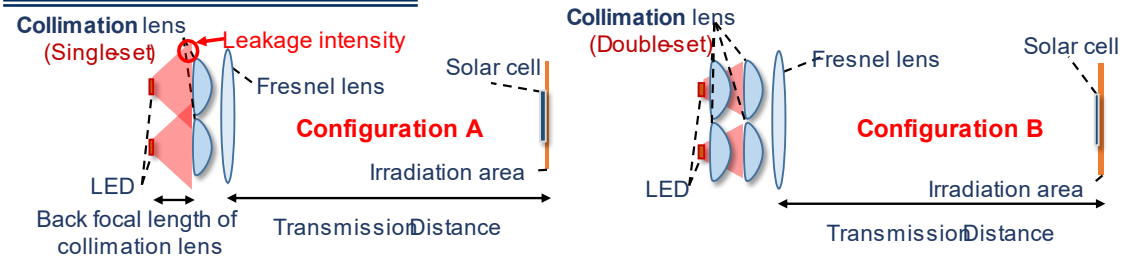

In the condition of same system dimension

- Exit pupil (focal length of the collimation lens) : Config. A > Config. B
- Smaller irradiation → Config. B has higher output
- Lower efficiency

In special conditions

Ideal condition (clear boundary of divergence)
Special condition (very short focal length or very large aperture) → Config. A has higher output

Performance: Config. B is better Cost or complexity: Config. A is better 16

Part. 2 Q&A

Q: How do you set the numerical targets of the OWPT system? (from Prof. Koyama)

Compact Receiver:

- Size: 1 cm² - 50 cm²
  (side length: 1 cm – 7 cm)

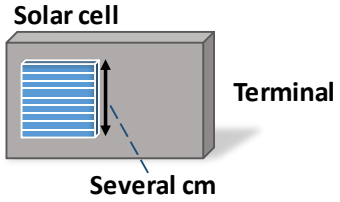

Can be compatible to most IoT devices

Although for ultra-small IoT device, it might unable to compact, the power consumption for such IoT is also small

Portable Transmitter:

- Dimension: 15 cm × 15 cm × 15 cm
  - Normal OWPT: easily put in bag
  - Mini OWPT: easily put in pocket

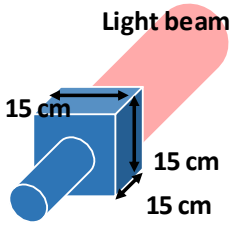

Portable OWPT transmitter 17

Part. 2 Q&A

- Weight of transmitter: ~ 700 g

Size (cm^3):
20.4 x 19.4 x 10.8

Weight: 700 g

Devices	Weight
Gopro	116 g
iPhone X	174 g
Samsung Galaxy Z Fold2	282 g
Can of Coke	412 g
iPad 4	662 g
LED flashlight	700 g
Surface Pro 3	800 g
MacBook Air	1.35 kg

Target transmission distance:

- Long range: 100 mm ~ 3 m range

1 m is the cut-off point of radiative WPT and non-radiative WPT

The normal height of the room and workplace is around 3 m

Output:

- High power: 100 mW ~ several watts class power transmission

100 mW ⟶ 35 mW/cm^2-75 mW/cm^2 ≈ Sunlight irradiance of whole day
(AM1.5G: 100 mW/cm^2)

18

Part. 2 Q&A

Q: What is the difference between the focused beam condition and unfocused beam condition? (from Prof. Tokuda)

Focused condition

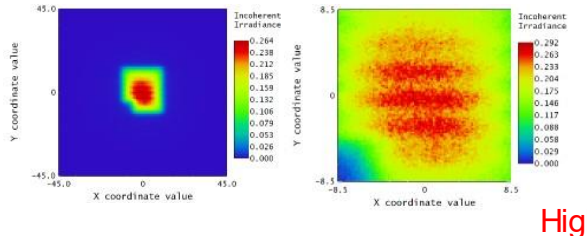

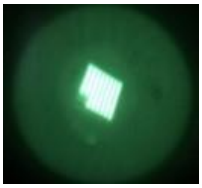

Peak irradiance:
0.292 W/cm^2
Total intensity:
575 mW

Higher PV effi., easy alignment

Unfocused condition

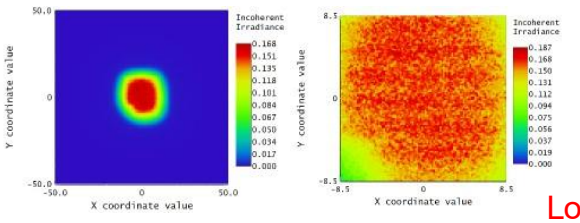

Peak irradiance:
0.187 W/cm^2
Total intensity:
438 mW

Lower PV effi., hard alignment

19

Part. 2 Q&A

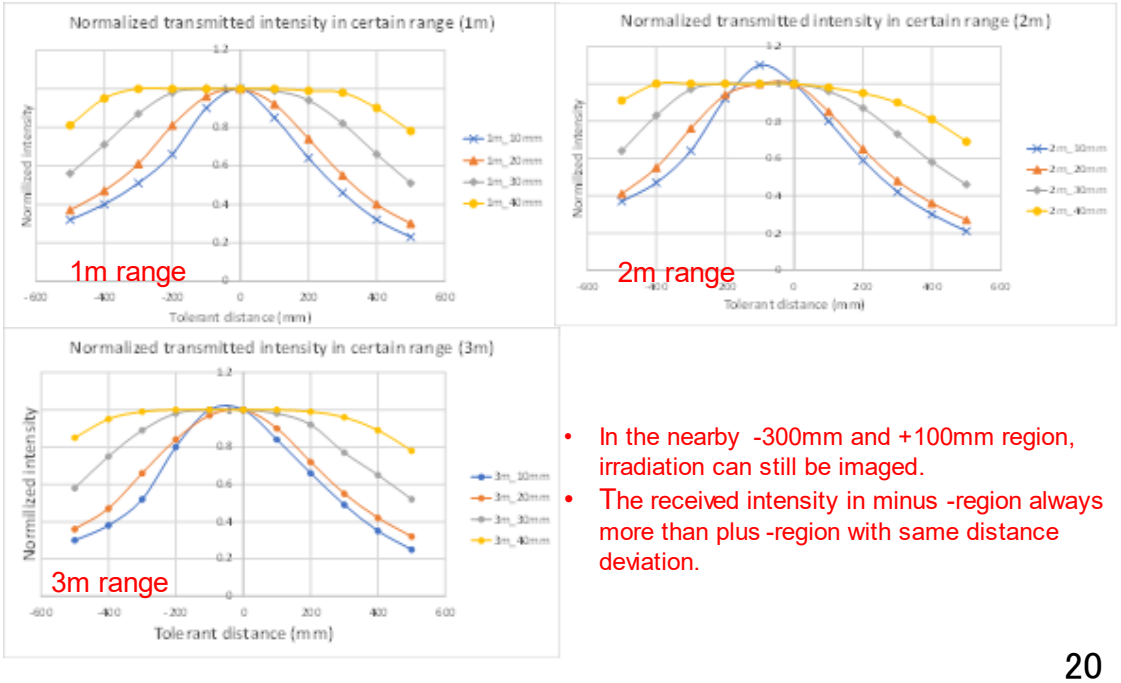

- In the nearby -300mm and +100mm region, irradiation can still be imaged.
- The received intensity in minus -region always more than plus -region with same distance deviation.

20

Part. 2 Q&A

Q: How do you align the multiple beams in LED -array OWPT system? (from Prof. Tokuda)

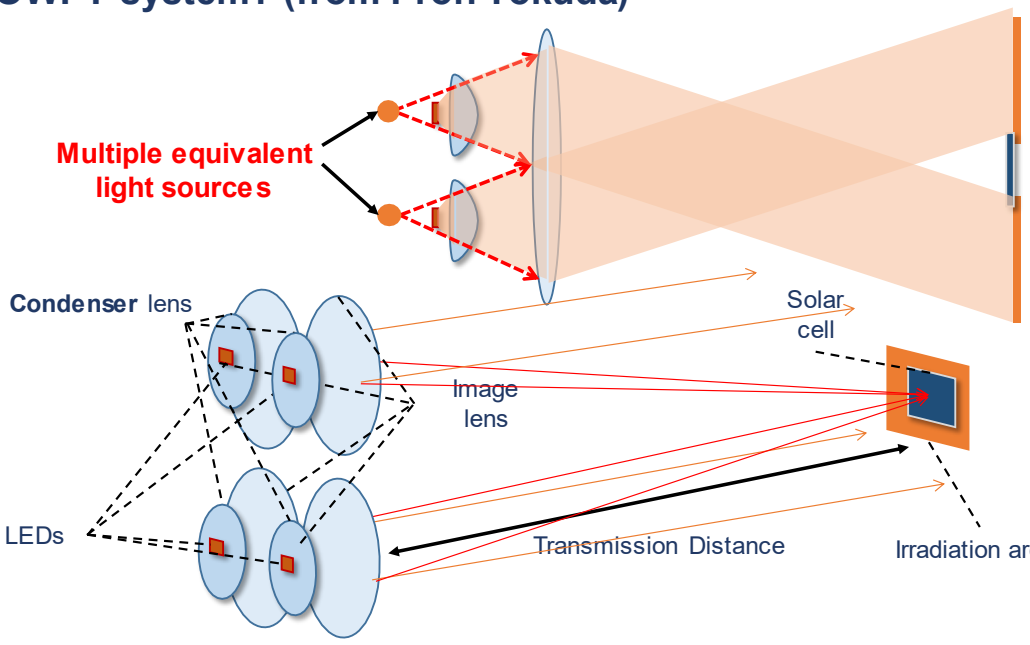

21

Part. 2 Q&A

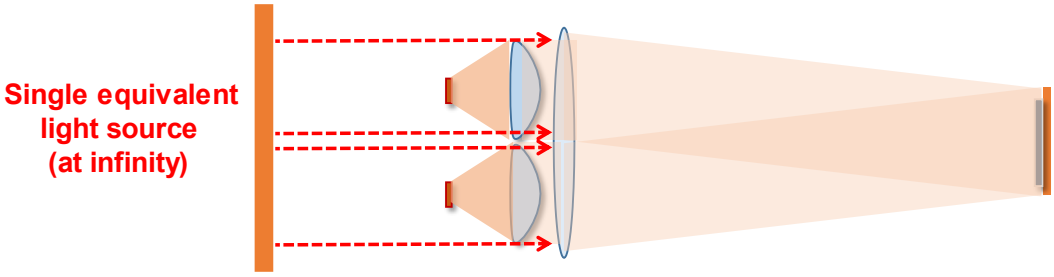

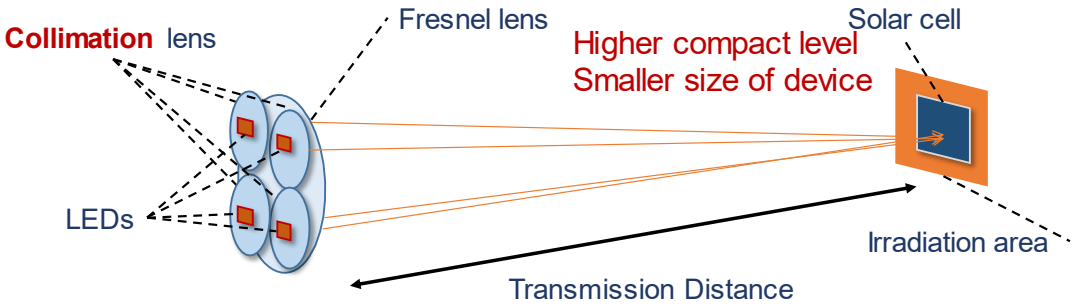

22

Part. 2 Q&A

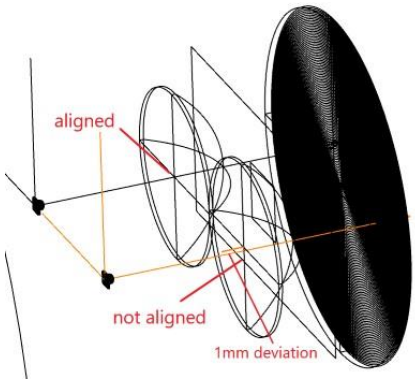

manufacturing deviation

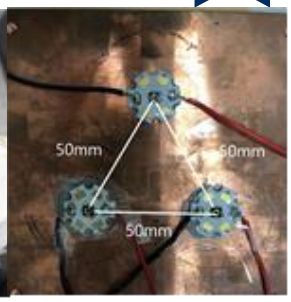

mounting deviation

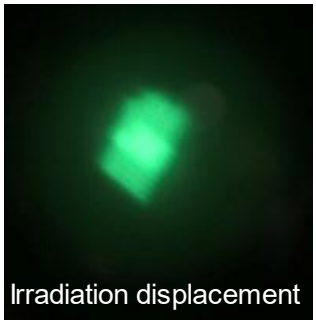

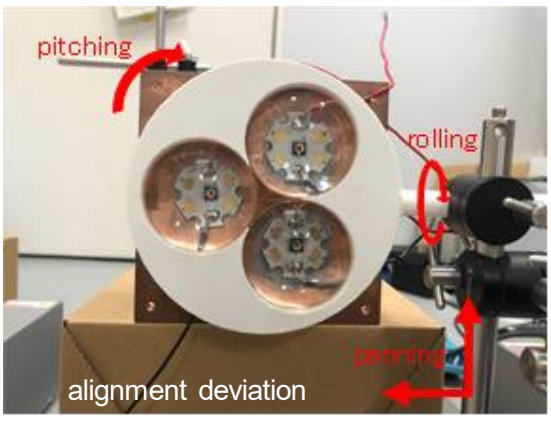

alignment deviation

23

Part. 2 Q&A

Q: The reason of using GaAs solar cell. (from Prof. Maruyama)

The selection of LED and solar cell should be considered together

- High-performance LED mainly in the near infrared region (800 nm – 870 nm)

Si: 1.14 eV
GaAs: 1.43 eV
Corresponds to NIR wavelength
Under same condition, GaAs solar cell generates less heat

GaAs solar cell has higher efficiency

Poly-crystalline Si solar cell + NIR LED → Around 30% PV conversion effi.
173 mW output power expected

- Even using corresponding wavelength LED (980 nm), Si solar cell still has lower efficiency due to higher current density

GaAs solar cell + NIR LED → Above 40% PV conversion effi.
230 mW

24

Part. 2 Q&A

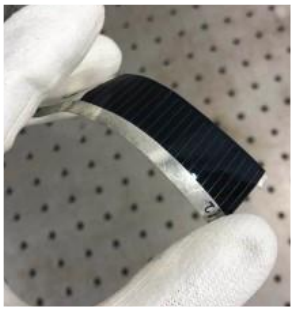

Single-junction GaAs solar cell

Poly-crystalline Si solar cell

- Flexible
- Light weight

GaAs solar cell: semiconductors deposited on metal (can be bent but not fold)

Conventional Si solar cell: semiconductors deposited on glass , indirect bandgap semiconductor (thick structure)

GaAs solar cell is much expensive, regarding the required GaAs solar cell for single IoT is small, the overall cost of entire system is low

25